Energetics of quantum measurements

Léa Bresque

THÈSE

Pour obtenir le grade de

DOCTEUR DE L'UNIVERSITÉ GRENOBLE ALPES

École doctorale : PHYS - Physique
Spécialité : Physique Théorique
Unité de recherche : Institut Néel

Énergétique de la mesure quantique

Energetics of quantum measurements

Présentée par :

Léa BRESQUE

Direction de thèse :

Alexia AUFFEVES Université Grenoble Alpes	Directrice de thèse

Rapporteurs :

DAVID GUERY-ODELIN
Professeur des Universités, UNIVERSITE TOULOUSE 3 - PAUL SABATIER
JANINE SPLETTSTOESSER
Professeur, Chalmers University of Technology

Thèse soutenue publiquement le **20 octobre 2022**, devant le jury composé de :

DAVID GUERY-ODELIN Professeur des Universités, UNIVERSITE TOULOUSE 3 - PAUL SABATIER	Rapporteur
JANINE SPLETTSTOESSER Professeur, Chalmers University of Technology	Rapporteure
JULIA MEYER Professeur des Universités, UNIVERSITE GRENOBLE ALPES	Présidente
BENJAMIN HUARD Professeur des Universités, ENS DE LYON	Examinateur
MICHELE CAMPISI Directeur de recherche, Istituto Nanoscienze CNR	Examinateur

Acknowledgements

MY PERSONAL JOURNEY in quantum physics started in Australia. There, years before obtaining a master in physics and an engineering diploma, I discovered the excitement and richness of research thanks to the guidance of André R. R. Carvalho. Then, after many other adventures for which I would already have too many people to thank (and who will probably never read this acknowledgment anyway: Sébastien Massenot, Laurent Sanchez Palencia, Alain Aspect, Mikhail Lukin, Emma Rosenfeld, Arthur Saphira, Samuel Deleglise, Thibault Capelle...), I discovered the field of quantum thermodynamics and with it the impressive energy of Alexia.

Thank you Alexia for your trust and for introducing me to the field of quantum thermodynamics. Now that I know better what it means to do research, I am even more impressed at your capability to find deep ideas and connections and at your courage to push them forward. I also want to thank you for the many wonderful researchers you allowed me to collaborate with.

I have had the chance to work with Natalia Ares, Janet Anders, Juan Parrondo, Robert Whitney, Cyril Branciard, Jacqueline Bloch, Alastair Abbott, Maxime Richard, Andrew Jordan, and Kater Murch, among others; all very impressive researchers whose works I greatly admire. They all have inspired me for their knowledge, powerful ideas, and profound kindness. I was also lucky to have met and discussed with several philosophers of science, especially Laurie Letertre, Owen Maroney and Cristian Mariani. Olivier Ezratty too was a very enriching encounter.

I don't forget Patrice Camati, of course, my unofficial supervisor at the start and soon a true friend that I can always count on. Working with you is always a happy and exciting moment. I was lucky to work with other very skilled friends such as: Nicolò Piccione, Juliette Monsel, Titta (Nicola Carlon Zambon), Irénée Frérot, Federico Fedele, Federico Cerisola, Jorge Tabanera, Florian Vigneau, Xiayu Linpeng, Spencer Rogers, Étienne Jussiau, and Maria Maffei. My thesis would not have been the same without the other members of our group, especially the anecdotes and gadgets of Bruno; the jokes, books, discussions and tea of Samyak, the hikes with Konstantina, the fascinating chemistry related email exchange with Jing Hao and the parties of Marco. Thank you Hippolyte, Raphaël, Kylia, Quentin, Zaynab, Jana and all those who are making our lab an enjoyable place. In this spirit, I also thank Laurence Magaud and Jean-Phillipe Poizat as well as Nathalie Bourgeat-Lami.

Although I have not seen a lot my family during these three years, I thank them for all they made me discover and experience during my childhood and thereafter. Finally, I would have too many reasons to thank you, Louis, and I wish to everyone to have a partner as caring, fascinating and charming as you are. Thanks to you, not a week went by that I can regret, and

not only because we have gone on so many adventures such as under ice diving, building an igloo and (almost) sleeping in it, camping surrounded by wolves, or on the top of a mountain, waking up at 6am to go by kayak on the wild side of the Bourget lake at sunrise or even buying an apartment. I feel like all dreams are possible with you and being a tired, excited or curious Ph.D student was definitely one of them.

I also warmly thank the organizers of the "New Mechanics" Houches school for these four fascinating weeks which allowed me to finish writting my thesis surrounded by all the excitement for physics and reassuring discussions I needed. Last but not least, I am very grateful to my jury members, especially Janine Splettstößer and David Guéry Odelin who accepted to be my rapporteurs.

Thank you to all the songs, poems, books and movies that are here everyday.
And I don't forget my ants and plants either!

Abstract

QUANTUM MEASUREMENTS disturb. By this, it is implied that quantum measurement can affect the state of the measured system. Such a measurement backaction is due to the interaction of the quantum system with the measuring device. When the measured observable and the system's Hamiltonian do not commute, the backaction can lead to a mean energy change of the system. This energy change has been dubbed "quantum heat" and, in association with feedback processes and/or the interaction with thermal bath(s), proves to be a genuinely quantum resource to fuel new kinds of quantum engines. We propose such a measurement powered engine exploiting the non-commutativity of local and non-local operations on a bipartite quantum system.

We then investigate the origin of the quantum heat. This task might appear impossible because one cannot model the full dynamics of a measurement due to the collapse of the wavefunction. However, the energetic aspects can still be investigated by modeling the so-called pre-measurement. During this pre-measurement step, the system interacts and gets correlated with a quantum system, which can be viewed as a small part of the measuring apparatus and called the quantum meter. Ideally, at the end of this process, the system's reduced state will be fully decohered in the measurement basis, thus corresponding to the averaged collapsed output states given by the measurement postulate. We find that the quantum heat received by the measured system corresponds to the energy necessary to turn on and off the coupling between the meter and the system. Using generalized definitions of heat and work, we moreover characterize the nature of these energy exchanges.

Tracing the source of this energy one step further, we propose an autonomous description of a measurement. This is done by considering a flying qubit measured by the quantum field of the cavity it crosses. The interaction being position dependent, the kinetic degree of freedom is providing the required energy to switch on and off the interaction between the qubit and the meter field. A full quantum treatment allows us to evaluate the impact of the finite spatial and momentum extension of the qubit wavepacket. Since the kinetic degree of freedom can be affected by the interaction, it does not simply generate a time dependent Hamiltonian for the other degrees of freedom. We find the correction to this ideal dynamic and analyse its consequences on the nature of the energy fluxes.

Taking the opposite point of view, we compare the cost needed to measure a qubit state via a cavity field, depending on their initial states. The measurement quality is quantified via its informational and energy efficiency. Given energy constraints, single photon are found to be more efficient than coherent field, themselves better than thermal fields. These results hence pinpoint an energetic advantage of quantum states over classical ones for measurement purposes.

The results presented in this thesis contribute to unravel the mysterious effects and mechanisms of quantum measurements. Notably, they open new possibilities to further analyse quantum measurement based engines and to understand the energetic resource that measurements cost and constitute at the same time.

Table of Contents

List of Figures

List of Symbols

Unless stated otherwise, the notations used in this manuscript are defined as follows.[1]

S^{sh}	Shannon entropy (units of log(2))
$S(\rho)$; S_A	Von Neumann entropy of a state ρ; of the state of the system A (units of log(2))

Bipartite Quantum Energetics (BQE) quantities

$\mathcal{U}_A$	Internal energy of the subsystem A
W_A	Generalized work done on the subsystem A
Q_A	Generalized heat done on the subsystem A
$V_{AB}^{\otimes}$	Generalized work done on the the interaction energy
V_{AB}^{χ}	Generalized heat done on the the interaction energy
W_{ext}^{A}	External work done on the subsystem A

Pre-measurement dynamics

S; M; SM	Measured system, quantum meter and joint system made of these two parts
t_0	Starting time of pre-measurement step
t_m	Ending time of pre-measurement step
H^A; H^S	Bare Hamiltonian of an arbitrary system A; of a measured system S
H^B; H^M	Bare Hamiltonian of an arbitrary system B; of a meter system M
V^{AB}; V^{SM}	Interaction term between A and B; S and M
χ	Coupling constant between a system and a meter
$\chi^{AB}(t)$	Correlation matrix of a bipartite system AB at time t

Autonomous measurement

H_0; V_1	Bare Hamiltonian of the internal degrees of freedom (IdoFs); part of the interaction Hamiltonian acting on the IDoFs
x_0; v_0; ρ_0	Initial average position, velocity and state of the wavepacket
$\hat{q} = \hat{p} - p_0$	Momentum operator displaced by the initial average momentum

[1] Operators are written without a hat symbol to lighten the notation unless a confusion is possible.

$f(\hat{x})$; $f(x)$	Potential shape as a function of the position operator; or value
$H_{NA}(t)$	Time dependent non autonomous Hamiltonian
$\tilde{H}(x) = H_0 + f(x)V_1$	Position dependent non automomous Hamiltonian
$\tilde{U}_x(t)$	Unitary evolution associated to a classical particle starting at position x and moving at the speed v_0
$\mathcal{C}(\rho_0, t)$	Correction term due do the spatial shape of the initial wavepacket
$\rho_I(t)$; $\rho_K(t)$	Reduced density matrix of the internal degrees of freedom; of the kinetic degree of freedom

Energetic cost of a measurement

$\bar{n}_{\text{in}}$	Average number of photon of the input field
f_c^e; f_c^g	Frequency of the cavity if the qubit is in $\|e\rangle$ (resp $\|g\rangle$)
ρ_{th}^e; ρ_{th}^g	Monochromatic thermal state at frequency f_c^e (resp f_c^g)
$\rho_{\text{SM, th}}^p$; $\rho_{\text{SM, coh}}^p$; $\rho_{\text{SM, 1ph}}^p$	Joint system and meter state after step "p" given an initially thermal field state (resp coherent of single photon)
$\eta_I = I/S_S$; $\eta_E = I/S_M$	Informational and energetic efficiencies

Appetizer

Whilst thermodynamic research extends its borders to the realm of plasma physics [1, 2], novel turbines [3] and non-equibrium aspects in biology [4] among other paths; quantum physics expands its domain towards eagerly awaited new practical usages with the emergence of quantum spatial communication [5, 6], quantum cryptography [7, 8], enhanced photovoltaïc cells [9, 10] and driven by the hopes for quantum computers [11]. In the meantime, quantum physics does not lose its affinity with pure fundamental theory by questioning the implications of causal order superposition [12, 13, 14], pushing the limit of the quantum world by cooling increasingly larger objects [15, 16, 17, 18, 19] in the hope to witness effects of gravity in quantum systems (perhaps decoherence), and even probing physics beyond the Standard Model [20].
At the confluence of these fields lies the, explicitly named, realm of Quantum Thermodynamics. The richness of this transdisciplinarity goes beyond the current appetite for blurring science's reassuring domains. Rather, it seems to arise from the very "paradoxically fertile" nature of this encounter. Indeed, it is no surprise that the very idea of quantification itself came from a discrepancy at the heart of thermodynamics: the Black-Body radiation [21]. Since then, the confrontation of quantum unexpected features with our classical intuitions lead to many other great unravellings in quantum physics. One could think for instance about Schrödinger's cat, illustrating the conceptual void, still puzzling us to this day, regarding the frontier of the classical and quantum worlds, or about the Einstein-Podolsky-Rosen (EPR) paradox proving that a concept such as entanglement appeared unrealistic even to some of the greatest minds. Moreover, within the classical realm, thermodynamics is perhaps the most fundamental theory since, as even Einstein once said:

> "It is the only physical theory of universal content, which I am convinced, that within the framework of applicability of its basic concepts will never be overthrown."

Thus, thermodynamics is arguably the strongest bound to quantum physics' annoying and fascinating habit to slip away from our grasp. Consequently, maybe within thermodynamics, can we hope to dive deeper into quantum's profound mechanisms.
This hope already resulted in great accomplishements. Although many subfields of Quantum Thermodynamics are still rather young, the following introduction will simply cover the prospects and achievements related to this thesis topics and many others are also worth exploring [22]. Interested readers might enjoy Figure. I.1's attempt to organize a mind map of quantum thermodynamics' main areas of research.

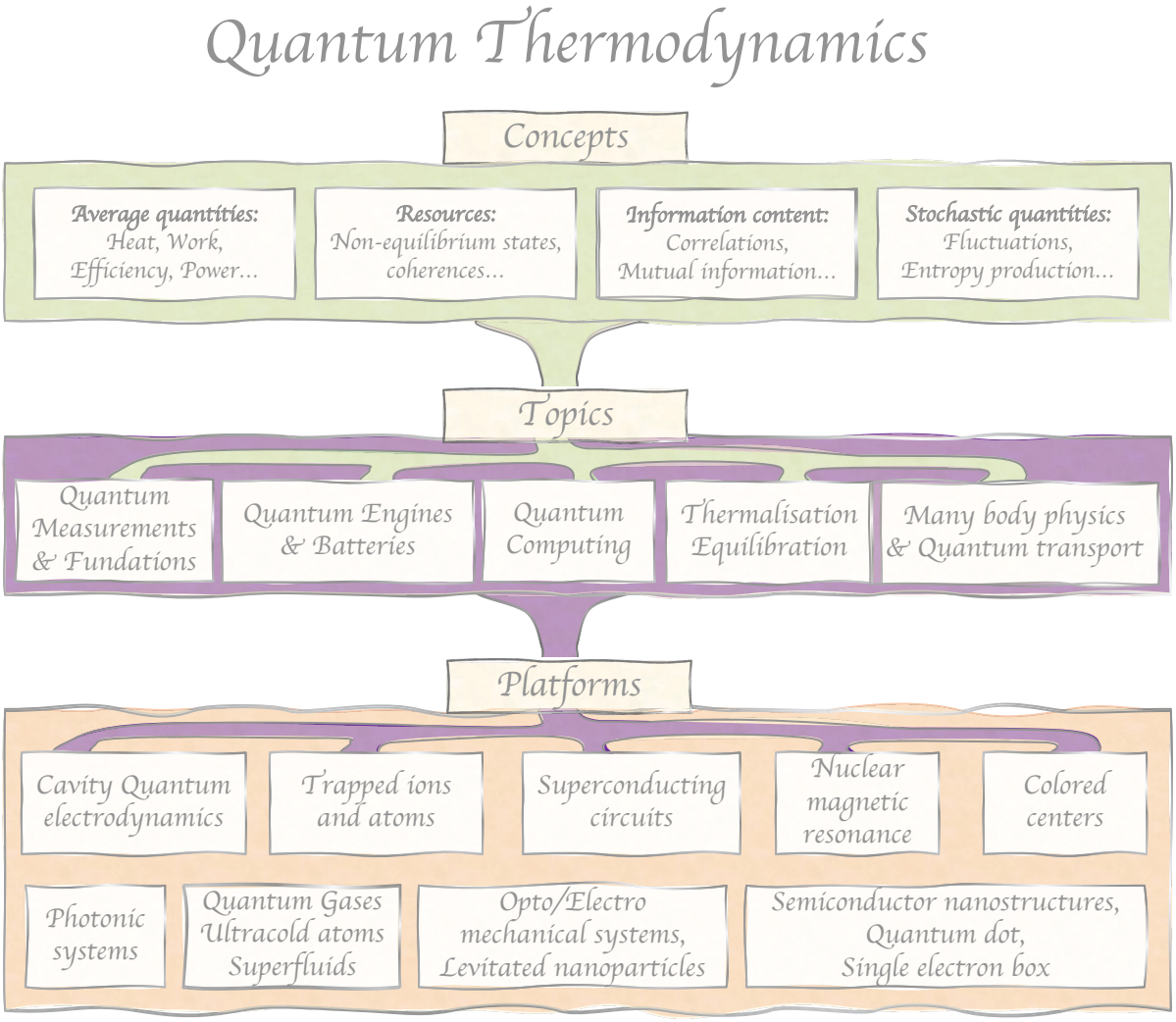

Figure I.1: An attempt of a Quantum Thermodynamics mind map

Chapter 1

Quantum thermodynamics and Measurement: an introduction

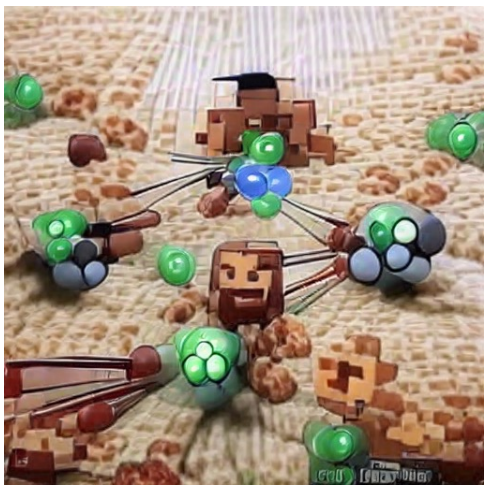

Generated using the artificial intelligence method VGLAN + CLIP

Contents

IF I WERE TO DEFINE a PhD thesis to a friend, with all the naivety of not having written mine yet, I would compare it to the notes of a XVIII's century navigator, once typed and organized. In other words, I view it as a personal, and yet as objective as possible, gathering of knowledge, insights and findings: a structured report and update on a recent exploration.
Firstly, and not to lose a reader on the other side of the sea, I will zoom in the thermodynamics of microscopic objects. Reaching the quantum world, I will highlight the stakes and prospects raised by these new possibilities and take the opportunity to introduce useful notations and achievements made within this quantum framework. The quantum to classical frontier remaining a vivid topic of research and an attractor point to my work, quantum measurement and their stakes will be discussed to complete our chosen tour of the beautiful field of quantum thermodynamics.

1.1 Thermodynamics: From Macro to Micro

1.1.1 Emergence of the core concepts

In order to appreciate the depth of our conceptual thermodynamic heritage, it is insigthful to remember that before the middle of the XVIII's century the concepts of temperature and heat were still mistaken for one another - the distinction is known to be own to Joseph Black. Often, we do not even realize how much our unified vision of energy was a mind-blowing understanding at the time. What a deep connection to be able to relate the energy of electrons moving in a wire with kinetic, gravitational and chemical energy due partly to Mayer and Helmholtz. Thanks to the work of Benjamin Thompson and James Joules, it became clear that mechanical work could be converted in heat, as demonstrated via the paddle-wheel experiment for instance [23]. On the pratical side, creative engineers, such as James Watt, did not wait to use heat flow in order to generate useful work for their machines. Quickly, along with the industrial revolution, thermodynamics, which was originally focusing on the field of thermometry and the study of the *caloric* (heat) exchanges, went on to characterize the spreading heat engines, depicted in Figure. 1.1, and their corresponding cycles and efficiencies. It is thus no surprise that in 1871, in the preface of his book, *Theory of Heat*, J. Clerk Maxwell defines the subject of Thermodynamics as the investigation of the thermal and mechanical properties of substances. However, whereas work could be completely dissipated to heat, the opposite conversion was found to be impossible. Kelvin no-go theorem is even stating that no work can cyclically be extracted using only a single bath. Using two baths is not enough either for a perfect retrieval of work from heat since, as Sadi Carnot has shown, even an ideal, perfectly reversible, cycle could not transform the total amount of heat going from a hot to a cold reservoir into work [24]. From these findings arose the understanding that heat is a degraded form of energy that cannot be fully converted into work. This realisation is very deep because it already prefigures the notion of time arrow. Indeed, coming back to Carnot's cycle, it appeared that the work extracted is less than the heat given by the heat bath. However, by running the cycle backwards, it is possible to reverse the

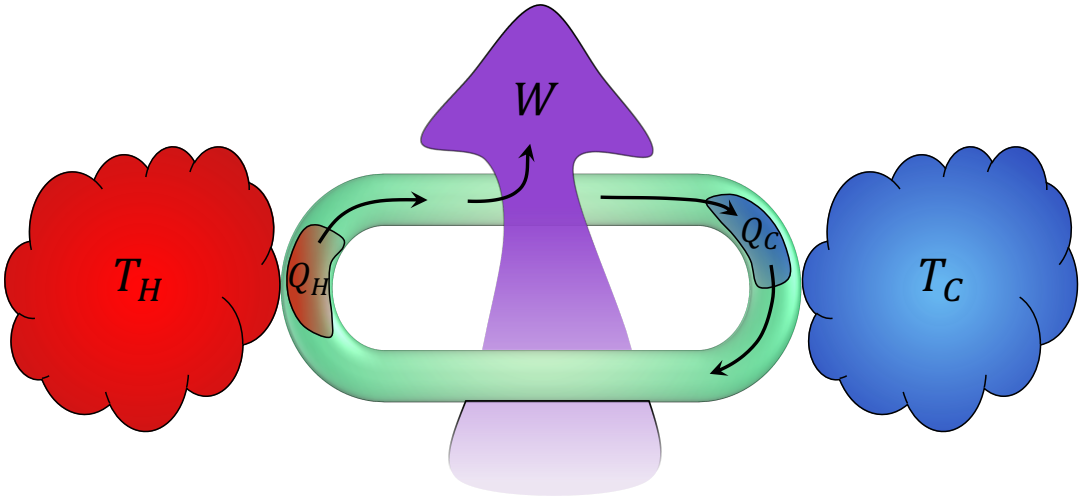

Figure 1.1: Working principle of a heat engine: The working substance (blob travelling in the green path) receives Q_H of heat by interacting with the hot bath from which some work W can be extracted upon increasing the entropy of the cold bath, of temperature T_C, by Q_C/T_C where Q_C is the heat received by this bath.

heat flow and come back to the initial state of the engine. As such, one could simply think that heat and work, just like two currencies, could simply be converted to one another at will given some specific exchange rate, this "rate" being the well-known Carnot efficiency $\eta = W/Q_H$, with W the work extracted from the working substance. However, as noticed by Clausius, when considering any other cycle than Carnot's, the amount of work extracted is not sufficient to generate, when reinvested in the backward cycle, an equal and opposite heat flow that the one used to obtain it in the first place: some extra charges apply upon each new conversion. Clausius noticed that, for all known cycles, the heat absorbed by the working substance during a cycle was such that $\oint \frac{dQ}{T} \geq 0$, with equality for the reversible Carnot cycle. This asymmetry lead him to invent the notion of reversible entropy change of a body in contact with a bath at temperature T defined as $\Delta S = Q_{\text{rev}}/T$, where Q_{rev} is the heat exchanged. For instance, if a container filled with gas at temperature T is connected to a bath, also at T, and is compressed or expanded by staying in contact with this bath, the heat exchanged will be reversible and the entropy will be given by the above formula. Instead, if this gas was initially at a temperature $T_1 \neq T$, the thermalisation process will be such that entropy change of the gas will be

$$\Delta S = Q_{\text{rev}}/T + \Delta_i S, \tag{1.1}$$

where $\Delta_i S$ is the, always positive, entropy production which quantifies the irreversibility and where Q_{rev} does not include the heat exchange associated to this irreversible step.
At this stage, introducing the notion of entropy might seem a bit artificial, although it already hightlights the time evolution asymmetry via the inequality $\Delta_i S \geq 0$ which later lead to the notion of time arrow. However, this idea becomes much deeper when related to Boltzmann

informational entropy. Indeed, as written on his grave, Bolztmann has defined the entropy of a system in equilibrium from the number of its microstate Ω such that:

$$S = k_B \log(\Omega) \tag{1.2}$$

with k_B the eponym constant. In a gas made of many particles, it is often more appropriate to regroup the microstates of same energy to rewrite the entropy in Gibbs' terms $S = -k_B \sum_i p_i \log\left(p_i\right)$ where p_i is the probability of a given particle of this gas to be having the corresponding energy E_i. This formulation is more general at it also applies to systems out of equilibrium for which not all microstates are as likely witnessed. Entropy is thus related to the probability distribution of the possible states: a very cold system for which all particles are likely to be moving at low speed will have less entropy than a hot system for which the distribution of kinetic energy will be much broader. From the perspective of thermal engines, work extraction is possible because it uses the natural flow of entropy from the hot to the cold reservoir. By mediating this exchange via a working substance we can gain some readily usable energy, however, this does not come from free since, outside of the ideal theory world, the thermal bath will eventually converge to the same temperature in the process: hence the need to keep the flamme burning.

1.1.2 Thermodynamics of information

From this early heritage, further insights about the thermodynamic consequence of the physical nature of information almost started as a joke. Indeed, Maxwell's original thought experiment [25] seemed like a playful game, except that it led to an apparent violation of the second law of thermodynamics which would puzzle scientist for many years. At the end of his book"Theory of Heat", in a section called "Limitation of the Second Law of Thermodynamics", Maxwell imagine a way to violate the common expectation that:

> "it is impossible in a system enclosed in an envelope which permits neither change of volume nor passage of heat, and in which both the temperature and the pressure are everywhere the same, to produce any inequality of temperature or of pressure without the expenditure of work."[25]

which can be seen as another statement of the second law. To do so, he considers a container fullfilling the above conditions (no change of volume and no heat exchange) and divided in two parts, initially at the same temperature. As in any gas, the individual particules would have different speed according on the thermal distribution. Between the two compartments, lies a small trap initially open.
The paradox arises by noticing that an intelligent being, later made demonic by Kelvin, knowing the position and velocities of the particles, could choose to open and close the trap at the appropriate instants such that the particles get sorted into faster and slower ones. Thereby he

would freely obtain two reservoirs of different temperature in clear violation with Maxwell's statement.

However simple, this pedagogical setting (for a playful and interactive simulation see: Maxwell Demon game) became highly disturbing for physicists. Indeed, from a single bath, one could obtain at apparently no cost, two different temperature reservoirs from which we know that useful work can be extracted. Once the temperature difference between them would vanish we could start again the demon game and thereby, seemingly cyclically extract work from a single bath in clear violation of Kelvin's statement of the second law.

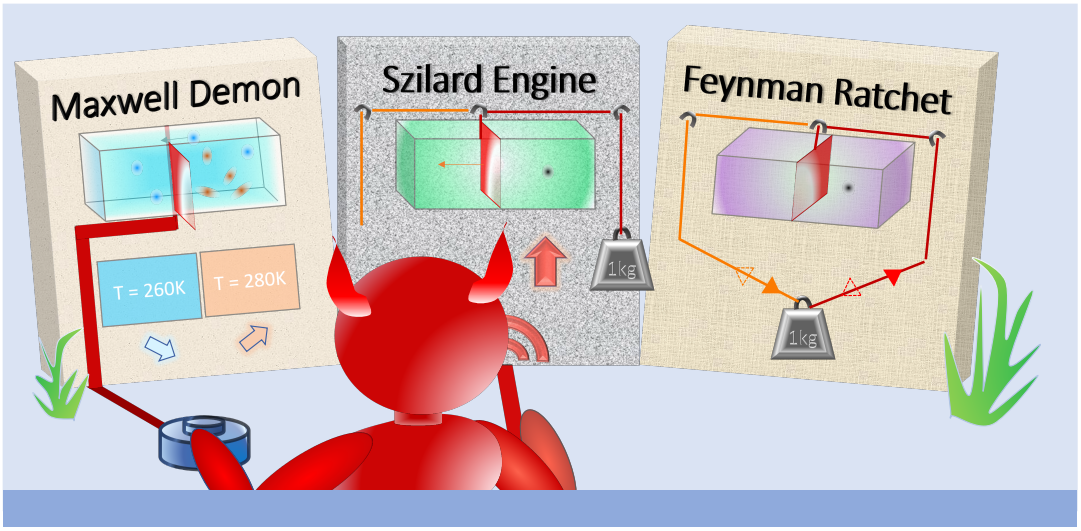

Figure 1.2: Depiction of a Demon facing its original game by Maxwell as well as Szilard's single molecule adaptation and an adaptation of the Feynman's ratchet thought experiment.

More than half a decade later, one of the most important steps towards understanding the missing brick was given by Leo Szilard in his seminal paper of 1929 [26]. There, he introduced a new version of the experiment in which the gas is replaced by a single particle, see Figure. 1.2. By placing a piston in the middle of the container we would end up with two sides: one containing the molecule and the other empty. The pressure difference will induce the piston to move toward the empty side and this motion can be used to extract some useful work retrieving here too an apparent violation of the second law. In order to extract this energy however, information about the side on which the molecule was found is needed to decide where to place the weight, as pictured in Fig. 1.2. Thanks to the works of Shannon, Bennett [27] and Landauer [28] it became clear that to repeat the experiment, the memory storing this information would have to be erased and that this logically irreversible operation implied a cost of at least $W = k_B T \ln(2)$.

To understand the reason behind this specific work cost, it is useful to come back to Clausius who came to the conclusion that the change of entropy of a system in contact with a bath was

such that:

$$\Delta S - \frac{Q}{T} \geq 0. \tag{1.3}$$

Using the first law $\Delta U = W + Q$ and the definition of free energy $F = U - TS$, where U is the internal energy of the system considered, he obtained his eponym inequality:

$$W - \Delta F = T\Delta_i S \geq 0, \tag{1.4}$$

showing that the extractable work in any such transformation is at best equal to the change of free energy of system. Applying this finding to the case of a degenerate memory of one bit of information, we deduce that the work required to erase this bit information, thereby changing the Gibbs entropy from $S = k_B \log(2)$ to $S = 0$ would cost a work $W \geq \Delta F = k_B T \log(2)$. This work cost, since it exactly corresponds to the maximal work that could be extracted from the Szilard engine, thus allowed to solved the paradox.

The main conclusion to this endeavour was that information can be used to extract useful work but that the manipulation of information itself was coming at a cost.
This cost is needed to reset the memory. Ideally, this can be done by reversing the Szilard procedure decribed above, i.e., starting with a container filled with a particle either on the right or on the left and with the barrier on the side of the container, as depicted in Fig. 1.3, and then pulling off the piston-barrier to force the particle to be reset in the right side for instance: this is Landauer erasure.

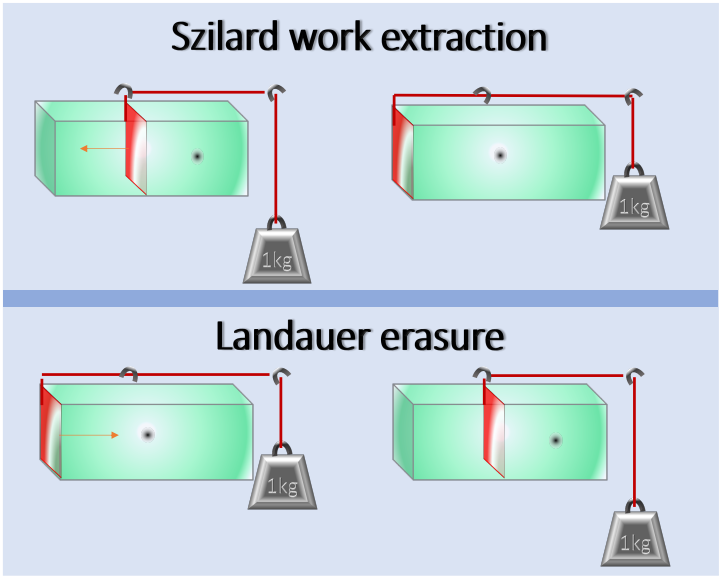

Figure 1.3: Landauer erasure and Szilard work extraction as two opposite mechanism.

At this stage, one could wonder if it is still possible to extract work without using a memory. Several attempts have been made to propose such engines which are usually based on fluctuations. Indeed, due to the discrete nature of matter, i.e., atoms and molecules, the pressure

felt by the piston is not constant over time but fluctuates around its average value. Of course the larger the system is, the smaller the fluctuations will be compared to this average. In the Feynman–Smoluchowski ratchet thought experiment, by using a ratchet that is only allowed to rotate in one direction, thermal fluctuations were thought to be able to induce rotation of the gear. This rotation could then be used to lift a weight for instance and therefore extract some useful work. In the same spirit, one could take again the single particle Szilard engine (in the classical case, where it does not cost anything to insert the barrier). There as depicted in Fig. 1.2, without even knowing the side of the particle, one could expect it will exert a pressure on the barrier and thus lead to a movement of the mass attached to the string, upward no matter the direction of the barrier. To solve these new paradoxes, since such engines would violate the second law of thermodynamics if they could work, Smolowski and Feynman; whose work were complemented in this regard by Parrondo, Pep Español, Magnasco and Stolovitzky [29, 30]; came to the understanding that, if everything is at the same temperature (particle(s), ratchet, mass), then no work can be extracted from the thermal fluctuations. This is because the fluctuating position of the pawl will let the ratchet rotate backward with equal probability than the thermal fluctuations will make it move forward. In the Szilard case, the effect of the particle on the barrier will induce a motion of the weight indistinguishable from the motion due to the fluctuations arising from the surrounding environment. This example, illustrated in the last pannel of Fig. 1.2 can be seen as the mechanical counterpart of the electrical circuit using diode bridges such as the one proposed by Aydin *et al.* [31]. Last but not least, it was recently understood that stepping away a little from the standard paradigm of measurement and feedback described in the original proposal of Maxwell, similar effects, such as heating a hot reservoir and cooling a cold one without providing work, can be obtained solely from the use of non equilibrium resources [32, 33]. In this case of so-called non-equilibrium demon, it is the equilibration of the non-equilibrium resource that generates the entropy production necessary to verify the second law. However simple and idealistic, these toy models have motivated many further investigations due to the richness of the conceptual questions they raise.

1.2 Quantum thermodynamics and measurements

Quantum systems are small and well isolated enough that their dynamics can be affected by quantification and superposition. Not only are they subject to important fluctuations but even at an average level, i.e., averaging over many runs of the same experiment, their quantum nature offers new possibilities. Such counter intuitive features include superposition; which can be witnessed in single photon interference experiments; entanglement; which allows for the striking "action at a distance" phenomenon; contextuality; which tells us that the result of a measurement depends on the set of the other measurement operators jointly measured, or measurement backaction; which comes from the invasiveness of quantum measurements. From these features, it is possible to secure communications from an eventual eavesdropper, to speed up some computations or to build very precise sensors. Thermodynamics is not left out as

the energetic exchanges between quantum systems also inherits quantum's fascinating's properties: it is the purpose of quantum thermodynamics to single out and characterize these new properties.

1.2.1 Quantum heat engines

As early as 1959 it became clear that; building on the first quantum revolution, i.e., quantification; one could make use of quantum working substances and the individual addressability of their energy level splittings to build quantum thermal engines [34]. Scovil and Schulz-DuBois famously first showed that a three energy level quantum system implementing a maser could be seen as a heat engine. A bit later, the ultimate Carnot cycle was adapted to quantum systems [35] as well as the Otto cycle [36]. Although even entanglement was reassuringly shown not to violate the second law of thermodynamics [37], going to the quantum world unlocked new possibilities such as extracting work from a single heat source [38], reaching efficiencies greater than their ideal classical counterpart [39] and even greater than Carnot's efficiency [40]. These striking phenomena were only in apparent contraction with the second law of thermodynamics and led to evolutions of the expression of the second law in the quantum regime to account for these new discovered possibilities [41, 42].

Aside from the deep insights these works provided, on both, quantum physics and the second law, the typical thermodynamic figures of merit such as maximal power, work extracted and efficiency were extended in the quantum regime.

Building on these first achievements, the community went further by implementing many of these proposals at the edge of the quantum world such as a single colloïdal particle to build a Stirling engine [43], a thermoelectric heat engine with ultracold atoms [44], a Carnot engine with a polystyrene microsphere [45], a single-atom heat engine [46], a circuit quantum electrodynamics (QED) absorption refrigerator [47] and a single-ion Otto engine [48]. The latest experiments started using purely quantum properties such as squeezed reservoirs [49] or spin-1/2 particles [50]. It allowed to build quantum absorption refrigerator [51] and other quantum engines [52, 53, 54]. For a more detailed review of the past realizations regarding quantum heat engines, see the very nice and recent work of Myers *et al*. [55].

One of the main new possibilities offered by quantum physics is to have pure states, i.e., states that are not probabilistic mixtures but which are neither in an energy eigenstate. Such superposition states can be seen as new resources, which are costly to keep when the system is in contact with a thermal bath [56] due to the detrimental effect of quantum irreversibility [57] and, conversely, from which work can be extracted [58]. It is thanks to this new resource, that quantum engines could outperform their classical counterparts [39]. Moreover, since interactions can influence the different energy eigenstates, the energy distribution of a quantum system can be used to quantify its entanglement to the surrounding environment [59].

In the quantum world, baths themselves are not necessarily thermal. They still interact in an uncontrolled manner with quantum systems and therefore lead to stochastic terms in their

reduced evolutions but their states can be squeezed or with population inversion all of which can also be considered as new resources.

1.2.2 Quantum measurement

We have seen that coherences and entanglement can be used as tools to unlock new possibilities for quantum engines. Measurements performed on quantum objects, a.k.a., quantum measurements, can also unveil purely quantum effects.

The goal of measurements is usually simply to update our knowledge about a system's property. As we have seen in section 1.1.2, information already comes with thermodynamic consequences as it allows, for instance, to extract useful work at the cost of resetting the memory state. This is also the case when manipulating quantum systems and quantum engines which are making use of the information and are usually called quantum information engines.

However, for this information to be accessible, measurements outcomes must be encoded on macroscopic systems. The interaction chain from the quantum system to this macroscopic meter usually causes the final state of the quantum system to be different from its initial one. This evolution is usually not modelled and measurements are considered as instantaneous processes. From the early days of quantum mechanics, quantum measurements indeed need a specific treatement: "The Measurement Postulate". This postulate states that:

> The result of measuring a physical quantity must be one of the eigenvalues of the corresponding observable.

to which we should add Born's rule, telling us that the probability to obtain a specific value a_k for the observable associated to the operator $A = \sum_k a_k \left|v_k\right\rangle \left\langle v_k\right|$ is $\mathrm{Tr}(\rho^S A)$, with ρ^S the state of the system before the measurement. Right after the measurement, this state becomes $\left|v_k\right\rangle$. These rules describe the effect of ideal and instantaneous projective measurements. The term "projective" refering to the projection of the system state to one of the observable eigenstates.

Box 1.1: Projective and generalized measurements

Projective measurements

The projective measure or projection-valued measure (PVM) of a system of interest S of initial state ρ^S, given the set of positive semi-definite, Hermitian, orthogonal projection operators $\Pi_i = |i\rangle\langle i|$, with $\sum_i \Pi_i = \mathbb{1}$, leads to the outcome k and the final state $\frac{\Pi_k \rho^S \Pi_k}{\mathrm{Tr}(\Pi_k \rho^S)}$ with probability $\mathrm{Tr}(\rho^S \Pi_k)$. If the measurement outcome is not read, the final state reads: $\sum_k \Pi_k \rho^S \Pi_k$.

Generalized measurements or POVM

If we now add to the model an ancillary system A and let it interact with S before projectively measuring this ancillary system, the effect this will have on S can be more general than that of a PVM. Such type of measurement is called positive-operator-valued-measure (POVM). From Naimark's dilation theorem, they are a generalisation of PVM since any POVM can be seen as a PVM acting on a larger space. Given the initial state of the ancilla $\rho_A = \sum_j p_j |j\rangle\langle j|$, the unitary operator U and the measurement projective operators $\{\Pi_i = \Pi_i^e \otimes \mathbb{1}^S\}_i$; the evolution will be the following:

$$\rho_S \otimes \rho_A \to U\rho_S \otimes \rho_A U^\dagger \to \sum_i \Pi_i U \rho_S \otimes \rho_A U^\dagger \Pi_i \xrightarrow[\mathrm{Tr}_A]{} \sum_{i,j} p_j \langle i|U|j\rangle \rho_S \langle j|U^\dagger|i\rangle . \tag{1.5}$$

Defining the Kraus operators $M_{ij} = \sqrt{p_j}\langle i|U|j\rangle$, one retrieves similar output states as with PVM, i.e., $\frac{M_k \rho^S M_k^\dagger}{\mathrm{Tr}(M_k \rho^S M_k^\dagger)}$ for a read measurement of output k and $\sum_k M_k \rho^S M_k^\dagger$ for a unread measurement . Of course, in order for the probabilities to make sense, and thus to sum to one, one should have $\sum_{ij} M_{ij}^\dagger M_{ij} = \mathbb{1}$.

Importantly, we call "read measurement", or "selective measurement", measurements whose result is read which implies that information acquired is taken into account to update the post measurement state. "Unread" or "unselective" measurements however assume that the measurement outcome is not read and the final state therefore is in the mixed state corresponding to each of the possible measurement outcomes with their respective probabilities. The state resulting from an unread measurement therefore correponds to the average state of the read ones. A more general class of measurements, generalised measurements, include cases in which the system to measure first interacts with an ancillary system which is itself projectively measured (see Box 1.1 for more information about these measurements).

When the measurement output state is not the same as its input state, we speak of measurement backaction. In classical physics, an initially mixed state is also modified after a measurement because our state of knowledge is updated. However, in quantum physics, even without knowing the measurement outcome, the state of the system can still be affected which is a crucial difference. For instance, an initially pure state, i.e., a perfectly known state, will not necessarily end up in the same state after the measurement. Even more surprising, measuring

such a state can increase its Von Neumann entropy, if the outcome of the measurement is not read.

Quantum measurements are already a vast field with many pratical applications such as sensing, quantum error correction, measurement based quantum computing, feedback controlled quantum trajectories, quantum parameter estimation, to cite only a few. For more details about these possibilities, I invite the reader to dive into the book "Quantum measurement and control" [60].

In particular, quantum measurements are known for their ability to destroy coherences in the measurement basis. Coherences which, as we have seen before, can affect energy exchanges. This phenomenon could be viewed as a drawback since it sets a fundamental limitation on our capability to know the state of a quantum system [61]. However, as astonishing as it is, this induced backaction can also serve as a fuelling mechanism for quantum measurement engines [62].

1.2.3 Quantum heat: definition, nature and example

We know that measuring a quantum system can affect its state, except in the particular case in which the system is initially in one of the measurement eigenstates. As a result of this backaction, the energy of the system measured can also change.

Definition and example

Take for instance a qubit of Hamiltonian $H_S = \frac{\hbar\omega}{2}\sigma_z$ initially in the state $\rho^S_{t_0} = \left|\psi_0\right\rangle\left\langle\psi_0\right|$ with $\left|\psi^S_{t_0}\right\rangle = a_e\left|e\right\rangle + a_g\left|g\right\rangle$ and $\{a_e, a_g\} \in \mathbb{C}^2$. At the beginning, its average energy is thus $\frac{\hbar\omega}{2}(|a_e|^2 - |a_g|^2)$. However, if we measure this qubit in the $\{\left|e\right\rangle, \left|g\right\rangle\}$ basis, we will obtain, with probability $|a_e|^2$, the state $\left|e\right\rangle$ and thus the qubit will gain $\frac{\hbar\omega}{2}(1 - |a_e|^2 + |a_g|^2)$ of energy or, with probability $|a_g|^2$, the state $\left|g\right\rangle$ and thus the qubit will lose $\frac{\hbar\omega}{2}(1 + |a_e|^2 - |a_g|^2)$ of energy. Already at this stage it might be surprising to notice that upon reading the result of the measurement, one can change the energy of the system. Due to the stochastic nature of this energy change, reminiscent of the one induced by a thermal bath, it was named "Quantum heat" by Elouard *et al.* [63]. However, if we prepare the same initial state and repeat this procedure, the gain and loss will compensate each other and no energy will be given to the system on average. More generally, any projective measurement of operators Π_i commuting with the system's Hamiltonian will lead to a zero average quantum heat. Indeed, the average energy would be $\mathrm{Tr}(H_S \sum_i \Pi_i \rho^S_{t_0} \Pi_i) = \mathrm{Tr}(H_S \rho^S_{t_0})$, using the commutative property of the trace and the fact that $\Pi_i^2 = \Pi_i$. Therefore, measuring in a basis that commutes with a system's Hamiltonian cannot affects its energy on average .

However, if the measuring basis does not commute with the Hamiltonian, the system can gain or lose energy even on average. Given an system of Hamiltonian H^S and of pre and post

measurement state $\rho^S_{t_0}$ and $\rho^S_{t_m}$, respectively; the average quantum heat is defined as:

$$Q_h = \langle H^S \rangle_{\rho^S_{t_m}} - \langle H^S \rangle_{\rho^S_{t_0}} = \mathrm{Tr}\left(H^S \sum_i \Pi_i \rho^S_{t_0} \Pi_i \right) - \mathrm{Tr}(H^S \rho^S_{t_0}) \tag{1.6}$$

where $\{\Pi_i\}_i$ is the set of measurement operators.

For instance, coming back to our example, if the qubit starts in the ground state $|g\rangle$, i.e., if $a_e = 0$, and that we projectively measure it in the $\{|+\rangle, |-\rangle\}$ basis, the unread measurement output of this operation would be $\frac{|-\rangle\langle -|+|+\rangle|+\rangle}{2}$ thus raising the average energy by $\hbar\omega/2$ as depicted in Figure. 1.4.

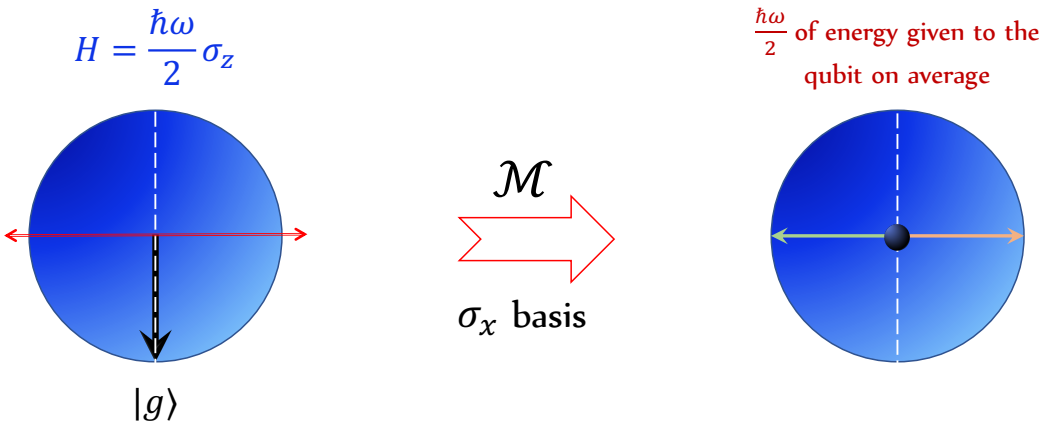

Figure 1.4: Exemple of a projective measurement induced energy exchange. Here by measuring the operator σ_x we can prodive $\hbar\omega/2$ of energy on average to the system given that it was initially in the ground state (black arrow) of its Hamiltonian $\frac{\hbar\omega}{2}\sigma_z$. The final state of the unread measurement is represented by the black sphere and the ones conditionned on obtaining a value $+1$ (in red) or -1 (in green) for the average of σ_x are arrows on the equatorial plane.

In general, measuring a system in a basis that does not commute with its bare Hamiltonian will change its average energy, except if the initial state is diagonal in the measurement basis. In other words, quantum heat is due to coherences of the initial system' state in the measurement basis and hence is a purely quantum phenomena.

Nature of the quantum Heat

The nature of the energy change between quantum systems is not settled in the quantum thermodynamic community. Inheriting classical views, one could want to use Clausius's second principle and Kelvin's no-go theorem in this regard. However, this implies defining effective temperatures to quantum system which we know can be strongly out of equilibrium and exhibit negative temperature among other such artifacts. These concerns have motivated the use of a

new, more agnostic fully quantum definitions to characterize the energy exchange within isolated (or closed) bipartite systems [64, 65]. In this spirit, we introduce a general framework to treat the energetics of bipartite quantum systems (See Chapter. 3.3.4).

Regarding the energy exchanged due to quantum measurements: quantum heat, a similar confusion reigns in the community. As an intrinsically irreversible process, leading to stochastic jumps, it can be classified as a new type of heat. But one can also set aside this denomination for thermal baths only and therefore identify the energy counterpart of backaction as work or introduce, there also, the notion of effective temperature (usually defined from the energy and entropy of the system).

Focusing on the first, fully quantum, step of the measurement, which can be shown to encompass all energy exchanges under reasonable constraints, we address this question of the nature of the quantum heat using our bipartite quantum energetics framework.

1.2.4 Quantum measurement engines

Understanding quantum measurements from a thermodynamic standpoint is one of the grand challenges of quantum thermodynamics, with strong fundamental and practical implications in various fields ranging from quantum foundations to quantum computing. Quantum measurement has a double status. On one hand, it is the process that allows the extraction of information from a quantum system [66]. In the spirit of classical information thermodynamics, its “work cost" was thus quantitatively analysed as the energetic toll to create correlations between the system and a memory [67, 68, 69]. On the other, quantum measurements also leads to wavefunction collapse. Measurements can thus behave as a source of entropy and energy, playing a role similar to a bath.

Even if it was not analyzed as such at the time, the first proposal for a quantum measurement engine using measurement backaction can be found in the work of Kim *et al.* [70] if the wall insertion, necessary to split in two a box containing a single quantum particle, is interpreted as being part of the measuring procedure. Since then, such quantum measurement engines were extended to the measurement of internal degrees of freedom of the quantum particle in combination with a feedback protocol [71, 72], without feedback on a spin-$1/2$ interacting with a single bath and undergoing adiabatic transformations [73, 74], with a bipartite working substance interacting between two thermal baths as a refrigerator [75] or with a single bath in a heat engine regime [76]. The realization that measurements can act as an energy source is crucial because, it provides a new, purely quantum, resource to fuel quantum engines not only due to the information they provide but also by the effect they directly have on the measured systems [77]. This changes our viewpoint on quantum measurements from mere tools to new types of processes. And the possibilities offered by quantum measurement are numerous, ranging from weak, to strong projective measurements, destructive or indirect ones, and with all possible measurement basis. Moreover, quantum measurement engine prove to be excellent platforms to study and characterize quantum measurements, which are themselves at the heart

of the many discrepancies between interpretations of quantum physics [78].

A simple an pedagogical example, first introduced by Elouard *et al.* [71], is the following. Consider a qubit with Hamiltonian $H_0 = \hbar\omega \left|e\right\rangle \left\langle e\right|$, interacting with a field modelled classically via $i\frac{\hbar\Omega}{2}(\left|0\right\rangle \left\langle 1\right| e^{i\omega_o t} - \left|1\right\rangle \left\langle 0\right| e^{-i\omega_o t})$ with Ω the Rabi frequency. If the qubit starts initially in the $\left|+\right\rangle$ state, its states will rotate under the influence of the drive reaching the state $\left|g\right\rangle$ after a duration $\pi/(2\Omega)$. At this stage, the qubit would thus have lost $\hbar\omega/2$ of energy compared to its initial state. Of course, this energy lost to the driving field will would be retrieved if we wait again for the same amount of time. However, if we projectively measure the state of the qubit in the $\{\left|+\right\rangle, \left|-\right\rangle\}$ basis much before it reached $\left|g\right\rangle$ for the first time, i.e., when the qubit is in the state $\cos(\theta)\left|+\right\rangle - \sin(\theta)\left|-\right\rangle$ with $\theta \ll \pi/2$, the qubit would already have given the energy $E_+ = \hbar\omega\cos(\theta)\sin(\theta)$ to the field and there is a probability $P_+ = \cos^2(\theta)$ finding the qubit back in the $\left|+\right\rangle$ state in which case this work can be extracted over again. Of course, there is also a probability $P_- = \sin^2(\theta)$ of finding the qubit to the state $\left|-\right\rangle$. In this case, one can freely rotate it back to $\left|+\right\rangle$ and extract energy again. This feedback operation however, requires the knowledge of the measurement result and the cost of the memory erasure should also be taken into account. Nevertheless, if the angle θ is small enough, i.e., if the duration of the evolution before the measurement is very short, one can provide energy to the field without any feedback operation. Indeed, without the knowledge of the measurement outcome, upon interaction with the field for the same short duration after the measurement, this field would gain the energy $P_+E_+ - P_-E_+ = \hbar\omega(\cos^2(\theta) - \sin^2(\theta))\cos(\theta)\sin(\theta) \approx \hbar\omega\theta > 0$. Making use of the quantum Zeno effect the state stabilization would ensure to find the qubit in the $\left|+\right\rangle$ state with near certainty. However, one would still need feeback operations to operate this engine in a steady state regime since, after many repetition of the evolution and unread measurements steps, the qubit will switch to the $\left|-\right\rangle$ state from which it will keep on loosing energy on average until the, equally unlikely event, of switching back to the measurement output state $\left|+\right\rangle$ occurs.

While it is possible to combine the backaction and information resources provided by quantum measurement, it is also possible to involve thermal baths. Buffoni *et al.* proposed such a measurement engine where two thermal bath are involved to build an engine but also a refrigerator [75].

1.2.5 Origin of the quantum heat

Of course, if measurements can be used to provide energy to a working substance in order to fuel an engine, it means that they can also have a cost.We already know, thanks to the pionnering works of Landauer, Bennett and Szilard [79, 27, 26], that resetting the state of any system acting as a memory can be costly. And, since what is meant by measurement is the act of imprinting some information about a given system's state onto another physical system's state, this erasure operation is always necessary in order to restore that other physical system's state to its original one. In the case of a degenerate memory, i.e., a memory on which information is

encode on states which have the same bare average energy, this erasure cost will be purely due to the change of entropy of the meter system acting as a memory. However, in pratice, the meter system can be of any kind, such as a cavity field, and thus can have non-degenerated energy levels. In this more general case, pioneering works have found a bound on this resetting cost. Combined to the cost of making the measurement, i.e., creating correlations and projectively measuring the meter system, it was shown that the total measurement cost is proportional to the QC-mutual information between the meter and the system [80, 68]. This means that it is possible to perform a measurement at no energetic cost, but only if no information was extracted in the process: we only pay for what we gain. The nature of this cost is one of the central questions of this thesis. Indeed, the energy of quantum measurement can be fully extracted in Maxwell demon type experiments and results from the interaction with a classical object pointing toward a work interpretation, however they result in stochastic jumps and lead to entropy change of the measured system, properties usually associated with heat exchanges.

We point out that it was recently argued that unbiased, faithful and non-invasive measurements would require infinite resources [81]. This claim is based on the third law of thermodynamics which prevents us from rigourously preparing pure states. It can also be understood as coming from the fact that projective measurements would need infinite resources to be performed. This important realization should however not be confused with an energetic cost. Indeed, whilst it is true that obtaining a pure state from a projective measurement would require infinite resources: via the interaction with an infinitely large meter or a meter in an initially pure state; this resource cannot be considered as a cost since it is not used nor consummed, i.e., most of it remains in the final state and does not have to be provided to reset the state of the meter.

This is however a hint regarding the perculiarity of quantum measurements. The measurement postulates of quantum physics, which tell us which output states and outcomes result from a measurement, assume idealistic projective measurements whose dynamics is not described within the quantum formalism. The definite outcome of projective measurements is only justified by a quantum to classical cut, i.e., by the interaction of quantum systems with a classical system which forces a specific result to emerge since it cannot be in a state of superposition. This gap in our understanding of quantum measurements, and therefore of the quantum to classical interface, has been fascinating physicists and philosophers for more than thirty years. It is at the heart of the many interpretations of quantum physics to which Box. 1.2 is dedicated. Currently, we understand that from the interaction with the environment, some "pointer states" are naturally selected which are the ones that are stable under these interactions. This "einselection" consitutes the natural basis upon which the information about the system is encoded on the meter system. This is Zurek's famous Quantum Darwinism [82, 83]. However, this does not explain by which dynamical evolution do the quantum states always seem to pick one of them in the end, i.e., the problem of definite outcome. The collapse of the wavefunction to a specific pointer state is still puzzling us [84].

Box 1.2: **Interpretations of quantum physics**

There are many different ways to view and understand the measurement problem and the main current interpretations of quantum physics provide different insights on it [85]. These interpretations include: Bohmian mechanics [86], Many world and Everttian interpretations, an ontologic interpretation based on the notions of Contextual Objectivity (CSM) [87] and Relational quantum mechanics [88].
A list of the requirements imposed on any potential solution was proposed recently [89]. This puzzle goes deep into the question of the wavefunction's nature; does it describe the physical state of an object or just the knowledge a certain observer has of it? Some physicists do not think that there is a measurement problem and even argue that "there is not real state of a physical system" [90].
On the experimental side, the manipulation of always larger objects with quantum properties, the description of many of which can be found in the last section of [91], offers great opportunities towards testing some of the proposed measurement dynamics such as those given by Ghirardi-Rimini-Weber (GRW) and Continuous Spontaneous Localization (CLS) stochastic collapse theories.

Since the external measuring apparatus is not included in the modelling, this could be a dead end for our quest towards the origin of the quantum heat. Indeed, even when introducing a quantum meter, at some point, we always invoke a classical device to projectively measure its state. This separation between the quantum and classical modelling is usually refered to as the "Heisenberg cut". The encounter of this frontier by a quantum system is associated with an intantaneous and stochastic "collapse" of its wavefunction.

Pre-measurement and classical measurement

Hopefully, at lot can already be said about quantum thermodynamics without collapse, i.e., about the thermodynamics exchanges between quantum systems at the average level. In this spirit of we can decompose a quantum measurement into two steps:

- A pre-measurement step in which the measurement system is interacting with a quantum meter. By choosing the interaction operator appropriately correlations are getting built in the desired basis between the system and the meter. The resulting decoherence of the reduced state of the system consitutes the average backaction effect.

- Once the quantum meter and the system are correlated, one should projectively measure the quantum meter itself with a larger, classical, meter. This operation will thus project the meter' state and thus the system' state correspondingly. The quantum to classical cut is necessary only for this step.

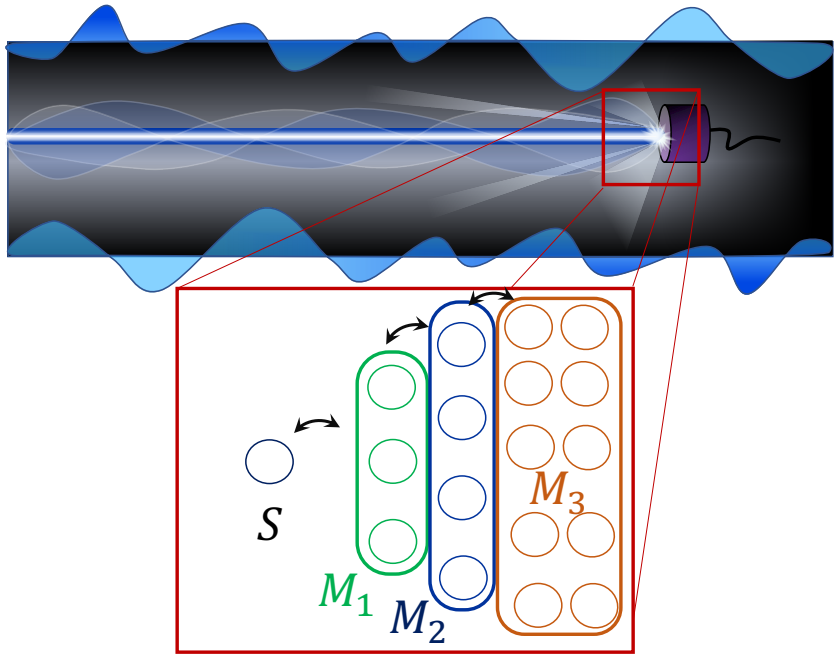

Figure 1.5: Von Neumann measurement chain: Case of a photodetector. Top pannel: a light field colliding with photodectector. Bottom pannel: Representation of the measurement chain. The dark double arrow symbolizes the interaction taking place between the system S and the first part of the meter: M_1, as well as with its neighbouring part M_2 and last part M_3

As a result of this decomposition, a measurement $\mathcal{M}$ is fully characterised by the unitary evolution corresponding to the pre-measurement U, the Hilbert space of the meter system $\mathcal{H}_{\mathrm{M}}$, the initial state of meter $\left|\psi_0^M\right\rangle$ and the pointer observable Z_M used to projectively measure it in the end. The last step is considered instantaneous due to the interaction with the classical world but the decoherence as well as the storage of information about the system' state in the meter is already encompassed in the first, quantum, step. One could, of course, apply the same reasonning to the classical measurement of the meter system, invoking a second meter system and so on and so forth. This would allow to shift always further the quantum to classical limit, i.e., Heisenberg limit. This is exactly the idea behing Von Neumann's measurement chain pictured in Fig. 1.5. While this opens a wide range of possibilities, one should not forget that it does not remove the need of a final classical measurement at the end to select a single measurement result.

As we will show in Section. 4.1.3, under some reasonable conditions, it is possible to witness all the energy exchanges in the first, pre-measurement, step. Our approach therefore moves from the standart paradigm of projective measurements. As depicted in Figure 1.6, in order to analyse the energy exchanges associated to a quantum measurement, we study of the pre-measurement process, first governed by a time dependent Hamiltonian (Chapter. 3 and 4) and then in a fully autonomous manner (Chapter 4).

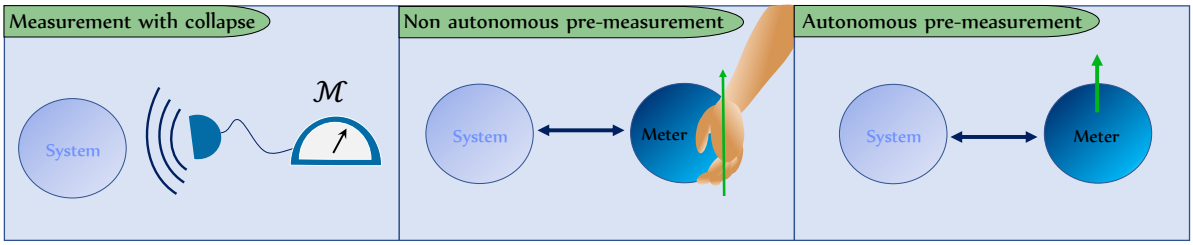

Figure 1.6: Quantum Measurement: Depiction of the measurement procedure as an interaction with a classical meter causing an instantaneous collapse of the wavefunction (left). The pre-measurement part of this measurement can be analyzed in a non-autonomous way with a classical degree of freedom used to generate a time dependent Hamiltonian (middle). A fully quantum modelling of the pre-measurement process is possible with an interaction strength between the system and the quantum meter that is position dependent. The green arrow represent the motion of the meter which could equivalent be the one of the measured system.

Studying the dynamic of closed quantum systems might seem trivial and easy but, to understand the fueling mechanism of measurement powered engines, one should remember that the measured operator should not commute with the Hamiltonian of the system. This means that the system state will evolve while it is measured. As generalized by the Wigner-Araki-Yanase (WAY) theorem and detailed in Box 1.3, backaction and ideal measurement are thus incompatible, even starting with pure initial states. By studying the pre-measurement we will characterize the nature of the associated energy fluxes and their relation to the quality of the measurement.

Box 1.3: **WAY theorem**

An ideal quantum measurement is defined by the following properties [81]:

- accurate, which means that, for all eigenstates of the measured observable $\mathcal{O}_S$, $\left|e_i^S\right\rangle$, and for the initial state of the meter $\left|\psi_0^M\right\rangle$ we have $\left|e_i^S\right\rangle \otimes \left|\psi_0^M\right\rangle \xrightarrow{U} \left|e_i^S\right\rangle \otimes \left|z_i^M\right\rangle$ upon the unitarity evolution U, given that $\{\left|z_i^M\right\rangle\}_i$ is the eigenbasis of the measurement operator Z_M,
- sharp, i.e., projective and thus leading to a single value,
- repeatable meaning that we would obtain the same outcome by performing immediatly the same measurement again.

A measurement verifying all these ideal properties is called a Von Neumann-Lüders' measurement. As first noticed by Wigner in 1954 [92, 93], such an ideal measurement cannot always be performed. It is the case if the system observable to be measured, $\mathcal{O}_S$, does not commute with a conserved quantity N, which acts on the system and/or meter. Indeed, when the unitary operator U, governing the state evolution of the system and meter, is such that $[N, U] = 0$ and that $[\mathcal{O}_S, N] \neq 0$, only an approximated measurement of $\mathcal{O}_S$ can be obtained with an error decreasing as the meter size increases [93, 61, 94]. This theorem is still valid if the repeatable condition is replaced by the Yanase condition which states that the matrix Z_M made of the pointer states of the meter $\left|M_i\right\rangle$ with $i \in [0, n]$, n being the number of such pointer states, must commute with the conserved quantity: $[Z_M, N] = 0$. This condition ensures that the no-go theorem about the measurement of the system's observable does not propagate to the measurement of the meter pointer observable (see [95, 96] for an historical aspects and extensions).
To better understand this theorem, consider an observable $\mathcal{O}_S$ which does not commute with the Hamiltonian associated to the unitary evolution U. The measurement of this observable cannot be accurate since its average value will evolve during the pre-measurement step such that $\mathrm{Tr}(\mathcal{O}_S \rho_0^S) \neq \mathrm{Tr}(\mathcal{O}_S U^\dagger \rho_0^S U)$, where ρ_0^S is the initial state of the system.

1.3 Outline of the thesis

Quantum measurements are at the heart of my personal contribution towards elucidating these problems, and, therefore, of this whole manuscript. Firstly, we proposed a new quantum measurement engine, the first such engine to work with a bipartite system and to make use of entanglement between its parts. This theoretical platform turned out to be ideal to investigate the energetic counterpart of measurement backaction. By modelling the pre-measurement step we gained deeper insights into the source of the extracted quantum heat, i.e., the average energy change of the system due to the measurement.

Pushing this analysis further, we imagine, a new thought experiment in which a flying qubit is sent to interact dispersively with the field within a cavity. Their interaction is chosen such that the field effectively measures the qubit state thereby implementing an autonomous measurement. In this framework, we investigate the energy and information exchange between the kinetic degree of freedom, the field and the qubit. The quantum heat can be non-zero on average if the measurement occurs in a basis that does not commute with the bare Hamiltonian of the qubit. This energy is shown to come from the kinetic degree of freedom, thereby acting as a work source to fuel the measuring process.

We then change perspective and study the resources needed to perform a good measurement. More specifically, in a circuit QED setup we witness the backaction and mutual information obtained when measuring a qubit embedded in a cavity using different input field states. The field acts as a meter and we show that thermal and coherent statistics can lead to similar performance of the measurement.

Chapter 2

Energetics of a bipartite quantum system

Contents

AS DISCUSSED in the introduction, quantum coherence effects have lead to a refinement of our understanding of the second law of thermodynamics and the way to apply it to quantum systems. The distinction, made by the first law, between heat and work energy exchanges also has to be interpreted in quantum terms. In this section, I introduce a formalism to address this need in the case of a bipartite closed quantum system and motivate it via some examples.

2.1 Classical heritage

In its most complete formulation, classical thermodynamics is governed by five fundamental laws. The zeroth one states that thermal equilibrium is a transitive property. The first and second laws, respectively, that the total energy of an isolated system is a conserved quantity and that the entropy of such a system can only increase (or stay constant) with time. The third law sets the minimum value of thermodynamic entropy to that of a pure state at a absolute zero temperature (in Kelvin) which is taken to be zero. And last but not least, there is the fourth law, i.e., Onsager's relations, that governs the non-equilibrium flow and force reciprocities.

Coming back to the first law, as Clausius first noticed, the change in energy of a closed system ΔU can be split into a heat Q and a work W contribution (here, unlike Clausius, we choose to count them both as positive when entering the system) such that:

$$\Delta U = Q + W, \tag{2.1}$$

where heat is the part of energy exchange that is associated with a change of entropy of the system of interest whilst work involves no such changes. In classical physics, the energy exchanges with/between bath(s) is counted as heat whereas work is associated to well-controlled

and reversible energy flows such as the one induced by a conservative force. Of course, average energy conservation remains valid in the quantum realm but the splitting between heat and work becomes far from trivial. If we take a quantum system S of initial state ρ_S interacting with an environment E of state ρ_E via a global unitary evolution U, by tracing over the environment, the effect this evolution has on the quantum system writes:

$$\rho_S \to \mathrm{Tr}_E(U\rho_S \otimes \rho_E U^\dagger). \tag{2.2}$$

Some of our classical intuitions can hence be retrieved. For instance, when the environment is a thermal bath, the energy change of the system comes in the form of heat [97, 98, 99]. Conversely, when the unitary evolution only acts on the system: $U = U_S \otimes \mathbb{1}_E$, the entropy of the system remains unchanged and it can only receive work [22].

Outside of these two consensual cases, depicted in the first panel of Fig. 2.1, the nature of the energy exchange between two quantum systems is still not settle and consensual in the community.

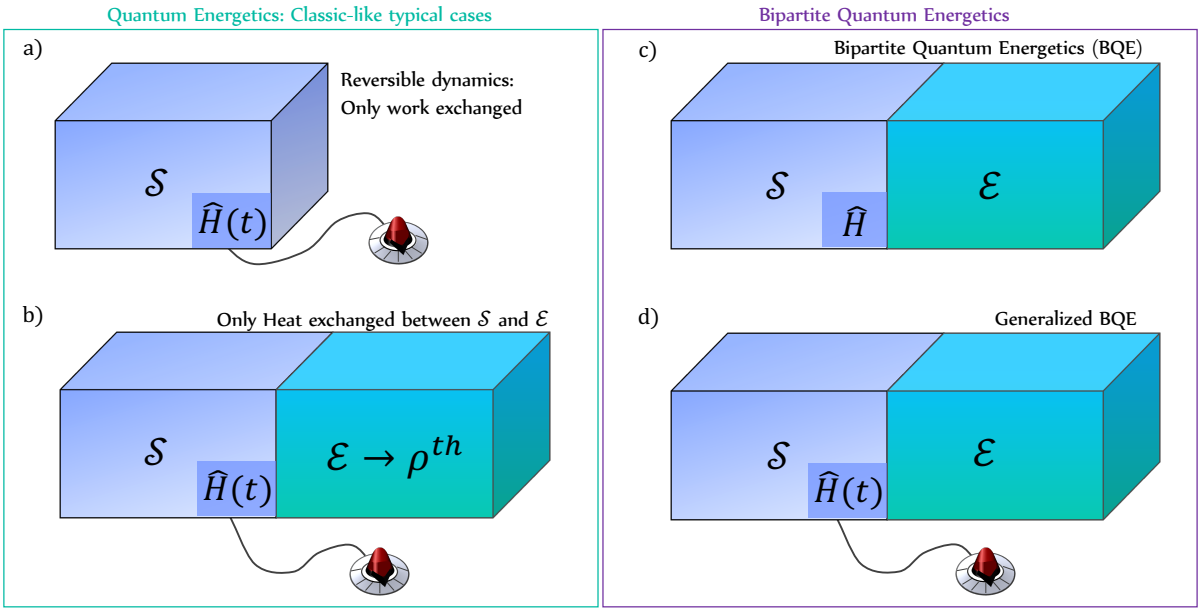

Figure 2.1: Typical classical-like situations in which a quantum system interacts with a classical environment are depicted in the left box. a) When a quantum system is closed that its Hamiltonian is monitored by external classical drive its evolution is unitary and it only exchanges work with its environment. b)When this system is in contact with a bath the energy exchanged with it is only in the form of heat. The bipartite quantum energetics formalism allows to characterize the energy exchange between two quantum systems, when the total Hamiltonian is time independent c) or time-dependent d)

2.2 A difficult quantum transposition

One reason behind this ongoing puzzle is that thermal baths are not the only environments capable of changing a system's entropy. For instance an electron spin interacting with a collection of nuclear spins can sees its entropy increase while undergoing a rotation of its quantization axis, therefore this environment acts as a source of heat and work at the same time. Similarily, a qubit resonantly interacting with a small coherent field can see its state rotate but the entanglement with the field state implies a increase of the qubit entropy as well. As a result, heat and work sources are often coming together when dealing with quantum systems and there is still no consensus about a unified way to distingush them especially when dealing both with classical and quantum systems. However, it is still important to sort them out because the nature of the energy exchange determines their reversibility and thus quality. Inheriting from the classical world the understanding that heat is a degraded form of energy, one can argue that it is not as costly to ask for a heat source than for a work source, which is a key point of view of quantum resource theory [100]. A mainstream approach to unravel these quantities is to associate the heat to a change of the system' state and work flux to a change of the Hamiltonian [101]. Work would therefore be, for instance, the energy given to a system when its energy levels are moving while their population, and with them the system's entropy, stays constant.

This definition is appreciabily simple and intuitive. For instance, when considering a system only evolving under a time changing Hamiltonian, it implies that the system only exchanges work with its environment. Likewise, a quantum system interacting with a weakly coupled thermal bath and with a time-independent Hamiltonian is found to only exchange heat with its environment. However, the Hamiltonian one considers is sometimes ambiguous. Take for instance two qubits A and B interacting via a time-independent coupling term V^{AB}. If we try to quantify the work and heat received by one qubit, should we include this coupling in the qubit Hamiltonian or not? And, if all terms in the Hamiltonian are time-independent, no work should be transfered between the qubits since, no matter if we include the coupling term in H or not, its derivative will always be zero and hence the work received by this subsystem. However, a coupling such as $V^{AB} = V^A \otimes V^B$ where V^A commutes with H^A but V^B not commuting with H^B would be expected to imply some work exchange with qubit A since its energy could change but its entropy will not. Thus, if we want to characterize the nature of the energy exchange between two quantum systems, one needs to complete these initial ideas. Even if many different definitions are known [101, 64, 102, 103, 104], there is not yet a general agreement on a mathematical definition that would apply to all quantum systems [105]. This question is even more important that it could have a crucial impact on the fundamental bounds to the energy consumption of quantum information processing which is becoming a vivid topic of research [106]. As was recently shown, this energy expenditure could rapidly come out of reach with the growth of quantum computers and whereas the work invested could possibly be retrieved, the heat part can never be completely recovered [107].

2.3 Bipartite quantum energetics (BQE)

We have been developping a general framework to answer these questions building on previous ideas [64, 108]. In this manuscript, I use the following definitions to characterize the energy exchanges with and within a fully quantum bipartite system that I will refer to as "Bipartite quantum energetics": BQE.
If we consider a bipartite system made of two interacting subsystems A and B the state of this full system can always be written as:

$$\rho^{AB}(t) = \rho^{A}(t) \otimes \rho^{B}(t) + \chi^{AB}(t), \tag{2.3}$$

where $\rho^{A}(t)$ and $\rho^{B}(t)$ are the reduced state of A and B respectively and $\chi^{AB}(t)$ is called the correlation matix, encoding all correlations between these subsystems and defined as $\chi^{AB}(t) = \rho^{AB}(t) - \mathrm{Tr}_{B}(\rho^{AB}(t)) \otimes \mathrm{Tr}_{A}(\rho^{AB}(t))$. This bipartite system is closed and even thermally isolated and evolves under its time-dependent Hamiltonian:

$$H^{AB}(t) = H^{A}(t) + H^{B}(t) + V^{AB}(t) \tag{2.4}$$

with H^{A}, H^{B} the bare Hamiltonians of the subparts and V^{AB} their interaction operator. The chosen definitions of heat and work, are based on the realization that the reduced equation of motion of subsystem A can be written as:

$$\frac{d}{dt}\rho^{A} = -\frac{i}{\hbar}[H^{A}, \rho^{A}] - \frac{i}{\hbar}\mathrm{Tr}_{B}([V^{AB}, \rho^{AB}]) \tag{2.5}$$

where the time dependence is kept implicit. By using Eq. (2.3), we obtain:

$$\frac{d}{dt}\rho^{A} = -\frac{i}{\hbar}[H^{A} + \mathrm{Tr}_{B}(V^{AB}\rho^{B}), \rho^{A}] - \frac{i}{\hbar}\mathrm{Tr}_{B}([V^{AB}, \chi^{AB}]) \tag{2.6}$$

where we can already see that some part of the interaction term can contribute to the unitary part of the dynamics of ρ^{A}. In the following we will denote this effective interaction, which is related to the Lamb shift, as $\mathcal{V}^{A} = \mathrm{Tr}_{B}(V^{AB}\rho^{B})$. Importantly, we do not include it in the definition of the internal energy of the subsystem A which simply writes:

$$\mathcal{U}_{A}(t) = \mathrm{Tr}_{A}(H^{A}\rho^{A}). \tag{2.7}$$

The time derivative of this energy can then be divided into an internal work flux $\frac{d}{dt}\mathcal{W}_{A}$ and a heat flux $\frac{d}{dt}\mathcal{Q}_{A}$by inserting Eq. (2.6) into the derivative of Eq. (2.7). It results that:

$$\frac{d}{dt}\mathcal{W}_{A} = -\frac{i}{\hbar}\mathrm{Tr}_{A}([H^{A}, \mathcal{V}^{A}]\rho^{A}) = -\frac{i}{\hbar}\mathrm{Tr}_{AB}([H^{A}, V^{AB}]\rho^{A} \otimes \rho^{B}) \tag{2.8}$$

$$\frac{d}{dt}\mathcal{Q}_{A} = -\frac{i}{\hbar}\mathrm{Tr}_{A}\left(\mathrm{Tr}_{B}\left([V^{AB}, \chi^{AB}]\right) H^{A}\right) = -\frac{i}{\hbar}\mathrm{Tr}_{AB}\left([H^{A}, V^{AB}]\chi^{AB}\right). \tag{2.9}$$

where we used the fact that $\mathrm{Tr}_{AB}\left(H^A[V^{AB},\chi^{AB}]\right) = \mathrm{Tr}_{AB}\left([H^A,V^{AB}]\chi^{AB}\right)$ from the cyclic property of the trace. With completely symetric definitions for the heat and work rates with respect to the subsystem B, we can also split the change of energy of the subsystem B in work and heat fluxes. In the most general case in which the bare Hamiltonian $H^B(t)$ is time dependent the change of energy of the subsystem B writes:

$$\frac{d}{dt}\mathcal{U}_B = \frac{d}{dt}\mathcal{W}_B + \frac{d}{dt}\mathcal{Q}_B + \frac{d}{dt}\mathcal{W}_B^{\mathrm{ext}} \tag{2.10}$$

where $\frac{d}{dt}\mathcal{W}_B^{\mathrm{ext}}$ is the external work flux done on the subsystem B by an external operator and defined as:

$$\frac{d}{dt}\mathcal{W}_B^{\mathrm{ext}}(t) = \mathrm{Tr}_B\left(\frac{dH^B}{dt}\rho^B(t)\right). \tag{2.11}$$

Notice here that we rather use the infinitesimal variation of heat and work, which we call fluxes, than their integrated counterpart because work and heat are path-dependent quantities and thus need the full state history in order to be computed.

With the addition of the external works, which are the work done by the external environment due to the possible time-dependence of the bare Hamiltonian and interaction term, we have all the contribution to the change of energy of the subsystems. However, given the chosen definition of internal energy of Eq. (2.7), the total energy of the bipartite system is not simply the addition of the internal energy of each subsystem. There is an additional energy contribution which comes from the interaction between the two subsystems. This energy is called interaction energy and it is defined as $\mathcal{V}_{AB} = \mathrm{Tr}_{AB}(V^{AB}\rho^{AB}(t))$. Making use again of the decomposition of Eq. (2.3), this term can also be split in a part due to the correlations $\mathcal{V}_{AB}^{\chi}$ and a part which is not, $\mathcal{V}_{AB}^{\otimes}$. Eventually we obtain the following first law for the total bipartite system :

$$\frac{d}{dt}\mathcal{U}_{AB} = \frac{d}{dt}\mathcal{U}_A + \frac{d}{dt}\mathcal{U}_B + \frac{d}{dt}\mathcal{V}_{AB} \tag{2.12}$$

given that the total energy is $\mathcal{U}_{AB} = \mathrm{Tr}_{AB}(H^{AB}\rho^{AB}(t))$. At this stage, it is very important to notice the crucial difference between this interaction energy $\mathcal{V}_{AB}$ which is a number and the effective interaction operator $\mathcal{V}^A$, resp. $\mathcal{V}^B$, which acts on the subsystem A, resp. B. In this manuscript, we will always use subscript for energetic quantities and other real values and superscript for density matrix and operators.

Based on these definitions, which are agnostic regarding the nature of the quantum system A and B, we find the generalized work, generalized heat, and external work balance equation:

$$\begin{aligned} 0 &= \dot{\mathcal{W}}_A + \dot{\mathcal{W}}_B + \dot{\mathcal{V}}_{AB}^{\otimes} \\ 0 &= \dot{\mathcal{Q}}_A + \dot{\mathcal{Q}}_B + \dot{\mathcal{V}}_{AB}^{\chi} \\ 0 &= \dot{\mathcal{W}}_A^{\mathrm{ext}} + \dot{\mathcal{W}}_B^{\mathrm{ext}} + \dot{\mathcal{V}}_{AB}^{\mathrm{ext}} \end{aligned} \tag{2.13}$$

as represented in Fig. 2.2

Interestingly, we can already notice that two interacting qubits can, for instance, exchange generalized heat by getting correlated. This feature is consistent with our classical intuitions, since, from these correlations, the entropy of their reduced state can change.

Since discussions are still ongoing in the quantum thermodynamic community regarding heat and work and the case in which it is legitimate to use these terminologies,we chose to call the two different energy terms we defined: generalized heat and generalized work to avoid any confusions. If, by simplicity, I use the terms heat and work in this thesis, it will always refer to the BQE quantities defined in this chapter from now on. A summary of the definition given above is provided in Fig. 2.2 where the external work done on the interaction energy is defined

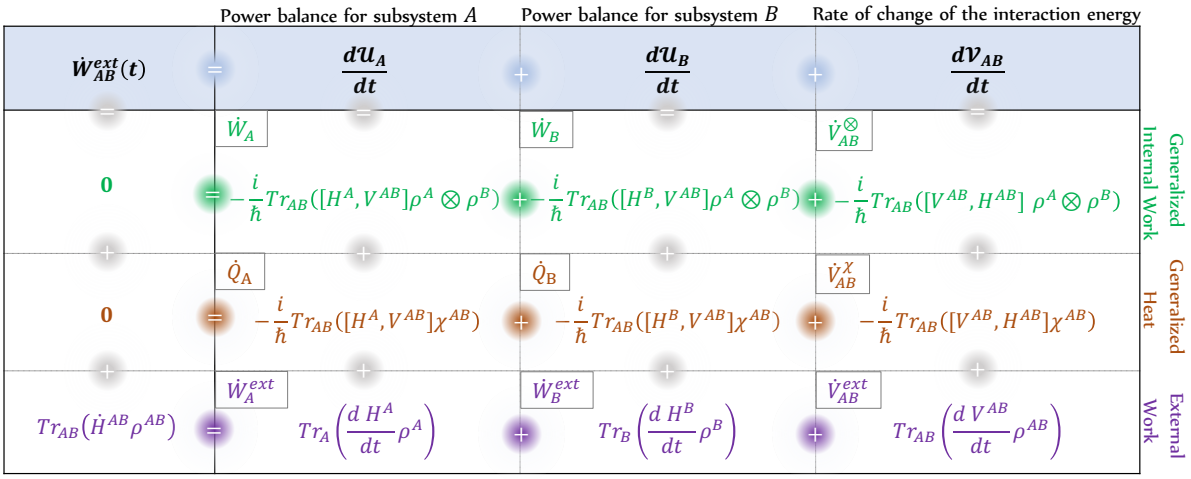

Figure 2.2: Bipartite quantum energetics (BQE) definitions. All time dependence are implicit to keep the expression concise. All lines and columns sum verify the equation indicated by the signs in between cells.

as:

$$\frac{d}{dt}\mathcal{V}^{\text{ext}}_{AB}(t) = \text{Tr}_B\left(\frac{dV^{AB}}{dt}\rho^{AB}(t)\right). \tag{2.14}$$

2.4 Examples

We now apply the definitions summerized in Fig. 2.2 to several typical examples. We consider that at time t_0^-, there is no energy exchanges of any king occuring and that at time 0 the full system starts evolving under H^{AB} (possibly time dependent). Therefore, if an energetic flux is null at every time it implies that the corresponding integrated quantity is also null.

2.4.1 Fully commuting interaction

When the bare Hamiltonian H^A and H^B both commute with V^{AB}, i.e.,:

$$[H^A, V^{AB}] = [H^B, V^{AB}] = 0, \tag{2.15}$$

this implies that all internal work flux and heat flux are zero. This will be the case, for instance, in the chapter 5 of this manuscript where a qubit is dispersively measured by a cavity field under the full Hamiltonian $\hbar\omega_{qb}\sigma_z + \hbar a^\dagger a + \hbar\frac{\chi}{2}\sigma_z \otimes a^\dagger a$.

The only possible energy changes will therefore happend at the frontier of the bipartite system, if the Hamiltonian is time dependent. This energy can only be in the form of work, since it does not affect the entropy of the global system nor of each subsystems. In this case, the only non-zero instantenous flux are such that:

$$\mathrm{Tr}_{AB}(\dot{H}^{AB}\rho^{AB}) = \mathrm{Tr}_A(\dot{H}^A\rho^A) + \mathrm{Tr}_B(\dot{H}^B\rho^B) + \mathrm{Tr}_{AB}(\dot{V}^{AB}\rho^{AB}), \tag{2.16}$$

i.e.,

$$\dot{W}^{ext}_{AB} = \dot{W}^{ext}_A + \dot{W}^{ext}_B + \dot{V}^{ext}_{AB}. \tag{2.17}$$

2.4.2 Conservation of the local energies

When the sum of the bare Hamiltonians $H^A + H^B$ commute with H^{AB} but not each of them individually, i.e.,:

$$[H^A + H^B, V^{AB}] = 0, \tag{2.18}$$

as for resonant Jaynes Cummings interaction, the interaction energy remains constant and the two subsystems can only exchange equal and opposite heat and work. We therefore have:

$$\dot{W}^A = -\dot{W}^B \quad \text{and} \quad \dot{Q}^A = -\dot{Q}^B. \tag{2.19}$$

In the next chapter, we consider a two qubit system. If we assumed the bare frequencies of these qubits to be equal, we would be in this situation.

2.4.3 Partially commuting interaction

When only one of the bare Hamiltonians, H^B for instance, does not commute with V^{AB} and that both bare Hamiltonians are taken time independent, i.e.,:

$$[H^A, V^{AB}(t)] = 0 \quad \text{and} \quad [H^B, V^{AB}(t)] \neq 0. \tag{2.20}$$

It is for instance the case when we use a system B to measure an operator that commutes with the bare Hamiltonian of a system A. The system A will not receive any heat and work and therefore its energy stays constant. No quantum heat will be involved in this case but the meter, i.e., the system B, can exchange heat and work with the interaction energy.

In the opposite case, when a system is measured in a basis that does not commute with its bare Hamiltonian but which does commute with the bare Hamiltonian of the meter, the information is therefore encoded in the relative phases of the meter state which should thus not start in an energy eigenstate. In this situation quantum heat can arise and the energy of the meter system is not changing. At the end of this interaction, i.e., when $V^{AB}(t) = 0$, projectively measuring the meter state will not induce any generalized heat flux nor work flux. Therefore, the information will be extracted from the quantum meter without affecting neither the total average energy of AB nor the individual ones. This case will therefore be of special interest in this manuscript.

Exploiting this useful feature, we will now focus on the specific exemple of a two qubit system measured by a third meter qubit to characterize the involved quantum heat. Before moving to our fourth chapter in which the measurement process is made autonomous, we will generalize our conclusions to a subset of partially commuting interaction of the type $V^{AB} = V^{A}(t) \otimes V^{B}(t)$.

Chapter 3

Energetics of a pre-measurement

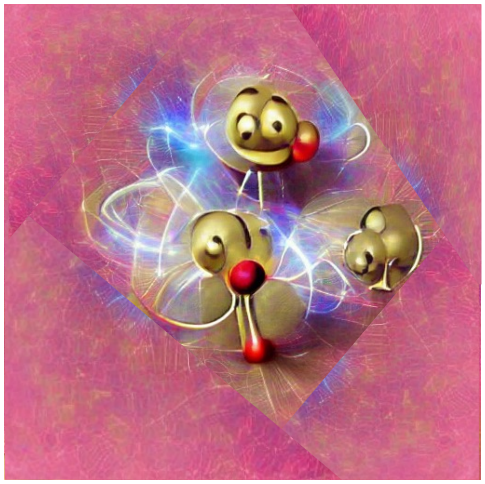

Generated using the artificial intelligence method VGLAN + CLIP

Contents

Some of this chapter content was published in:

Léa Bresque, P. A. Camati, S. Rogers, K. Murch, A. N. Jordan, and A. Auffèves, *Two-Qubit Engine fuelled by Entanglement and Local Measurements.* Phys. Rev. Lett. 126, 120605 (2021).

Editor's suggestion, reported in INP communication and phys.org.

QUANTUM MEASUREMENT ENGINES are ideal plateforms to study the energetics of quantum measurements [78]. In this chapter, we focus on and extend the pre-measurement analysis of such an engine that we proposed recently [109].

At the average level, focusing on the pre-measurement step is enough to access the energy exchanges. During this step, a qubit quantum meter M is introduced and the interaction is chosen such that it will become correlated to the system S. Since the classical projective measurement of this degenerate meter will not affect the reduced state of the system nor the one of the meter on average, no more energy exchanges will be missing in our description. Building on this convenient fact, we can now ask ourselves the following questions:

- When a measurement is giving (or receiving) energy to a quantum system on average, where does this energy comes from (or go to)?
- Should this energy change of the system be considered as heat or work?
- How much energy can be extracted from imperfect measurements ?

A naive answer to the first question would be that: it is the meter that provides this missing energy. But what if the quantum meter only has degenerate energy levels ? Then it is clear that its energy cannot change and the question becomes more vivid.
Regarding the second one, since the term "quantum heat" was coined [63] to refer to such energy change it would be natural to expect it to come in the form of heat. However, when thinking about Zeno measurement, all the energy seems to be given in the form of work since for short enough time intervals between two measurements the effect is to compensate for the rotation induced by a classical drive for instance.
To answer these questions, we will first focus on the working substance of a two-qubits measurement engine we have been proposing and then extend our conclusion to a more general case. More information and details about the engine itself and one of its possible generalisation are given in the Appendix. 3.5 for interested readers but are not necessary to our main discussion.

3.1 Two-qubit system

We consider a system made of two qubits A and B of respective transition frequencies ω_A and ω_B whose evolution is governed by the Hamiltonian

$$H_{\text{2qb}} = \underbrace{\hbar\omega_A\sigma_A^\dagger\sigma_A + \hbar\omega_B\sigma_B^\dagger\sigma_B}_{H_{\text{loc}}} + \underbrace{\hbar\frac{g(t)}{2}(\sigma_A^\dagger\sigma_B + \sigma_B^\dagger\sigma_A)}_{V}, \tag{3.1}$$

where we have introduced the lowering operator $\sigma_i = |0_i\rangle\langle 1_i|$ for the qubit $i \in \{A, B\}$. The first term of H_{2qb} is the free Hamiltonian of the qubits. It thus features “local" one-body terms

that we shall denote as H_{loc}. The second term, which we denote by V, couples the qubits, giving rise to entangled states. The coupling channel can be switched on and off, which is modelled by the time-dependent coupling strength $g(t)$. Without loss of generality, we consider a positive detuning $\delta = \omega_B - \omega_A$ and for simplicity, we denote the product states $|x_A\rangle \otimes |y_B\rangle$ as $|xy\rangle$, where $x, y \in \{0, 1\}$. Importantly, the two-qubit system is closed except during the measurement part.

It is interesting to notice that any evolution under this Hamiltonian will conserve both the total energy and the total number of excitations. As the initial state of the qubits is $|10\rangle$, i.e., a state with one excitation in qubit A, we can thus focus our study in the subspace spanned by the vectors $|10\rangle, |01\rangle$. This property allows us to picture the qubits dynamics in the Bloch sphere representation in Fig. 3.10(a). The eigenvectors of $H_{2\text{qb}}$ and of the total number of excitations operator $\sigma_A^\dagger \sigma_A + \sigma_B^\dagger \sigma_B$ are $|+_\theta\rangle$ and $|-_\theta\rangle$ with:

$$\begin{aligned} |+_\theta\rangle &= \sin(\theta/2)\,|10\rangle + \cos(\theta/2)\,|01\rangle \\ |-_\theta\rangle &= \cos(\theta/2)\,|10\rangle - \sin(\theta/2)\,|01\rangle\,, \end{aligned} \tag{3.2}$$

where the angle θ is given by $\tan(\theta) = g/\delta$. These states' respective energies are $\hbar(\omega_A + \omega_B)/2 \pm \hbar\Omega/2$, where $\Omega = \sqrt{g^2 + \delta^2}$ is the generalized Rabi frequency associated with the coupling between the qubits.

We can then directly derive the evolution of the state of the system at time t after its preparation in the initial state $|10\rangle$, to be:

$$|\psi(t)\rangle = (c_\theta^2 e^{i\Omega t/2} + s_\theta^2 e^{-i\Omega t/2})\,|10\rangle - c_\theta s_\theta (e^{i\Omega t/2} - e^{-i\Omega t/2})\,|01\rangle\,, \tag{3.3}$$

where $c_\theta = \cos(\theta/2)$, $s_\theta = \sin(\theta/2)$ and we neglected the very fast global oscillating phase $e^{\frac{-i(\omega_A+\omega_B)t}{2}}$.

3.2 Work value of information

For now on we consider the measurement of second qubit in the basis $\{|0\rangle, |1\rangle\}$ when the two-qubit state is given by Eq. 3.3 at $t_0 = \pi/\Omega$. In this subsection, the measurement will be considered instantaneous, an assumption that we will relax in the following discussion.

It should now be clear that quantum measurements can provide energy via two complementary features: on the one hand their ability to directly affect the average energy of a system via the backaction, and, on the other hand, their capability to extract information, that can be further used to convert the energy input into work. Before focusing on the backaction energy exchange, we analyze here the informational resource as quantified by the mutual information. In the case of a measurement, the mutual information I_{meas} between the system and the memory used in the feedback loop writes:

$$I_{meas} = S_S + S_M - S_{SM}, \tag{3.4}$$

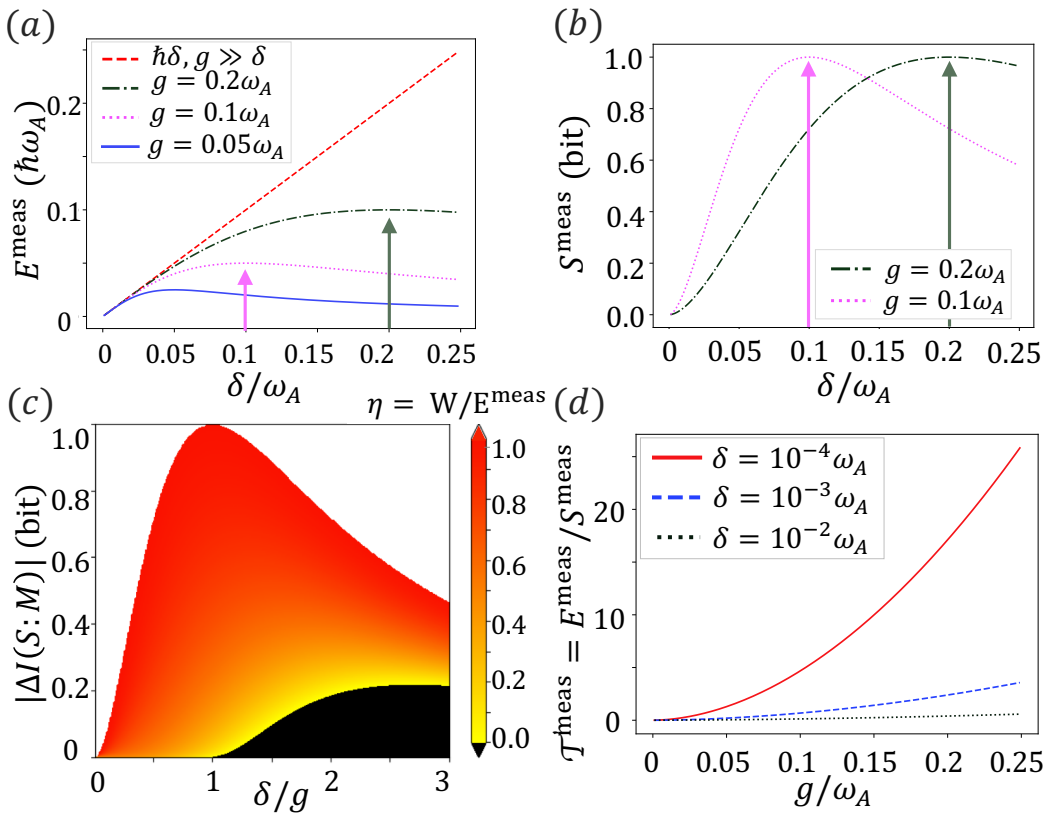

Figure 3.1: Measurement energy vs information as fuel. (a), (b) Energy E^{meas} (a) and entropy S^{meas} inputs as a function of the detuning δ, for various coupling strengths g. (c) Work extraction ratio $\eta = W/E^{\text{meas}}$ (color scale) as a function of δ/g and consumed mutual information $|\Delta I(S:M)|$. The black region corresponds to $\eta = 0$. d) Yield of information to work conversion $\mathcal{T}^{\text{meas}}$ as a function of g for various δ.

where S_{SM} is the entropy of the system SM and memory M. The average energy E^{meas} input by the measurement channel is

$$E^{\text{meas}} = \langle V\rangle(t_0^+) - \langle V\rangle(t_0^-) = \langle H_{2\text{qb}}\rangle(t_0^+) - \langle H_{2\text{qb}}\rangle(t_0^-) = \hbar\delta\sin^2(\theta) \geq 0, \tag{3.5}$$

where t_0^- and t_0^+ refer to the time just before and just after the measurement. The energy given by the measurement is unsurprisingly positive since, at time $t = 0$, the qubits were in the state $|10\rangle$ and that, under the unitary evolution, the excitation got delocalized toward the second qubit of higher splitting energy. This implies that the local energy increased and that the coupling one became negatice. Since, $\langle V\rangle(t_0^+) = 0$ and $\langle H_{\text{loc}}\rangle(t_0^+) = \langle H_{\text{loc}}\rangle(t_0^-)$ the measurement effect was to cancel a negative term, therefore increasing the average energy as ploted in Figure. 3.10(b). Conversely, the von Neumann entropy of the qubit pair increases by an amount

$S^{\text{meas}} = -\text{Tr}[\rho(\theta)\log_2(\rho(\theta))]$, that reads

$$S^{\text{meas}} = -\cos^2(\theta)\log_2[\cos^2(\theta)] - \sin^2(\theta)\log_2[\sin^2(\theta)]. \tag{3.6}$$

Where we used $\log_2$, such that all entropies are expressed in bits. These two quantities are plotted in Figs. 3.1(a) and 3.1(b) as a function of the detuning δ, for various coupling strengths g. Since the two-qubit system is in a pure state before the measurement, S^{meas} corresponds to the two-qubit entropy after the measurement. As it appears in the figure, E^{meas} and S^{meas} are both maximized for $\delta = g$ which corresponds to an equal probability of finding the system in $|01\rangle$ and $|10\rangle$ and to a maximal mutual information between the system and memory states.

Converting the measurement energy into work requires the processing of this information during the feedback step. Here it consists of doing nothing if the high energy qubit is found empty and to apply two π-pulses to flip the state of both qubits if not. On average the energy E^{meas} can be extracted from the system in this way. The conversion is optimal ($W = E^{\text{meas}}$) when all information is consumed, which corresponds to the ideal cycle considered until now. Non-optimal work extraction results from an incomplete consumption, $|\Delta I(S : M)| < I^{\text{meas}}(S : M)$, yielding a conversion ratio $\eta = W/E^{\text{meas}} < 1$. Ideally, the probability to measure the meter in the state $|1\rangle$ (resp. $|0\rangle$) knowing that the system is in the state $|01\rangle$ (resp. $|10\rangle$) would equal one. However, if we consider a more realistic measurement, the probability to measure the meter in $|0\rangle$ even though the excitation is in the qubit B can be nonzero. This can be due to the fact that our access to this information is limited (reading error) or that the mutual information between the system and the meter is not yet equal to the system's entropy (incomplete measurement). In the following, we denote by p, either the reading error probability or the degree to which the meterand system are imperfectly correlated or the lack of information regarding the system's state. In our analysis we will denote S_S the Shannon entropy of the system and $I(S : M)$ the mutual information between the system and the memory. From this error probability p, we define $P(i|k)$, the probability that the classical memory is in i, with $i \in \{0, 1\}$ given that the excitation is localized in $k \in \{A, B\}$:

$$\begin{aligned} P(1|A) &= p \\ P(1|B) &= 1 - p \\ P(0|A) &= 1 - p \\ P(0|B) &= p. \end{aligned} \tag{3.7}$$

In order to derive the work extracted, we consider that if the meter is found in $|0\rangle$, no pulses are applied and no work is extracted whereas if it is found in $|1\rangle$ the two π-pulses are applied and $\pm\hbar\delta$ of work is extracted or performed (work is performed rather than extracted if the π-pulses are applied while the excitation is actually in qubit A). From this simple model we find that the mean work extracted after one measurement reads:

$$\begin{aligned} W &= P(B)P(1|B)\hbar\delta - P(A)P(1|A)\hbar\delta, \\ &= \sin^2(\theta)(1-p)\hbar\delta - \cos^2(\theta)p\hbar\delta, \\ &= \hbar\delta[\sin^2(\theta) - p], \end{aligned} \tag{3.8}$$

where $P(B)$ (resp. $P(A)$) is the probability for the excitation to be localized in qubit B (resp. qubit A). In Fig. 3.1(c), p is taken to vary from zero to one-half because, when $p = 1/2$, the probabilities to read the memory in 1 or 0 does not depend anymore on the system's state. Notice here that if $p = 0$, we recover the average work extracted $E^{\text{meas}} = \hbar\delta \sin^2(\theta)$.

The Shannon entropy and mutual information are given in bits, justifying the use of the $\log_2$. We can now derive the mutual information, which reads:

$$\begin{aligned}
&I(S : M) = S_S + S_M - S_{SM} \\
&= [-\cos^2(\theta)\log_2(\cos^2(\theta)) - \sin^2(\theta)\log_2(\sin^2(\theta))] - \\
&[(\sin^2(\theta)(1-p) + \cos^2(\theta)p)\log_2(\sin^2(\theta)(1-p) + \cos^2(\theta)p) \\
&+ (\sin^2(\theta)p + \cos^2(\theta)(1-p))\log_2(\sin^2(\theta)p + \cos^2(\theta)(1-p))] \\
&+ [\sin^2(\theta)(1-p)\log_2(\sin^2(\theta)(1-p)) \\
&+ \sin^2(\theta)p\log_2(\sin^2(\theta)p) \\
&+ \cos^2(\theta)(1-p)\log_2(\cos^2(\theta)(1-p)) \\
&+ \cos^2(\theta)p\log_2(\cos^2(\theta)p)]. \qquad (3.9)
\end{aligned}$$

Here, we notice that when $p = 0$, $I(S : M) = -\cos^2(\theta)\log_2(\cos^2(\theta)) - \sin^2(\theta)\log_2(\sin^2(\theta)) = S_S = S_M$, i.e., it corresponds to maximal correlation. It is then clear that without noise the system and the meter can be maximally correlated. If we further assume $\delta = g$ we obtain $I(S : M) = 1$. The upper boundary of the coloured area is the regime for which $p = 0$, i.e., $\Delta I(S : M) = S_S$. In the lower boundary we have $p = 1/2$ which leads to $\Delta I(S : M) = 1 - \sin^2(\theta) - \cos^2(\theta) = 0$ as expected. This clearly shows the work value of information—the larger the consumed information, the larger the conversion ratio. Interestingly, the figure reveals that work can be extracted even if $\Delta I(S : M) = 0$. This is the case when $P_{\text{succ}}(\theta) > 1/2$, which happens when $\delta/g < 1$. Then π-pulses can be blindly applied, still leading to a net work extraction $W = \hbar\delta(\sin^2(\theta) - \cos^2(\theta))$. This mechanism solely exploits the energy input by the measurement, but not the extracted information; it is at play, e.g. in single temperature engines [73, 74]. Importantly, one could think that in this regime, one could fuel an engine only from measurement backaction (without involving any bath) by repeatedly measuring and extracting the energy without feedback. It is indeed true for a finite duration which can be very long if $g \gg \delta$. However, if no feedback operation nor bath is involved to garantee a cyclic process, the measurement will not give any energy on average over a sufficent number of repeatitions as well explained already in the case of Zeno measurements [71]. This is why no engine can be fuelled *only* from measurement backaction. By contrast, even for short time scale, information processing is necessary when $\delta \geq g$. Note that in all non-ideal cases where information is not fully consumed, an additional step must be included in the cycle, to reset the qubits' state.

From now on we suppose that the feedback is perfect, such that the information available in the memory is fully consumed and all the energy input by the measurement channel is converted into work. In this situation, the net work extracted is $W = E^{\text{meas}}$. It is thus related to the size of the memory used S^{meas} by the effective parameter $\mathcal{T}^{\text{meas}}$ defined above. Interestingly, now

$\mathcal{T}^{\text{meas}}$ is a measure of efficiency of information-to-work conversion. Such efficiency is usually bounded by the bath temperature in Maxwell's demons fuelled by a thermal bath [67, 110]. $\mathcal{T}^{\text{meas}}$ is plotted on Fig. 3.1(d) as a function of g for various values of the detuning δ. As it appears on the figure, it is not bounded and increases as a function of g. This reveals that in the limit $g \gg \delta$, a finite amount of work can be extracted by processing a vanishingly small amount of information. This effect is similar to the Zeno regime identified in Ref. [71], where work extraction relies on measurements whose outcomes are nearly deterministic.

3.3 Energetics of the pre-measurement

We now investigate the measurement-based fueling mechanism, based on the modeling of the "pre-measurement process" by which the qubits are entangled with a quantum meter while still coupled. It is well-known that such an entanglement accounts for the entropy increase of the measured system. Below we show that it also explains the measurement energy input.

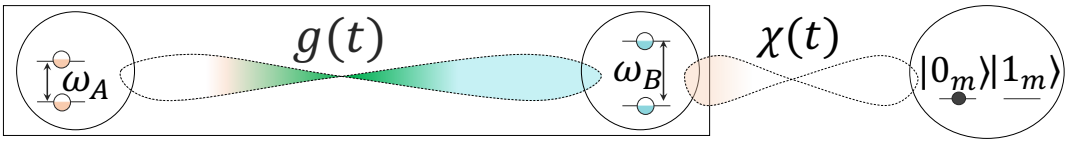

Figure 3.2: A local quantum measurement of qubit B allows for the creation of correlations between the meter M and the AB system and destroys correlations between the qubits.

The measurement process takes place between $t = t_0$ and $t = t_{\text{m}}$, and is depicted in Fig. 3.2. The meter is chosen to be a third qubit M with degenerate energy levels $|0_{\text{M}}\rangle$ and $|1_{\text{M}}\rangle$. It is coupled to the qubit B through the Hamiltonian:

$$V_{\text{M}} = \hbar\chi(t)\sigma_B^\dagger\sigma_B \otimes \sigma_x^M. \tag{3.10}$$

$\chi(t)$ is the measurement strength, with $\chi(t) = \chi$ for $t = [t_0, t_{\text{m}}]$ and 0 otherwise. We choose $\chi \gg g$, to ensure the readout takes place on small time-scales with respect to the Rabi period. This defines the parameter $\epsilon = g/\chi$, which is small but finite since the measurement is implemented on still-interacting qubits. Notice that if χ was not large enough the operator $\sigma_B^\dagger\sigma_B$ would evolve significantly during the measurement leading to a low accuracy of the measurement.

3.3.1 Pre-measurement dynamics

Here we derive the analytical expression for the joint ABM system' state $|\Psi\rangle(t)$ during the pre-measurement process, which is governed by the total Hamiltonian:

$$\begin{aligned} H &= H_{\text{loc}} + V + V_{\text{M}} \\ &= \hbar\omega_A \sigma_A^\dagger \sigma_A + \hbar\omega_B \sigma_B^\dagger \sigma_B + \hbar\frac{g}{2}(\sigma_A^\dagger \sigma_B + \sigma_A \sigma_B^\dagger) + \frac{\hbar\chi}{2}\sigma_B^\dagger \sigma_B \otimes \sigma_x^M. \end{aligned} \tag{3.11}$$

In what follows, we treat V as a perturbation with respect to the unperturbed Hamiltonian $H_0 = H_{\text{loc}} + V_{\text{M}}$. Introducing the small parameter $\epsilon = g/\chi \ll 1$ and $V = \epsilon V'$, the joint state is computed up to first order in ϵ.

To simplify our analytical expressions, we took the time just before the pre-measurement process, denoted t_0^-, to be our initial time 0 in the following analysis. At that time, the joint state reads $|\Psi_0\rangle = (a_0 |10\rangle + b_0 |01\rangle) \otimes |0_M\rangle$ with $|a_0|^2 + |b_0|^2 = 1$. From this initial state and the structure of the Hamiltonian in Eq. (3.11), the state at any time has the general form:

$$|\Psi\rangle(t) = a_t |100\rangle + b_t |010\rangle + c_t |101\rangle + d_t |011\rangle, \tag{3.12}$$

where $a_t, b_t, c_t, d_t \in \mathbb{C}$ and $|a_t|^2 + |b_t|^2 + |c_t|^2 + |d_t|^2 = 1$. The subscript t indicates the dependency on time. Here, as in the rest of the chapter, we shall omit the subscript M for the meter.

The eigenstates of H_0 are $|10-\rangle, |10+\rangle, |01-\rangle, |01+\rangle$ with $|+\rangle = \frac{|1\rangle+|0\rangle}{\sqrt{2}}$ and $|-\rangle = \frac{|1\rangle-|0\rangle}{\sqrt{2}}$. The associated eigenvalues read $E_{10-} = \hbar\omega_A$, $E_{10+} = \hbar\omega_A$, $E_{01-} = \hbar(\omega_B - \chi/2)$, $E_{01+} = \hbar(\omega_B + \chi/2)$ as we took the eigenvalues of the meter to be both zero.

We can now write the joint state as

$$\begin{aligned} |\Psi\rangle(t) &= \left|\Psi^{(1)}\right\rangle(t) + o(\epsilon) \\ &= \sum_{n\in\{10-,10+,01-,01+\}} \gamma_n(t) e^{-iE_n t/\hbar} |n\rangle, \end{aligned} \tag{3.13}$$

where

$$\left|\Psi^{(1)}\right\rangle(t) = \sum_{n\in\{10-,10+,01-,01+\}} \gamma_n^{(1)}(t) e^{-iE_n t/\hbar} |n\rangle \tag{3.14}$$

contains all terms of first order or lower and $\gamma_n = \gamma_n^{(1)} + o(\epsilon)$. Projecting the Schrödinger equation onto the eigenstate $|k\rangle$ of H_0 and using Eq. (3.14), we find:

$$i\hbar\frac{d}{dt}\gamma_k(t) = \epsilon \sum_n \langle k|V'|n\rangle(t)\gamma_n(t) e^{i(E_k - E_n)t/\hbar}. \tag{3.15}$$

Thus, at order zero, we have $\frac{d}{dt}\gamma_k^{(0)}(t) = 0$ for all $k \in \{10-, 10+, 01-, 01+\}$ and as the state just before the pre-measurement reads:

$$\begin{aligned}\left|\Psi^{(0)}\right\rangle(0) &= \sum_{n\in\{10-,10+,01-,01+\}} \gamma_n^{(0)} |n\rangle \\ &= (a_0 |10\rangle + b_0 |01\rangle) \otimes |0\rangle \\ &= \frac{a_0}{\sqrt{2}} |10+\rangle - \frac{a_0}{\sqrt{2}} |10-\rangle + \frac{b_0}{\sqrt{2}} |01+\rangle - \frac{b_0}{\sqrt{2}} |01-\rangle ,\end{aligned} \tag{3.16}$$

we have:

$$\begin{aligned}\gamma_{10-}^{(0)} &= -\frac{a_0}{\sqrt{2}}; \quad \gamma_{10+}^{(0)} = \frac{a_0}{\sqrt{2}} \\ \gamma_{01-}^{(0)} &= -\frac{b_0}{\sqrt{2}}; \quad \gamma_{01+}^{(0)} = \frac{b_0}{\sqrt{2}}.\end{aligned} \tag{3.17}$$

From these coefficients we obtain, at order zero,

$$\left|\Psi^{(0)}\right\rangle(t) = \sum_n \gamma_n^{(0)} e^{-iE_n t/\hbar} |n\rangle \tag{3.18}$$

$$= a_0 e^{-i\omega_A t} |100\rangle + \frac{b_0}{2}(e^{-i(\omega_B+\chi/2)t} - e^{-i(\omega_B-\chi/2)t}) |011\rangle + \frac{b_0}{2}(e^{-i(\omega_B+\chi/2)t} + e^{-i(\omega_B-\chi/2)t}) |010\rangle .$$

To find the first order coefficients, we use Eq. (3.15) to first order:

$$i\hbar \frac{d}{dt}\gamma_k^{(1)}(t) = \epsilon \sum_n \langle k|V'|n\rangle \gamma_n^{(0)} e^{i(E_k-E_n)t/\hbar} \tag{3.19}$$

where $V' = \hbar\frac{\chi}{2}(\sigma_A^\dagger \sigma_B + \sigma_B^\dagger \sigma_A)$. Using the initial conditions $\gamma_{10-}^{(1)}(0) = \gamma_{10+}^{(1)}(0) = \gamma_{01-}^{(1)}(0) = \gamma_{01+}^{(1)}(0) = 0$, these equations can be solved to obtain:

$$\begin{aligned}\gamma_{10-}^{(1)} &= -\frac{\epsilon\chi b_o}{2\sqrt{2}(\delta-\chi/2)}(e^{-i(\delta-\chi/2)t} - 1); & \gamma_{10+}^{(1)} &= \frac{\epsilon\chi b_o}{2\sqrt{2}(\delta+\chi/2)}(e^{-i(\delta+\chi/2)t} - 1) \\ \gamma_{01-}^{(1)} &= \frac{\epsilon\chi a_o}{2\sqrt{2}(\delta-\chi/2)}(e^{i(\delta-\chi/2)t} - 1); & \gamma_{01+}^{(1)} &= -\frac{\epsilon\chi a_o}{2\sqrt{2}(\delta+\chi/2)}(e^{i(\delta+\chi/2)t} - 1).\end{aligned}$$

We can now simply write the coefficients introduced in Eq. (3.12) at zeroth order:

$$\begin{aligned}a_t^{(0)} &= a_0 e^{-i\omega_A t} + O(g/\chi) \\ b_t^{(0)} &= \frac{b_0}{2}(e^{-i(\omega_B+\chi/2)t} + e^{-i(\omega_B-\chi/2)t}) + O(g/\chi) \\ c_t^{(0)} &= o(1) \\ d_t^{(0)} &= \frac{b_0}{2}(e^{-i(\omega_B+\chi/2)t} - e^{-i(\omega_B-\chi/2)t}) + O(g/\chi)\end{aligned} \tag{3.20}$$

and up to first order:

$$
\begin{aligned}
a_t^{(1)} &= a_0 e^{-i\omega_A t} + \frac{\gamma_{10+}^{(1)} e^{-i(\omega_A+\chi/2)t} - \gamma_{10-}^{(1)} e^{-i(\omega_A-\chi/2)t}}{\sqrt{2}} + O(g^2/\chi^2) \\
b_t^{(1)} &= \frac{b_0}{2}(e^{-i(\omega_B+\chi/2)t} + e^{-i(\omega_B-\chi/2)t}) + \frac{\gamma_{01+}^{(1)} e^{-i(\omega_B+\chi/2)t} - \gamma_{01-}^{(1)} e^{-i(\omega_B-\chi/2)t}}{\sqrt{2}} + O(g^2/\chi^2) \\
c_t^{(1)} &= \frac{\gamma_{10+}^{(1)} e^{-i(\omega_A+\chi/2)t} + \gamma_{10-}^{(1)} e^{-i(\omega_A-\chi/2)t}}{\sqrt{2}} + O(g^2/\chi^2) \\
d_t^{(1)} &= \frac{b_0}{2}(e^{-i(\omega_B+\chi/2)t} - e^{-i(\omega_B-\chi/2)t}) + \frac{\gamma_{01+}^{(1)} e^{-i(\omega_B+\chi/2)t} + \gamma_{01-}^{(1)} e^{-i(\omega_B-\chi/2)t}}{\sqrt{2}} + O(g^2/\chi^2). \quad (3.21)
\end{aligned}
$$

From a more qualitative point of view, we can now obtain the density matrix of the subsystem AB (tracing out the meter M) during the pre-measurement. The quantum state tomography of this state is presented on Fig. 3.3 for three times of interest: before, during, and after the measurement. As expected, the reduced density matrix of the two-qubit state exhibits initially nonzero correlations which progressively decrease during the coupling to the meter.

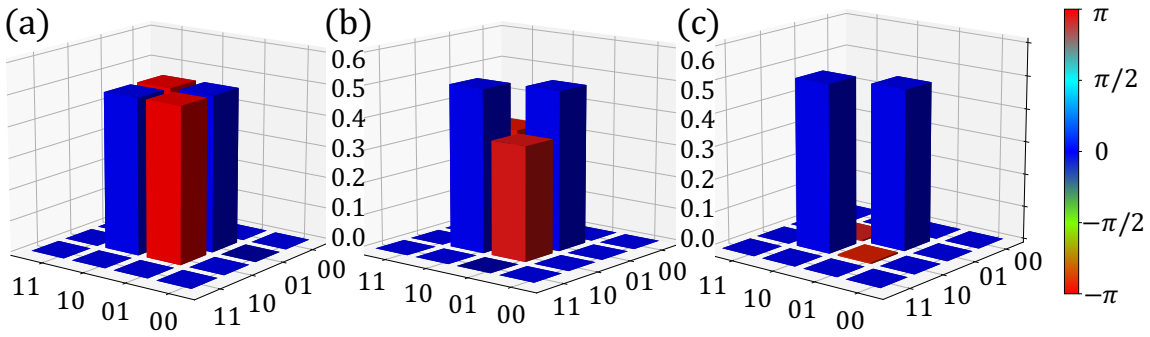

Figure 3.3: Quantum state tomography of the reduced density matrix of the two qubits (a) before the measurement process (b) during the measurement process and (c) at the end of the measurement process. The color represents the phase and the height represents the modulus of each element of the density matrix. One should notice here the decreasing of the cross terms during the measurement process due to the decreasing of $|b_t|$ and the small value of $|c_t|$.

3.3.2 Energy dynamics

At t_0^-, the meter M is prepared in $|0_M\rangle$, while A and B are in the entangled state $|\psi(t_0)\rangle$, such that their joint state reads $|\Psi(t_0)\rangle = i(\cos(\theta)\,|100_M\rangle - \sin(\theta)\,|010_M\rangle)$. Since $\langle V_M(t_0)\rangle = 0$,

the measurement channel is switched on at no energy cost.The joint qubits-meter system then evolves under the total Hamiltonian $H = H^{(0)} + H^{(1)}$, where $H^{(0)} = H_{\rm loc} + V_{\rm M}$ (resp. $H^{(1)} = V$) rules the evolution at zeroth order (resp. at first order) in the small parameter ϵ. The evolution equations are solved at first order, yielding $\left|\Psi^{(1)}(t)\right\rangle = \left|\Psi^{(0)}(t)\right\rangle + |\delta\Psi(t)\rangle$ where $|\delta\Psi(t)\rangle$ is of order ϵ. The populations up to first order are plotted on Fig. 3.4(a). To lowest order in ϵ, the measurement is quantum non-demolition, resulting in state $\left|\Psi^{(0)}(t)\right\rangle$ [111, 81]. The readout is complete at time $t_{\rm m} = t_0 + \pi/\chi$ where $\left|\Psi^{(0)}(t_{\rm M})\right\rangle = i(\cos(\theta)\left|100_{\rm M}\right\rangle - \sin(\theta)\left|011_{\rm M}\right\rangle)$. Conversely, the first order correction $|\delta\Psi(t)\rangle$ accounts for the remaining coupling between the qubits during the measurement.

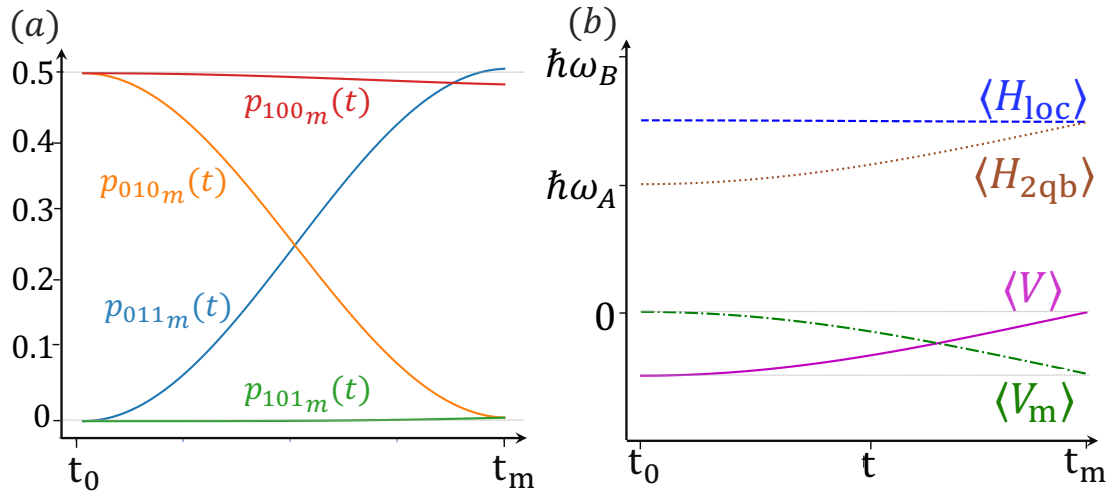

Figure 3.4: Dynamics of measurement induced energy transfer. (a) Full state decomposition in the $\{\left|100_m\right\rangle, \left|101_m\right\rangle, \left|010_m\right\rangle, \left|011_m\right\rangle\}$ basis during the pre-measurement step. (c) Expectation values of $\langle H_{\rm 2qb}\rangle$, $\langle H_{\rm loc}\rangle$, $\langle V_{\rm M}\rangle$, and $\langle V\rangle$ as a function of the pre-measurement time $t \in [t_0, t_{\rm m}]$. The curves in the figure are calculated for $\chi = 10\Omega$ and $g = \delta$. The grey lines indicate constant values as guides to the eye.

At zeroth order, the full system only evolves under $H_{\rm loc} + V_{\rm M}$. In this case the average value of $V_{\rm M}(t)$ reads:

$$\begin{aligned}\langle V_{\rm M}^{(0)}\rangle/\hbar\chi &= \langle\Psi^{(0)}|V_{\rm M}|\Psi^{(0)}\rangle/\hbar\chi \\ &= b_t^{*(0)}d_t^{(0)} + d_t^{*(0)}b_t^{(0)} = 2{\rm Re}(b_t^{(0)}d_t^{*(0)}).\end{aligned} \tag{3.22}$$

Using zeroth order coefficients given in Eq. (3.20), we find $b_t^{(0)}d_t^{*(0)} = \frac{b_0^2}{4}2i\sin(\chi t)$ from which it follows that ${\rm Re}(b_t^{(0)}d_t^{*(0)}) = 0$ and $\langle V_{\rm M}^{(0)}\rangle = 0$ for any time during the pre-measurement process. To derive the average value of $\langle H_{\rm loc}^{(1)}\rangle$ up to first order in ϵ we develop $\langle\Psi^{(1)}|H_{\rm loc}|\Psi^{(1)}\rangle$ and keep

only the zero and first order terms. Since $c_t^{*(0)} = 0$, the average evolution of $H_{\text{loc}}(t)$ reads:

$$\begin{aligned}\langle H_{\text{loc}}^{(1)}\rangle &= \hbar\omega_A a_t^{*(1)} a_t^{(1)} + \hbar\omega_B b_t^{*(1)} b_t^{(1)} + \hbar\omega_B d_t^{*(1)} d_t^{(1)} + O(\epsilon) \\ &= (a_0^* \hbar\omega_A \frac{\gamma_{10+}^{(1)} e^{-i\chi t/2} - \gamma_{10-}^{(1)} e^{i\chi t/2}}{\sqrt{2}} + b_0^* \hbar\omega_B \frac{\gamma_{01+}^{(1)} - \gamma_{01-}^{(1)}}{\sqrt{2}} + \text{c.c.}) \\ &\quad + |a_0|^2 \hbar\omega_A + |b_0|^2 \hbar\omega_B, \end{aligned} \tag{3.23}$$

where c.c. stands for complex conjugate. Since at the beginning of the pre-measurement process we have $b_0 = -i\sin(\theta)$ and $a_0 = i\cos(\theta)$, we find that, in the limit where $\chi \gg \delta$ this average value writes:

$$\begin{aligned}\langle H_{\text{loc}}^{(1)}\rangle \underset{\chi>>\delta}{\rightarrow} & |a_0|^2 \hbar\omega_A + |b_0|^2 \hbar\omega_B \\ & + \epsilon b_0 a_0^* \hbar\omega_A \text{Re}[e^{i\chi t/2} - e^{-i\chi t/2} + e^{-i\chi t} - e^{i\chi t}] \\ & + \epsilon \hbar\omega_B b_0 a_0^* \text{Re}([e^{-i\chi t/2} - e^{i\chi t/2}]) \\ = & |a_0|^2 \hbar\omega_A + |b_0|^2 \hbar\omega_B \end{aligned} \tag{3.24}$$

and thus $\langle H_{\text{loc}}^{(1)}\rangle$ is constant and equal to its zeroth order value.

Finally, we study the evolution at first order of $V_{\text{M}}(t)$. We obtain

$$\begin{aligned}\langle V_{\text{M}}^{(1)}\rangle &= \frac{\hbar\chi}{2}(b_t^{*(0)} d_t^{(1)} + d_t^{*(0)} b_t^{(1)}) + O(\epsilon) = \frac{\hbar\chi}{2}[\frac{b_0^*}{\sqrt{2}}(\gamma_{01+}^{(1)} + \gamma_{01-}^{(1)})] + \text{c.c.} \\ &\underset{\chi>>\delta}{\rightarrow} \frac{\hbar\chi}{2}\frac{\epsilon b_0^* a_0}{2}[e^{i\chi t/2} - 1 + e^{-i\chi t/2} - 1] + \text{c.c.} = \frac{\hbar g b_0^* a_0}{4}[e^{i\chi t/2} + e^{-i\chi t/2} - 2] + \text{c.c.} \\ &\underset{t=\pi/\chi}{=} \frac{\hbar g b_0^* a_0}{2}[i - i - 2] + \text{c.c.} = -\hbar g b_0^* a_0 + \text{c.c.} = -\hbar g \text{Re}(b_0^* a_0). \end{aligned} \tag{3.25}$$

Taking the initial state to be the one at $t_0 = \pi/\Omega$, i.e., $b_0 = -i\sin(\theta)$ and $a_0 = i\cos(\theta)$, we find that the average value of the interaction term V_{M} at the end of the pre-measurement process is:

$$\langle V_{\text{M}}^{(1)}\rangle(t = \pi/\chi) \underset{\chi>>\delta}{\rightarrow} -\hbar g \cos(\theta)\sin(\theta) = -\hbar\delta \sin^2(\theta), \tag{3.26}$$

which is exactly what we observe in our simulations, i.e, a non-negligible average value for V_{M} at the end of the pre-measurement process, even for $\chi \gg g$.

Lastly, the evolution at first order of $V(t)$ is given by

$$\begin{aligned}\langle V^{(1)}\rangle &= \langle \Psi^{(0)}|V|\Psi^{(0)}\rangle \\ &= \frac{\hbar g}{2}(a_t^{*(0)}b_t^{(0)} + b_t^{*(0)}a_t^{(0)}) \\ &= \hbar g \mathrm{Re}(a_t^{*(0)}b_t^{(0)}) \\ &= \frac{\hbar g}{2}\mathrm{Re}(a_0^* b_0 (e^{-i(\delta+\chi/2)t} + e^{-i(\delta-\chi/2)t})) \\ &= \text{-}\hbar g \cos(\theta)\sin(\theta)\cos(\chi t/2)\mathrm{Re}(e^{-i\delta t}) \\ &= \text{-}\hbar\delta \sin^2(\theta)\cos(\chi t/2)\mathrm{Re}(e^{-i\delta t}). \end{aligned} \tag{3.27}$$

This last result is very insightful when looking at the initial and final times of the pre-measurement. Just before the pre-measurement process, at $t = 0$, the interaction term between the two qubits is, as expected, $\langle V^{(1)}\rangle(0) = \text{-}E^{meas}$. At the end of the process, we find that at first order, $\langle V^{(1)}\rangle(\pi/\chi) = 0$.

Comparing the first and second order In Fig. 3.5(a), we have plotted the modulus of the first order coefficients describing the state $|\psi\rangle$ during the pre-measurement process. Here, with parameters $\chi = 10g = 10\delta$, we find an evolution similar to that obtained by simulation in Fig. 4(c). This shows that, for these parameters, the first order description is sufficient to reproduce the system state evolution.

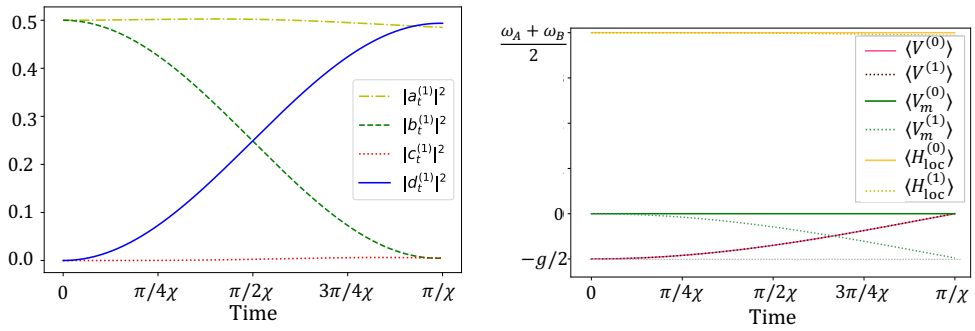

Figure 3.5: Pre-measurement dynamics. (a) First order probabilities of the different states during the pre-measurement process. (b) Zeroth and first order evolution of the energetic terms: $\langle V\rangle$, $\langle V_{\mathrm{M}}\rangle$, $\langle H_{\mathrm{loc}}\rangle$ Parameters: $\chi = 10g = 10\delta$.

In Fig. 3.5(b), the energy of the system is split into its different components at first and zeroth orders. At zeroth order, $\langle V_{\mathrm{M}}\rangle$ and $\langle H_{\mathrm{loc}}\rangle$ stay constant. The term $\langle V\rangle$ evolves, but this is not in contradiction with energy conservation since, at zeroth order, the system evolves under only $H_{\mathrm{loc}} + V_{\mathrm{M}}$. The evolution that this interaction term follows at zeroth order is qualitatively

the same as that obtained at first order; however, at first order, since it is included in the unitary dynamics, its increase is compensated by a similar decrease of the term $\langle V_{\mathrm{M}} \rangle$. Meanwhile, the term $\langle H_{\mathrm{loc}} \rangle$ stays mostly constant but, due to the first order terms, actually decreases slowly with time.

Conclusion

Since the process is unitary, $\langle H_{\mathrm{loc}} \rangle$, $\langle V \rangle$ and $\langle V_{\mathrm{M}} \rangle$ sum up to $\hbar\omega_A$ which was the average initial energy before the pre-measurement. We saw that $\langle H_{\mathrm{loc}} \rangle$ (resp. $\langle V \rangle$ and $\langle V_{\mathrm{M}} \rangle$) remain constant up to first order in ϵ (resp. at zero order) whereas the first order contribution of the binding energy between A and B, $\langle V^{(1)} \rangle = \left\langle \Psi^{(0)}(t) \right| V \left| \Psi^{(0)}(t) \right\rangle$, scales like the coherences of the AB density matrix in the $|01\rangle, |10\rangle$ basis. Its absolute value decreases together with the quantum correlations between A and B, and vanishes when the readout is complete. This evolution is compensated by an equivalent decrease of $\langle V_{\mathrm{M}}^{(1)} \rangle(t)$, yielding at time t_{m}: $\langle V_{\mathrm{m}}^{(1)}(t_{\mathrm{m}}) \rangle = -E^{\mathrm{meas}}$. Importantly, since V_{M} scales as χ, $\langle V_{\mathrm{m}}^{(1)}(t_{\mathrm{m}}) \rangle$ remains finite and of the order of g even if $g/\chi \ll 1$. This calculation reveals the direction of the energy flow during the measurement process:

> The binding energy initially localized between the qubits is transferred between the qubits and the meter. This energy flow follows the same dynamics as the decoherence in the local energy basis, and can be seen as its energetic counterpart. Finally, when the readout is complete, the measurement channel must be switched off before a new cycle can start. This switching off has a work cost of $\langle -V_{\mathrm{M}}(t_{\mathrm{m}}) \rangle = E^{\mathrm{meas}}$.

This gives a first answer to the question of the origin of the quantum heat energy: it comes from the time dependent coupling to the measuring device. In the next chapter we will see how this turning on and off can be implemented and even be made autonomous, i.e., modelled with a time independent Hamiltonian and an additional degree of freedom.

3.3.3 Heat or Work?

Since we have shown that the full qubits and meter system ABM receives energy via the switching off of their coupling V_{M}, it is clear that the nature of this energy exchange is work as it comes from the reversible action of a classical operator. Coming back to the perspective of our two-qubit system however, the final energy exchange E^{meas} is also associated with an increase of its entropy (at the average level of an unread measurement) resulting from its entangling interaction with the meter qubit M. Moreover, this energy input by the measurement backaction was coined "Quantum Heat" [63] for its stochastic nature, reminiscent of thermal baths. However, as discussed in Chapter 2, quantum energy exchanges can, a priori, contain both a generalized heat and a generalized work contribution. Using the dynamical evolution of the system and its environment (here the meter) we can now sort out these possible contributions in the quantum

heat E^{meas}.
We apply the formalism, described in Chapter. 2 and summerized in Fig. 2.2,[1], to the measurement Hamiltonian given in Eq. (3.11):

$$\begin{aligned} H &= H_{2qb} + V_{\text{M}} \\ &= \hbar\omega_A \sigma_A^\dagger \sigma_A + \hbar\omega_B \sigma_B^\dagger \sigma_B + \hbar\frac{g}{2}(\sigma_A^\dagger \sigma_B + \sigma_A \sigma_B^\dagger) + \frac{\hbar\chi}{2}\sigma_B^\dagger \sigma_B \otimes \sigma_x^M \end{aligned} \tag{3.28}$$

and consider our two separate systems to be the two system qubits, denoted by S, on one side and the meter qubit M on the other. The absence of a bare Hamiltonian for the meter qubit immediately implies that $\dot{Q}_M = \dot{W}_M = 0$ i.e., that the meter is not exchanging any energy during the pre-measurement process.
From the system point of view, the interaction term $\mathcal{V}^S = \text{Tr}_M(\frac{\hbar\chi}{2}\sigma_B^\dagger \sigma_B \otimes \sigma_x^M \rho_S \otimes \rho_M) = \frac{\hbar\chi}{2}\sigma_B^\dagger \sigma_B \langle\sigma_x^M\rangle$ and the resulting generalized heat and work exchanged by the system qubits can therefore be written as:

$$\begin{aligned} \dot{Q}_S(t) &= -\frac{i\chi}{2}\text{Tr}_{SM}([H_{2qb}, \sigma_B^\dagger \sigma_B \otimes \sigma_x^M]\chi^{SM}) \\ &= -\frac{i\chi}{2}\text{Tr}_{SM}((\sigma_A \sigma_B^\dagger \sigma_z^B - \sigma_A^\dagger \sigma_z^B \sigma_B) \otimes \sigma_x^M \chi^{SM}) \\ \dot{W}_S(t) &= -\frac{i}{\hbar}\text{Tr}([H_{2qb}, \mathcal{V}^S]\rho^S) \\ &= -\frac{i\chi}{2}\text{Tr}((\sigma_A \sigma_B^\dagger \sigma_z^B - \sigma_A^\dagger \sigma_z^B \sigma_B)\rho^S)\langle\sigma_x^M\rangle, \end{aligned} \tag{3.29}$$

where we remind that $S = AB$. Since $\dot{W}_M(t) + \dot{W}_S(t) + \dot{V}_{SM}^{\otimes}(t) = 0$ and $\dot{Q}_M(t) + \dot{Q}_S(t) + \dot{V}_{SM}^{\chi}(t) = 0$, the interaction energy contribution can be derived by substraction. Moreover, as σ_x^M commutes with H, it stays constant during the evolution, and as the initial state of the meter qubit is $|0\rangle$ this constant value is 0. Thus, all the work flux are zero and, the energy exchange witnessed, simply corresponds to a generalized heat exchange between the measurement system and the interaction energy:

$$\dot{Q}_S(t) = -\dot{V}_{SM}^{\chi}(t) \tag{3.30}$$

as shown in Fig. 3.6.

[1] We remind the reader that there is no general and always applicable consensus about the definition of heat and work (nor about the correct usage of these names) in the quantum community. Given that the formalism introduced in Chapter. 2 has no free parameter and uses the most usual definition of the internal energy of a quantum system we choose it to characterize the energy exchanges.

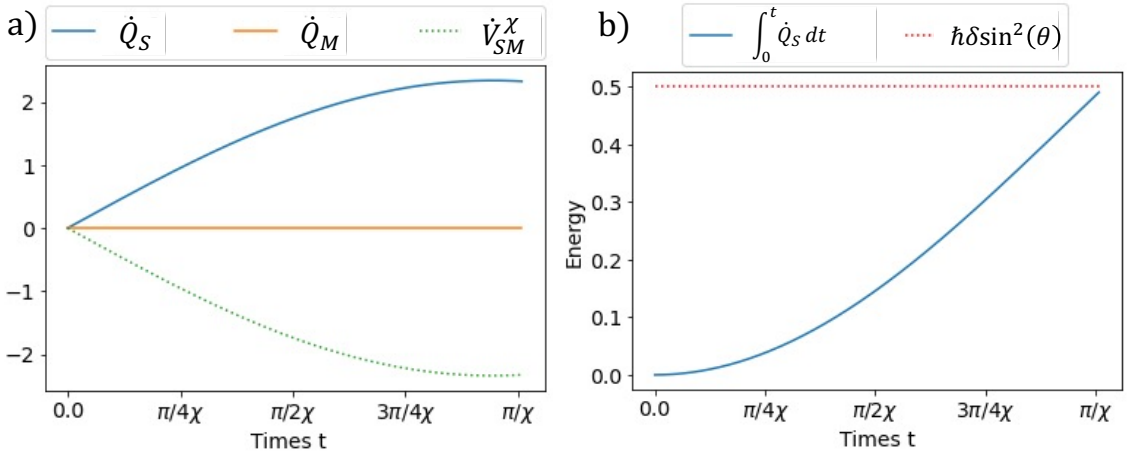

Figure 3.6: Energetics of our two qubit engine during the measurement step. a) Time derivative of the heat exchanges. b) Integral of the heat received by the two-qubit system. Parameters: $\omega_A = 1, \omega_B = 2, g = 1, \chi = 10g$

As shown on Fig. 3.6(a), the heat received by our two-qubit working substance S increases until the final measurement time π/χ and this increase is exactly compensated by the decrease of correlated interaction energy V^{SM}_{χ}. This tells us that during the pre-measurement, heat flows from the interaction term $\langle V^M \rangle$ to the system qubit explaning why it is legitimate to call the fuel of our engine "Quantum Heat". The integral of this flow is given in Fig. 3.6(b) where we observe that this total amont of heat exactly matches the energy input by the switching off: E^{meas}.

3.3.4 Generalization

We generalize the previous reasoning to the pre-measurement process of an arbitrary system S and meter M evolving under the Hamiltonian:

$$H = H^S + H^M + f(t)\, V^{SM} \tag{3.31}$$

where the function $f(t)$ characterizes the interaction and is null outside of the pre-measurement time interval $[t_0, t_m]$. Hence, t_0 and t_m correspond to the initial and final times of the pre-measurement process. We define the time-averaged interaction strength A such that $A\tau = \int_{t_0}^{t_m} f(t)dt$ with $\tau = t_m - t_0$. Until now, we considered a specific pre-measurement dynamics governed by a time-independent Hamiltonian. Here, we generalize this study to an arbitrary system and meter and allow their coupling to be turned on and off smoothly (f should only be differentiable in $]t_0, t_m[$ and such that $f(t_0) = f(t_m) = 0$) .

As was the case so far, we restrict this generalisation to conservative pre-measurements: measurements for which the energy of the (quantum) meter is a constant of motion, i.e., for which $\left[H^M, V^{SM}\right] = 0$. In this manner, no energy is exchanged with the meter on average. Moreover, the interaction is chosen to be of the form $V^{SM} = V^S \otimes V^M$, i.e., a tensor product between a part acting on the meter: V^M and a part acting on the system: V^S. This choice is motivated by its common use in the literature of measurement processes since von Neumann [112, 113, 114, 115, 109]. Such an interaction allows to identify V^S as the measured observable of the system. The outcome probabilities to obtain each of its eigenvalues are encoded in the probabilities of measuring the meter in some specific states: the pointer states. These states should be different from the eigenstates of V^M. Indeed, since V^M and H^M commute, the probabilities to find the meter in the eigenstates of V^M will stay constant during the pre-measurement and hence contain no information about the system.

The average energy change of the system is given by $\Delta E^S = \left\langle H^S \right\rangle (t_{\mathrm{m}}^+) - \left\langle H^S \right\rangle (t_0^-)$, where t_0^-, resp. t_{m}^+, is the time immediately before, resp. after, the pre-measurement. To identify the nature of this energy, we apply Eq. (2.8). The work flux performed on the system thus writes: $d\mathcal{W}^S/dt = -f(t)\left\langle V^M \right\rangle \left(d\left\langle V^S \right\rangle/dt\right)$, which can be integrated by parts to give:

$$\begin{aligned}\mathcal{W}^S\left(t_0 \to t_{\mathrm{m}}\right) &= -\langle V^M \rangle \left[f(t)\langle V^S\rangle(t)\right]_{t_0^-}^{t_{\mathrm{m}}^+} + \langle V^M \rangle \int_{t_0}^{t_{\mathrm{m}}} \dot{f}(t)\langle V^S\rangle dt \\ &= \langle V^M \rangle \int_{t_0}^{t_{\mathrm{m}}} \dot{f}(t)\langle V^S\rangle(t) dt, \end{aligned} \tag{3.32}$$

since $f(t_{\mathrm{m}}^+) = f(t_0^-) = 0$. The average value $\langle V^M \rangle$ was removed from the integral for being a constant of motion, since $[V^M, H^{SM}] = 0$. Equation (3.32) shows that the energy received by the measured system can have a non-zero work contribution. Since the quantum meter is, by assumption, not exchanging any heat or work, this work done on S must come from an equal and opposite work received by the coupling energy. In this case, it means that there is an uncorrelated contribution to the change of coupling energy or equivalently, that the measurement induces a rotation of the system's state, although unwanted. This effect is reminiscent of the WAY theorem, and can be seen as one of its energetic consequences. Indeed, due to the non-commutativity of the measured observable with the initial Hamiltonian $H^S + H^M$, a perfectly accurate measurement of V^S is not possible given finite resources due to the evolution of $\langle V^S\rangle(t)$ in time.

When $\langle V^M \rangle = 0$, however, even if $\langle H^S\rangle(t)$ evolves during the measurement, this would have no effect on the work done on S. It was the case in our previous example where the work flux received by the system was null because we had $\langle V^M \rangle = \langle \sigma_x^M \rangle = 0$. When this condition is fullfield, the total work received by the system vanishes, no matter the shape of the interaction, its duration, strenght or the meter size.

In general, the total energy change of the system during the pre-measurement process, $\Delta\mathcal{U}^S(t_0^- \to t_{\mathrm{m}}^+)$, is divided into heat $\mathcal{Q}^S(t_0^- \to t_{\mathrm{m}}^+)$ and work $\mathcal{W}^S(t_0^- \to t_{\mathrm{m}}^+)$. It is equal and opposite to the change of the interaction energy, since the meter is not exchanging heat nor

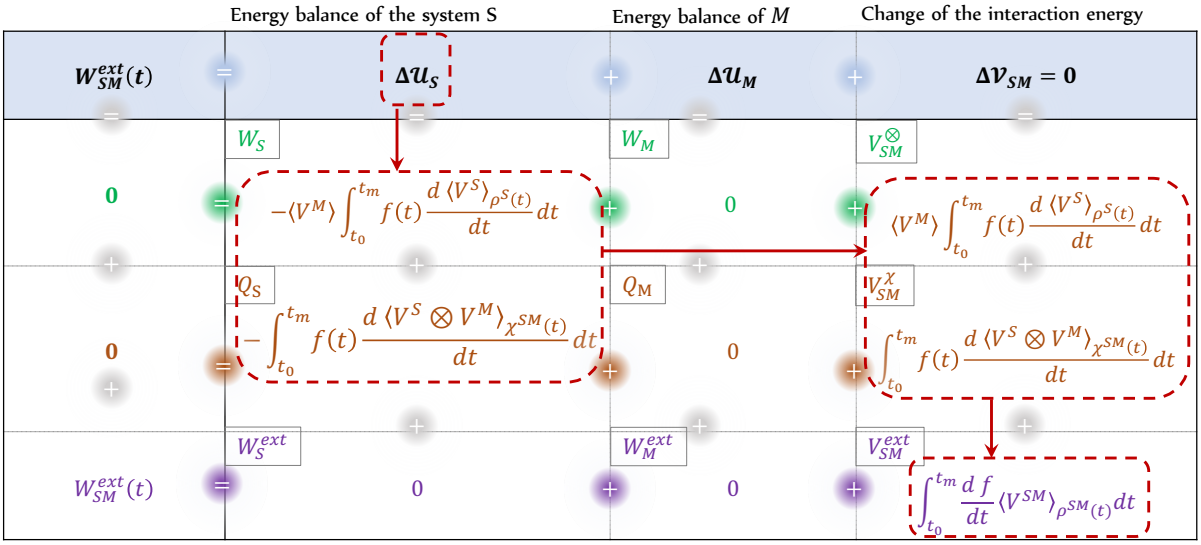

Figure 3.7: Bipartite quantum energetics (BQE) for pre-measurements with $V^{SM} = f(t)V^S \otimes V^M$. This table corresponds to the integrated quantities defined in Fig. 2.2, from t_0 to t_m. The energy received by the measured system can have generalized heat and work contributions and is traced back to the one received by the interaction energy and eventually to the external work done on the bipartite system to vary the interaction strength between the system and meter.

work, as $[H^M, H^{SM}] = 0$ (from Eq. 2.12) . Hence, our framework reveals that,

$$\Delta \mathcal{U}^S(t_0^- \to t_m^+) = \int_{t_0^-}^{t_m^+} \frac{df}{dt} \langle V^S \otimes V^M \rangle(t) dt. \tag{3.33}$$

This unveils that this energy change is due to the modulation of the interaction strength during the measurement process. Moreover, since the net coupling energy exchanged during the process is $\Delta \mathcal{V}^{SM} = 0$ as $f(t_0^-) = f(t_m^+) = 0$, $\Delta \mathcal{U}^S$ is also the total external work done on the meter and system, i.e., $\Delta \mathcal{U}^S(t_0^- \to t_m^+) = W_{SM}^{\text{ext}}(t_0^- \to t_m^+)$, as shown in Figure. 3.7.

To go further, it is useful to consider a square potential of amplitude A and duration τ, such that $f(t) = A\left[\Theta\left(t - t_0\right) - \Theta\left(t - t_m\right)\right]$ and that the work done on S given in Equation (3.32) becomes

$$\begin{aligned} \mathcal{W}^S\left(t_0^- \to t_m^+\right) &= -A\langle V^M \rangle (\langle V^S \rangle(t_m) - \langle V^S \rangle(t_0)) \\ &= -A\tau \langle V^M \rangle \left(\frac{\langle V^S \rangle(t_m) - \langle V^S \rangle(t_0)}{\tau} \right). \end{aligned} \tag{3.34}$$

Perhaps surprisingly, even for τ much shorter than the typical evolution time evolution induced by H^S, which implies $\langle V^S \rangle(t_m) \approx \langle V^S \rangle(t_0)$, this work can be non-null in the limit of an infinitely short measurement. Indeed, when the pre-measurement duration $\tau = t_m - t_0$ goes to

zero,

$$\mathcal{W}^S\left(t_0^- \to t_{\mathrm{m}}^+\right) = -A\tau\langle V^M\rangle\frac{d\langle V^S\rangle}{dt}(t) \tag{3.35}$$

and the work done on the system is found to be proportional to the derivative of the average value of $\langle V^S\rangle$ at the time of the measurement. Notice that prior to the pre-measurement, this average value was already evolving since the system was evolving under H^S with $[H^S, V^S] \neq 0$. Moreover, this work is not a perturbation to a main heat exchange. On the contrary, when the meter size increases to reach the one of a classical measuring device, the absolute value of the average value $|\langle V^M\rangle|$ will also increase or remain null. Hence, if $A\tau$ remains constant, this will also lead to an increase work exchange with S.

Of course, one could argue that in this classical limit the duration τ should be vanishingly small and hence $A\tau$ could tend to zero in such a way that $A\tau\langle V^M\rangle$ goes to zero and similarily for the work $\mathcal{W}^S\left(t_0^- \to t_{\mathrm{m}}^+\right)$. This is true, however one should also be carefull about the overlap between the meter pointer states.

Indeed, an implicit requirement regarding measurement is that the overlap between the final states of the meter associated to the different measurement outcomes should be as small as possible. Therefore, since in the interaction picture with respect to $H^S + H^M$, the unitary operator will be given by $U_I(t) = e^{-i/\hbar\int_{t_0}^{t_{\mathrm{m}}} f(t)V_I^S(t)\otimes V^M dt}$ and that at lower order in τ, this unitary evolution becomes $U_I(t) = e^{-iA\tau V^S\otimes V^M/\hbar}$, if the system is in the eigenstate $\left|e_i^S\right\rangle$ of V^S associated to the eigenvalue a_i, the meter will evolve through $e^{-iA\tau a_i V^M/\hbar}$. Thus, the overlap between two meter states associated with different system states, denoted by p and l, will be $|\langle e_0^M|e^{iA\tau a_p V^M/\hbar}e^{-iA\tau a_l V^M/\hbar}|e_0^M\rangle| = |\langle e_0^M|e^{iA\tau(a_p-a_l)V^M/\hbar}|e_0^M\rangle|$, given that the initial meter state is $\rho_0^M = \left|e_0^M\right\rangle\left\langle e_0^M\right|$. Hence taking $A\tau = 0$ would lead to a unit overlap and thus to a measurement unable to extract information about the system S. Having both only heat done on the measured system, an instantaneous measurement and extract some information seems like a tricky task. The example of the pre-measurement of a qubit by a cavity field (also known as dispersive readout in circuit QED) illustrates well these difficulties. In such a case we have:

$$V^S \otimes V^M = \sigma_z \otimes a^\dagger a \tag{3.36}$$

given a coherent initial state for the meter of average photon number $\bar{n} = |\alpha|^2$, such that $\left|e_0^M\right\rangle = |\alpha\rangle$. Applying the previous reasonning, we find that the overlap between the meter's pointer states associated to $|e\rangle$ and $|g\rangle$ writes:

$$|\langle\alpha e^{-iA\tau}|\alpha e^{iA\tau}\rangle| = |e^{-|\alpha|^2(1-e^{2iA\tau})}| = e^{-2\bar{n}\sin^2(A\tau)}. \tag{3.37}$$

Whilst the work done on the qubit is:

$$\mathcal{W}^{qb}\left(t_0^- \to t_{\mathrm{m}}^+\right) = -A\tau\bar{n}\left(\frac{\langle\sigma_z\rangle(t_{\mathrm{m}}) - \langle\sigma_z\rangle(t_0)}{\tau}\right) \propto A\tau\bar{n} \tag{3.38}$$

As it appears, as long as $\frac{\langle\sigma_z\rangle(t_{\mathrm{m}})-\langle\sigma_z\rangle(t_0)}{\tau} \neq 0$, having both an overlap different from one and a vanishing work implies that $A\tau\bar{n} \to 0$ whist $\bar{n}\sin^2(A\tau) \neq 0$. This last condition implies that

$\bar{n} \neq 0$ and $A\tau \neq 0[\pi]$ which is clearly not compatible with $A\tau\bar{n} \to 0$. Hence, it is not possible to fullfill these two conditions at the same time. And the only way to have only heat done on the measured system, an instantaneous measurement and extract some information is to measure the qubit at a time t where $\frac{d\langle\sigma_z\rangle(t)}{dt} = 0$.

Our BQE framework therefore reveals in which conditions the external work provided by ideal classical measurements is directly converted into heat on the measured system. It also underlines that when the meter remains of small size, this received energy can also have a work contribution. The BQE formalism therefore prolongates the notion of quantum heat by bringing new insights to the nature of the energy exchange during a pre-measurements.

3.4 Conclusion

In the specific case of a two qubit system measured by a qubit meter, we derived the pre-measurement dynamics. This allowed us to conclude that the quantum heat comes from the turning off of the interaction between them. We then generalized this result to any system measured via an interaction of the form $V^S \otimes V^M$. This energetic counterpart of measurement backaction was hence also traced back to the modulation of the interaction between meter and measured system.

The nature of the quantum heat was shown to depend on the average value of the meter part of the interaction. When $\langle V^M \rangle = 0$, it is indeed received in the form of heat by the measured system.

In the next chapter, we model the autonomous dynamics of a similar measurement, where the switching on and off of the interaction V^{SM} is driven by the evolution of another degree of freedom. Therefore, we move one step closer in a full quantum measurement modelling, still without invoking the controversial collapse of the wavefunction. This analysis could prove useful to the design of engines exploiting decoherence as a resource which is of special interest as it contributes to bridging the gap between the field of quantum measurement engines, in which a measuring environment can serve as a work source, and the field of dissipation engineering [116, 117], where dissipation is harnessed to produce nontrivial quantum states and desirable quantum dynamics. Such reservoir engineering has been recently employed in the circuit-QED architecture[118, 119, 120, 121] and could be an ideal platform on which to realize the engine resulting for these ideas as described in the following Appendix.

3.5 Appendix: A two qubit engine based on measurement

Measurement driven engines can be fuelled by the information extracted about a working substance and/or by the measurement backaction effect. Until recently however, the working substance was usually a single qubit and the measurement step was not itself modeled . Bipartite working substances were first introduced for Maxwell type, information-based only, quantum heat engines [122]. Buffoni *et al.* were the first to propose a two-qubit engine fuelled by

measurement backaction [75] by adapting Campisi *et al.* [123] swap heat engine from its information fuelled version [77]. Thanks to this new type of working substance, their engine features all possible regimes: heater, refrigerator, thermal accelator and work extraction. Their protocol involves two thermal baths and a measurement of the joint state of the qubits. Since this measurement occurs in a basis that does not commute with the Hamiltonian of the qubits, it can exchange energy with this system. Therefore heat can be transfered from a cold reservoir to a hot one not by a sequence of time dependent operations on the working substance, as in classical heat engines, neither via the information obtained by measuring the system, as in Maxwell demon type protocols, but rather due to the measurement backaction on the joint two qubit system.

By adding a coupling between the two qubits and without the need of thermal bath (except for the resetting phase), we proposed a two-qubit quantum engine that is powered by entangling operations and projective local quantum measurements. An important novelty is that the fueling of our bipartite working substance comes from the local measurement of this global system. Thus instead of rotating the measurement basis with respect to the Hamiltonian eigenbasis, we chose the local Hamiltonian eigenbasis as our measurement basis. Compared to the inspiring work of Buffoni, our setup allows to extract work by the amplification of a coherent field and can also serve as an almost deterministic frequency upconverter. Additionnaly, we investigated the measuring process to complete our understanding of the quantum heat injected.

3.5.1 Principle of the engine

As summerized in Fig. 3.8 the engine cycle encompasses four steps:

(i) *Entangling evolution*

At time $t = 0$, the qubits are prepared in the state $|\psi_0\rangle = |10\rangle$ of mean energy $\langle H_{2\mathrm{qb}}\rangle = \langle\psi_0| H_{2\mathrm{qb}} |\psi_0\rangle = \hbar\omega_A$. The coupling term is switched on at time $t = 0^+$ with a strength g. Since $|\psi_0\rangle$ is a product state, its mean energy does not change during this switching process, which is thus performed at no cost. The qubits' state then evolves into an entangled state $|\psi(t)\rangle$, given in Eq. 3.3, where the initial excitation gets periodically exchanged between the two qubits. $\langle H_{\mathrm{loc}}\rangle(t)$ and $\langle V\rangle(t)$ are plotted on Fig. 3.10(b). As expected from a unitary evolution, their sum remains constant and equal to its initial value $\hbar\omega_A$. The periodic exchange of the single excitation between A and B gives rise to oscillations of the local energy component. This evolution is compensated by the opposite oscillations of the coupling energy $\langle V\rangle(t) \leq 0$. This term appears here as a binding energy and is or purely quantum origin since without entanglement between the two qubits this average energy contribution would vanish. Its presence ensures that the total energy and the number of excitations are both conserved.

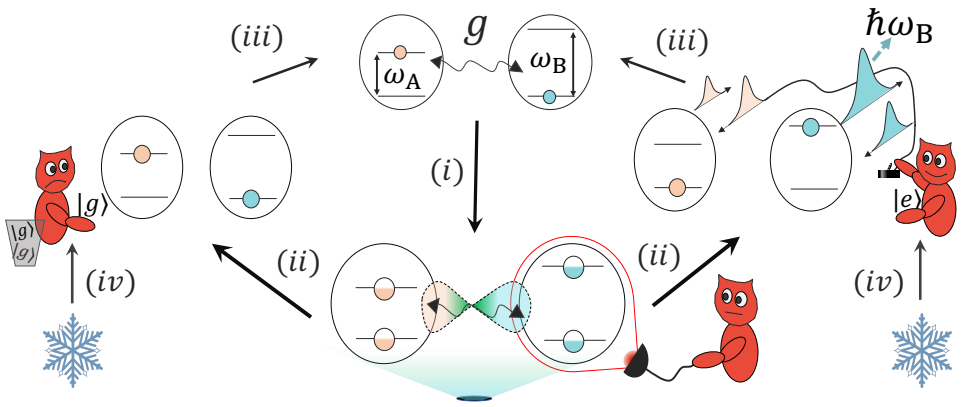

Figure 3.8: Scheme of the two-qubit engine cycle. *(i)* Starting from $|10\rangle$, the qubits get entangled by coherently exchanging an excitation. *(ii)* A demon performs a selective energy measurement on qubit B at $t_0 = \pi/\Omega$. *(iii)* Feedback. If B is found in the excited state, a π pulse is applied to each qubit. The energy of B is extracted and A is re-excited. If not, nothing is done. At the end of this step, the qubits are back to their initial state. *(iv)* Reset of the demon's memory.

(ii) *Measurement*

The average energies $\langle H_{\rm loc}\rangle$ and $|\langle V\rangle(t)|$ reach a maximum when $t_0 = \pi/\Omega$ where $|\psi(t_0)\rangle = i(\cos(\theta)\,|10\rangle - \sin(\theta)\,|01\rangle)$. At this time, a local projective energy measurement is performed on qubit B, and its outcome is encoded in a classical memory. Here we consider an instantaneous process, performed with a classical measuring device. We will study in more details the energy exchanges happening during this measurement at the end of the chapter. On average, the qubits' state becomes a statistical mixture $\rho(\theta) = \cos^2(\theta)\,|10\rangle\langle 10| + \sin^2(\theta)\,|01\rangle\langle 01|$, erasing the quantum correlations between them and thus bringing the binding energy $\langle V\rangle$ to zero. The average energy input by the measurement channel is $E^{\rm meas}$, defined in Eq. (3.5) and the change of the two-qubit system entropy is $S^{\rm meas}$, as given by Eq. (3.6). The ratio $\mathcal{T}^{\rm meas} = E^{\rm meas}/S^{\rm meas}$ characterizes the measurement process from a thermodynamic standpoint. For a fixed detuning δ, it diverges for large coupling such that $\theta \to \pi/2$ where it typically scales like $\mathcal{T}^{\rm meas} \sim -\hbar\delta/[2(\pi/2-\theta)^2\log_2(\pi/2-\theta)]$. In this limit of large coupling and small detuning, quantum measurement can input a finite amount of energy with vanishing entropy. This contrasts with isothermal processes, where energy and entropy inputs are related by the bath temperature.

From an informational standpoint, the measurement creates classical correlations between the qubits and the memory in the basis $|10\rangle, |01\rangle$. If the measurement is ideal, these correlations are perfect, such that the entropies of the qubits and the memory at the end of the process are equal. They are also equal to the mutual information they share, further denoted $I^{\rm meas}(S:M)$.

(iii) *Feedback*

The information stored in the memory is now processed to extract the energy input by the measurement. To do so, the coupling term is switched off at time $t_0{}^+$. Since the correlations between the qubits have been erased by the measurement, the switching-off can be implemented at no energetic cost. If the excitation is measured in B, which happens with probability $P_{\text{succ}}(\theta) = \sin^2(\theta)$, A and B both undergo a resonant π pulse, such that B emits a photon while A absorbs one. The work $W = \hbar\delta$ is extracted and the qubits are reset to their initial state $|10\rangle$. Conversely if the excitation is measured in A, no pulse is implemented and the cycle restarts. Eventually, the mean work extracted is $W = E^{\text{meas}}$. At the end of this feedback step, the qubits' entropy vanishes, and a maximal amount of mutual information $|\Delta I(S : M)| = I^{\text{meas}}(S : M)$ is consumed.

(iv) *Erasure.*

Immediately after the feedback, the memory's entropy still equals $S^{\text{meas}} = I^{\text{meas}}(S : M)$. The memory is finally erased in a cold bath, the minimal work cost of this operation being proportional to S^{meas} [28].

3.5.2 Generalization of the working principle

One could worry about the cost for the necessary resetting of the memory that will be necessary in order to repeat the cycles of our engine. Indeed, since we know that this reset will cost at least $k_B T$ of work if the probability of obtaining 0 and 1 are the same, it seems quite device dependent and arbitrary to include it since it depends on the environment temperature T. However, our engine can be generalized to a regime in which the resetting cost vanishes solving this legitimate concern. This generalisation builts on the realization that this two qubit engine can be seen as a frequency up-converter. Its effect is indeed to convert an excitation at frequency ω_A to a higher frequency excitation. Now, if we gradually increase the energy splitting along a chain of qubits, the initial low energy of the first qubit can be up-converted deterministically to an arbitrarily high energy at the last qubit by successive neighbor swap operations and local measurements.

The protocol is based on the efficient transfer of a single excitation through a chain of N qubits of increasing frequency as depicted in Fig. 3.9(a). We denote the frequency of the qubit i by $\omega_i = \omega_A + (i-1)\delta/(N-1)$, with $i \in \{1, 2, ..., N\}$. As above, $\delta = \omega_B - \omega_A$, such that the frequency of qubit N is ω_B and $\omega_1 = \omega_A$. At time $t = 0$, the qubit 1 is excited and the coupling g between qubit 1 and qubit 2 is switched on, its Rabi frequency being $\Omega_N = \sqrt{g^2 + (\delta/(N-1))^2}$. At time $t_N = \pi/\Omega_N$, the energy of qubit 2 is measured. The process stops if it is found in the ground state, which happens with probability $\cos^2(\theta_N)$, where $\tan(\theta_N) = (N-1)g/\delta = (N-1)\tan(\theta)$. If the excitation is successfully transferred to qubit 2, the coupling

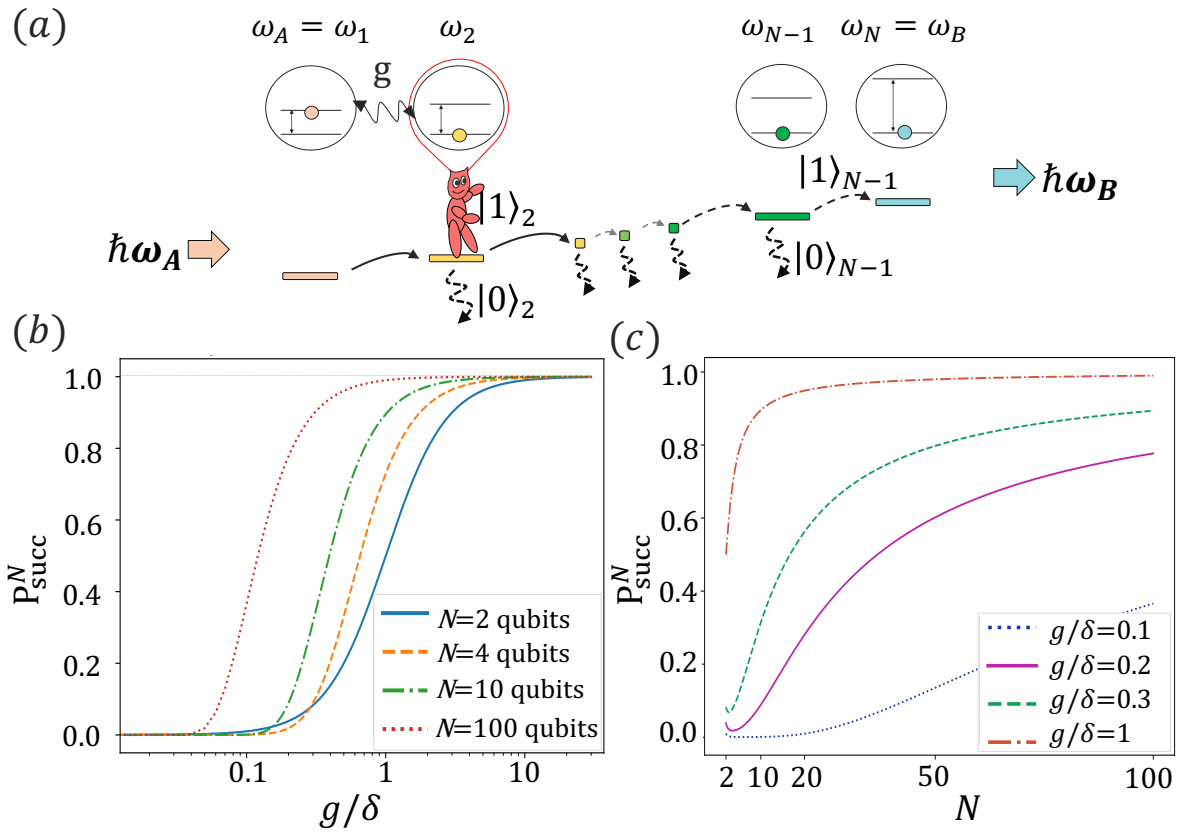

Figure 3.9: Entanglement and measurement based up-conversion mechanism. (a) Scheme of the frequency up-converter (See text). (b),(c) Probability of transfer P^N_{succ} as a function of g/δ for various N ((b)) and as a function of N for various g/δ ((c)).

between 1 and 2 is switched off and the coupling between 2 and 3 is switched on. The same process is repeated between qubits k and $k+1$ until the excitation gets detected in qubit N, which happens with probability $P^N_{\text{succ}} = \sin^{2(N-1)}(\theta_N)$. P^N_{succ} is plotted in Fig. 3.9(b) and 3.9(c) as a function of g/δ and N. For fixed values of g and δ, it is clearly advantageous to increase the number of intermediate qubits. The mechanism at play is reminiscent of the quantum Zeno effect. Indeed, the probability for the excitation to be transferred to the last qubit goes to 1 as the number of intermediate qubits increases (for fixed $\frac{\delta}{g}$) since we have:

$$\begin{aligned} \tan(\theta_N) &= \frac{(N-1)g}{\delta} \\ \sin(\theta_N) &= \frac{(N-1)g}{\sqrt{\delta^2+(N-1)^2g^2}} = \frac{1}{\sqrt{(\delta/(N-1)g)^2+1}} = e^{-\frac{1}{2}\ln\left(1+(\frac{\delta}{(N-1)g})^2\right)} \end{aligned} \tag{3.39}$$

and thus:

$$P^N_{\text{succ}} = e^{-(N-1)\ln\left(1+(\frac{\delta}{(N-1)g})^2\right)} \approx e^{-\frac{1}{(N-1)}(\frac{\delta}{g})^2} \tag{3.40}$$

where the latter approximation holds and, furthermore, approaches 1 as long as $N-1 \gg (\frac{\delta}{g})^2$. Using the Bloch sphere representation can help visualize the cyclic nature of the evolution as in Fig. 3.10(a).

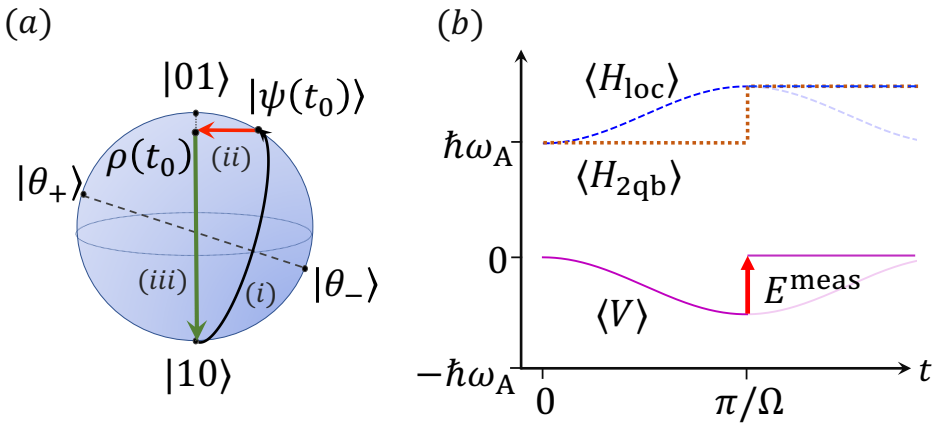

Figure 3.10: Two qubit dynamics. (a) Representation of the qubits' quantum state in the Bloch sphere spanned by $\{|01\rangle, |10\rangle\}$. The eigenstates of H_{2qb} are denoted by $|\theta_+\rangle$ and $|\theta_-\rangle$. At the end of (i) the qubit's state is $|\psi(t_0)\rangle$. After an unselective measurement, the state is $\rho(t_0)$. (b) Evolution of $\langle H_{2qb}\rangle$ (dotted brown), $\langle H_{loc}\rangle$ (dashed blue), and $\langle V\rangle$ (solid magenta) as a function of time (See text).

3.5.3 Photonic implementation

Using the spatial distribution and polarization of photon travelling in a linear optic setup it is possible to obtain experimentally results in good agreement with our theoretical prediction concerning the work value of information.
As explained in:

Kunkun Wang, Ruqiao Xia, Léa Bresque, and Peng Xue,

Experimental demonstration of a quantum engine driven by entanglement and local measurements

Physical Review Research **4**, no. 3 (2022),

the engine is simulated by encoding the states $|0\rangle$ and $|1\rangle$ of the first qubit onto the left and right transverse spatial modes of single photons, and the states of the second qubit onto their horizontal $|H\rangle$ and vertical polarizations $|V\rangle$. This results in the following mapping:

$$|10\rangle \rightarrow |RH\rangle$$
$$|01\rangle \rightarrow |LV\rangle\,.$$

To account for the pre-measurement, the longitudinal spatial modes up $|U\rangle$ and down $|D\rangle$ are used as an additional third qubit. This ingenious setup also allows for the simulation of the working principle generalization to N-qubit.

Chapter 4

Energetics of an Autonomous Measurement

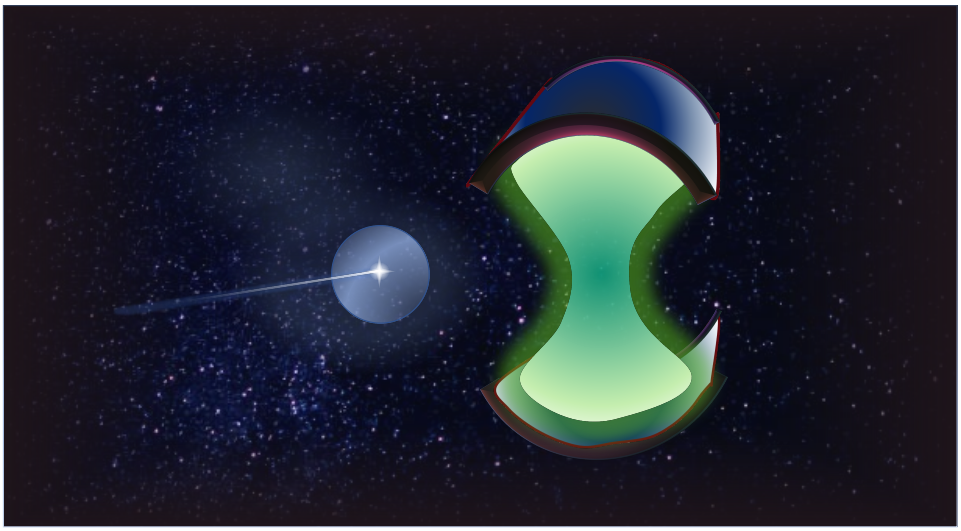

Contents

IN THE PREVIOUS CHAPTER, we were able to witness energy exchanges during the, fully quantum, step of pre-measurement. We found that the average energy change of the system due to the measurement, i.e., the quantum heat, was paid for by switching off the interaction between the meter and the system or more generally by modulating the strength of this interaction. This modulation was simply modelled by a time dependent coupling strengh $\chi(t)$. Such a time dependent evolution is a sign that some parts of the system are not included in the model which therefore prevents us from further tracking and accessing the origin of the quantum heat. Therefore, we now proceed to analyse the closed dynamic of a pre-measurement. This natural endeavour toward considering fully closed, autonomous quantum system was already fruitful in quantum optics setups [**?**], Maxwell Demons using tape models [124, 125] or a three level atom [54], and quantum engines [126, 127]. It allows for a description of the dynamics fully within the realm of quantum physics, i.e., without invoking a extra classical degree of freedom to generate a time-dependent Hamiltonian.

Coming back to the case of quantum measurements, nothing prevents us from imagining a situation in which the switching on and off of the coupling between the measuring apparatus and the system is mediated by another system included in the description, thus making the full model autonomous. This typically corresponds to what happens in many quantum optics experiments where Rydberg atoms are send in a cavity [128]. In these cases, the interaction between the field in the cavity and the flying particle's internal degree of freedom varies in time due to the change in position of the particle. Therefore, the cost of the turning on and off the interaction should be paid for by the kinetic degree of freedom of this flying particle.

In this chapter, we will particularize this situation to the case of a cavity field which measures the flying particule's internal degree of freedom. Choosing a conservative interaction such that the energy of the meter field is conserved and in a situation in which the energy of the particule's measured IDoF changes implies that this energy can only come from the kinetic degree of freedom of the flying particle.

We focus on the near ideal regime, in which the particle is not too massive, such that the energy change of its KDoF could be experimentally tractable, while keeping the motion of the particle only slightly affected by the state of the IDoF throughout the evolution. Therefore, the flying particle's IDoF remains measured by the scatter's IDoF and not by the KDoF. The KDoF serves here to provide the necessary energy to modulate this dispersive interaction. The nature of the induced energy exchanges and the conditions for such an autonomous interaction to induce a good measurement are some of the main questions adressed in this chapter.

> *The approximated solution to the Autonomous dynamic was found thanks to my collaboration with Nicolò Piccione on this project.*

Some of this chapter content will soon be published as:

Nicolò Piccione, Léa Bresque, R. Whitney, A. N. Jordan, and A. Auffèves,
How good are kinetic degrees of freedom as work sources ?

4.1 A flying particle interacting with a fixed scatterer

In this chapter, we derive the dynamic and the energy exchanges caused by the interaction of a flying particle with a fixed scatter. We will model this situation via a time-dependent, non autonomous Hamiltonian and also using a more refined, autonomous, time-independent model whose solution makes use of the non-autonomous dynamics.

These two situations are presented in Fig. 4.1 in our specific case of interest which is the measurement of the particule's internal degree of freedom (IDoF) via the IDoF of a cavity field mediated by their position dependent interaction.

4.1.1 General situation

In the most general situation, we consider a one-dimensional moving particle with internal degree of freedom (IDoF) sent on the potential of spatial shape $f(x)$ generated by a fixed scatterer which can itself have IDoF. The joint internal degrees of freedom of the particle and scatterer will be denoted IDoFs. The IDoF of the flying particle could be for instance the spin orientation of the particle; its orbital decomposition or its angular momentum. They are called "Internal" as opposed to the position/kinetic one. The full Hamiltonian of this particle, of mass m, and its scatterer is given by:

$$H = \frac{\hat{p}^2}{2m} + H_0 + f(\hat{x}) \otimes V_1, \tag{4.1}$$

where $\hat{p}$ is the momentum operator, $\hat{x}$ the position operator, H_0 is the bare Hamiltonian of the IDoFs and V_1 is the interaction term for the IDoFs. There are thus three degrees of freedom: kinetic degree of freedom of the flying particle (KDoF); its internal degree of freedom and the internal degree of freedom of the scatterer. Note that H_0 could be acting on the flying particle, the scatterer or both. Moreover, the situations described by Eq. (4.1) are not limited to the case of measurements since V_1 could for instance be chosen to act only on the flying particle's IDoF and hence implement rotation of its initial state.

When the interaction strength is of the same order than the initial kinetic energy of the particle, flying particles sent on such an effective potential can get reflected [129, 128]. Therefore, the KDoF can be strongly influenced by the state of the IDoF. This means that the KDoF can become strongly correlated to the state of the IDoFs. This regime is not interesting for our purpose since, as the interaction term is position dependent, it does not commute with the bare KDoF Hamiltonian. This implies that the energy of this possible KDoF meter would change during the interaction. Instead, we here want to track the energy exchanges in the counter intuitive case in which, the system received some energy but the conservative interaction prevents this energy to come from the meter system. In other words, we do not want the KDoF to act as a meter for the particle IDoF because it would not correspond to a conservative measurement.

In semi-classical limit, attained for a massive-enough point-like particle, whose spatial extension is much smaller that the typical lenght of the interaction region, the reduced dynamic of

the IDoFs will be well approximated by the one induced by the corresponding time dependent Hamiltonian [130]:

$$H_{\mathrm{NA}}(t) = H_0 + f(x_0 + v_0 t)V_1 \tag{4.2}$$

with x_0 the starting position of the particle and v_0 its constant velocity. By massive enough, we imply here that the kinetic energy of the particle should be large enough that any reflection and recoil of the particle can be neglected and that the amount of information exchanged between the KDoF and IDoFs is negligible. This means that the global state can always be written as a tensor product of the kind $\rho_K \otimes \rho_{\mathrm{IDoFs}}$, where ρ_K corresponds to the kinetic state and ρ_{IDoFs} to the internal ones. This will allow us to investigate the energetic dynamics during the switching on and off of the interaction term V_1. In this case it is as if an operator was modulating this interaction instead of simply turning it on and off as in the previous chapter.

This modulation can be accounted for by the KDoF of the particle, making the global evolution autonomous. In the limit in which the KDoF state would be unaffected by the interaction with the IDoF, i.e., for an infinitely massive and perfectly localized particle, all the work previously attributed to the operator would now come from the KDoF without affecting the evolution of the IDoFs. Therefore, the KDoF would act as a perfect work source. i.e., a degree of freedom, usually classical, which can exchange energy without changing entropy. Modelling the KDoF in the quantum formalism allows us to go beyond this ideal case and describe the impact of the finite spatial extension of the flying particle. Ultimately, the entanglement between the KDoF and IDoFS will reduce the quality of the energy transfer between them. This will lead to a decrease of the proportion of the IDoFS energy change that comes in the form of work. Using an approximated version of the autonomous time independent Hamiltonian of Eq. (4.1) will allow us to access this quantity.

4.1.2 A qubit measured by a single mode cavity field

This general case can prove useful for our endeavour to better understand the energy flows due to quantum measurements. Therefore, we particularize it to the case of single mode cavity meter C measuring a qubit flying whose IDoF constitute our measured system S. In this case, we choose the bare Hamiltonian of the IDoFs to be:

$$H_0 = \underbrace{\frac{\hbar}{2}\omega_{\mathrm{q}}\sigma_\Theta}_{H^{\mathrm{S}}} + \underbrace{\hbar\omega_{\mathrm{c}}a^\dagger a}_{H^{\mathrm{C}}} \tag{4.3}$$

with a and $a^\dagger$ the photon annihilation and creation operators of the cavity, H^{S} the Hamiltonian of the measured qubit and H^{C} the Hamiltonian of the electromagnetic field inside the cavity. The interaction Hamiltonian is given by

$$V_1 = \frac{\hbar}{2}\chi\sigma_z a^\dagger a, \tag{4.4}$$

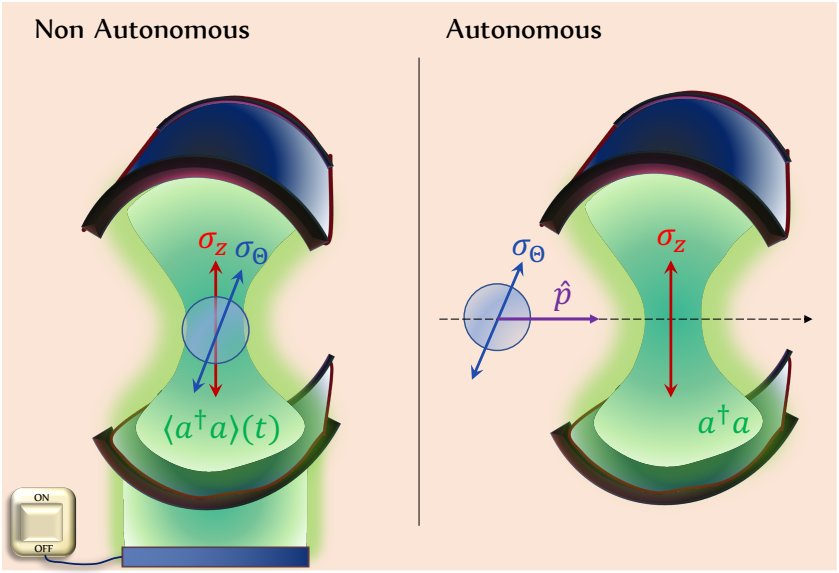

Figure 4.1: Non Autonomous and Autonomous interaction of a qubit with a single mode cavity.

where we also introduced the qubit and cavity's respective resonant frequency ω_q and ω_c as well as the coupling strength χ. The qubit's bare Hamiltonian H_S contains the operator $\sigma_\Theta = x\sigma_x + z\sigma_z$ with $x, z >= 0$ and $x^2 + z^2 = 1$. We will also use the polar parametrisation: $x = \sin(\Theta)$ and $z = \cos(\Theta)$ and refer to σ_Θ's diagonalisation basis as the initial quantization basis.

Note that in this case, the last term of Equation. 4.1 will correspond to a three-partite interaction between the cavity field, the qubit and the KDoF.

4.1.3 Unravelling pre-measurement's energy exchanges

In order to motivate the interest of looking at the non-autonomous dynamics, aside for its use in the autonomous one, we give some more context here about the energy exchanges caused by a pre-measurement. Indeed, although its only difference with the measurement of a qubit by another qubit derived in the previous chapter it that here the meter is a cavity field, the impact of these difference of the nature of the energy exchange will not be negligible.

As we have seen in Chapter 1, the collapse of the wavefunction caused by projective measurement is not associated with a consensual equation that would rule the dynamic of the measured system. That is to say that we do not know the time evolution of the system and meter during the collapse. However, averaging the effect of such projective measurements leads to the final state obtained from an unread measurement. Since, this state can be obtain from a fully quantum, unitary evolution by invoking an ancillary quantum meter system: the pre-

measurement, the average energy change of the system becomes accessible.

For this purpose, the general framework is composed of a system S of bare Hamiltonian H^S is being pre-measured by a meter system M of bare Hamiltonian H^M via the time dependent interaction term V_{SM} such that the total Hamiltonian is:

$$H^{SM} = H^S + H^M + V^{SM}(t). \tag{4.5}$$

When the bare Hamiltonian of the system does not commute with the interaction term, i.e., $[H^S, V^{SM}] \neq 0$, the system can lose or gain energy due to the measurement. Moreover, we choose $[H^M, V^{SM}] = 0$ such that the meter can not provide and take this energy: the measurement is thus conservative. If $V^{SM}(t_0) = V^{SM}(t_m) = 0$, i.e., that the interaction term is null before and after the measurement, this term will also not contribute to the final energy balance.

Until now, we considered the case in which $H^M = 0$ since there were no bare Hamiltonian for the meter qubit in the previous chapter (See Eq. (3.11)). Moreover, the interaction term of the form $V^{SM} = f(t)V^S \otimes V^M$ was such that $\langle V^M \rangle(t) = 0$ for all time t. This lead to us to conclude that the quantum heat was received by the system in the form of a generalized heat and to trace back its origin to the external work done to turn on and off the interaction (See Figure. 3.7).

Here we consider a more general case in which we still have $[H^M, V^{SM}] = 0$ but with a non zero bare Hamiltonian of the meter. More importantly, the interaction term, still of the form $V^{SM} = f(t)V^S \otimes V^M$, will be such that $\langle V^M \rangle(t) = \langle a^\dagger a \rangle \neq 0$ for all time t. The labelling of the energy exchanges as work or heat will therefore prove to be more complicate in this context.

4.2 Non autonomous modelling

4.2.1 Non-Autonomous dynamics

First here, we derive the evolution induced by the time dependent Hamiltonian given by Eq. (4.2) using the bare Hamiltonian from Eq. (4.3) and the interaction term of Eq. (4.4). This Hamiltonian only acts on the IDoFs and the kinetic degree of freedom generates this time dependence. Therefore, the entropy of the IDoFs will stay constant during this dynamics and the energy they receive will come in the form of an external work done on their interaction energy as defined in Equation. (2.14). We can think about $H_{\mathrm{NA}}(t)$ as resulting from the change of position of the particle in the position dependent potential of shape $f(x)$ at constant velocity. The validity of considering a fixed velocity and a motion uncorrelated from the internal state evolution will be discussed in next section.

Since the photon number operator $a^\dagger a$ commutes with H_{NA} at all times, it is useful to introduce the qubit Hamiltonian associated to the n photon subspace:

$$H^n_{\mathrm{NA}}(t) = \langle n| H_{\mathrm{NA}} |n\rangle (t) = \frac{\hbar}{2}\begin{pmatrix} \omega_q z + n\chi(t) & \omega_q x \\ \omega_q x & -\omega_q z - n\chi(t) \end{pmatrix} + \hbar\omega_c n \tag{4.6}$$

where, for simplicity, we took $x_0 = 0$ and $v_0 = 1$ and introduced $\chi(t) \equiv \chi f(t)$. This Hamiltonian has for eigenstates:

$$\begin{aligned} \left|e_{\Theta,n}\right\rangle &= \cos\left(\Theta_n/2\right)\left|e_z\right\rangle + \sin\left(\Theta_n/2\right)\left|g_z\right\rangle \\ \left|g_{\Theta,n}\right\rangle &= -\sin\left(\Theta_n/2\right)\left|e_z\right\rangle + \cos\left(\Theta_n/2\right)\left|g_z\right\rangle \end{aligned} \tag{4.7}$$

with $\tan\left(\Theta_n(t)\right) = \frac{\omega_q x}{\omega_q z + n\chi(t)}$ and respective eigenvalues $\hbar\omega_c n + E_n(t)$ and $\hbar\omega_c n - E_n(t)$ given that:

$$E_n(t) = \frac{\hbar}{2}\sqrt{(\omega_q z + n\chi(t))^2 + (\omega_q x)^2}. \tag{4.8}$$

Notice that for $n = 0$, omitting the subscript 0 to lighten the notations, we have

$$\begin{aligned} \sigma_\Theta \left|e_\Theta\right\rangle &= \left|e_\Theta\right\rangle, \\ \sigma_\Theta \left|g_\Theta\right\rangle &= -\left|g_\Theta\right\rangle \end{aligned} \tag{4.9}$$

and $E_0 = \frac{\hbar\omega_q}{2}$. In this subspace, the qubit and cavity state can always be written as:

$$\left|\psi_n(t)\right\rangle = (A_n(t)\left|e_z, n\right\rangle + B_n(t)\left|g_z, n\right\rangle)e^{-i\omega_c nt} \tag{4.10}$$

and the Schrödinger equation leads to:

$$i\hbar\begin{pmatrix} \dot{A}_n(t)e^{-i\omega_c nt} \\ \dot{B}_n(t)e^{-i\omega_c nt} \end{pmatrix} + i\hbar\begin{pmatrix} -i\omega_c n A_n(t)e^{-i\omega_c nt} \\ -i\omega_c n B_n(t)e^{-i\omega_c nt} \end{pmatrix} = H^n_{\text{na}}(t)\begin{pmatrix} A_n(t)e^{-i\omega_c nt} \\ B_n(t)e^{-i\omega_c nt} \end{pmatrix}. \tag{4.11}$$

Which simplifies to:

$$i\hbar\begin{pmatrix} \dot{A}_n(t) \\ \dot{B}_n(t) \end{pmatrix} = \begin{pmatrix} Z_n(t) & X \\ X & -Z_n(t) \end{pmatrix}\begin{pmatrix} A_n(t) \\ B_n(t) \end{pmatrix}, \tag{4.12}$$

by defining

$$\begin{aligned} X &= \hbar\omega_q x/2, \quad \text{and} \\ Z_n(t) &= \hbar(\omega_q z + n\chi(t))/2. \end{aligned} \tag{4.13}$$

To solve this system analytically, we need to make some further assumptions. Especially, since we want to apply this model to the specific case of the σ_z operator measurement on the initial qubit state, the total duration of the interaction, and hence the speed v_0, must be carefully chosen.

Since we want to track the origin of the quantum heat we have no other choice but to take a bare Hamiltonian of the qubit which does not commute with σ_z, i.e., take $x \neq 0$. However, ideally, we would like to perform the pre-measurement associated to a quantum non demolition

(QND) measure of the qubit in the σ_z basis. Although measurement are usually considered as instantaneous, we here want to zoom in the dynamics of this measurement. However, the average value of σ_z should still remain almost constant in order for the measurement to provide some information about this observable. Thus, the dynamics has to happen on a time-scale t_m such that $\langle\sigma_z\rangle(0) \approx \langle\sigma_z\rangle(t_m)$. Two regimes are interesting in this regard:

- the **very strong interaction** one: $\omega_q \ll \chi$, where, starting at some time t_1 and until a time t_2, we have $X \ll Z_n(t)$. In this case, the tilt of the initial quantization axis with respect to the measurement one: Θ with $\tan(\Theta) = x/z$, can be arbitrary and the small parameter is $\boldsymbol{\mu = \omega_q/\chi}$. Notice that with a gaussian shaped potential t_1 can be taken arbitrarily close to 0 and t_2 to t_m as long as χ is large enough to ensure $n\chi(t_1) \gg x\omega_q$ and $n\chi(t_2) \gg x\omega_q$. In this case, the measurement time t_m will be fast enough that the evolution under σ_Θ will only be a small perturbation to the dynamics.
- the **small tilt regime**, where $x \ll z$ leading to the small parameter $\boldsymbol{\epsilon = x/z}$ and thus $\Theta \ll 1$. In this case $X \ll Z_n(t)$ at every time $t \in [0, t_m]$.

In both these regimes, we can use a perturbative expansion with respect to the small parameter $\epsilon_n = \max\{X/Z_n(t)\}_t$ in the appropriate time window ($[t_1, t_2]$ in the strong interaction case and $[0, t_m]$ in the small tilt one). Indeed no mather if $x \ll z$ or if $\omega_q \ll \chi$, we will have $\epsilon_n \ll 1$. For notation simplicity we will take the time window associated to the small tilt case. At zeroth order in ϵ_n, we obtain the ideal evolution:

$$(A|e_z\rangle + B|g_z\rangle) \otimes |\alpha\rangle \xrightarrow[e^{-i\int_0^t H_{\mathrm{NA}}(t)dt}]{\text{0th order}} Ae^{-i\omega_q zt/2}|e_z\rangle|\tilde{\alpha}_-^t\rangle + Be^{i\omega_q zt/2}|g_z\rangle|\tilde{\alpha}_+^t\rangle, \tag{4.14}$$

with

$$\tilde{\alpha}_-^t = \alpha e^{-i/2\int_0^t \chi(t')dt'}e^{-i\omega_c t} \quad \text{and} \quad \tilde{\alpha}_+^t = \alpha e^{i/2\int_0^t \chi(t')dt'}e^{-i\omega_c t}, \tag{4.15}$$

since $e^{-|\alpha|^2/2}\sum_n \frac{\alpha^n e^{-i\int_0^t \chi(t)dtn/2}e^{-i\omega_c nt}}{\sqrt{n!}}|n\rangle = \left|\alpha e^{-i\int_0^t \chi dt/2}e^{-i\omega_c t}\right\rangle$.

We solve Eq. (4.12) by cutting the total time duration into slices. Over a sufficently small duration $[0, 2dt]$, this first slice is such that $\chi(t) \approx \chi(dt)$. Thus, by considering Z_n constant and at first order in $X/Z_n(dt)$, the resulting coefficients can be written as:

$$\begin{aligned} A_n(t) &= A_n(0)e^{-iZ_n(dt)t/\hbar} - \frac{X}{2Z_n(dt)}B_n(0)(-e^{-iZ_n(dt)t/\hbar} + e^{iZ_n(dt)t/\hbar}) \\ B_n(t) &= B_n(0)e^{iZ_n(dt)t/\hbar} - \frac{X}{2Z_n(dt)}A_n(0)(-e^{-iZ_n(dt)t/\hbar} + e^{iZ_n(dt)t/\hbar}) \end{aligned} \tag{4.16}$$

for $t \in [0, 2dt]$. Repeating this procedure for the next time intervals and going back to continuous time, we obtain for $t > 0$:

$$\begin{aligned} A_n(t) =& A_n(0)e^{-i\int_0^t Z_n(t')dt'/\hbar} - iB_n(0)\frac{X}{\hbar}\int_0^t e^{i\int_0^{t'} Z_n(t'')dt''/\hbar}e^{-i\int_{t'}^t Z_n(t'')dt''/\hbar}dt' \\ B_n(t) =& B_n(0)e^{i\int_0^t Z_n(t')dt'/\hbar} - iA_n(0)\frac{X}{\hbar}\int_0^t e^{-i\int_0^{t'} Z_n(t'')dt''/\hbar}e^{i\int_{t'}^t Z_n(t'')dt''/\hbar}dt', \end{aligned} \tag{4.17}$$

interestingly, these coefficients can also be obtained by using the Dyson serie formalism. The mathematical details about this method and the time discretization used to go from Eq. (4.16) to Eq. (4.17) are given in the Appendix 4.5
Using the assumption that $\frac{d\chi}{dt} \ll \omega_q^2 z^2$, i.e., that the spatial shape of the interaction profil is smooth enough, these coefficients simplify to (see Appendix 4.5 for more details):

$$\begin{aligned} A_n(t) =& A_n(0)P_n^*(t) - B_n(0)\frac{\omega_q x}{2}\left(\frac{P_n(t)}{\omega_q z + n\chi(t)} - \frac{P_n^*(t)}{\omega_q z + n\chi(0)}\right) \\ B_n(t) =& B_n(0)P_n(t) + A_n(0)\frac{\omega_q x}{2}\left(\frac{P_n^*(t)}{\omega_q z + n\chi(t)} - \frac{P_n(t)}{\omega_q z + n\chi(0)}\right) \end{aligned} \tag{4.18}$$

where the phase factor is given by $P_n(t) = e^{i\int_0^t Z_n(t')dt'/\hbar} = e^{i\omega_q zt/2}e^{\frac{i}{2}n\int_0^t \chi(t')dt'}$. From Eq. (4.18), we recognize the zeroth order evolution given by the time dependent phase factor and the first order evolution in ϵ_n which is given by the terms on the right. Note that the only assumptions about the f function here is that it is a smooth integrable $\mathcal{C}^1$ function. Without loss of generality, we take $\int_0^{t_m} f(t)dt = 1$, the strength of the interaction being set by χ such that $\int_0^{t_m} \chi(t)dt = \chi$ with $\chi(t) = \chi f(t)$.
Defining $U_{\text{NA}}(t) = e^{-\frac{i}{\hbar}\int_0^t (H_0 + V_1 f(t))dt} = \sum_n U_{\text{NA}}^n |n\rangle\langle n|$, Eq. (4.18) implies that:

$$\begin{aligned} U_{\text{NA}}^n(t) &= e^{-\frac{i}{\hbar}\int_0^t (H_0 + \frac{\hbar\chi}{2} n\sigma_z f(t))dt} \\ &= \begin{pmatrix} P_n^*(t) & -\frac{x}{2z}\left(\frac{P_n(t)}{1+n\chi(t)/\omega_q z} - \frac{P_n^*(t)}{1+n\chi(0)/\omega_q z}\right) \\ \frac{x}{2z}\left(\frac{P_n^*(t)}{1+n\chi(t)/\omega_q z} - \frac{P_n(t)}{1+n\chi(0)/\omega_q z}\right) & P_n(t) \end{pmatrix} \end{aligned} \tag{4.19}$$

where we recall that $P_n(t) = e^{i\omega_q zt/2}e^{in/2\int_0^t \chi(t')dt'}$. At the end of the interaction, when $t = t_m$ such that $\chi(t_m) = \chi(0) = \chi$, the unitary operation U_{NA}^n can be simplified to:

$$U_{\text{NA}}^n(t_m) = \begin{pmatrix} e^{-i\omega_q zt_m/2}e^{-in/2\int_0^{t_m}\chi(t')dt'} & -i\frac{x}{z}\frac{\sin\left(\omega_q zt_m/2 + n/2\int_0^t \chi(t')dt'\right)}{1+n\chi/\omega_q z} \\ -i\frac{x}{z}\frac{\sin\left(\omega_q zt_m/2 + n/2\int_0^{t_m}\chi(t')dt'\right)}{1+n\chi/\omega_q z} & e^{i\omega_q zt_m/2}e^{in/2\int_0^{t_m}\chi(t')dt'}. \end{pmatrix}$$

The Equation 4.20 is the most general one, i.e., it is valid even if $\mu = \omega_q/\chi$ **or** $\epsilon = x/z$ are small parameters. Notice however than is can be simplied to

$$U_{\text{NA},\mu}^n(t) = \begin{pmatrix} (1 - i\omega_q zt/2)e^{-in/2\int_0^t \chi(t')dt'} & -\frac{\omega_q x}{2n}\left(\frac{e^{in/2\int_0^t\chi(t')dt'}}{\chi(t)} - \frac{e^{-in/2\int_0^t\chi(t')dt'}}{\chi(0)}\right) \\ \frac{\omega_q x}{2n}\left(\frac{e^{-in/2\int_0^t\chi(t')dt'}}{\chi(t)} - \frac{e^{in/2\int_0^t\chi(t')dt'}}{\chi(0)}\right) & (1 + i\omega_q zt/2)e^{in/2\int_0^t\chi(t')dt'} \end{pmatrix} \tag{4.20}$$

at first order in $\mu = \omega_q/\chi$.

Coming back to the most general case and using the coefficients of Eq. (4.18) in Eq. (4.10), we obtain the solution of the non-autonomous dynamics under the hypothesis that:

- Either $\omega_q \ll \chi$ (large coupling regime) or $x \ll z$ (small tilt regime).
- The derivative of the potential $\frac{d\chi}{dt}$ is much smaller that $\omega_q^2 z^2$.

This solution also works in the autonomous case if (as will be shown in next section):

- the particule is massive enough that it can be considered point-like and its position does not get correlated with the IDoF.
- the kinetic energy $\langle \frac{\hat{p}^2}{2m} \rangle$ is much larger that the potential amplitude $\frac{\hbar}{2}\chi\langle a^\dagger a\rangle$ to allow us to neglect any reflexion of the particle wavefunction.

If the initial state of the cavity is the coherent state $|\alpha\rangle$ (α is taken real to lighten a bit the notation) and the qubit in the arbitrary state $A_n(0)|e\rangle + B_n(0)|g\rangle$, with $A_n^2(0) + B_n^2(0) = 1$, which at time zero do not depend on n, the final solution can eventually be written as:

Box 3.2: Non Autonomous solution (cavity meter)

$$\begin{aligned}
|\psi_{\mathrm{NA}}\rangle(t) &= U_{\mathrm{NA}}(t)\left(A_n(0)|e\rangle + B_n(0)|g\rangle\right)\otimes|\alpha\rangle \\
&= \sum_n U^n_{\mathrm{NA}}(t)e^{-\alpha^2/2}\frac{\alpha^n}{\sqrt{n!}}\left(A_n(0)|e\rangle + B_n(0)|g\rangle\right)e^{-i\omega_c nt}|n\rangle \qquad (4.21)\\
&= |\psi\rangle^{(0)}(t) + |\psi\rangle^{(1)}(t) \qquad (4.22)
\end{aligned}$$

where the zeroth and first order contributions in , resp. $|\psi\rangle^{(0)}(t)$ and $|\psi\rangle^{(1)}(t)$, write:

$$\begin{aligned}
|\psi\rangle^{(0)}(t) &= A_n(0)e^{-i\omega_q zt/2}\left|e_z,\tilde{\alpha}^t_-\right\rangle + B_n(0)e^{i\omega_q zt/2}\left|g_z,\tilde{\alpha}^t_+\right\rangle \\
|\psi\rangle^{(1)}(t) &= -\sum_n \frac{B_n(0)x}{2z\sqrt{n!}}e^{-|\alpha|^2/2}\left(\frac{e^{i\omega_q zt/2}(\tilde{\alpha}^t_+)^n}{1+n\chi(t)/\omega_q z} - \frac{e^{-i\omega_q zt/2}(\tilde{\alpha}^t_-)^n}{1+n\chi(0)/\omega_q z}\right)|e_z,n\rangle \\
&\quad + \sum_n \frac{A_n(0)x}{2z\sqrt{n!}}e^{-|\alpha|^2/2}\left(\frac{e^{-i\omega_q zt/2}(\tilde{\alpha}^t_-)^n}{1+n\chi(t)/\omega_q z} - \frac{e^{i\omega_q zt/2}(\tilde{\alpha}^t_+)^n}{1+n\chi(0)/\omega_q z}\right)|g_z,n\rangle
\end{aligned}$$

with the complex numbers $\tilde{\alpha}^t_-$ and $\tilde{\alpha}^t_+$ defined in Eq. (4.15).

When $\chi = \chi(t) = \chi(0)$ and that the initial state of the cavity $|\alpha\rangle$ is such that $|\alpha|^2 \gg 1$ with $\alpha \in \mathbb{R}$ and $|\alpha|^2\chi \gg 1$, or if $\omega_q \ll \chi$, the first order contribution in $\mu = \omega_q/\chi$ becomes :

$$
\begin{aligned}
|\psi\rangle^{(1)}(t) = &- \sum_n \frac{B_n(0)x\omega_q}{\sqrt{n!}n\chi}\alpha^n e^{-|\alpha|^2/2}\left(\frac{e^{i\omega_q zt/2}e^{in\chi t/2} - e^{-i\omega_q zt/2}e^{-in\chi t/2}}{2}\right)e^{-in\omega_c t}\,|e_z, n\rangle \\
&+ \sum_n \frac{A_n(0)x\omega_q}{\sqrt{n!}n\chi}\alpha^n e^{-|\alpha|^2/2}\left(\frac{e^{-i\omega_q zt/2}e^{-in\chi t/2} - e^{i\omega_q zt/2}e^{in\chi t/2}}{2}\right)e^{-in\omega_c t}\,|g_z, n\rangle \\
= &- \sum_n \frac{iB_n(0)x\omega_q}{\sqrt{n!}n\chi}\alpha^n e^{-|\alpha|^2/2}\sin\big(\omega_q zt/2 + n\chi t/2\big)e^{-in\omega_c t}\,|e_z, n\rangle \\
&- \sum_n \frac{iA_n(0)x\omega_q}{\sqrt{n!}n\chi}\alpha^n e^{-|\alpha|^2/2}\sin\big(\omega_q zt/2 + n\chi t/2\big)e^{-in\omega_c t}\,|g_z, n\rangle \\
= &- \frac{ix\omega_q}{\chi}e^{-|\alpha|^2/2}\sum_n \frac{\alpha^n}{\sqrt{n!}n}\sin(n/2\chi t)e^{-in\omega_c t}(B_n(0)\,|e_z, n\rangle + A_n(0)\,|g_z, n\rangle) \qquad (4.23)
\end{aligned}
$$

where the last equality is obtained by only keeping the zeroth order contribution from the sine function in order for the full term to be of order one.

The result of Box 3.2 conveys important messages. Firstly, it clearly appears that the cavity states evolves according on the IDoF of the particle and that the information is encoded in the phase of the field. Two pointer states indeed emerge: $|\tilde{\alpha}_+\rangle$ and $|\tilde{\alpha}_+\rangle$ which only differ by a phase factor exactly as expected from the zeroth order solution given in Eq. (4.14). However, the first order correction tells us that when $x \neq 0$, these pointer states are not perfectly correlated with the qubit's internal states. i.e., the information extraction is incomplete. This result is reminiscent of the WAY theorem introduced in Box 1.3. Indeed, once the interaction is turned on and assuming that the total Hamiltonian stays constant during the creation of correlations between the IDoFs, we are in the case of the measurement of an observable $\mathcal{O}^S = \sigma_z$ which does not commute with the total Hamiltonian which is a conserved quantity in this time interval.

Hence, the measurement cannot be fully accurate, i.e., the final state of the meter does not allow to know exactly the initial probabilities of the system to be in the $|e_z\rangle$ and $|g_z\rangle$ states.

4.2.2 Non-Autonomous energy exchanges

For now on focussing on the strong coupling case, for which $\omega_q \ll \chi$, we investigate the energy exchange cause by the obtained non-autonomous dynamic.

Maximizing the quantum heat

When $A_n(0) = -\sin(\theta/2)$ and $B_n(0) = \cos(\theta/2)$, i.e., for an initial state parametrized by θ in the zy plane of the Bloch sphere, the state at time t writes :

$$\begin{aligned}\left|\psi_{\mathrm{NA}}\right\rangle(t) = &-\sin(\theta/2)e^{-i\omega_q zt/2}\left|e_z, \tilde{\alpha}_-^t\right\rangle + \cos(\theta/2)e^{i\omega_q zt/2}\left|g_z, \tilde{\alpha}_+^t\right\rangle \\ &- \frac{ix\omega_q}{\chi}e^{-|\alpha|^2/2}\sum_n \frac{\alpha^n}{\sqrt{n!n}}\sin(n/2\chi t)e^{-in\omega_c t}(\cos(\theta/2)\left|e_z, n\right\rangle - \sin(\theta/2)\left|g_z, n\right\rangle)\end{aligned} \tag{4.24}$$

If $\theta = \Theta$, the initial state corresponds to the ground state of $H_{\mathrm{NA}}(t = 0)$ such that its average energy is $-E_0(0) = -\frac{\hbar}{2}\omega_q$, as defined in Eq.4.8. We then wonder how to choose θ in order to maximize the energy received by the measured qubit during the pre-measurement. Since the average energy of the meter cavity is not affected by the pre-measurement, due to $[H^S M, H^M] = 0$ and that the coupling energy is null at the beginning and end, due to the time dependent coupling constant being such that $\chi(0) = \chi(t_m) \approx 0$, we have that the change in the system average energy due to the pre-measurement, is also equal to the total energy change of the global system and meter system. At lowest order, using the quantities derived in Appendix 4.5.2 we find that they write:

$$\Delta\langle H_{\mathrm{S}}\rangle = \Delta\langle H_{\mathrm{NA}}\rangle = \frac{\hbar}{2}\omega_q(x\Delta\langle\sigma_x\rangle + z\Delta\langle\sigma_z\rangle) = x^2\frac{\hbar}{2}\omega_q \tag{4.25}$$

with $\Delta\langle.\rangle = \langle.\rangle(t_m^+) - \langle.\rangle(t_0^-)$.

The energy given to the total system is thus maximal when $x^2 = \sin^2(\theta) = 1$, i.e., when $\theta = \pi/2$. This means that the larger the angle between the initial qubit eigenenergy basis and measurement basis is, the more energy can be extracted. This is the case when the initial state of the qubit, i.e., the ground state of the bare Hamiltonian of the system qubit is $(\left|e_z\right\rangle + \left|g_z\right\rangle)/\sqrt{2}$.

Characterizing the energy exchanges

To characterize the nature of the energy exchanges, one can apply the BQE model described in Chapter 2, to the global Hamiltonian H_{NA} and its two associated subsystems: the qubit S and the cavity C. Independently of their initial state, doing so we find the generalized work and heat rates :

$$\begin{aligned}\frac{d}{dt}\mathcal{W}_{\mathrm{S}} &= -\frac{i}{\hbar}\mathrm{Tr}_{\mathrm{S}}\{[H^S, \mathcal{V}^S(t)]\rho^S(t)\} = -\frac{\hbar}{2}\chi(t)\omega_q x\langle a^\dagger a\rangle_{\rho^C}\langle\sigma_y\rangle_{\rho^S}(t) \\ \frac{d}{dt}\mathcal{Q}_{\mathrm{S}} &= \mathrm{Tr}\{[H^S, f(t)V_1]\chi^{SC}\} = -\frac{\hbar}{2}\chi(t)\omega_q x\langle\sigma_y \otimes a^\dagger a\rangle_{\chi^{QC}}(t) \\ \frac{d}{dt}\mathcal{W}_{\mathrm{C}} &= -\frac{i}{\hbar}\mathrm{Tr}_C\{[H^C(t), \mathcal{V}^C(t)]\rho^C(t)\} = -\frac{i}{\hbar}\mathrm{Tr}_C\{\left[\frac{\hbar}{2}\omega_c a^\dagger a, \frac{\hbar}{2}\chi(t)a^\dagger a\langle\sigma_z\rangle(t)\right]\rho^C(t)\} = 0 \\ \frac{d}{dt}\mathcal{Q}_{\mathrm{C}} &= \mathrm{Tr}\{[H^C, V_1]\chi^{SC}\} = 0\end{aligned}$$

since $[H^C, V_1] = 0$ and with $\mathcal{V}^S(t) = \chi(t)\sigma_z\langle a^\dagger a\rangle_{\rho^{C}(t)}$ and $\mathcal{V}^C(t) = \chi(t)a^\dagger a\langle\sigma_z\rangle_{\rho^{S}(t)}$. From these last equations, it appears that the cavity does not receive heat nor work whereas the measured qubit exchanges both heat and work. The external work done by modulating the interaction strength directly affects the interaction energy $\mathcal{V}_{SC}$ whose flux can be decomposed into:

$$\begin{aligned}
\dot{V}^{\otimes}_{SC} &= -\frac{i}{\hbar}\mathrm{Tr}([f(t)V_1, H_{\mathrm{NA}}]\rho^S \otimes \rho^C) = \frac{\hbar}{2}\omega_q\chi(t)\langle\sigma_y\rangle_{\rho^S}(t)\langle a^\dagger a\rangle_{\rho^C} \\
\dot{V}^{\chi}_{SC} &= -\frac{i}{\hbar}\mathrm{Tr}([f(t)V_1, H_{\mathrm{NA}}]\chi^{SC}) = \frac{\hbar}{2}\omega_q\chi(t)\langle\sigma_y \otimes a^\dagger a\rangle_{\chi^{SC}}(t) \\
\dot{V}^{ext}_{SC} &= \mathrm{Tr}(\frac{df(t)}{dt}V_1\rho^{SC}) = \frac{\hbar}{2}\frac{d\chi}{dt}(t)\langle\sigma_z \otimes a^\dagger a\rangle_{\rho^{SC}}(t).
\end{aligned} \tag{4.26}$$

The different quantities are summerized in the Table. 4.2. The path of the energy from the ex-

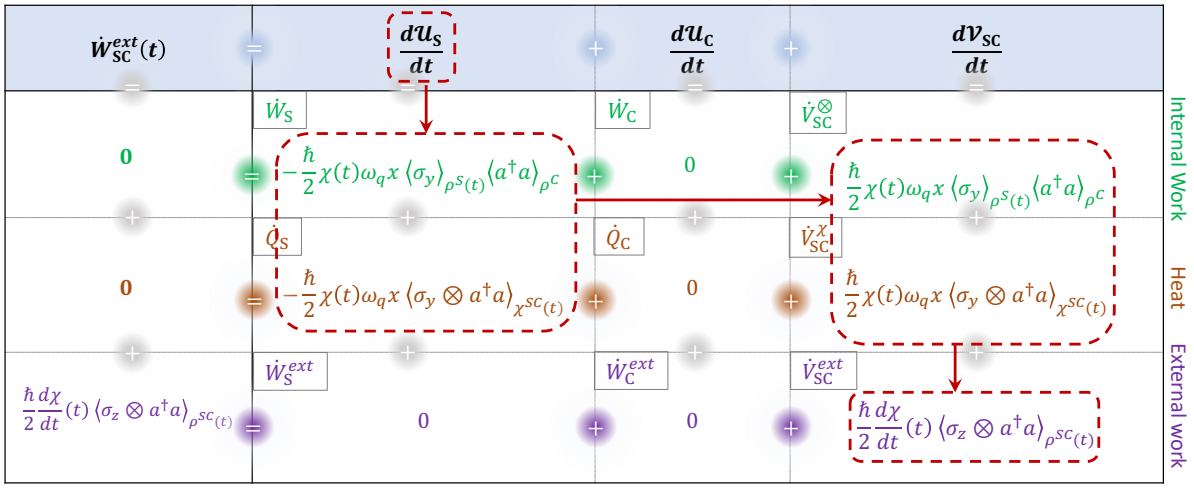

Figure 4.2: Energy fluxes leading to a change of the qubit system's energy due to its non autonomous measurement by a cavity field meter. The quantum heat received by the system appears to come from generalized heat *and* work fluxes, using the definitions of Chapter 2.

ternal work done on the total system W^{ext}_{SC} to the change of the system energy $\Delta\mathcal{U}_S = \int_{t_0}^{t_m}\frac{d\mathcal{U}_S}{dt}dt$ is similar to the one presented in Figure. 3.7 but with the addition of a work exchange between the interaction energy and the qubit system energy.

Simulating the total evolution using the python module qutip, we find that, with a gaussian shaped potential, as shown in Fig. 4.3, the total energy received almost exactly corresponds to the expected value of $\hbar\omega_q x^2/2$.

More surprisingly, the quantum heat is here found to partly come from the generalized work done on the system. This result is in contrast to the ones found in the previous chapter where we had $\langle V^M\rangle = \langle\sigma^M_x\rangle = 0$ at all times. Here instead, $\langle V^M\rangle_{\rho^{SM}(t)} = \langle V^M\rangle_{\rho^{M}(t)} = \langle V^C\rangle_{\rho^{C}(t)} = \langle a^\dagger a\rangle \neq 0$ since the meter is the cavity. This quantity is very important because, as we found in Eq. 3.32, the work done on the system, between the initial and final time t_0 and t_m, can be

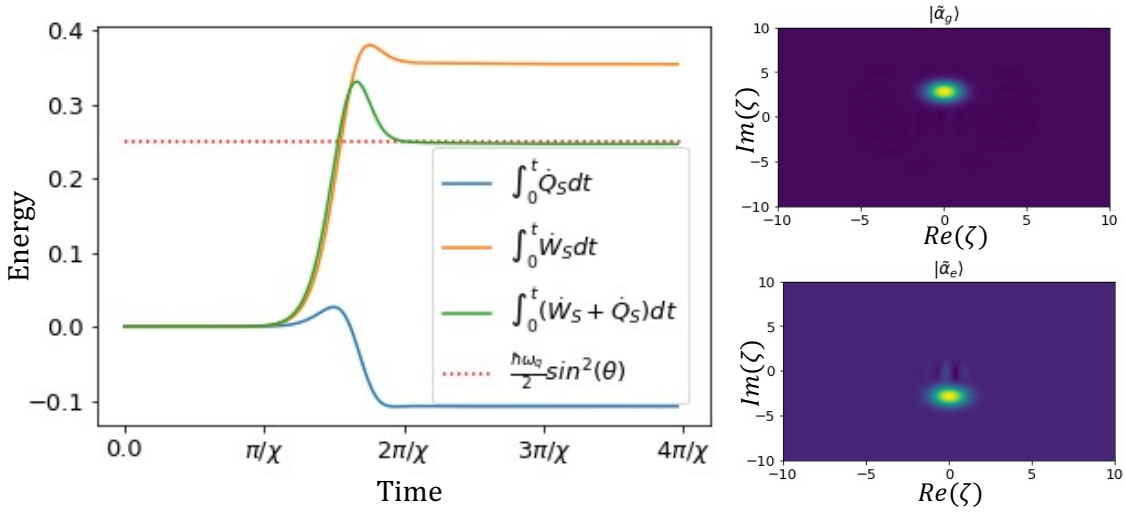

Figure 4.3: Non autonomous pre-measurement of a flying particule's IDoF. Left: Total work and heat received by the qubit during the pre-measurement. Right: Wigner distribution $W(\xi) = W(x = \mathrm{Re}(\xi), p = \mathrm{Im}(\xi)) = \frac{1}{\pi\hbar}\int_{-\infty}^{\infty} \langle x+y|\,\tilde{\alpha}^*(t_m)\,|x+y\rangle\,\langle x-y|\,\tilde{\alpha}(t_m)\,|x-y\rangle\, e^{-2ipy/\hbar} dy$ of the final state of the pointer state associated to $\left|\tilde{\alpha}_g\right\rangle(t_m)$ (up) and $\left|\tilde{\alpha}_e\right\rangle(t_m)$ (down). The function f is a gaussian function such that $f(t) = \frac{1}{\sigma\sqrt{2\pi}} e^{-(t-\mu)/2\sigma^2}$ with σ the width and μ the middle position of the potential. Parameters: $\omega_q = \omega_c = 1$; $\chi = 100$; $\Theta = \theta = \pi/4$; $\alpha = 2$; $\mu = 5\sigma/2$; $\sigma = \sqrt{\pi/2}/\chi$; duration $= 5\sigma$, Hilbert space dimension for the cavity DoF $= 20$.

written as:

$$\mathcal{W}^S\left(t_0 \to t_\mathrm{m}\right) = \langle V^M\rangle \int_{t_0}^{t_m} dt\,\dot{\chi}(t)\langle V^S\rangle(t). \tag{4.27}$$

which is hence proportional to $\langle V^M\rangle$.

One could suspect that increasing the coupling constant χ would lead to vanishingly small changes in $\langle V^S\rangle(t)$ during the interaction. This is indeed correct since, using Eq. 4.76, one has:

$$\langle V^S\rangle(t_m) - \langle V^S\rangle(0) = \langle\sigma_z\rangle(t_m) - \langle\sigma_z\rangle(0) \approx -2\sin(\theta)\omega_q t_m \underset{\chi\to\infty}{\propto} \frac{1}{\chi}.$$

assuming that the total duration time $\tau = t_\mathrm{m} - t_0 = t_m$ should be such that $n\chi\tau$ remain constant (and ideally close to π) in order to extract information about the qubit. However, one cannot remove $\langle V^S\rangle$ for the integral appearing in Eq. 4.27 and conclude that the work should vanish for symetric potential for which $\int_{t_0}^{t_m} dt\,\dot{\chi}(t) = 0$. Indeed, for a constant potential $\chi(t) = \chi$ for $t \in]t_0, t_m[$, applying the result of Eq. 3.38, the work done on the system can be rewritten as

$$\mathcal{W}^S\left(t_0 \to t_\mathrm{m}\right) = -A\tau\bar{n}\left(\frac{\langle\sigma_z\rangle(t_\mathrm{m}) - \langle\sigma_z\rangle(t_0)}{\tau}\right) = 2\sin(\theta)\omega_q A\tau\bar{n} \tag{4.28}$$

It is fascinating to notice that here, assuming an initial coherent state, minimizing $\langle V^M \rangle = \langle a^\dagger a \rangle$ would imply using a very low number of photon in the cavity and therefore result in low correlations between the system and meter due to large the overlap of the two pointer states $\left|\tilde{\alpha}^t_+\right\rangle$ and $\left|\tilde{\alpha}^t_-\right\rangle$. This is similar to the case of the previous chapter in which the measurement of a qubit by another qubit would have not created any correlations if the initial state of the meter qubit was maximizing or mimizing $\langle V^M \rangle_{qb:qb} = \langle \sigma_x \rangle$.

These results confirm that a larger indeterminacy of the meter initial state in the basis of the interaction term V^M, which is here a conserved quantity, leads to a higher accuracy of the measurement. They also pinpoint the non trivial relation between the quality of the correlation between the system and the meter and the nature of the energy received by the system.

Note also that, no matter the choice of bipartite time-independent Hamiltonian and the nature and initial state of the sub-systems, the work and heat fluxes are identically null if the interaction term commutes with the bare energy of the system, i.e., when there is no quantum heat.

4.3 Autonomous modelling

Coming back to the general case of a flying particle interacting with a fixed scatter, we here derive the dynamic of the IDoF from the autonomous modelling. Since the KDoF will not be considered classical enough that it is not affected by the interaction with the scatterer anymore, the IDoFs' reduced dynamic will depart from the non-autonomous unitary one. We are interested here in the effect of this perturbation on the quality of the KDoF as a work source. Note that the autonomous solution derived here is very general and could be applied to any type of meter and even to situations other than pre-measurements.

4.3.1 Autonomous dynamics

In the previous analysis, the dynamics was non-autonomous since the total Hamiltonian was time dependent. Here instead, we model the varying interaction by considering a quantum description of the flying particle position during its passage through an interaction region, as depicted in the right pannel of Figure 4.1. By including its kinetic degree of freedom into the model we can use the Hamiltonian given in Eq.4.1 which is indeed time independent. To study

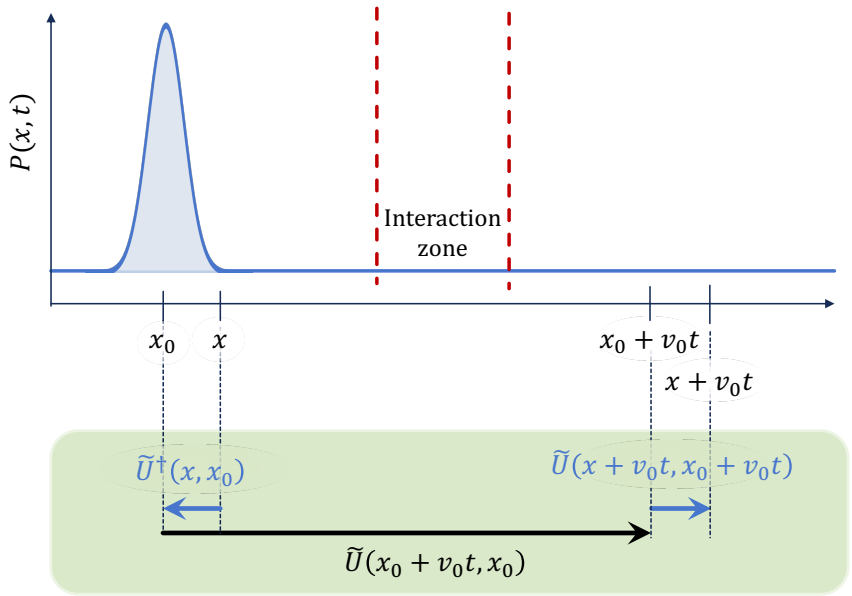

Figure 4.4: Top Panel: Initial space probability distribution of a heavy particle. The interaction zone is pictured by the red dashed lines. Bottom Panel: representation of the decomposition employed to Taylor expand the unitary evolution $\tilde{U}(x + v_0 t, x)$ around the evolution given by $\tilde{U}(x_0 + v_0 t, x_0)$. If the wavepacket is sufficiently localized, we can Taylor expand $\tilde{U}^\dagger(x, x_0)$ and $\tilde{U}(x + v_0 t, x_0 + v_0 t)$.

the dynamics of a heavy particle, we make use of an approximation which, to the best of our knowledge, was first introduced in Ref. [131]. We define the operator $\hat{q} = \hat{p} - p_0$ where p_0 is the average momentum of the initial state of the particle. By substituting back $\hat{p}$ in Eq. (4.1) we get

$$H \simeq v_0 \hat{q} + H_0 + f(\hat{x}) \otimes V_1, \tag{4.29}$$

where $v_0 = p_0/m$ and we neglected the term $p_0^2/(2m)$ for being a constant and the term $\hat{q}^2/(2m)$, associated to momentum fluctuations, because we assume it is negligible. Once v_0 is fixed, the term $\hat{q}^2/(2m)$ goes to zero for $m \to \infty$. The regime described by Eq. (4.29) is of special interest because it is solvable while maintaining the motion quantum. Due to the form of Eq. (4.29) the wavepacket travels at constant speed v_0 without being deformed. This can be easily seen in the Heisenberg representation of the position operator. We get $\hat{x}_H(t) = \hat{x}_H(0) + v_0 t$, where we assumed $t_0 = 0$ and the subscript H denotes Heisenberg representation. For this reason, a system described by the Hamiltonian of Eq. (4.29) is sometimes referred to as a *Quantum Clock* [131, 132, 133], especially in connection to theory of quantum measurements. We will adhere to this terminology by referring to the Hamiltonian of Eq. (4.29) as the *clock Hamiltonian*. It may seem counter intuitive that the particle momentum can change even if its velocity is constant. As we will show later, this effect can be traced back to the fact that the phase of the spatial wavepacket will vary differently, with respect to the position, depending on the interaction strength and IDoF state.

The Hamiltonian of Eq. (4.29) can be exactly solved when the exact solution of the non-autonomous dynamics is known. The formal solution for the non-autonomous dynamics of the IDoF associated to the evolution from x to $x + v_0 t$ is given in the form of the unitary operator

$$\tilde{U}(x + v_0 t, x) = \mathcal{T} \exp\left[-\frac{i}{\hbar} \int_0^t \mathrm{d}s \, \tilde{H}(x + v_0 s)\right], \tag{4.30}$$

where $\mathcal{T}$ is the time-ordering operator and we defined the position-dependent Hamiltonian $\tilde{H}(x) \equiv H_0 + f(x)V_1 = H_{\mathrm{NA}}(\frac{x - x_0}{v_0})$. Notice that, unlike the two last terms in Eq 4.29, $\tilde{H}(x)$ only acts on the IDoF and not on the KDoF.

The most generic state at time $t = 0$ can be written as $\langle x|\rho(0)|y\rangle = A_0(x, y)\rho_0(x, y)$, where $|x\rangle$ and $|y\rangle$ are position eigenstates in the kinetic degree of freedom (KDoF) Hilbert space and $\rho_0(x, y)$ is an operator in the IDoFs Hilbert space associated to the couple of spacial points (x, y). We take $A_0(x, x) \geq 0$ and $\rho_0(x, x)$ to be a proper density matrix, so that $A_0(x, x)$ represents the probability density function of finding the particle at point x at $t = 0$. When the initial state is a product state, $\rho_0(x, y)$ does not depend on (x, y) and one can simply write ρ_0. Moreover, if the initial state of the KDoF is pure, $A_0(x, y) = \psi_0(x)\psi_0^*(y)$, where $\psi_0(x)$ is the wavefunction of the KDoF at time $t = 0$. Therefore, by linearity of the Schrödinger equation, the solution for a generic wavepacket $\psi_0(x)$ is given by

$$\langle x + v_0 t|\psi(t)\rangle = \psi_0(x)\tilde{U}(x + v_0 t, x)\,|\psi_{\mathrm{int}}\rangle\,, \tag{4.31}$$

where $|\psi_{\text{int}}\rangle$ is the initial state of the IDoF, which we assumed to be uncorrelated with the KDoF at the start of the dynamics. In the most general case, at time t, the state can be written as:

$$\langle x + v_0 t|\rho(t)|y + v_0 t\rangle = A_0(x, y)U_x(t)\rho_0(x, y)U_y^\dagger(t), \tag{4.32}$$

where we defined $U_x(t) \equiv \tilde{U}(x + v_0 t, x)$. By tracing over the IDoFs, the density operator for the KDoF is

$$\langle x + v_0 t|\rho_K(t)|y + v_0 t\rangle = A_0(x, y)\,\mathrm{Tr}\left[U_x(t)\rho_0(x, y)U_y^\dagger(t)\right], \tag{4.33}$$

while tracing over the KDof, the density matrix of the IDoFs is

$$\rho_I(t) = \int_{-\infty}^{+\infty} \mathrm{d}x\, A_0(x, x)U_x(t)\rho_0(x, x)U_x^\dagger(t). \tag{4.34}$$

Notice that $\langle x|\rho_K(t)|x\rangle = A_0(x - v_0 t, x - v_0 t)$, i.e., the position probability density function travels at constant velocity v_0 no matter the interaction due to the form of the Clock Hamiltonian. Thus the solution can be written in terms of the non-autonomous solution given in Eq. (4.22) as long as the Clock Hamiltonian is a good approximation of the initial one.

If the traveling wavepacket is well localized in space (narrow but finite width) and that $\tilde{H}(x)$ varies on a larger scale than the wavepacket localization, we can greatly simplify Eq. (4.31). Within the Clock Hamiltonian formalism, the wavepacket moves from left to right at constant velocity v_0. After a time t the center of the wavepacket is located at $x_0 + v_0 t$. The evolution of the IDoF associated to x_0 is simply given by $U_{\text{NA}}(t) = \tilde{U}_{x_0}(t) = \tilde{U}(x_0+v_0 t, x_0)$, i.e., corresponds to the non autonomous solution. For all the other points, we can first evolve the IDoF from x to x_0 by means of $\tilde{U}(x_0, x)$, then from x_0 to $x_0 + v_0 t$ by means of $\tilde{U}(x_0 + v_0 t, x_0)$ and, finally, from $x_0 + v_0 t$ to $x + v_0 t$ by means of $\tilde{U}(x + v_0 t, x_0 + v_0 t)$. This consideration, illustrated in the bottom pannel of Fig. 4.4, allows us to simplify Eq. (4.31) as long as we can legitimately approximate $\tilde{U}(x_0, x)$ and $\tilde{U}(x + v_0 t, x_0 + v_0 t)$ by means of a Taylor expansion such that:

$$\tilde{U}_x(t) = \tilde{U}(x + v_0 t, x) = \tilde{U}(x + v_0 t, x_0 + v_0 t)\tilde{U}(x_0 + v_0 t, x_0)\tilde{U}^\dagger(x, x_0). \tag{4.35}$$

To obtain the contribution of the narrow wavepacket's spatial extension on the dynamic, we use the Dyson serie expansion of $\tilde{U}(x + v_0 t, x_0 + v_0 t) = \mathcal{T}\exp\left[-\frac{i}{\hbar}\int_0^{(x-x_0)/v_0} \mathrm{d}s\, \tilde{H}(x + v_0(t + s))\right]$ which writes:

$$\tilde{U}(x+v_0 t, x_0+v_0 t) \approx \mathbb{1} - \frac{i}{\hbar}\int_0^{t'} ds\tilde{H}(x_0+v_0(t+s)) - \frac{1}{2\hbar^2}\int_0^{t'}\int_0^{t'} dsds'\tilde{H}(x_0+v_0(t+s))\tilde{H}(x_0+v_0(t+s'))$$

where $t' = \delta x/v_0$ with $\delta x = x - x_0$.

Using the expansion $\tilde{H}(x_0 + v_0(t+s)) \approx \tilde{H}(x_0 + v_0 t) + v_0 s \partial_x \tilde{H}(x_0 + v_0 t)$ this becomes:

$$\begin{aligned}\tilde{U}(x + v_0 t, x_0 + v_0 t) \approx \mathbb{1} &- \frac{i}{\hbar}\int_0^{t'} ds(\tilde{H}(x_0 + v_0 t) + v_0 s \partial_x \tilde{H}(x_0 + v_0 t)) \\ &- \frac{1}{2\hbar^2}\int_0^{t'}\int_0^{t'} ds ds'(\tilde{H}(x_0 + v_0 t) + v_0 s \partial_x \tilde{H}(x_0 + v_0 t))(\tilde{H}(x_0 + v_0 t) + v_0 s' \partial_x \tilde{H}(x_0 + v_0 t)) \\ &= \mathbb{1} - i\frac{\delta x}{\hbar v_0}\tilde{H}(x_0 + v_0 t) - i\frac{\delta x^2}{2\hbar v_0^2} v_0 \partial_x \tilde{H}(x_0 + v_0 t) - \frac{1}{2}\left(\frac{\delta x}{\hbar v_0}\right)^2 \tilde{H}^2(x_0 + v_0 t).\end{aligned} \tag{4.36}$$

Thus, a similar Dyson serie expansion on $\tilde{U}^\dagger(x, x_0)$ we obtain:

$$\tilde{U}^\dagger(x, x_0) \simeq \mathbb{1} + i\frac{\delta x}{\hbar v_0}\tilde{H}(x_0) + \frac{i\delta x^2}{2\hbar v_0}\partial_x \tilde{H}(x_0) - \frac{1}{2}\left(\frac{\delta x}{\hbar v_0}\right)^2 \tilde{H}^2(x_0). \tag{4.37}$$

If the wavepacket starts at a position x_0, far from the interaction region, introducing $\tilde{H}_0 \equiv \tilde{H}(x_0) \approx H_0$, $\tilde{H}_t \equiv \tilde{H}(x_0 + v_0 t)$, $\tilde{H}_0' \equiv \partial_x \tilde{H}(x)|_{x_0}$ and $\tilde{H}_t' \equiv \partial_x \tilde{H}(x)|_{x_0 + v_0 t}$, and replacing Eq.(4.36) and Eq.(4.37) into Eq. (4.35), we get:

$$\begin{aligned}&\tilde{U}(x + v_0 t, x) \simeq \\ &\left(\mathbb{1} - i\frac{\delta x}{\hbar v_0}\tilde{H}_t - \frac{i\delta x^2}{2\hbar v_0}\partial_{x_0}\tilde{H}_t - \frac{1}{2}\left(\frac{\delta x}{\hbar v_0}\right)^2 \tilde{H}_t^2\right) U_{\mathrm{NA}}(t) \left(\mathbb{1} + i\frac{\delta x}{\hbar v_0}\tilde{H}_0 + \frac{i\delta x^2}{2\hbar v_0}\partial_{x_0}\tilde{H}_0 - \frac{1}{2}\left(\frac{\delta x}{\hbar v_0}\right)^2 \tilde{H}_0^2\right) \\ &= U_{\mathrm{NA}}(t) - \frac{i}{\hbar v_0}\delta x(\tilde{H}_t U_{\mathrm{NA}}(t) - U_{\mathrm{NA}}(t)\tilde{H}_0) \\ &\quad + \delta x^2\left[\frac{1}{\hbar^2 v_0^2}\left(\frac{-\tilde{H}_t^2 U_{\mathrm{NA}}(t) - U_{\mathrm{NA}}(t)\tilde{H}_0^2}{2} + \tilde{H}_t U_{\mathrm{NA}}(t)\tilde{H}_0\right) - \frac{i}{2\hbar v_0}(\partial_{x_0}\tilde{H}_t U_{\mathrm{NA}}(t) - U_{\mathrm{NA}}(t)\partial_{x_0}\tilde{H}_0)\right] \\ &= U_{\mathrm{NA}}(t) - i\frac{\delta x}{\hbar v_0}U_1(t) + \left(\frac{\delta x}{\hbar v_0}\right)^2 U_2(t)\end{aligned} \tag{4.38}$$

with the first and second order contribution:

$$\begin{aligned}U_1(t) &= \tilde{H}_t U_{\mathrm{NA}}(t) - U_{\mathrm{NA}}(t)\tilde{H}_0 \\ U_2(t) &= \tilde{H}_t U_{\mathrm{NA}}(t)\tilde{H}_0 - \frac{\tilde{H}_t^2 U_{\mathrm{NA}}(t) + U_{\mathrm{NA}}(t)\tilde{H}_0^2}{2} - \frac{i\hbar v_0}{2}\left(\tilde{H}_t' U_{\mathrm{NA}}(t) - U_{\mathrm{NA}}(t)\tilde{H}_0'\right).\end{aligned} \tag{4.39}$$

When the measurement is not tilted with respect to the bare Hamiltonian H_0, i.e., $[H_0, V_1] = 0$, it means that at all times $[\tilde{H}_t, U_{\mathrm{NA}}(t)] = 0$. However, the spatial extension still has some influence on the dynamics as long as $\tilde{H}_t \neq \tilde{H}_0$. At the final time however, long after the spatial wavepacket has left the interaction region, $\tilde{H}_t \approx \tilde{H}_0$ and U_1 and U_2 vanish. Indeed,

the component of the initial IDoF will acquire a slightly different phase during the interaction according on each possible initial position leading to correlations between the IDoFs and KDoF. But at the end, no matter the initial position, each of them will have interacted with the scattered IDoF for the same amount of time and therefore will have acquired the same phase.

We note that the initial spread of the wavepacket Δx is such that $(\Delta x)^2 = \int_{-\infty}^{\infty} (\delta x)^2 A_0(x,x)dx$. Moreover, we introduce the quantity $E_I(t)$, which is the typical energy scale of the IDoFs' bare Hamiltonian, such that the parameter $\varepsilon = \frac{E_I(t)\Delta x}{\hbar v_0}$ is dimensionless. From the result of Eq. (4.38) applied to the initial state ρ_0 of the IDoFs, we obtain, in the case when the initial state of the system is a product state of KDoF and IDoF, the global Autonomous solution:

Box 3.3: Autonomous solution

$$\rho(t) = \int_{-\infty}^{\infty}\int_{-\infty}^{\infty} dxdy A_0(x,y) \left|x + v_0 t\right\rangle \left\langle y + v_0 t\right| \tilde{U}_x(t)\rho_0 \tilde{U}_y^\dagger(t). \tag{4.40}$$

given that the global initial state is $\int_{-\infty}^{\infty}\int_{-\infty}^{\infty} A_0(x,y)\left|x\right\rangle\left\langle y\right| dxdy \otimes \rho_0$. And the reduced state of the IDoFs is given by:

$$\rho_{\text{IDoFs}}(t) \simeq \rho_C(t) = \rho_{NA}(t) + \left(\frac{E_I(t)\Delta x}{\hbar v_0}\right)^2 \mathcal{C}(\rho_0, t) \tag{4.41}$$

where the density operator $\rho_{NA}(t) = U_{\text{NA}}(t)\rho_0 U_{\text{NA}}^\dagger(t)$ is the solution of the non-autonomous dynamics governed by the time-dependent Hamiltonian $\tilde{H}(x_0 + v_0 t)$. Moreover, $\mathcal{C}(\rho_0, t)$ is what we call the *Correction Term*, defined as:

$$\mathcal{C}(\rho_0,t) = \frac{1}{E_I^2(t)}\Big(\left[\tilde{H}_t, U_{\text{NA}}\left[\tilde{H}_0,\rho_0\right]U_{\text{NA}}^\dagger\right] + U_{\text{NA}} D_{\tilde{H}_0}(\rho_0) U_{\text{NA}}^\dagger + D_{\tilde{H}_t}(U_{\text{NA}}\rho_0 U_{\text{NA}}^\dagger)$$
$$-\frac{i\hbar v_0}{2}[\tilde{H}_t', U_{\text{NA}}(t)\rho_0 U_{\text{NA}}^\dagger] - U_{\text{NA}}[\tilde{H}_0', \rho_0]U_{\text{NA}}^\dagger\Big), \tag{4.42}$$

where the time dependence of U_{NA} is kept implicit for concision and we recall that $\tilde{H}_0 \equiv \tilde{H}(x_0)$ and $\tilde{H}_t \equiv \tilde{H}(x_0 + v_0 t)$, and that their spatial derivatives are denoted by $\tilde{H}_0' \equiv \partial_x \tilde{H}(x)|_{x_0}$ and $\tilde{H}_t' \equiv \partial_x \tilde{H}(x)|_{x_0+v_0 t}$. We also introduced the notation $D_X(\rho) = X\rho X^\dagger - (1/2)\{X^\dagger X, \rho\}$.

Interestingly, the correction to the IDoF dynamics does not have a first order contribution. If the initial state is diagonal in the bare Hamiltonian basis, i.e., $[\rho_0, H_0] = 0$, such as when we start in its ground state, and that at the final time $\rho_{\text{NA}}(t_m)$ also commutes with H_0, the correction term completly vanishes at the final time t_m where $\tilde{H}_0' \approx \tilde{H}_t'(t_m) \approx 0$, $\tilde{H}_0 \approx H_0 \approx \tilde{H}_t(t_m)$. This is expected because in these conditions, the free evolution before and after entering the interaction region only comes as a phase factor on the IDoFs which are therefore in the same state when entering (and leaving) this region no matter the initial position of the wavepacket. At the

end of the evolution, an initial state $|\psi_{IDoF}\rangle(0) \otimes |\psi(x)\rangle$ becomes $|\psi_{IDoF}\rangle(t_m) \otimes |\psi'(x)\rangle$, i.e., no correlation remain between the KDoF and IDoFs. We must not conclude that this correction term is useless in this case however. Indeed, at intermediate times, the IDoF associated to a position on the left of the interaction region will have reached its final state whereas those associated to position still inside of this region not. There are thus correlations between KDof and IDoF at intermediate times which are important to take into account to characterize the nature of energy exchanges.

Moreover, in the perpective of the measurement of the operator V_1 such that $[H_0, V_1] \neq 0$, even when starting with a state such that $[\rho_0, H_0] = 0$, we will not have $[\rho_{\mathrm{NA}}(t_m), H_0] = 0$ except in very specific cases. However, before coming back to the particular measurement case, note that the results of the above box are very general and can be applied to any massive system with internal degrees of freedom interacting with a fixed system having itself internal degrees of freedom, via a position dependent term. Therefore, it is not limited to the study of quantum measurements. The KDoF could therefore very well serve as a work source to fuel the unitary manipulation of a qubit state for instance, in the limit of a classical particle. Thus, Equation. 4.41 is useful to access the second order departure from this ideal situation.

4.3.2 Autonomous measurement

In our specific measurement case, i.e., using the bare Hamiltonian from Eq. (4.3) and the interaction term of Eq. (4.4), and starting from the state ρ_0 for which the qubit is in the ground state of H^S we have $[\tilde{H}_0, \rho_0] = 0$ when the particle starts far enough from the interaction region such that $\tilde{H}(x_0) \approx H_0$. Hence, $\rho_{\mathrm{NA}}(t)$ is given by Eq. (4.22) and

$$\mathcal{C}(\rho_0, t) = \frac{1}{E_I^2(t)} \left(D_{\tilde{H}_t}(\rho_{\mathrm{NA}}(t)) - \frac{i\hbar v_0}{2} [\tilde{H}'_t, \rho_{\mathrm{NA}}(t)] \right), \tag{4.43}$$

since $D_{\tilde{H}_0}(\rho_0) = 0$ and $\tilde{H}'_0 \approx 0$. Moreover, at the final time t_m when the particle is far enough to the right of the interaction region, $\tilde{H}'_{t_m} \approx 0$ and the final state of the IDoFs reads:

$$\rho_C(t_m) = \rho_{NA}(t_m) + \left(\frac{\Delta x}{\hbar v_0} \right)^2 D_{H_0}(\rho_{\mathrm{NA}}(t_m)) \tag{4.44}$$

since at time t_m, $\tilde{H}_t = H_0$.

As a result, the final energy of the IDoF will be:

$$\langle H_0 \rangle_{\rho_c(t_m)} = \langle H_0 \rangle_{\rho_{NA}(t_m)} + \left(\frac{\Delta x}{\hbar v_0} \right)^2 \mathrm{Tr}(H_0 D_{H_0}(\rho_{\mathrm{NA}}(t_m))) = \langle H_0 \rangle_{\rho_{NA}(t_m)} \tag{4.45}$$

from the fact that $D_{H_0}(\rho_{\mathrm{NA}}(t_m)) = H_0 \rho_{\mathrm{NA}}(t_m) H_0^\dagger - (1/2)\{H_0^\dagger H_0, \rho_{\mathrm{NA}}(t_m)\}$ and the cyclicity property of the trace. Hence, the quantum heat received by the IDoFs derived in Eq. (4.25) is unaffected by the spatial extension of the KDoF at second order in $\frac{\Delta x}{\hbar v_0}$.

Efficiency of the Kinetic Degree of Freedom as a work source

Since we want to measure the IDoF of the flying particle via the cavity state, the KDoF would ideally couple and uncouple the IDoFs for the right amount of time without getting itself correlated with any of them. Assuming a gaussian shape for the initial wavepacket of the incoming particle, the narrower this distribution is in position, the closer to the ideal non-autonomous dynamic the evolution will be. From Heisenberg uncertainty relation, this implies that the initial momentum distribution Δp of the particle is large (at least such that $\Delta p > \hbar/\Delta x$). In this case, the IDoF's state dependent shift in momentum will lead to highly overlapping distribution associated to each of these possible states. Hence, there is a trade-off between the information acquired by the KDoF about the IDoF (which we want to avoid) and the quality of the measurement (here to be understood at the proximity to the ideal non autonomous dynamics).

When the KDoF acts as an ideal work source, the entire energy change of the IDoFs (of the meter and system) can be regarded as work, and the von Neumann entropy of the IDoFs does not change. This is not the case for a non-ideal work source. Therefore, the ratio between work done on the IDoF and energy change of the IDoF can be used to characterize the quality of the KDoF as a work source.

To define the work, we use again the definition of Chapter 2 where, this time,
the two parts of the bipartite system are: all the IDoFs (of the cavity and qubit) treated as a single system denoted I and the KDoF, denoted K.

Since the interaction between them is of the form $V^{KI} = V^K \otimes V^I$, the work fluxes within this bipartite system can be written as:

$$\dot{W}_K(t) = -\left\langle V^I \right\rangle_t \frac{\mathrm{d}}{\mathrm{d}t}\left\langle V^K \right\rangle_t ; \quad \dot{W}_I(t) = -\left\langle V^K \right\rangle_t \frac{\mathrm{d}}{\mathrm{d}t}\left\langle V^I \right\rangle_t ; \quad \dot{V}^{\otimes}_{KI}(t) = \frac{\mathrm{d}}{\mathrm{d}t}\left[\left\langle V^K \right\rangle_t \left\langle V^I \right\rangle_t\right].$$

with $V^K = f(\hat{x})$ and $V^I = V_1 = \frac{\hbar}{2}\chi\sigma_z \otimes a^\dagger a$. This implies, from integrating the equation $\dot{W}_K + \dot{W}_I + \dot{V}^{\otimes}_{IK} = 0$ between the initial time $t = 0$ and the final time $t = t_m$, that the work done on the IDoFs I is equal and opposite to the one done on the KDoF K since $\left\langle V^K \right\rangle_0 = \left\langle V^K \right\rangle_{t_m} = 0$. This does not imply, however, that the work fluxes are equal and opposite at intermediate times. To go farther, we note that the effective interaction term acting on the IDoFs is:

$$\mathcal{V}_I(t) = V_1 \,\mathrm{Tr}_K\left\{f(\hat{x})\rho_K(t)\right\}, \tag{4.46}$$

where $\rho_K(t)$ is the reduced density matrix of the KDoF at time t. Because of the structure of the Clock Hamiltonian, this effective Hamiltonian can be computed without the exact knowledge of the KDoF density operator such that:

$$\mathcal{V}_I(t) = V_1 I(t), \quad \text{where} \quad I(t) \equiv \int_{-\infty}^{+\infty} dx f(x) A_0(x - v_0 t, x - v_0 t). \tag{4.47}$$

where the function $I(t)$ only depends on the spatial profile of the potential $f(x)$, and the initial state of the KDoF.

In the case of a narrow wavepacket with respect to the typical scale over which the potential varies, we can use the approximated evolution given by $\rho_{\mathcal{C}}(t)$ (see Eq. (4.40)) and decompose the work flux done on the IDoFs into its ideal non-autonomous value plus another term. To do this, we expand the function $I(t)$ to first order in $\Delta x/L$ where L is the typical size of the interaction region:

$$I(t) = I_0(t) + I_\Delta(t), \text{where} \quad I_0(t) \equiv \int_{-\infty}^{+\infty} dx f(x)\delta(x - v_0 t - x_0) = f(x_0 + v_0 t)$$
$$\text{and} \quad I_\Delta(t) \equiv \int_{-\infty}^{+\infty} \frac{1}{2}\frac{\mathrm{d}^2 f}{\mathrm{d}x^2}\Big|_{x_0+v_0 t}(x - x_0)^2 A_0(x, x)\,\mathrm{d}x = \frac{(\Delta x)^2}{2}\frac{\mathrm{d}^2 f}{\mathrm{d}x^2}\Big|_{x_0+v_0 t}. \tag{4.48}$$

such that $I(t)$ becomes $I_0(t)$ in the limit of a point-like particle.
The work flux received by the IDoFs, can then be written:

$$\dot{W}_{\mathrm{I}} = -\frac{i}{\hbar}\mathrm{Tr}([H_0, \mathcal{V}_I(t)]\rho_I(t)) = -\frac{iI(t)}{\hbar}\mathrm{Tr}([H_0, V_1]\rho_I(t)) \tag{4.49}$$

with $\rho_I(t)$ the IDoFs reduced state at time t. We can now decompose this work flux into four pieces:

$$\dot{W}_{\mathrm{I}} = \dot{W}_{\mathrm{I}}^{NA} + \varepsilon^2\dot{W}_{\mathrm{I}}^{\mathcal{C}} + \dot{W}_{\mathrm{I}}^{\Delta} + \varepsilon^2\dot{W}_{\mathrm{I}}^{\Delta,\mathcal{C}}, \quad \text{where} \quad \varepsilon \equiv \frac{E_I \Delta x}{\hbar v_0}, \tag{4.50}$$

with the non-autonomous work flux defined as:

$$\dot{W}_{\mathrm{I}}^{NA} \equiv -\frac{\hbar\omega_q x\chi}{2} I_0(t)\mathrm{Tr}\left[\sigma_y \otimes a^\dagger a \rho_{\mathrm{NA}}(t)\right] \quad \text{and} \quad W_{\mathrm{I}}^{NA} = \int_0^{t_m} \dot{W}_{NA}\,\mathrm{d}t\,. \tag{4.51}$$

The correction terms are given by:

$$\dot{W}_{\mathrm{I}}^{\mathcal{C}} = -\frac{\hbar\omega_q x\chi}{2} I_0(t)\mathrm{Tr}\left[\sigma_y \otimes a^\dagger a\mathcal{C}(t)\right],$$
$$\dot{W}_{\mathrm{I}}^{\Delta} = -\frac{\hbar\omega_q x\chi}{2} I_\Delta(t)\mathrm{Tr}\left[\sigma_y \otimes a^\dagger a \rho_{NA}(t)\right],$$
$$\dot{W}_{\mathrm{I}}^{\Delta,\mathcal{C}} = -\frac{\hbar\omega_q x\chi}{2} I_\Delta(t)\mathrm{Tr}\left[\sigma_y \otimes a^\dagger a\mathcal{C}(t)\right]. \tag{4.52}$$

Since $I_\Delta(t)$ is of second order in Δx, so is $\dot{W}_{\mathrm{I}}^{\Delta}$ whereas $\dot{W}_{\mathrm{I}}^{\Delta,\mathcal{C}}$ is of order four and thus considered negligible. In the case of a spatially-narrow wavepacket with respect to the interaction region length-scale, the function $I_\Delta(t)$ is much smaller than $I_0(t)$ so that $\dot{W}_{\mathrm{I}}^{\Delta}$ is small with respect to $\dot{W}_{\mathrm{I}}^{NA}$. A non-autonomous energy exchange value can also be defined as

$$\Delta U_{\mathrm{I}}^{NA} \equiv \mathrm{Tr}\left\{H_0 \rho_{NA}(t_m)\right\} - \mathrm{Tr}\left\{H_0 \rho_{NA}(0)\right\}. \tag{4.53}$$

Since this is the ideal case scenario, one has that $W_{\mathrm{I}}^{NA} = \Delta U_{\mathrm{I}}^{NA}$. By using the IDoFs state obtained in Eq. (4.40) we can write the total energy exchange as

$$\Delta U_I \equiv \mathrm{Tr}\left[H_0\rho_C(t_m)\right] - \mathrm{Tr}\left[H_0\rho_C(0)\right] = \Delta U_I^{NA} + \varepsilon^2\Delta U_{\mathcal{C}}, \quad \text{where} \quad \Delta U_{\mathcal{C}} \equiv \mathrm{Tr}\left\{H_0\mathcal{C}(t_m)\right\}, \tag{4.54}$$

since $\mathcal{C}(0) = 0$. Building on these definitions, we introduce the following figure of merit η,

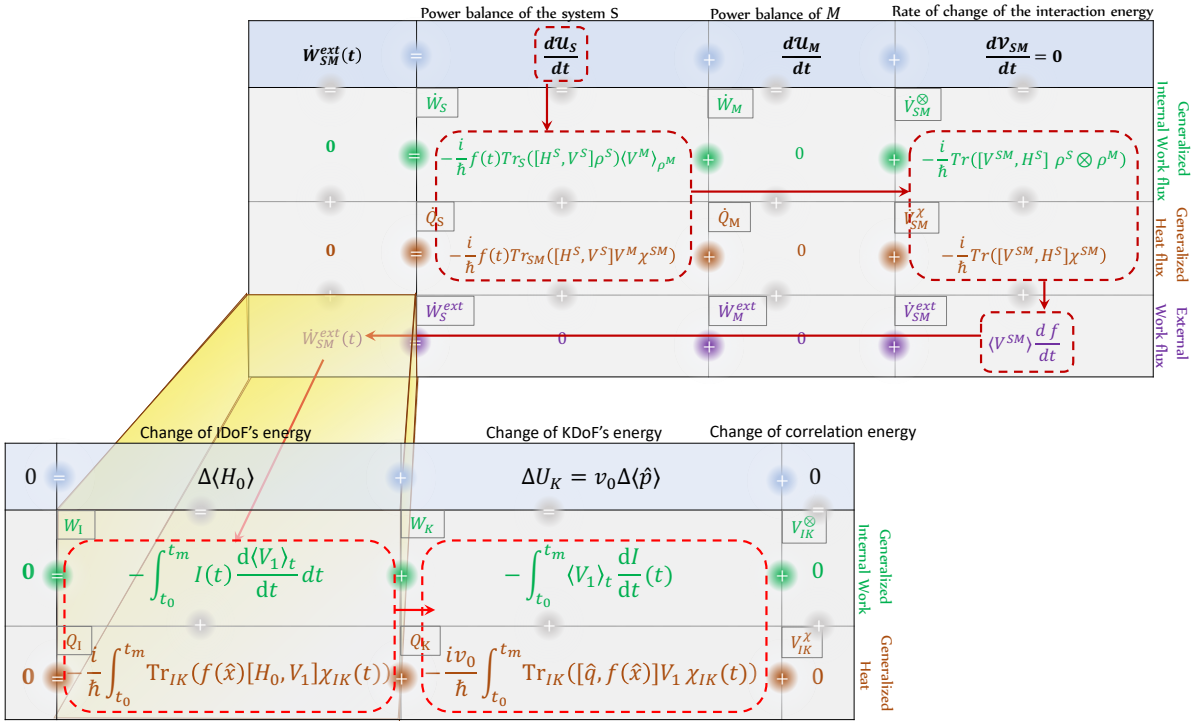

Figure 4.5: Origin of the Quantum heat in the Autonomous modelling. The above table links the energy exchanges between IDoFs obtained in the non-Autonomous analysis and summerized in Table. 4.2 and the current quantification of the generalized heat and work exchanges between the KDoF and IDoFs.

which we call "work transfer efficiency", for the work source:

$$\eta \equiv W_I/\Delta U_I, \quad \text{where} \quad W_I = \int_0^{t_m} \dot{W}_I \, \mathrm{d}t\,, \tag{4.55}$$

and t_m is a time such that the interaction between KDoF and IDoFs is practically zero. Importing the work and total energy decomposition given by the Eq. (4.51) and (4.54), we obtain the work transfer efficiency as a quadratic function of the wavepacket spatial extension:

$$\eta(\Delta x) \simeq \frac{W_{\mathrm{I}}^{NA} + \varepsilon^2 W_{\mathrm{I}}^{\mathcal{C}} + W_{\mathrm{I}}^{\Delta}}{\Delta U_{\mathrm{I}}^{NA} + \varepsilon^2 \Delta U_{\mathcal{C}}} \simeq 1 + \frac{W^{\Delta}}{\Delta U_{\mathrm{I}}^{NA}} + \varepsilon^2 \left(\frac{W_{\mathrm{I}}^{\mathcal{C}} - \Delta U_{\mathrm{I}}^{\mathcal{C}}}{\Delta U_{\mathrm{I}}^{NA}}\right). \tag{4.56}$$

Change of Kinetic energy

The change of energy of the momentum itself can also be computed and writes:

$$\begin{aligned}
\langle \hat{p} \rangle &= \mathrm{Tr}(\hat{p}\rho(t)) \\
&= \mathrm{Tr}\left[-i\hbar \int dx_2 \int_{-\infty}^{\infty}\int_{-\infty}^{\infty} |x_2\rangle \frac{d}{dx_2}\left(\langle x_2| \, x+v_0 t\rangle \langle y+v_0 t| \, A_0(x,y)\mathrm{Tr}\left[\tilde{U}_x(t)\rho_0\tilde{U}_y^\dagger(t)\right]\right) dxdy\right] \\
&= -i\hbar\mathrm{Tr}\left[\int dx_2 \int_{-\infty}^{\infty} |x_2\rangle \langle y+v_0 t| \frac{d}{dx_2}\left(A_0(x_2-v_0 t,y)\mathrm{Tr}\left[\tilde{U}_{x_2-v_0 t}(t)\rho_0\tilde{U}_y^\dagger(t)\right]\right) dy\right] \\
&= -i\hbar \int dx_2 \int_{-\infty}^{\infty} \mathrm{Tr}\left[|x_2\rangle \langle y+v_0 t|\right] \frac{d}{dx_2}\left(A_0(x_2-v_0 t,y)\mathrm{Tr}\left[\tilde{U}_{x_2-v_0 t}(t)\rho_0\tilde{U}_y^\dagger(t)\right]\right) dy \\
&= -i\hbar \int dx_2 \frac{d}{dx_2}\left(A_0(x_2-v_0 t,y)\mathrm{Tr}\left[\tilde{U}_{x_2-v_0 t}(t)\rho_0\tilde{U}_y^\dagger(t)\right]\right)_{|y=x_2+v_0 t} \\
&= -i\hbar \int dx \left(\frac{d}{dx}A_0(x,y)\right)_{|y=x} \mathrm{Tr}\left[\tilde{U}_x(t)\rho_0\tilde{U}_x^\dagger(t)\right] - i\hbar\int dx A_0(x,x)\mathrm{Tr}\left[\frac{d}{dx}\left(\tilde{U}_x(t)\right)\rho_0\tilde{U}_x^\dagger(t)\right] \\
&= \langle\hat{p}\rangle_0 - i\hbar\int dx A_0(x,x)\mathrm{Tr}\left[\frac{d}{dx}\left(\tilde{U}_x(t)\right)\rho_0\tilde{U}_x^\dagger(t)\right]. \qquad (4.57)
\end{aligned}$$

In order to analyse this formula, we introduce the change of kinetic energy which is given by:

$$\Delta U_K = v_0[\langle\hat{p}\rangle_{t_m} - \langle\hat{p}\rangle_0]. \qquad (4.58)$$

This energy change can be expanded in $\delta x = x - x_0$ by recalling that $\tilde{U}_x(t) = U_{\mathrm{NA}}(t) - i\frac{\delta x}{\hbar v_0}U_1(t) + \left(\frac{\delta x}{\hbar v_0}\right)^2 U_2(t)$, which implies $\frac{d}{dx}\left(\tilde{U}_x(t)\right) = \frac{-i}{\hbar v_0}U_1(t) + 2\left(\frac{\delta x}{(\hbar v_0)^2}\right)U_2(t)$. At zeroth order in δx, the momentum change is thus given by $\frac{-1}{v_0}\mathrm{Tr}\left[U_1(t)\rho_0 U_{\mathrm{NA}}^\dagger(t)\right]$ since, from the normalisation of the initial state, $\int dx A_0(x,x) = 1$. Therefore, at the final time t_m, when $U_1(t_m) = H_0 U_{NA}(t_m) - U_{\mathrm{NA}}(t_m)H_0$, the zeroth order kinetic energy change is $\Delta U_K^{(0)}(t_m) = \langle H_0\rangle_{\rho_0} - \langle H_0\rangle_{\rho_{\mathrm{NA}}(t_m)}$. This shows that, as expected from energy conservation, the change of energy of the IDoFs is exactly compensated by an equal and opposite change of kinetic energy.

Now, we analyse the impact of the spatial extension on this kinetic energy change. Given that $\int \delta x A_0(x,x)dx = \int x A_0(x,x)dx - x_0 = 0$, the first order contribution vanishes and at second order, for any intermediate time, we have:

$$\Delta U_K^{(2)}(t) = -\mathrm{Tr}\left[U_1(t)\rho_0 U_{\mathrm{NA}}^\dagger(t)\right] + \left(\frac{\Delta x}{\hbar v_0}\right)^2\left(2\mathrm{Tr}[U_2(t)\rho_0 U_1^\dagger(t)] - \mathrm{Tr}[U_1(t)\rho_0 U_2^\dagger(t)]\right)$$

At time t_m, since $\tilde{H}_{t_m} = \tilde{H}_0 = H_0$ and $H'_{t_m} = \tilde{H}_0 = 0$; when $[\rho_0, H_0] = 0$, we have:

$$\mathrm{Tr}(2U_2\rho_0 U_1^\dagger - U_1\rho_0 U_2^\dagger) = \frac{3}{2}\left(\langle H_0^3\rangle_{\rho_{\mathrm{NA}}(t_m)} - \langle H_0^3\rangle_{\rho_0} + \mathrm{Tr}(U_{\mathrm{NA}}^\dagger H_0^2 U_{\mathrm{NA}}\rho_0 H_0) - \mathrm{Tr}(U_{\mathrm{NA}}H_0^2\rho_0 U_{\mathrm{NA}}^\dagger H_0)\right)$$

where of course, when $[H_0, U_{\mathrm{NA}}(t)] = 0$, the change in kinetic energy vanishes because there is no quantum heat.

Measuring the work quantities

In order to experimentally access the work quantities described above, one particular case is of special interest. Consider a potential of shape:

$$f(x) = \begin{cases} A & \text{if } x \in [l, L-l] \\ \frac{Ax}{l}(1+\frac{x}{2l}) + \frac{A}{2} & \text{if } x \in [-l, 0] \\ \frac{Ax}{l}(1-\frac{x}{2l}) + \frac{A}{2} & \text{if } x \in [0, l] \\ -\frac{A(x-L)}{l}(1+\frac{(x-L)}{2l}) + \frac{A}{2} & \text{if } x \in [L-l, L] \\ -\frac{A(x-L)}{l}(1-\frac{(x-L)}{2l}) + \frac{A}{2} & \text{if } x \in [L, L+l] \\ 0 & \text{otherwise.} \end{cases} \tag{4.59}$$

This choice might seem very specific but it is simply an almost squared shape of arbitrary amplitude A and such that its second derivative is constant piecewise. The raising and diminishing regions are of lenght $2l$. Since the work flux done on the system is $\dot{W} = -I(t)\frac{d\langle H_1\rangle}{dt}$, we can decompose it into:

$$\begin{aligned} W_{NA} &= -\int_0^{t_m} I_0(t)\frac{d\langle H_1\rangle_{\rho_{NA}}}{dt}dt \approx -A\left(\langle H_1\rangle^L_{\rho_{NA}} - \langle H_1\rangle^0_{\rho_{NA}}\right) \\ \epsilon^2 W_{\mathcal{C}} &= -\epsilon^2\int_0^{t_m} I_0(t)\frac{d\langle H_1\rangle_{\mathcal{C}}}{dt}dt \approx -\epsilon^2 A\left(\langle H_1\rangle^L_{\mathcal{C}} - \langle H_1\rangle^0_{\mathcal{C}}\right) \end{aligned} \tag{4.60}$$

where $\langle H_1\rangle^x_\rho = \mathrm{Tr}(H_1\rho(t = (x-x_0)/v_0))$, we denote $I(x) = I(t = \frac{x-x_0}{v_0})$ and we neglected the integral over $[-l, l]$ and $[L-l, L+l]$ which goes to 0 with $l \to 0$. This is justified if we assume that $\langle H_1\rangle$'s evolution in these region is negligible. The remaining part of the work is proportional to $I_\Delta(t) = \frac{(\Delta x)^2}{2}\frac{\mathrm{d}^2 f}{\mathrm{d}x^2}\Big|_{x_0+v_0t}$ where

$$\frac{\mathrm{d}^2 f}{\mathrm{d}x^2}\Big|_{x_t} = \begin{cases} \frac{A}{l^2} & \text{if } x_t \in [-l, 0] \\ -\frac{A}{l^2} & \text{if } x_t \in [0, l] \\ -\frac{A}{l^2} & \text{if } x_t \in [L-l, L] \\ \frac{A}{l^2} & \text{if } x_t \in [L, L+l] \\ 0 & \text{otherwise.} \end{cases} \tag{4.61}$$

such that :

$$
\begin{aligned}
W_\Delta &= -\int_0^{t_m} I_\Delta(t)\frac{d\langle H_1\rangle_{\rho_{NA}}}{dt}dt = -\int_{-l}^{L+l} I_\Delta(x)\frac{d\langle H_1\rangle_{\rho_{NA}}}{dx}dx \\
&\approx -\frac{A(\Delta x)^2}{2l^2}\left[\int_{-l}^{0}\frac{d\langle H_1\rangle}{dx}dx - \int_0^{l}\frac{d\langle H_1\rangle}{dx}dx - \int_{L-l}^{L}\frac{d\langle H_1\rangle}{dx}dx + \int_{L}^{L+l}\frac{d\langle H_1\rangle}{dx}dx\right] \\
&= -\frac{A(\Delta x)^2}{l^2}\left(2\langle H_1\rangle_{\rho_{NA}}^{0} - 2\langle H_1\rangle_{\rho_{NA}}^{L} - \langle H_1\rangle_{\rho_{NA}}^{-l} - \langle H_1\rangle_{\rho_{NA}}^{l} + \langle H_1\rangle_{\rho_{NA}}^{L-l} + \langle H_1\rangle_{\rho_{NA}}^{L+l}\right)
\end{aligned}
\tag{4.62}
$$

by expansion. By assumption, we want the spatial extension of the wavepacket to be much smaller than the typical lenght of change of the potential, i.e., $\Delta x \ll l$. The work term W_Δ is therefore of second order in the small parameter $\Delta x/l$. The contribution of the correction term $\mathcal{C}$, is smaller than this last term if $\epsilon^2 \ll \frac{(\Delta x)^2}{l^2}$ which is equivalent to $\frac{E_I l}{\hbar v_0} \ll 1$. In this case, measuring the average quantities given by Eq. (4.62) would allow to deduce the heat and work exchange between KDoF and IDoFs during the pre-measurement process.

4.4 Conclusion

When a quantum system interacts with a quantum meter and receives quantum heat, we have seen in Chapter 3 that the incoming energy does not have to come from the meter itself but instead can come from the time dependent global Hamiltonian by which the interaction is turned on and off. In this chapter, we considered the case of a meter cavity field for which the energy levels are not degenerate. The average value of the interaction term acting on this field was hence chosen to be a constant, but non-null, quantity. This lead to modifications in the nature of the quantum heat which was found to be partially received in the form of work by the measured system. Its origin, however, is still the time-dependent modulation of the interaction between the meter and system. Such time dependence implicitly comes from the interaction with another system which is assumed to be classical, i.e., large enough that it is considered unaffected by the interaction with the quantum system and meter.

Here, we included this additional system, which is taken to be the kinetic degree of freedom of the measured particle, in the model. Therefore, the global system was isolated and the pre-measurement step autonomous. However, when the particle is not perfectly localized and hence that this kinetic degree of freedom is not perfectly classical anymore, the measurement dynamic can be affected. We found the correction to this dynamic at second order with respect to the spatial extension of the wavepacket.

This shines a new light on the question of the origin of the "quantum heat" which is now provided by the kinetic degree of freedom. Hence, a measurement can be fuelled by the one of the degree of freedom of the object it measures.

To go further, it is important to consider the cost of the full measurement cycle: including the reset of the meter state. Since we have seen how much the initial state of the meter and

hence the average value $\langle V^M \rangle$ matters to the nature of the energy exchanges, it is natural to study its impact on this total cost. We therefore compare the quality of a qubit measurement depending on the cavity field initial state in the following chapter.

4.5 Appendix

In order to keep the main discussion efficient and in order to help an interested reader who would like to follow the details of the derivations, we give here the explicit steps required to reach the conclusions discussed in this chapter.

4.5.1 Non Autonomous solution derivation

Time discretization method

We solve Eq. (4.12) by cutting the total time duration into slices. Over a sufficently small duration $[0, dt]$, this first slice is such that $\chi(t) \approx \chi(dt)$ and thus by considering Z_n constant and we obtain:

$$\begin{aligned}
A_n(t) = &\frac{1}{2\sqrt{X^2+Z_n^2}} e^{-it\sqrt{X^2+Z_n^2}/\hbar} \left(A_n(0) \left[\sqrt{X^2+Z_n^2}(1+e^{2it\sqrt{X^2+Z_n^2}/\hbar}) - Z_n e^{2it\sqrt{X^2+Z_n^2}/\hbar} + Z_n \right] \right. \\
&\left. - B_n(0) X (-1+e^{2it\sqrt{X^2+Z_n^2}/\hbar}) \right) \\
B_n(t) = &\frac{1}{2\sqrt{X^2+Z_n^2}} e^{-it\sqrt{X^2+Z_n^2}/\hbar} \left(B_n(0) \left[\sqrt{X^2+Z_n^2}(1+e^{2it\sqrt{X^2+Z_n^2}/\hbar}) + Z_n e^{2it\sqrt{X^2+Z_n^2}/\hbar} - Z_n \right] \right. \\
&\left. - A_n(0) X (-1+e^{2it\sqrt{X^2+Z_n^2}/\hbar}) \right)
\end{aligned} \tag{4.63}$$

At first order in $X/Z_n(dt)$, we use the following equivalence relationship:

$$\begin{aligned}
\sqrt{Z_n^2+X^2} &= Z_n + o(X/Z_n) \\
\frac{1}{\sqrt{Z_n^2+X^2}} &= \frac{1}{Z_n} + o(X/Z_n) \\
e^{-i\sqrt{Z_n^2+X^2}t/\hbar} &= e^{-iZ_n t/\hbar} + o(X/Z_n)
\end{aligned} \tag{4.64}$$

omitting the time dependence for concision. For $t \in [0, dt]$, the resulting coefficients thus are:

$$\begin{aligned} A_n(t) &= A_n(0)e^{-iZ_n(dt)t/\hbar} - \frac{X}{2Z_n(dt)}B_n(0)(-e^{-iZ_n(dt)t/\hbar} + e^{iZ_n(dt)t/\hbar}) \\ B_n(t) &= B_n(0)e^{iZ_n(dt)t/\hbar} - \frac{X}{2Z_n(dt)}A_n(0)(-e^{-iZ_n(dt)t/\hbar} + e^{iZ_n(dt)t/\hbar}) \end{aligned} \tag{4.65}$$

Solving Eq. (4.13) again starting from these new coefficients, $A_n(dt)$ and $B_n(dt)$, over the time period $t \in [dt, 2dt]$, such that $Z_n(t) \approx Z_n(2dt)$ we find:

$$\begin{aligned} A_n(2dt) =& A_n(0)e^{-i(Z_n(dt)+Z_n(2dt))dt/\hbar} \\ &- \frac{1}{2}B_n(0)\left[\frac{X}{Z_n(dt)}(-e^{-iZ_n(dt))dt/\hbar} + e^{iZ_n(dt)dt/\hbar})e^{-iZ_n(2dt))dt/\hbar}\right. \\ &\left. + \frac{X}{Z_n(2dt)}(-e^{-iZ_n(2dt)dt/\hbar} + e^{iZ_n(2dt)dt/\hbar})e^{iZ_n(dt)dt/\hbar}\right] \\ B_n(2dt) =& B_n(0)e^{i(Z_n(dt)+Z_n(2dt))dt/\hbar} \\ &- \frac{1}{2}A_n(0)\left[(\frac{X}{Z_n(dt)})\,(-e^{-iZ_n(dt)dt/\hbar} + e^{iZ_n(dt)dt/\hbar})e^{iZ_n(2dt)dt/\hbar}\right. \\ &\left. + (\frac{X}{Z_n(2dt)})(-e^{-iZ_n(2dt)dt/\hbar} + e^{iZ_n(2dt)dt/\hbar})e^{-iZ_n(dt)dt/\hbar}\right] \end{aligned} \tag{4.66}$$

eventually we obtain the formula at time kdt given by:

$$\begin{aligned} A_n(kdt) =& A_n(0)e^{-i\sum_{p=0}^{k} Z_n(pdt)dt/\hbar} \\ &- \frac{1}{2}B_n(0)\left[\sum_{j=1}^{k}\frac{X}{Z_n(jdt)}(-e^{-iZ_n(jdt)dt/\hbar} + e^{iZ_n(jdt)dt/\hbar})\prod_{l<j}e^{iZ_n(l.dt)dt/\hbar}\prod_{p>j}e^{-iZ_n(p.dt)dt/\hbar}\right] \\ B_n(kdt) =& B_n(0)e^{i\sum_{p=0}^{k} Z_n(pdt)dt/\hbar} \\ &- \frac{1}{2}A_n(0)\left[\sum_{j=1}^{k}\frac{X}{Z_n(jdt)}(-e^{-iZ_n(jdt)dt/\hbar} + e^{iZ_n(jdt)dt/\hbar})\prod_{l<j}e^{-iZ_n(l.dt)dt/\hbar}\prod_{p>j}e^{iZ_n(p.dt)dt/\hbar}\right] \end{aligned} \tag{4.67}$$

going back to continuous time we obtain (for $t > 0$):

$$\begin{aligned} A_n(t) =& A_n(0)e^{-i\int_0^t Z_n(t')dt'/\hbar} - iB_n(0)\frac{X}{\hbar}\int_0^t e^{i\int_0^{t'} Z_n(t'')dt''/\hbar}e^{-i\int_{t'}^t Z_n(t'')dt''/\hbar}dt' \\ B_n(t) =& B_n(0)e^{i\int_0^t Z_n(t')dt'/\hbar} - iA_n(0)\frac{X}{\hbar}\int_0^t e^{-i\int_0^{t'} Z_n(t'')dt''/\hbar}e^{i\int_{t'}^t Z_n(t'')dt''/\hbar}dt'. \end{aligned} \tag{4.68}$$

Dyson serie method

Interstingly, this coefficients can also be obtained by using the Dyson serie formalism with the perturbative operator:

$$U_I(t) = \mathbb{1} - \frac{i}{\hbar}\int_0^t U_0^\dagger(t) X \sigma_x U_0(t) dt \tag{4.69}$$

given that $U_0(t) = e^{-i\int_0^t Z_n(t)\sigma_z dt}$ is the zeroth order unitary operator.

Simplification of the coefficients A_n and B_n

In order to simplify the integral appearing in $A_n(t)$, we notice that:

$$\begin{aligned}
&\frac{d}{dt'}\left(-i\frac{e^{i\omega_q z(2t'-t)/2}e^{\frac{i}{2}n\int_0^{t'}\chi(t'')dt''}e^{-\frac{i}{2}n\int_{t'}^{t}\chi(t'')dt''}}{\omega_q z + n\chi(t')}\right)\\
&= \frac{e^{i\omega_q z(2t'-t)/2}e^{\frac{i}{2}n\int_0^{t'}\chi(t'')dt''}e^{-\frac{i}{2}n\int_{t'}^{t}\chi(t'')dt''}}{\omega_q z + n\chi(t')}(\omega_q z + n\chi(t')) - i\frac{e^{i\omega_q z(2t'-t)/2}e^{\frac{i}{2}n\int_0^{t'}\chi(t'')dt''}e^{-\frac{i}{2}n\int_{t'}^{t}\chi(t'')dt''}}{(\omega_q z + n\chi(t'))^2}(-n\frac{d\chi}{dt})
\end{aligned} \tag{4.70}$$

$$\approx e^{i\omega_q z(2t'-t)/2}e^{\frac{i}{2}n\int_0^{t'}\chi(t'')dt''}e^{-\frac{i}{2}n\int_{t'}^{t}\chi(t'')dt''} = e^{i\int_0^{t'}Z_n(t'')dt''/\hbar}e^{-i\int_{t'}^{t}Z_n(t'')dt''/\hbar}$$

where we neglected the second term in Eq. (4.70) by using the assumption that $\frac{d\chi}{dt} \ll \omega_q^2 z^2$. We therefore conclude:

$$\int_0^t e^{i\omega_q z(2t'-t)/2}e^{\frac{i}{2}n\int_0^{t'}\chi(t'')dt''}e^{-\frac{i}{2}n\int_{t'}^{t}\chi(t'')dt''}dt' \approx -i\left(\frac{e^{i\omega_q zt}e^{\frac{i}{2}n\int_0^t\chi(t'')dt''}}{\omega_q z + n\chi(t)} - \frac{e^{-i\omega_q zt}e^{-\frac{i}{2}n\int_0^t\chi(t'')dt''}}{\omega_q z + n\chi(0)}\right) \tag{4.71}$$

thus the coefficients of Eq. (4.17) can be rewritten as:

$$\begin{aligned}
A_n(t) =& A_n(0)e^{-i\int_0^t Z_n(t')dt'/\hbar} - B_n(0)\frac{\omega_q x}{2}\left(\frac{e^{i\omega_q zt/2}e^{\frac{i}{2}n\int_0^t\chi(t'')dt''}}{\omega_q z + n\chi(t)} - \frac{e^{-i\omega_q zt/2}e^{-\frac{i}{2}n\int_0^t\chi(t'')dt''}}{\omega_q z + n\chi(0)}\right)\\
B_n(t) =& B_n(0)e^{i\int_0^t Z_n(t')dt'/\hbar} + A_n(0)\frac{\omega_q x}{2}\left(\frac{e^{-i\omega_q zt/2}e^{\frac{-i}{2}n\int_0^t\chi(t'')dt''}}{\omega_q z + n\chi(t)} - \frac{e^{i\omega_q zt/2}e^{\frac{i}{2}n\int_0^t\chi(t'')dt''}}{\omega_q z + n\chi(0)}\right).
\end{aligned} \tag{4.72}$$

Eventually, by introducing the phase factor is given by $P_n(t) = e^{i\int_0^t Z_n(t')dt'/\hbar} = e^{i\omega_q zt/2}e^{\frac{i}{2}n\int_0^t\chi(t')dt'}$ we obtain:

$$\begin{aligned}
A_n(t) =& A_n(0)P_n^*(t) - B_n(0)\frac{\omega_q x}{2}\left(\frac{P_n(t)}{\omega_q z + n\chi(t)} - \frac{P_n^*(t)}{\omega_q z + n\chi(0)}\right)\\
B_n(t) =& B_n(0)P_n(t) + A_n(0)\frac{\omega_q x}{2}\left(\frac{P_n^*(t)}{\omega_q z + n\chi(t)} - \frac{P_n(t)}{\omega_q z + n\chi(0)}\right).
\end{aligned} \tag{4.73}$$

4.5.2 Useful quantities for average energy calculations

Taking, for the initial qubit state, the ground state of $H_{\text{na}}(0)$, i.e., $\theta = \Theta$ and $A_n(0) = -\sin(\theta/2)$, $B_n(0) = \cos(\theta/2)$, and choosing a strong coupling $\chi \gg \omega_q$, constant between t_0^+ and t_m^-, the dynamics writes (Eq. 4.24):

$$\begin{aligned}\left|\psi_{\text{NA}}\right\rangle(t) = &-\sin(\theta/2)e^{-i\omega_q zt/2}\left|e_z, \tilde{\alpha}_-^t\right\rangle + \cos(\theta/2)e^{i\omega_q zt/2}\left|g_z, \tilde{\alpha}_+^t\right\rangle \\ &-\frac{ix\omega_q}{\chi}e^{-|\alpha|^2/2}\sum_n \frac{\alpha^n}{\sqrt{n!}n}\sin(n/2\chi t)e^{-in\omega_c t}(\cos(\theta/2)\left|e_z, n\right\rangle - \sin(\theta/2)\left|g_z, n\right\rangle).\end{aligned}$$

In order to derive the change of average qubit energy $\Delta\langle H^S\rangle$, we first notice that:

$$\langle H^S\rangle(t) = \frac{\hbar\omega_q}{2}(x\langle\sigma_x\rangle(t) + z\langle\sigma_z\rangle(t)). \tag{4.74}$$

and that before the pre-measurement, at time $t_0^- = 0^-$:

$$\begin{aligned}\langle\sigma_z\rangle(t_0^-) &= \text{Tr}_C(\langle\psi_{\text{NA}}\left|\sigma_z\right|\psi_{\text{NA}}\rangle(t_0^-)) = \sin^2(\theta/2) - \cos^2(\theta/2) = -\cos(\theta) \\ \langle\sigma_x\rangle(t_0^-) &= \text{Tr}_C(\langle\psi_{\text{NA}}\left|\sigma_x\right|\psi_{\text{NA}}\rangle(t_0^-)) = -2\sin(\theta/2)\cos(\theta/2) = -\sin(\theta) \\ \langle\sigma_\theta\rangle(t_0^-) &= \text{Tr}_C(\langle\psi_{\text{NA}}\left|\sigma_\theta\right|\psi_{\text{NA}}\rangle(t_0^-)) = -x\sin(\theta) - z\cos(\theta) = -1.\end{aligned} \tag{4.75}$$

The last equality confirms that the chosen initial state is indeed the ground state of H^S. At first order in ω_q/χ, these quantities writes at an intermediate time $t \in [t_0, t_m]$:

$$\begin{aligned}\langle\sigma_z\rangle(t) = &\sum_n \left(-\sin(\theta/2)e^{-i\omega_q zt/2}e^{-|\alpha|^2/2}\frac{\alpha^n}{\sqrt{n!}}e^{-in\chi t/2} - \frac{ix\omega_q}{\chi}e^{-|\alpha|^2/2}\frac{\alpha^n}{\sqrt{n!}n}\sin(n/2\chi t)\cos(\theta/2)\right)(c.c) \\ &-\sum_n \left(\cos(\theta/2)e^{i\omega_q zt/2}e^{-|\alpha|^2/2}\frac{\alpha^n}{\sqrt{n!}}e^{in\chi t/2} + \frac{ix\omega_q}{\chi}e^{-|\alpha|^2/2}\frac{\alpha^n}{\sqrt{n!}n}\sin(n/2\chi t)\sin(\theta/2)\right)(c.c) \\ &= \sin^2(\theta/2) - \cos^2(\theta/2) \\ &-\frac{ix\omega_q}{\chi}\sin(\theta/2)\cos(\theta/2)e^{-|\alpha|^2}\sum_n \frac{\alpha^{2n}}{n!n}\left(e^{-i\omega_q zt/2}e^{-in\chi t/2} - e^{i\omega_q zt/2}e^{in\chi t/2}\right)\sin(n\chi t/2) \\ &+\frac{ix\omega_q}{\chi}\sin(\theta/2)\cos(\theta/2)e^{-|\alpha|^2}\sum_n \frac{\alpha^{2n}}{n!n}\left(e^{i\omega_q zt/2}e^{in\chi t/2} - e^{-i\omega_q zt/2}e^{-in\chi t/2}\right)\sin(n\chi t/2) \\ &\approx \langle\sigma_z\rangle(t_0^-) - 2\frac{x\omega_q}{\chi}\sin(\theta)e^{-|\alpha|^2}\sum_n \frac{\alpha^{2n}}{n!n}\sin^2(n\chi t/2)\end{aligned}$$

and

$$\begin{aligned}
\langle\sigma_x\rangle(t) =& -\sin(\theta/2)\cos(\theta/2)\left(e^{-i\omega_q zt}\left\langle\tilde{\alpha}_+^t\middle|\tilde{\alpha}_-^t\right\rangle + e^{i\omega_q zt}\left\langle\tilde{\alpha}_-^t\middle|\tilde{\alpha}_+^t\right\rangle\right)\\
&+\frac{ix\omega_q}{\chi}\sin^2(\theta/2)e^{-|\alpha|^2}\sum_n\frac{\alpha^{2n}}{n!n}\left(e^{-i\omega_q zt/2}e^{-in\chi t/2}-e^{i\omega_q zt/2}e^{in\chi t/2}\right)\sin(n\chi t/2)\\
&+\frac{ix\omega_q}{\chi}\cos^2(\theta/2)e^{-|\alpha|^2}\sum_n\frac{\alpha^{2n}}{n!n}\left(e^{i\omega_q zt/2}e^{in\chi t/2}-e^{-i\omega_q zt/2}e^{-in\chi t/2}\right)\sin(n\chi t/2)\\
=& -\sin(\theta)e^{-|\alpha|^2(1-\cos(\chi t))}\cos\left(\omega_q zt+|\alpha|^2\sin(\chi t)\right)-\frac{2x\omega_q}{\chi}\cos(\theta)e^{-|\alpha|^2}\sum_n\frac{\alpha^{2n}}{n!n}\sin^2(n\chi t/2)\\
\approx& -\sin(\theta)e^{-|\alpha|^2(1-\cos(\chi t))}\left(\cos\left(|\alpha|^2\sin(\chi t)\right)-\omega_q zt\sin\left(|\alpha|^2\sin(\chi t)\right)\right)\\
&-\frac{2x\omega_q}{\chi}\cos(\theta)e^{-|\alpha|^2}\sum_n\frac{\alpha^{2n}}{n!n}\sin^2(n\chi t/2)
\end{aligned}$$

where for the before last equality we used the fact that

$$\begin{aligned}
\left\langle\tilde{\alpha}_+^t\middle|\tilde{\alpha}_-^t\right\rangle &= \left\langle\alpha e^{i\chi t/2-i\omega_c t}\middle|\alpha e^{-i\chi t/2-i\omega_c t}\right\rangle\\
&= e^{-|\alpha|^2+\alpha e^{-i\chi t/2-i\omega_c t}\alpha^* e^{-i\chi t/2+i\omega_c t}}\\
&= e^{-|\alpha|^2(1-e^{-i\chi t})}\\
&= e^{-|\alpha|^2(1-\cos(\chi t))}e^{-i|\alpha|^2\sin(\chi t)} = e^{-2|\alpha|^2\sin(\chi t/2)}e^{-i|\alpha|^2\sin(\chi t)}.
\end{aligned}$$

Noticing that $\sum_n \frac{\alpha^{2n}}{n!n}\frac{\sin^2(n\chi t/2)}{\chi t} \underset{|\alpha|^2\to\infty}{\to} 1$, we obtain, at first order,:

$$\begin{aligned}
\langle\sigma_z\rangle^{(1)}(t) =& \langle\sigma_z\rangle(t_0^-) - 2x\omega_q t\sin(\theta) \qquad (4.76)\\
\langle\sigma_x\rangle^{(1)}(t) =& \langle\sigma_x\rangle(t_0^-)e^{-|\alpha|^2(1-\cos(\chi t))}\left(\cos\left(|\alpha|^2\sin(\chi t)\right)-\omega_q zt\sin\left(|\alpha|^2\sin(\chi t)\right)\right)-2x\omega_q t\cos(\theta)\\
\langle\sigma_\theta\rangle^{(1)}(t) =& x\langle\sigma_x\rangle^{(1)}(t)+z\langle\sigma_z\rangle^{(1)}(t)
\end{aligned}$$

which at zeroth order simplifies to

$$\begin{aligned}
\langle\sigma_z\rangle^{(0)}(t) =& \langle\sigma_z\rangle(t_0^-)\\
\langle\sigma_x\rangle^{(0)}(t) =& \langle\sigma_x\rangle(t_0^-)e^{-|\alpha|^2(1-\cos(\chi t))}\cos\left(|\alpha|^2\sin(\chi t)\right)\\
\langle\sigma_\theta\rangle^{(0)}(t) =& x\langle\sigma_x\rangle(t_0^-)e^{-|\alpha|^2(1-\cos(\chi t))}\cos\left(|\alpha|^2\sin(\chi t)\right)+z\langle\sigma_z\rangle(t_0^-)
\end{aligned}$$

The change in average energy of the measured system thus is:

$$\begin{aligned}
\Delta\langle H^S\rangle^{(0)}(t) &= \frac{\hbar\omega}{2}(x\Delta\langle\sigma_x\rangle^{(0)}(t)+z\Delta\langle\sigma_z\rangle^{(0)}(t))\\
&= \frac{\hbar\omega}{2}x\langle\sigma_x\rangle(t_0^-)\left(e^{-|\alpha|^2(1-\cos(\chi t))}\cos\left(|\alpha|^2\sin(\chi t)\right)-1\right)\\
&= \frac{\hbar\omega}{2}x^2\left(1-e^{-|\alpha|^2(1-\cos(\chi t))}\cos\left(|\alpha|^2\sin(\chi t)\right)\right) \qquad (4.77)
\end{aligned}$$

and when $t_m = \tau = \pi/\chi$ we retrieve the expression given in Eq. 4.25:

$$\Delta\langle H^S\rangle^{(0)}(t) = \frac{\hbar\omega}{2}x^2\left(1 - e^{-2|\alpha|^2}\right) \underset{|\alpha|^2\gg 1}{\approx} \frac{\hbar\omega}{2}x^2 \tag{4.78}$$

Interestingly, we assumed that the initial state of the cavity meter is the pure state $|\alpha\rangle$. However, as argued by Yelena Guryanova *et al*. [81], the preparation of such state would require infinite resources due to Kelvin's third law of thermodynamics. Since the pure state $|\alpha\rangle$ can be approach arbitrarily close with finite resources this does not undermine the value of these calculations. Deriving the effect of taking for the initial state of the cavity $(1-\epsilon)\,|\alpha\rangle\langle\alpha| + \epsilon|0><0|$ with $\epsilon \ll 1$ on our results could be useful to model an experimental implementation of this measurement.

Chapter 5

Resources to perform a good Measurement

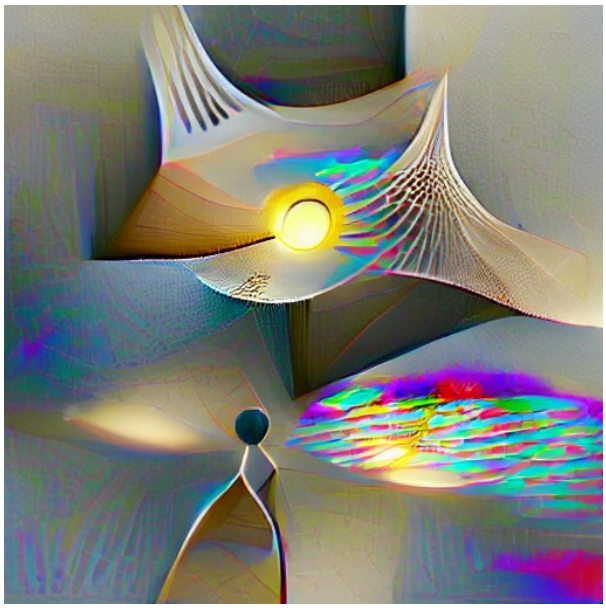

Generated using the artificial intelligence method VGLAN + CLIP

Contents

THE ENERGETIC COST of manipulating quantum resources will become a more pressing issue as quantum technologies and quantum ambitions florish [106]. With it, identifying the fundamental energy constraint set by each element will be of great value.

Recently, the cost of implementing unitary gates was explored [134, 135] as well as the global energy cost of quantum computing [107]. Quantum measurements are also very useful tools towards building measurement based quantum computers [136, 137], in many communication protocols and for sensing applications. A lower bound to their fundamental cost was first derived by Sagawa and Ueda [80, 68], and generalized to inefficient measurement by Abdelkhalek *et al.* [138]. Since, depending on the change of the memory's free energy, this bound can be negative, the measurement process is said to have no fundamental energy cost per se. Adding the resetting step, during which the meter is brought back to its initial state as shown in Figure. 5.1, instead sums to a positive fundamental cost which only vanishes when no information is extracted.

Note that in the case of a classical measurement, the information storing system is usually called memory. Since, in the quantum case, the quantum meter plays a similar role, the "meter", denoted M, we will indifferentially refer to the "memory" and to the "quantum meter".

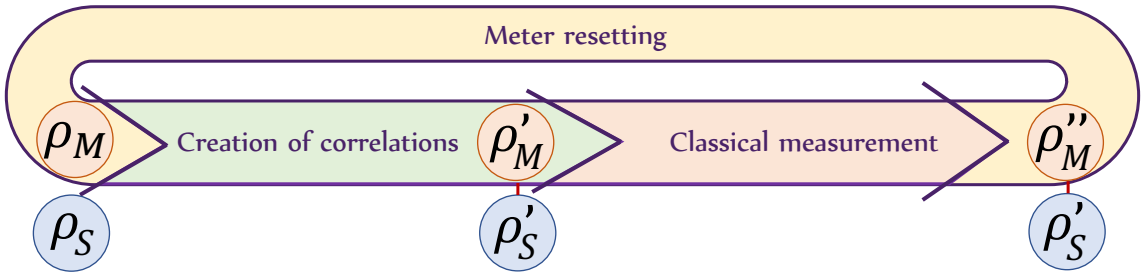

Figure 5.1: The three steps of a cycle of measurement and erasure can in the most general case affect both the system S and meter M's respective states ρ^S and ρ^M, if the system has coherences in its measurement basis. At the end, only the meter state has to be resetted which implies that the correlations built during the pre-measurement step and represented with a red line are destroyed.

The existence of a fundamental cost for the measurement and resetting process might come as a suprise. Indeed, one could expect that it is simply the substraction between the final and initial energy of the system which can be positive or negative. However, even when measuring a system in its eigenenergy basis, as will be the case in this chapter, this cost does not vanish. This is because correlations will be created during the pre-measurement step and will results in an increase of the meter's entropy. Consequently, the resetting step will have to decrease the meter's entropy and hence will have an energetic cost. The minimal energy cost was hence found to be "essentially determined by the entropy change in the memory" [138] which our quantum meter $\mathcal{M}$ models.

Finding such a lower bound has been a crutial step in the understanding of the energy cost of cycle of measurement and erasure but other questions remain. Some of them were already

adressed regarding the work extractable using the measurement output state and outcome [69] and obtained by performing a dephasing operation [58]. Others are still pending such as the impact of the meter's initial state on the measurement cost and quality.

In this chapter, we explore the impact of the system's and meter's coherence on these quantities. The measurement quality is evaluated via three figure of merit: the measurement backaction on the qubit state, the measurement informational efficiency and the measurement energetic efficiency. They allow to quantify respectively: how much the measurement affects the measured system, how much information is extracted from it and how much the cost amounts to this information. Thanks to these quantifiers, we can fairly compare the energy cost of the cycle of measurement and erasure of a qubit by a cavity field.

> These theoretical results were motivated and extend the concepts of a previous work:
> Xiayu Linpeng, Léa Bresque, M.Maffei, A. N. Jordan, Alexia Auffèves, and K. W. Murch
> *Energetic cost of measurements using quantum, coherent, and thermal light*
> Phys. Rev. Lett. 128, 220506 (2022)

The experimental part of this project was carried in Washington University in St. Louis, Missouri, by Xiayu Linpeng under the supervision of Kater Murch

5.1 Quantifying the energy cost of measurements

In order to understand the impact of the quantum nature of the measured system S and of the meter system M on the measurement cost and quality, we first consider the fully classical case. This implies that nor the measured system S nor the meter M have coherences in their respective measurement basis; where the measurement basis of the system is the eigenbasis of the system's operator that we ultimately want to measure, whereas the measurement basis of the meter is defined by the set of projective operator used to measure the meter after the correlations are built.

In this classical case, Figure. 5.1 can be simplified by bringing together the first two steps into a simple "measurement step", since an unread measurement of a classical system will not affect its state. We take the point of view of an external operator who performs this measurement in order to motivate the figures of merit used to characterize the measurement quality.

5.1.1 Ideal classical case

Initially, the meter and system state is separable such that the initial mutual information:

$$I = S_S + S_M - S_{SM}; \tag{5.1}$$

where $S_S = S(\rho^S)$, $S_M = S(\rho^M)$ and $S_{SM} = S(\rho^{SM})$ are respectively the initial entropy of the reduced state of S and M, and of their joint state; is null.

The measurement step's purpose is to create correlations between the meter and the system's states. Interestingly, the mutual information can also be rewritten in terms of the conditional entropy $S(\rho^S|\rho^M) = S_{SM} - S_M$, which characterize the remaining ignorance about the system once the state of the meter is known, as:

$$I = S_S - S(\rho^S|\rho^M) \geq 0. \tag{5.2}$$

Therefore, the mutual information can be interpreted as the information acquired about the system from knowing the meter state or, equivalently, the information that the S and M possess on their mutual states. Thus, the larger the mutual information, the better. Ideally, we would have $I = S_S$, i.e., all the possible information about the system would have been extracted. The energy required to perform this measurement step, corresponds to the total change in free

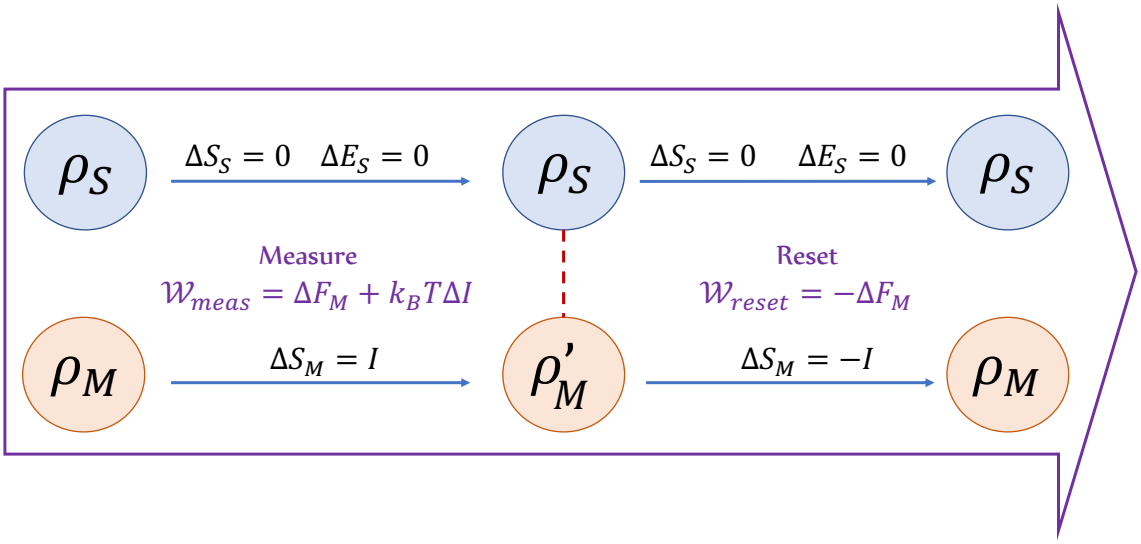

Figure 5.2: Work cost of an ideal classical cycle of measurement and erasure. This full measurement is splitted in two steps: the measurement during which the meter is extracting information from the measured system, and the resetting step. The dashed red lines represents the correlations between system and meter. We denote ΔS_A and ΔE_A, with $A \in \{S, M\}$, the change of entropy and energy of the system A.

energy of the total system SM such that:

$$\mathcal{W}_{meas} = \Delta F_{SM} = \Delta E_M + \Delta E_S - k_B T \Delta S_{SM} = \Delta E_M + k_B T (I - \Delta S_M) \tag{5.3}$$

where E_S (resp. E_M) is the average energy of the system S (resp. M) and T is the temperature of the available bath used in order to reset the state of the meter. The last equality comes from the assumption that the entropy and energy of the system are unaffected by the measurement ($\Delta E_S = 0$ and $\Delta S_S = 0$) as expected for an ideal classical measurement. Moreover, since the initial mutual information was null, ΔI is simply the final mutual information denoted I.

When the correlation building step is done unitarily, as when the correlations are built via a unitary pre-measurement dynamics, the second term of $\mathcal{W}_{meas}$ vanishes since $\Delta S_M = I$ by conservation of the total entropy of SM. It means that the increase in the meter entropy corresponds to the mutual information between meter and system. Ideally, in this case, the mutual information should be such that $I = S_S^0 = \Delta S_M \geq 0$ where S_S^0 is the initial entropy of the system which should remain unaffected by a classical measurement process. Therefore the measurement cost turns out to be $\mathcal{W}_{meas} = \Delta E_M$, i.e., only coming from the change of average energy of the meter.

There are now two possibilities depending on the structure of the physical system storing the information: either the energy of the meter is unchanged or it is not. The first possibility can happen if the meter energy level are degenerate. It is the case, for instance, when the information is encode in the right and left position of particle in a symmetric double well potential [139]. In this case, $\mathcal{W}_{meas} = 0$ and the measurement step can be performed at no cost. For an asymmetric meter however, the measurement cost will have to include the eventual increase of the meter energy. Note that, if the entropy of the meter increases more than the mutual information, which can happend under a non-unitary transformation, some energy could even be extracted during this measurement process.

As depicted in Figure. 5.2, the measurement is then followed by a resetting of the meter state. The mutual information aquired during the measurement step can be exploited by a feedback loop in order to extract some useful work, as shown in Figure. 5.3. Hence, the energy cost of the resetting step amounts to the change of free energy of the meter which is exactly equal and opposite to its change during the measurement step such that:

$$\mathcal{W}_{eras} = -\Delta F_M = -\Delta E_M + k_B T \Delta S_M \tag{5.4}$$

Therefore, in the case of a degenerate memory, since $\Delta E_M = 0$, the erasure cost corresponds to the one needed in order to decrease back to its initial value the entropy of the meter. Here, ΔS_M is the positive increase of meter entropy caused by the measurement step. Eventually, the cost for an ideal cycle of measurement and erasure writes:

$$\mathcal{W}_{meas} + \mathcal{W}_{eras} = k_B T I \tag{5.5}$$

which exactly corresponds to the amount of work extractable from the potential feedback loop and which is consistent with the results of Sagawa and Ueda [68].

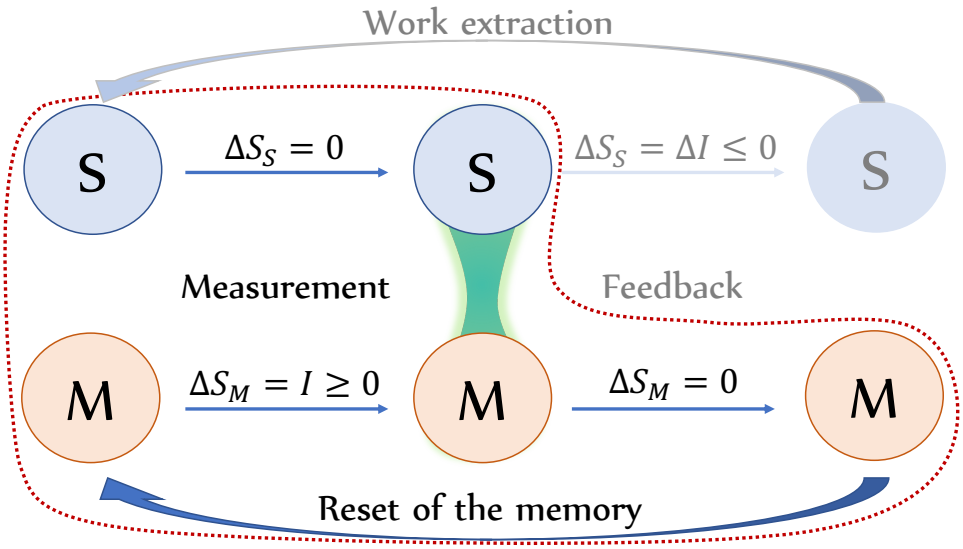

Figure 5.3: Local entropy change in an information measurement engine. The global measurement analyzed in this chapter corresponds to the region circled in dotted red. As it appears, the mutual information can serve to decrease the entropy of the system via a feedback step which leads to and optimal work extraction if $\Delta S = I$.

5.1.2 Measurement efficiencies

As we have seen, the amount of information extracted during the measurement process is quantified by the mutual information I reached at the end of this step. The maximal information available however is given by the initial entropy of the system S_S^0. In order to quantify the performance of the measurement at extracting the available information, we therefore define the measurement informational efficiency as:

$$\eta_I = I/S_S^0. \tag{5.6}$$

In the ideal case, one can gain full knowledge about the state of the system from the one of the meter, $I = S_S^0$ and thus $\eta_I = 1$. In the worse case, no information is extracted and therefore $\eta_I = 0$. As described by Equation. 5.2, this happends when the state of the meter is not sufficient to determine exactly the one of the system. This can occur if the system state evolves while it is being measured, or if the meter initial state has some components whose evolution are not affected by the system' state or if the meter states associated to the each of the system measurement basis are not orthogonal. Moreover, since the mutual information is such that $0 < I < S_S^0$, this efficiency always remains between 0 and 1. Note that when $S_S^0 = 0$, i.e., that the initial state of the system is pure, it is impossible to reduce our ignorance about this state and the information extracted does not correspond to the one contained in the initial state. This

efficiency therefore only makes sense, and remains finite, when the initial state is not pure. This quantity can also be motivated from the schematic of an information measurement engine, as depicted in Figure. 5.3. Indeed, the higher the mutual information given a fixed S_S^0, the more negative the change of system entropy during the feedback step can be. This implies that during the work extraction, a high mutual information will result in a larger possible increase of the system entropy and therefore more possible work extracted.

Regarding the measurement cost, we have seen that if this step is done unitarily such that $\Delta S_{SM} = 0$, then $\Delta S_M = I$ and $\mathcal{W}_{meas}$ should only compensate for the change of average energy of the meter. However, it could happend that $\Delta S_M > I$ for instance due to measurement error such as if the meter state evolved when it should not have based on the system's state. These errors being unknown are associated to an irreversible increase of the meter entropy. In this case, the work cost of the measurement $\mathcal{W}_{meas} = k_B T(I - \Delta S_M)$ will be negative (assuming degenerate meter levels). But this energy will not be extractable due to its irreversible origin. Therefore, the measurement will simply be performed at no cost while the resetting step will still cost $k_B T \Delta S_M$ resulting in a total measurement cost of the same amount. Therefore $\mathcal{W}_{meas} + \mathcal{W}_{eras} = k_B T \Delta S_M > k_B T I \geq 0$. The energetic performance of the cycle of measurement and erasure can thus be quantified via the measurement energy efficiency defined as:

$$\eta_E = I / \Delta S_M. \tag{5.7}$$

Ideally $\eta_E = 1$ and the measurement cost is minimal, whilst in the worse case, no information is extracted while the meter entropy is increased by the measurement step such that $\eta_E = 0$. In this case one has to use energy to perform a non informative measurement.

5.2 Quantum measurement: impact of the coherences

To this classical measurement we now add the possibility for the system and the meter to have coherences in their respective measurement basis. It is necessary in this case to divide the measurement step into a pre-measurement evolution during which the correlation are built and which is denoted by 1 and the classical measurement of the meter, denoted 2 [112, 140]. As shown in Figure. 5.4, the last, resetting step is denoted by a 3.

Since the system is measured via the classical measurement of the quantum meter, the two types of coherences will play a role on the extracted information and modify the classical case described so far. These coherences are the ones of the system S in the basis according to which the meter evolves and, the ones of the meter M in the classical measurement basis.

Moreover, quantum correlations between S and M will possibly arise and can be quantified by comparing the two expressions of the mutual information introduced in Eq. (5.1) and Eq. (5.2). While these quantities are equal for classical systems, they can be distinct in the quantum realm. The substraction of these two quantities is called the quantum discord [141] and is such that:

$$D_{SM} = I - J_{\{\Pi_j\}_j} \geq 0 \tag{5.8}$$

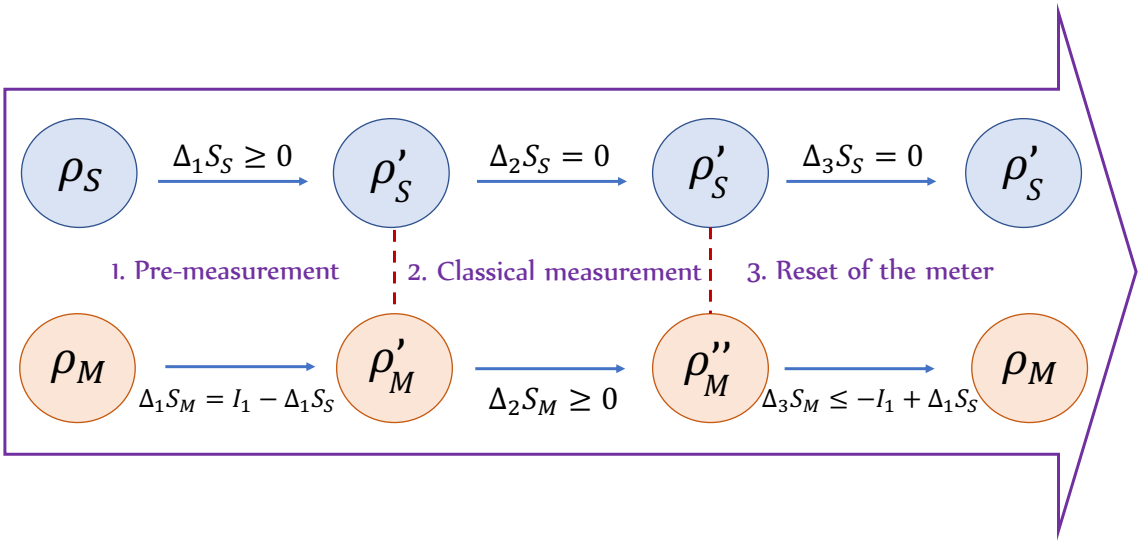

Figure 5.4: Work cost of a quantum cycle of measurement and erasure. This full measurement is splitted in three steps: the measurement during which the meter is extracting information from the measured system, the projective measurement of the meter and the resetting step. The dashed red lines represents the correlations between system and meter. We denote $\Delta_k S_A$ and ΔE_A, with $A \in \{S, M\}$, with $A \in \{S, M\}$, the change of entropy and energy of the system A during the step k.

with $I = S_S + S_M - S_{SM}$ the quantum mutual information, and $J_{\{\Pi_j\}_j} = S_S^{\text{sh}} - \sum_j p_j S^{\text{sh}}(\Pi_j \rho^S \Pi_j / \text{Tr}(\Pi_j \rho^S))$ the classical correlations given the specific choice of basis $\{\Pi_j\}_j$. This last quantity, usually refered to as Holevo's quantity, is the substraction of the Shannon entropy of the system's initial state S_S^{sh} by the weigthed average of the chosen selective projective measurement.

Coherences in the meter

Here, we still consider a system initial state with no coherences in its measurement basis. When the state of the meter has coherences in the basis in which it is classically measured, nothing changes during the pre-measurement in that if this step is unitary the change of the meter entropy is given by the mutual information. During the classical measurement however, in constrast with the fully classical case, the meter entropy can further increase. Therefore, the total change of mutual information after the steps 1 and 2: $\Delta I_{12} = I_2$ is such that:

$$I_2 = \Delta_{12} S_S + \Delta_{12} S_M - \Delta_{12} S_{SM} \leq \Delta_{12} S_M \tag{5.9}$$

since $\Delta_{12} S_S = 0$ and $\Delta_{12} S_{SM} \geq 0$. Hence the measurement energy efficiency, which writes from this decomposition: $\eta_E = I_2 / \Delta_{12} S_M$, will decrease due to these meter coherences (compared to a more classical meter state without these coherences).

Coherences in the system

When the measured system also has coherences in its measurement basis, its entropy can change during the pre-measurement step. This is due to the destruction of the system's coherences. Hence during the pre-measurement, the mutual information increases by:

$$I_1 = \Delta_1 S_S + \Delta_1 S_M \geq \Delta_1 S_M. \tag{5.10}$$

It will therefore not be a given that $I_1 = \Delta_1 S_M$, even during this first step. This increase of the mutual information due to $\Delta_1 S_S$ is however of purely quantum origin and can lead to mutual information greater than one. This is for instance the case for the state $\frac{|e\rangle|1\rangle^e + |g\rangle|0\rangle^e}{\sqrt{2}}$ for which the mutual information is 2. Once projectively measured in the Fock basis this state will however become $\frac{|e\rangle\langle e|1\rangle\langle 1|^e + |g\rangle\langle g|0\rangle\langle 0|^e}{2}$ for which the mutual information is 1 due to the erasure of the quantum correlations.

Notice that in the derivation of the work cost of the measurement, if ΔS_S is not assumed to be null, Equation. 5.3 can be rewritten:

$$\mathcal{W}_{meas} = \Delta F_M + k_B T I - k_B T \Delta S_S. \tag{5.11}$$

Hence, coherences in the measurement basis could potentially be exploited in order to reduce the cycle of measurement and erasure cost since one would ideally have $\mathcal{W}_{meas} + \mathcal{W}_{eras} = k_B T(I - \Delta S_S)$. However, this effect comes from the fact that the entropy of the system would have increased during the full measurement. There is therefore no suprise that this entropy increase can be exploited to do some useful work (or here to provide work necessary for the implementation of the full measurement).

Measurement backaction

The reason behind the modifications caused by the presence of coherences in the measurement basis of the system S is the measurement backaction [142]. This effect is due to the building of correlation with the meter system and results in the destruction of these coherences. In order to quantify directly its effect, on should compare the initial coherence of the system in the measurement basis to the final one. The coherence of state ρ^S in a given orthogonal basis $\{|e_i\rangle\}_i$ being defined as:

$$C_{\{|e_i\rangle\}_i}(\rho^S) = \sum_{i,j,i\neq j} |\langle e_i|\rho^S|e_j\rangle| \tag{5.12}$$

and is the l_1 matrix norm of the state in this basis [143]. In the case of a qubit measured in the basis $\{|e_\phi\rangle, |g_\phi\rangle\}$, one has $C_{eg}(\rho^S) = 2|\langle e_\phi|\rho^S|g_\phi\rangle|$.

5.3 Measurement of a qubit by a cavity field

We now consider the case of the measurement of a qubit by a cavity field. This quantum non demolition measurement (QND) is performed in the $\{|e\rangle, |g\rangle\}$ basis. By QND measurement,

we here imply that the measurement operator commute with the bare Hamiltonian of the system. The creation of correlation is performed via a conditionnal excitation of the meter field which initially starts in its ground state $|0\rangle$.

The specific measurement considered in this chapter was inspired by the possibilities offered by circuit QED plateforms. There, as depicted on Figure. 5.5, a transmon qubit can be measured by the field of a cavity in which it is embedded. Since this cavity is itself connected to two waveguides; one weakly coupled input waveguide and one strongly coupled output waveguide; the field leaking out the cavity can then be classically measured. While our analysis remains purely theoretical, a comparison with previous experimental results will be discuss in the end of the chapter. More information about the experimental implementation of this measurement is provided in Section. 5.7.2 of the Appendix.

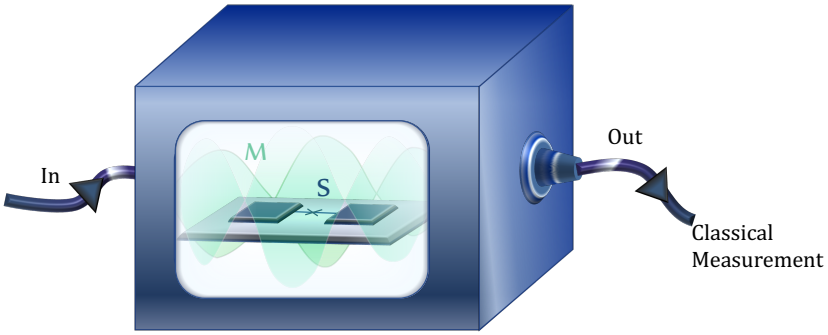

Figure 5.5: Illustration of a system S transmon qubit on its chip embedded in a 3-dimensional aluminium cavity filled with a meter field M and with input port on the left and output port on the right. This output port serve to collect the cavity field in order to measure it classically. This setup operates at mK temperature.

Conditional excitation

We are interested in the influence of the system and meter states on the measurement cost and quality. In order to investigate this aspect, we will consider two possible qubit states: a fully mixed state:

$$\rho_i^{qb} = \frac{|e\rangle\langle e| + |g\rangle\langle g|}{2}, \tag{5.13}$$

and a pure state with coherences in the measurement basis:

$$|\psi\rangle_i^{qb} = \frac{|e\rangle + |g\rangle}{\sqrt{2}}, \tag{5.14}$$

which will allow us to study the impact of the coherences in the measured system.

The meter field is initialized in the vacuum, $|\psi\rangle_i^c = |0\rangle$ and conditionally excited depending on the qubit state. The idea behind these transformations is that a qubit can dress a cavity's

resonant frequency according on its state if they are dispersively coupled. Therefore, the field entering the cavity is filtered according on the qubit state and on the field frequency (See appendix. 5.7.2 for more information). The resonant frequency associated to the qubit being in the state $|e\rangle$, resp. $|g\rangle$, is denoted f_c^e, resp. f_c^g. We will consider here three possible kinds of excitations all sent at the frequency f_c^g, i.e., only entering the cavity if the field is in the state $|g\rangle$.

One is a **purely quantum excitation** which induces the following transformation:

$$\begin{aligned} |e\rangle \otimes |0\rangle &\to |e\rangle \otimes |0\rangle\,, \\ |g\rangle \otimes |0\rangle &\to |g\rangle \otimes (\cos(\theta/2)\,|0\rangle + \sin(\theta/2)\,|1\rangle)\,, \end{aligned} \tag{5.15}$$

where the angle θ controls the average number of photon in the field (which is here between 0 and 1). Such as transformation can be unitarily implemented from the evolution associated to the Hamiltonian:

$$H_{1p} = \frac{\hbar\Omega}{2}\,|g\rangle\langle g| \otimes (|0\rangle\langle 1| + |1\rangle\langle 0|)\,, \tag{5.16}$$

where Ω sets the time scale of the transformation. The average number of excitations injected in the cavity if the qubit is in the state $|g\rangle$ will be $\bar{n} = |\sin(\theta/2)|^2$.

The second excitation will generate a conditional **coherent field** in the cavity such that:

$$\begin{aligned} |e\rangle \otimes |0\rangle &\to |e\rangle \otimes |0\rangle\,, \\ |g\rangle \otimes |0\rangle &\to |g\rangle \otimes |\alpha\rangle\,, \end{aligned} \tag{5.17}$$

where $|\alpha\rangle$ is a coherent field at frequency f_c^g of average photon number $\bar{n} = |\alpha|^2$, and which can also be implemented unitarily from:

$$H_{coh} = \frac{\hbar\Omega}{2}\,|g\rangle\langle g| \otimes \left(a_e^\dagger e^{i\omega t} + a_e e^{-i\omega t}\right). \tag{5.18}$$

Eventually, we will also consider a **thermal excitation** such that

$$\begin{aligned} |g\rangle\langle g| \otimes |0\rangle\langle 0| &\to |g\rangle\langle g| \otimes \rho_{th}, \\ |e\rangle\langle e| \otimes |0\rangle\langle 0| &\to |e\rangle\langle e| \otimes |0\rangle\langle 0|\,, \\ |g\rangle\langle e| \otimes |0\rangle\langle 0| &\to |g\rangle\langle e| \otimes \sum_n \sqrt{p_n}\,|n\rangle\langle 0| \\ |e\rangle\langle g| \otimes |0\rangle\langle 0| &\to |e\rangle\langle g| \otimes \sum_n \sqrt{p_n}\,|0\rangle\langle n|\,, \end{aligned} \tag{5.19}$$

where $\rho_{th} = \sum_n p_n\,|n\rangle\langle n|$ is a thermal field of average number of photon $\bar{n}$. This value is chosen such that, for a qubit in a state of equal populations in $|e\rangle$ and $|g\rangle$, the average number of photons in the cavity will be same no matter the field statistics. Notice that this last transformation does

not result from a unitary pre-measurement dynamics since it changes the entropy of the joint qubit and field system, as long as the thermal field is associated to a non zero temperature. In this case, the previous analysis should only be understood as a guide line to motivate the figure of merit.

Conveniently, since the intial state $|0\rangle$ always has a zero entropy, the variation of the meter entropy will always be equal to the final meter entropy which which just denote by S_M.

After this correlation building transformations, the field state is undergoing an classical measured in the Fock state basis in order to end the measurement process over which we average.

5.4 Theoretical results: influence of the meter state

5.4.1 On the information extracted

No coherences in the system

When the qubit system initially is in the mixed state given by Eq. 5.13, the final state of the field meter and qubit system after the interaction and unread projective measurement of the field in the Fock basis are:

$$\begin{aligned}
\rho_{\text{1ph}}^{\text{mix}} &= \frac{(|e\rangle\langle e| + |g\rangle\langle g|\cos^2(\theta/2))\,|0\rangle\langle 0|}{2} + \frac{\sin^2(\theta/2)\,|g\rangle\langle g| \otimes |1\rangle\langle 1|}{2} \\
\rho_{\text{coh}}^{\text{mix}} &= \frac{(|e\rangle\langle e| + |g\rangle\langle g|\,e^{-|\alpha|^2})\,|0\rangle\langle 0|}{2} + \sum_{k\neq 0} \frac{e^{-|\alpha|^2}\alpha^{2k}\,|g\rangle\langle g| \otimes |k\rangle\langle k|}{2 * k!} \\
\rho_{\text{th}}^{\text{mix}} &= \frac{|e\rangle\langle e| \otimes |0\rangle\langle 0|}{2} + \frac{|g\rangle\langle g| \otimes \rho_{\text{th}}}{2}
\end{aligned} \tag{5.20}$$

In Figure. 5.6 (a) and (b), we plot the entropy of the qubit system S and meter field M as function of the average number of photon $\bar{n}$ for these three different initial field states. Since the qubit starts in a fully mixed state, its entropy is unaffected by the measurement and therefore does not depend on $\bar{n}$ and is equal to one due to the equal probabilities to obtain $|e\rangle$ and $|g\rangle$. Therefore, the final mutual information and informational efficiency are equal, see Figure. 5.6 (c) and (d) which are here plotted with a different $\bar{n}$ range. As it appears, the single photon field reaches the maximal efficiency for $\bar{n} = 1$ whilst thermal and coherent fields only tend to 1 at higher number of photons. The thermal resource does not allow to extract as much information for an equal energetic investment as the coherent one. However, as shown in Figure. 5.6 (b) its resetting cost will be lower since $S^M(\rho_{th}^{\text{mix}}) < S^M(\rho_{coh}^{\text{mix}})$. Nevertheless, overall the coherent field will have a higher energy efficiency than the thermal field itself. The single photon field being even better than the coherent one. This simple comparison exibit a case in which the quantum nature of the meter system can prove useful in order to efficiently extract information given fixed energetic resources.

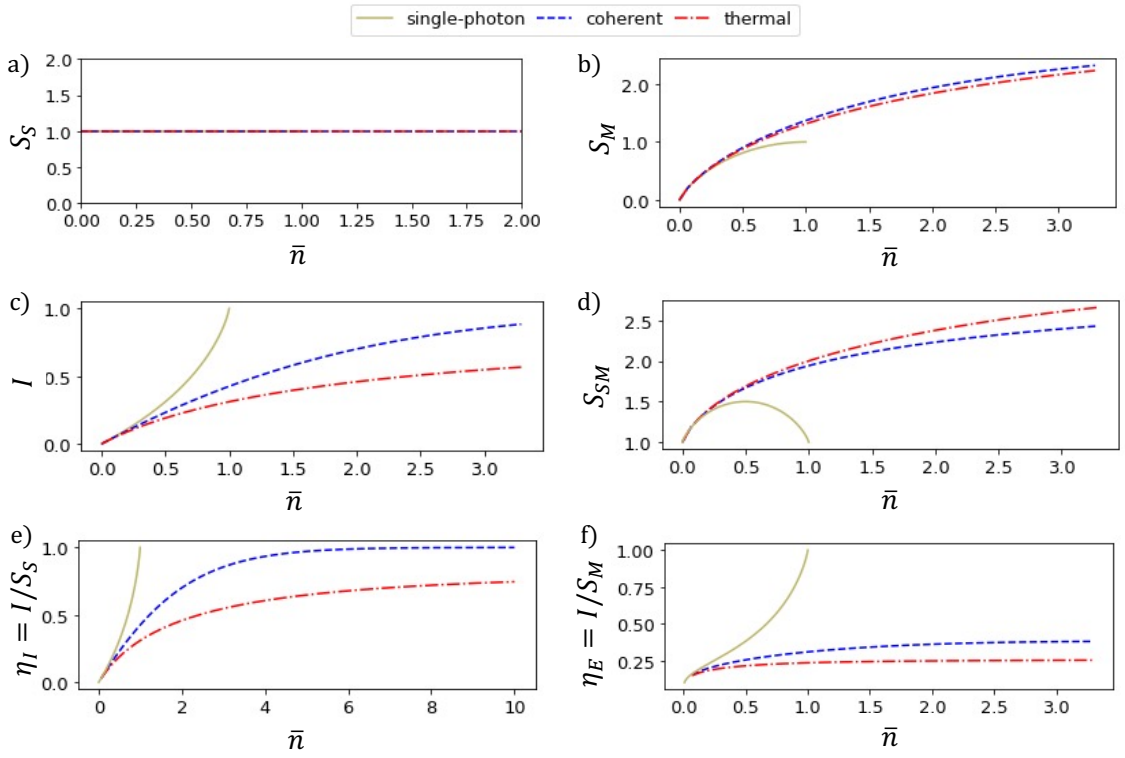

Figure 5.6: Mutual information and entropies of an initially mixed qubit state measured by single photon (yellow solid), coherent (blue dashed) and thermal (red dash-dotted) fields. The qubit system entropy a), meter field entropy b) amutual information I between them c) and their total entropy S_{SM} d) are plotted as functions of the average number of photon in the fields $\bar{n}$. The ultimate measurement efficiency is given by comparing the final information gain I to the system entropy S_S e). The maximum is only reached with a purely quantum measurement resource: a single photon Fock. The energetic efficiency as quantified by the ratio between the mutual information and the meter entropy is also presented in f).

To understand the origin of these different informational efficiencies, it is useful to notice that all the states of Equations. 5.20 can be written as:

$$\rho = \frac{|e\rangle\langle e| \otimes |0\rangle\langle 0|}{2} + \frac{|g\rangle\langle g|}{2} \otimes \sum_k p_k^{\text{distrib}} |k\rangle\langle k|\,, \tag{5.21}$$

where $p_k^{\text{distrib}} = p_k$ in the thermal case, $e^{-\bar{n}}\frac{\bar{n}^k}{k!}$ in the coherent case and $\bar{n}$ if $k = 1$ and $1 - \bar{n}$ if

$k = 0$ in the single photon case. Therefore, the mutual information reads:

$$\begin{aligned} I^{\text{distrib}} &= 1 + S^{\text{sh}}\left(\frac{p_0^{\text{distrib}}+1}{2}, \frac{p_1^{\text{distrib}}}{2}, \frac{p_2^{\text{distrib}}}{2}...\right) - S^{\text{sh}}\left(\frac{1}{2}, \frac{p_0^{\text{distrib}}}{2}, \frac{p_1^{\text{distrib}}}{2}, \frac{p_2^{\text{distrib}}}{2}...\right) \\ &= 1 + S^{\text{sh}}\left(\frac{p_0^{\text{distrib}}+1}{2}\right) - S^{\text{sh}}\left(\frac{1}{2}, \frac{p_0^{\text{distrib}}}{2}\right) \end{aligned} \tag{5.22}$$

where $S^{\text{sh}}(a_0, a_1, a_2...) = \sum_i S^{\text{sh}}(a_i) = -\sum_i a_i \log\left(a_i\right)/\log(2)$ where the a_i are real number in the range $[0, 1]$ and S^{sh} is the Shannon entropy in unit of $\log(2)$. Thus, the higher mutual information extracted by the coherent and single photon fields amount to the maximisation of the quantity: $l(p_0^{\text{distrib}}) = \frac{p_0^{\text{distrib}}}{2}\log\left(\frac{p_0^{\text{distrib}}}{2}\right) - \left(\frac{p_0^{\text{distrib}}+1}{2}\right)\log\left(\frac{p_0^{\text{distrib}}+1}{2}\right)$ and hence only to the probability of measuring the initial field in the Fock state $|0\rangle$. This is consistent with the fact that, in this context, only the Fock state $|0\rangle$ does not allow to discriminate between $|e\rangle$ and $|g\rangle$. Moreover, since the function $l(p_0^{\text{distrib}})$ is monotonously decreasing as $p_0^{\text{distrib}} \in [0, 1]$ increases, and that $p_0^{\text{th}} = \frac{1}{1+\bar{n}} > p_0^{\text{coh}} = e^{-\bar{n}} > p_0^{\text{1ph}} = 1 - \bar{n}$, for all $\bar{n} \in [0, 1]$, one indeed finds that the single photon field leads to a higher mutual information, and thus here a higher informational efficiency, than the coherent field itself better than the thermal field. The energy efficiency, depends on the full distribution, i.e., on all the p_k^{distrib} and is also better for the single photon, then coherent and eventually thermal distributions.

Coherences in the system

We now allow the system to have coherences in its measurement basis. Starting from such an initial state of the qubit given by $|\psi\rangle_i^{\text{qb}} = \frac{|e\rangle+|g\rangle}{\sqrt{2}}$, the system and meter joint states after the pre-measurement and classical measurement in the Fock basis are:

$$\begin{aligned} \rho_{\text{1ph}}^{\text{sup}} &= \frac{(|e\rangle + |g\rangle\cos(\theta/2))(\langle e| + \langle g|\cos(\theta/2))\,|0\rangle\langle 0|}{2} + \frac{\sin^2(\theta/2)\,|g\rangle\langle g| \otimes |1\rangle\langle 1|}{2} \\ \rho_{\text{coh}}^{\text{sup}} &= \frac{(|e\rangle + |g\rangle\, e^{-|\alpha|^2/2})(h.c.)\,|0\rangle\langle 0|}{2} + \sum_{k\neq 0}\frac{e^{-|\alpha|^2}\alpha^{2k}\,|g\rangle\langle g| \otimes |k\rangle\langle k|}{2 * k!} \\ \rho_{\text{th}}^{\text{sup}} &= \sqrt{p_0}\frac{|e\rangle\langle g| + |g\rangle\langle e|}{2} \otimes |0\rangle\langle 0| + \frac{|e\rangle\langle e| \otimes |0\rangle\langle 0|}{2} + \frac{|g\rangle\langle g| \otimes \rho_{\text{th}}}{2} \end{aligned} \tag{5.23}$$

As Figure 5.7(b) and Figure 5.6(b) illustrate, the meter entropy is unaffected by the presence of the coherences in the system state. The total entropy, also plotted in Figure 5.7(b) now starts at 0 when $\bar{n} \to 0$ since the initial entropy of the system is 0. Overall, the mutual information keeps the same ordering as in the previous case, without coherence in the system, with higher values the more quantum the field is as plotted on Figure 5.7(a).

In constrast, the system entropy, Figure 5.7(a) is strongly affected by this change and is now equal to the mutual information $S_S = I$. Starting from a pure system state, which is therefore

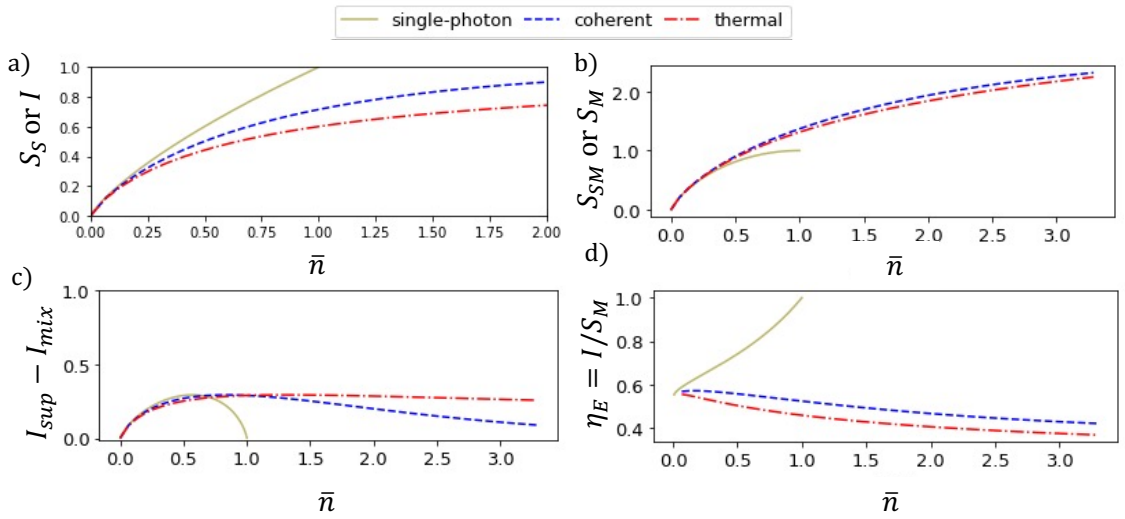

Figure 5.7: Mutual information and entropies of an initially pure qubit state measured by single photon (yellow solid), coherent (blue dashed) and thermal (red dash-dotted) fields. The qubit system entropy or equivalently mutual information I a), meter field entropy or equivalently total entropy b) are plotted as functions of the average number of photon in the fields $\bar{n}$. The mutual information is compared between the case with and without coherences in the measured system c). The energetic efficiency, as quantified by the ratio between the mutual information and the meter entropy is also presented in d), which only reaches it maximum value for single photon field.

strongly perturbed by the measurement, the informational efficiency does not apply and indeed would be infinite since the initial entropy of the system is nul. Unlike with a classical system state, the energetic efficiency is here found to decrease with the average number of photon involved for the thermal and coherent fields, Figure 5.7(d).

The impact of allowing coherences in the measured system is thus to induce a dependence with respect to $\bar{n}$ on the final system entropy and to modify the final mutual information. This final mutual information is found to always be greater in the case of a pure initial system than for a mixed one as shown in Figure. 5.7(c).

Notice that the mutual information obtained in Figure. 5.7(a) corresponds to the information the meter has on the system after the full measurement was performed. It does no quantify the information acquired about the initial state of the system in constrast to the information gain (See Appendix. 5.7.1). However, it quantifies the information one can exact about the system's projection in the $\{|e\rangle, |g\rangle\}$ basis from the meter state.

5.4.2 On the induced backaction

We now move on to characterize the measurement backaction of the thermal, coherent and single photon field statistics. In this case the initial state of the system should have coherence and therefore we take:

$$|\psi\rangle_i = |\psi\rangle_i^{qb} \otimes |0\rangle = \left(\frac{|e\rangle + |g\rangle}{\sqrt{2}}\right) \otimes |0\rangle \tag{5.24}$$

The coherence of the qubit initially is 1. In order to derive the final qubit coherence, we trace the fields from Equation. (5.23).

Single-photon light

In the case of the quantum field this leads to:

$$\rho_{1\text{ph}}^{\text{qb}} = \frac{1}{2}\begin{pmatrix} 1 & \cos(\theta/2) \\ \cos(\theta/2) & 1 \end{pmatrix} \tag{5.25}$$

and therefore the coherence reads $|2\rho_{1\text{ph},ge}| = |\cos(\theta/2)| = \sqrt{1-\bar{n}} \xrightarrow[\bar{n}\to 0]{} e^{-\bar{n}/2}$.

Coherent light

For the coherent light, we obtain the qubit's reduced state and its coherence in the $\{|e\rangle, |g\rangle\}$ basis to be:

$$\begin{aligned} \rho_{\text{coh}}^{\text{qb}} &= \frac{1}{2}\begin{pmatrix} 1 & e^{-\bar{n}/2} \\ e^{-\bar{n}/2} & 1 \end{pmatrix} = e^{-\bar{n}/2}\,|+\rangle\langle+| + \frac{1-e^{-\bar{n}/2}}{2}\mathbb{I} \\ |2\rho_{\text{coh},ge}| &= |\langle\alpha|0\rangle| = e^{-|\alpha|^2/2} = e^{-\bar{n}/2}. \end{aligned} \tag{5.26}$$

Thermal light

In the case of a thermal light, the reduced state of the qubit therefore reads:

$$\begin{aligned} \rho_{\text{th}}^{\text{qb}} &= \frac{1}{2}\begin{pmatrix} 1 & \sqrt{p_0} \\ \sqrt{p_0} & 1 \end{pmatrix} = \sqrt{p_0}\,|+\rangle\langle+| + \frac{1-\sqrt{p_0}}{2}\mathbb{I} \\ |2\rho_{\text{th},ge}| &= \sqrt{p_0} = \frac{1}{\sqrt{1+\bar{n}}} \xrightarrow[\bar{n}\to 0]{} e^{-\bar{n}/2}. \end{aligned} \tag{5.27}$$

As a result, we plot these three coherences as a function of $\bar{n}$ in Figure. 5.8(b). At very low number of photons, $\bar{n} \ll 1$, all the field considered lead to a coherence proportional to $e^{-\bar{n}/2}$. Hence, in this regime, all field induces the same backaction on the qubit.

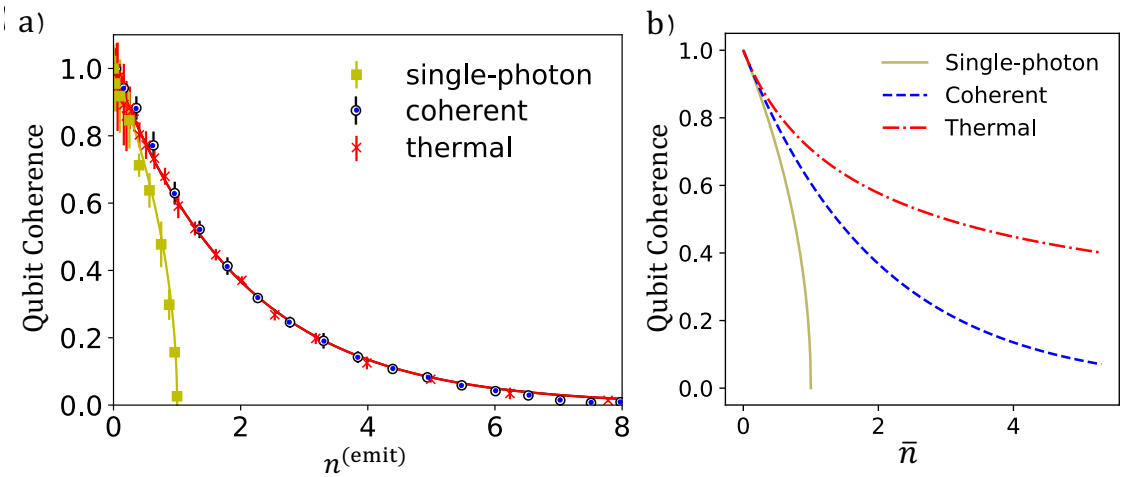

Figure 5.8: Decoherence of the measured qubit state for an initialy coherent, thermal and single-photon field. a) Experimental data point and theoretical fit as a function of the total emitted photon number assuming the measurement results from several interactions of the qubit with fields of very low number of photons. b) Qubit coherence for different total number of photon inside the cavity.

5.5 Comparison with the experimental results

Experimentally, it was however measured that the coherent and thermal field lead to similar decoherence as shown in Figure. 5.8(a). This exponential decoherence is well fitted by the exponential decay found in Equation. (5.26). Therefore, even though thermal field can be considered as free resources, as in the framework of quantum Resource theory, and are ideed easily obtained in pratice, in this circuit electrodynamic setup, they prove to be comparable in terms of measuring capabilities as coherent fields.

However, this is in contradiction with the simple model described so far, since, already below $\bar{n} = 2$, the difference between the coherent and thermal field is clearly visible in Figure. 5.8(b).

This discrepancy can be understood by noticing that, in pratice, the number of photon which have interacted with the qubit: $n^{(emit)}$ were not all inside of the cavity at the same time. Experimentally, the cavity is open, such that the conditional input field is continuously dissipated in a waveguide. Indeed, unlike the single photon field, which is created by an almost instantaneous process (see Appendix. 5.7), the thermal field is built by sending a continuous pulse on the cavity. This results in the repeated application of N infinitesimal maps each corresponding to $n^{(\text{emit})}/N$ average photons. According to Equation. 5.27, such unital map $\mathcal{M}$ will act on the qubit state ρ such that:

$$\rho \to \sqrt{p_{0_N}}\rho + \frac{1-\sqrt{p_{0_N}}}{2}\mathbb{I} \tag{5.28}$$

where $p_{0_N} = \langle 0|\, \rho_{\text{th}}^N \,|0\rangle$ with ρ_{th}^N a thermal field with $n^{(\text{emit})}/N$ photons on average. Upon N application of this map, the final qubit state becomes:

$$\mathcal{M}^N\rho = p_{0_N}^{N/2}\rho + \frac{1-p_{0_N}^{N/2}}{2}\mathbb{I}. \tag{5.29}$$

For $n^{(\text{emit})}/N$
1, the coherence is thus given by $p_{0_N}^{N/2} \approx (1-n^{(\text{emit})}/N)^{N/2} \approx e^{-n^{(\text{emit})}/2}$ at first order in $n^{(\text{emit})}/N$. This pragmatic approach allows to understand of the behavior observed experimentally taking advantage of the fact that the thermal fields have a classical statistics due to the final projective measurement in the Fock basis.

Notice that this reasoning could also apply to the coherent case resulting in a coherence for the qubit of $(e^{-n^{(\text{emit})}/2N})^N = e^{-n^{(\text{emit})}/2}$ and thus does not affect the exponential decoherence already obtained in Equation. 5.26.

In [144], we used a similar approach but taking into account the fact that the thermal field is broadband and hence that it can partially enter the cavity even if the qubit it excited. From this modelling the same exponential decoherence was derived and therefore, the same backaction obtained in the thermal and coherent field can be understood. The purpose of this chapter, is however not to provide a realistic modelling of the measurement process in the context of a circuit QED plateform. For this purpose, theoretical and experimental works [145, 146] provide

a much more complete modelling using the qubit and cavity master equation. Notably, they reach the same conclusion of a decoherence rate proportional to the average photon number $\bar{n}$ in the case of a thermal field and in the strong dispersive regime due to the quantum fluctuations in the photon number populating the resonator [145, 146].

Instead, we focused here on informational and energetic aspects in the case of a closed cavity. Nevertheless, as shown in Figure 5.8, our conclusion that the single photon field is much more efficient at inducing decoherence, at fixed average photon number, is also in good agreement with the experimental datas.

5.6 Conclusion

We analysed the energetic cost of a measurement using different initial state for the field meter. For this purpose, we introduced energetic and informational efficiencies. For the standard measurement of a classical qubit state, we found that the quantum nature of the field could prove useful in order to reach maximum efficiencies. This quantum advantage could be traced back to the distribution of the photon number and especially to the probability of having zero photon. It resulted in higher performances for the single-photon field compared to the coherent field, itself outperforming the thermal field.

When the initial state of the qubit is pure, the quantumness of the meter also proves useful in order to generate a strong backaction at a given energy cost. However, this also imply a more negative information gain and hence a larger loss of information about the initial state of the system. The mutual information, quantifying the information about the final system state encoded in the meter state, is nevertheless increased by the presence of coherences in the initial state of the system and larger for single-photon and to a lesser extent for coherent field. However, in this case is loses its original interpretation as the information extracted on the initial state of the system.

Since, at fixed number of photon, the final reduced state of the field in the case of an initially thermal field is smaller than the one associated to the coherent field, after dephasing in the Fock basis; this implies that theoretically the coherent field will cost more energy during the resetting step than the thermal field.

The similar backaction obtain experimentally for these two fields was explained by an effective model in which the total incoming photon number is divided into small cells. Since, at low average photon number, the thermal and coherent field have the same probabilities to be found in the zero photon subspace, we were able to understand theoretically this behaviour with a basic model.

Notice that the energetic cost of measurement and work extraction is upper bounded by a positive quantity to which one should add the quantum heat when the measured system exchanges energy.

5.7 Appendix:

5.7.1 Information gain

Another relevant quantity to quantify the information aquired during a measurement is the information gain. At the level of individual trajectories, it was for instance shown via this quantity that the backaction could lead to information loss compared to the case of a classical state [147]. This information gain is defined as [148]:

$$I_{gain} = S_S^0 - \sum_r p(r) S_S(r) \tag{5.30}$$

with r spanning over all possible final projective measurement result, $S_S(r)$ the von Neumann entropy of the system after the global measurement conditionned on the measurement result being r and S_S^0 its initial entropy. Classically, this quantity is equal to the classical mutual information.

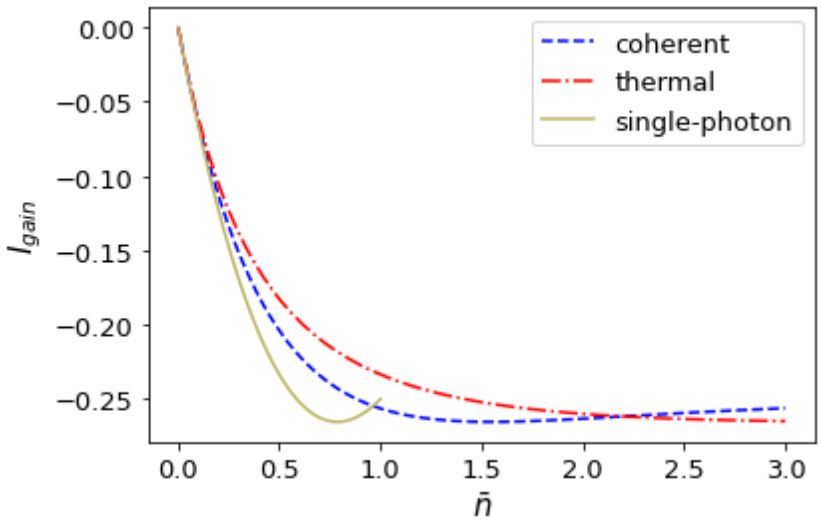

Figure 5.9: Information gain for single photon, coherent and thermal meter state as a function of the average photon number $\bar{n}$

Here we consider the initial state of the qubit with superposition in its measurement basis defined in Eq. (5.14). Since, the entropy of the qubit associated to the Fock state $|k\rangle$ with $k > 0$ is nul, since in this case the qubit is in the state $|g\rangle$, no matter the field statistics, the information gain writes:

$$I_{gain} = -\left(\frac{1+p_0^{\text{distrib}}}{2}\right) S\left(\frac{1}{2}\begin{pmatrix} 1 & \sqrt{p_0^{\text{distrib}}} \\ \sqrt{p_0^{\text{distrib}}} & p_0^{\text{distrib}} \end{pmatrix}\right). \tag{5.31}$$

From Figure. 5.9 it appears that the information gain is always negative, this is expected since we here started from a perfectly known state and only lost information during the measurement process. This lost of information is larger for the single photon field and the coherent field at low number of photon. This is consistent with the larger backaction induced by these fields discussed in the section 5.4.2.

5.7.2 Experimental implementation

In order to implement the measurement of a qubit by a field, it is possible to use a circuit quantum electrodynamics (cQED) plateform. This is indeed the setup used to obtain the results of Figure. 5.8(a).

Circuit QED setups are very versatile and offer many advantages such as well protected qubit leading to coherence time T_2 of the order of μs with good adressability via non destructive measurements. The tunability of Josephson Junctions (JJ) as well as the possibility to couple many of them, pushed this technology amongst the top plateforms envisionned to build quantum computers [11]. Thanks to these features, cQED offer great possibilities in terms of measuring capabilities, for rather recent enlightning reviews see [149, 150] . It was already demonstrated, for instance, that a qubit state could be controled via quantum measurements [151] and that one could measure the extractable work regenerated in a Maxwell demon experiment [152].

Qubit: In cQED plateforms, qubits are often transmon qubit. A transmon qubit, litteraly transmission line shunted plasma oscillation qubit, is made from a Josephson junction (JJ) shunted by a large capacitor such that $E_J \gg E_C$ whith E_C the capacitive charging energy and E_J the Josephson one. The induced non linearity effectively builds a qubit made from the first two level of the tunable non-harmonic oscillator that constitute the Josephson junction. The typical frequency of such a transmon qubit is in the GHz regime and can be tuned via current bias or magnetic flux. The qubit used in the experiment has for frequency $f_{\mathrm{q}} = \omega_q/2\pi = 5.122\,\mathrm{GHz}$ and the anharmonicity of the non-linear oscillator is $\alpha^{\mathrm{anharm}}/2\pi = -316\,\mathrm{MHz}$. Notice that the qubit and cavity are operated inside of a cryogenic fridge at $10mK$. The qubit temperature is of the order of $50mK$.

Cavity: This qubit is embedded in a superconducting circuit itself inside a 3-dimensional aluminum cavity whose field serves as the quantum meter as illustrated in Fig. 5.5. This field is then transmitted to the output waveguide and classically measured.

The cavity has two ports; a weakly coupled input port and a strongly coupled output port such that intracavity photons predominantly leak out of the output port. The input field consistenty comes from the input port.

Interaction: The qubit and cavity field interact via the dispersive Hamiltonian:

$$H_{cQED} = \hbar\omega_q\sigma_z + \hbar\omega_c a^\dagger a + \hbar\chi\sigma_z a^\dagger a, \tag{5.32}$$

where χ is the dispersive shift, $\omega_q/2\pi$ the qubit frequency and ω_c the one of the cavity. The dispersive shift is much larger that the dissipation rate of the cavity κ, i.e., $\chi \gg \kappa$, ensuring us to be in the strong dispersive regime where this Hamiltonian allows for a good modelling of the dynamics . Notice that here, the interaction term commutes with both the measurement system (the qubit) bare Hamiltonian and the one of the meter system (the cavity field). Therefore, neither the system nor the meter are exchanging energy via this interaction.

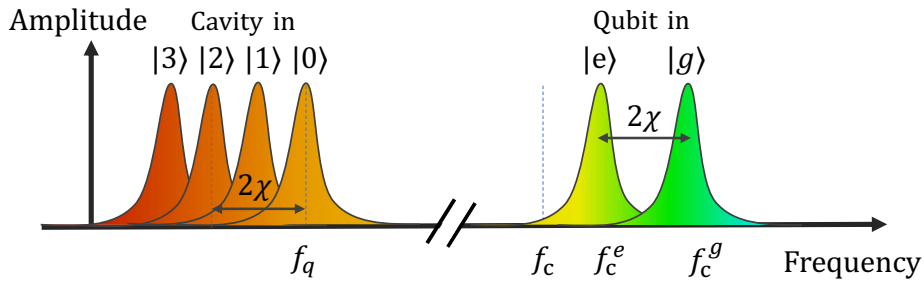

Figure 5.10: Schematic representation of the frequency shifts in the dispersive regime of the qubit from its interaction with the cavity (red/orange) and of the cavity from its interaction with the qubit (yellow/green).

This interaction however induces a shift of the effective frequency of the cavity, as illustrated in Fig. 5.10. Indeed, when regrouping the last to term of the Hamiltonian, we find that this effective frequency, $\omega_c + \chi\langle\sigma_z\rangle$, depends on the qubit state. We denote f_c^g the dressed frequency of the cavity when the qubit is in the ground state $|g\rangle$, and f_c^e the one associated to the qubit in the excited state $|e\rangle$. This effect is the one exploited to infer the state of the qubit from the one of the field. Similarily, the qubit's effective frequency is affected by its interaction with the cavity. This effect is the one used in order to characterize the number of photon in the cavity.

A summary of the notation and experimental values is given in Table. 5.1

Input field implementation

Thermal field A 300 K, 50 Ω resistor is used in order to generate thermal light.The Johnson noise from the resistor is filtered, amplified, and attenuated before it is directed to the weakly coupled port of the cavity, resulting in broadband light that uniformly illuminates the f_c^g and f_c^e resonances of the cavity.

Single-photon field An effective single-photon input can be realized utilizing the $|f\rangle$ state of the transmon qubit to transfer a photon into the cavity. Using a resonant rotation on the

Table 5.1: List the experimental values corresponding to Figure. 5.8

Definition	Quantity	Value
Qubit frequency	$f_q = \omega_q/2\pi$	5.122 GHz
Cavity bare frequency	$f_c = \omega_c/2\pi$	5.6047 GHz
Dressed cavity frequency (qubit in $\|g\rangle$)	f_c^g	5.6185 GHz
Dressed cavity frequency (qubit in $\|e\rangle$)	f_c^e	5.6060 GHz
Anharmonicity of the non-linear oscillator	$\alpha^{\text{anharm}}/2\pi$	-316 MHz
Dispersive shift	$\chi/2\pi$	-6.3 MHz
Dissipation rate of the cavity	$\kappa/2\pi$	0.5 MHz
Qubit relaxation time	T_1	9 μs
Qubit dephasing time	T_2^*	8 μs

$\{|e\rangle, |f\rangle\}$ manifold by the angle θ will map the $|e\rangle$ state to a superposition $\cos(\theta/2)|e\rangle + \sin(\theta/2)|f\rangle$. Then, two sideband pumps are applied to yield a coherent rotation between $|f\rangle \otimes |0\rangle$ and $|e\rangle \otimes |1\rangle$. Following these rotations, the quantum state of the system changes as:

$$|g\rangle \otimes |0\rangle \rightarrow |g\rangle \otimes |0\rangle,$$
$$|e\rangle \otimes |0\rangle \rightarrow \cos(\theta/2)|e\rangle \otimes |0\rangle + \sin(\theta/2)|e\rangle \otimes |1\rangle.$$

Coherent light To implement the readout step using coherent light, the initially empty cavity is probed with a single-frequency microwave tone at frequency f_c^g. In the strong dispersive limit ($\chi \gg \kappa$), as the two cavity resonances are well separated, the cavity is excited to a coherent state $|\alpha\rangle$ only if the qubit is in the state $|g\rangle$.

Characterization of the emitted photon number and measurement backaction

The emitted photon number $n^{(\text{emit})}$ is obtained experimentally by deduction of the angle of rotation θ applied to generate the field in superposition between 0 and 1 photon for the single-photon light and by integrating the intracavity photon number for the coherent and thermal state. This intracavity photon number is itself obtained using the ac-Stark effect which causes modifications in the qubit spectrum.

To characterize the measurement backaction, a Ramsey measurement can be used. It consists of two $\pi/2$ pulses separated with a fixed time delay . The measured qubit state population after the Ramsey sequence oscillates due to the phase change of the second $\pi/2$ pulse, and the amplitude of the oscillation is proportional to the qubit coherence.

Conclusion

QUANTUM PHYSICS is so counterintuitive that a puzzling phenomenon such as energy exchange caused by the measuring process could almost have gone unnoticed. Our old intuition should not be too quickly overlooked however, and average energy conservation remains a requirement in the realm of quantum physics.

As a challenge to this expectation, quantum measurement are capable of affecting the energy of the system they measure. This extra energy, sometimes called quantum heat, nonetheless has to come from somewhere.

In order to track the fundamental origin of this energy and to assess its nature, we focused on the energy exchanged induced by a pre-measurement evolution, i.e., the step during which information is extracted by the meter. Using the notions of generalized heat and work, we identified in which cases this energy comes in the form of heat. Moreover, we found that when the measured system gains energy on average, this energy can come from the cost of turning on and off the interaction with the meter system. We then described how this turning on and off could be made autonomous by making a position dependent interaction. This allowed to fully analyse all the energy exchange due to pre-measurements within the quantum formalism. When the initial state of the KDoF has some finite spatial extension, it does not act a perfect work source and gets correlated with the measured and meter degrees of freedom during the interaction. The quality of the energy exchange between the measured system and this kinetic degree of freedom (KDoF) could be investigated using an energetic efficiency. Even if the correlations vanish at the end of the process, the efficiency of the work transfer between the KDoF and the other DoF allows for the characterization of the unitarity of evolution from the system and meter point of view, as long are there are indeed some energy exchanges.

We then explored the impact of the meter initial state on the measurement cost and quality given energy constraints. The quality was quantified by the decoherence of the measured qubit and the mutual information between qubit and meter field. We found that, using a specific type of interaction and a given final classical measurement basis, the quantum field was a better meter than the coherent field and even more than the thermal. Indeed, quantum superposition of 0 and 1 photon are less energy demanding for the same measurement quality. However, since thermal states are often treated as free resources and are usually very easy to obtain, this result could prove useful to measurement based devices.

These results help clarify the link between measurement and energy at the quantum level and could allow to design more energy efficient measurement for future quantum objects. They also show that the quantum to classical cut is not necessarily a dead end to investigate fundamental aspects related to quantum measurements, such as the energetic ones.

What is life without fun?

Résumé en français

TANDIS QUE les domaines de la thermodynamique et de la physique quantiques s'étendent et fêtent respectivement leur 200ième et 120ième presque-anniversaires, leurs liens n'ont rien perdu de leur fertilité.

La première révolution quantique, qui a émergée suite à la découverte de la quantification des niveaux energétiques de la lumière et de la matière, est elle-même issue de l'analyse énergétique du rayonnement de corps noir. Depuis, les phénomènes de superposition et l'intrication sont devenus accessibles et leur impact sur les échanges d'énergie et d'information entre objects quantiques est au coeur de nombreuses questions.

Introduction

La thermodynamique classique caractérise et régit l'évolution de deux quantités fondamentales: l'energie et l'entropie. D'une part, elle postule la conservation de l'energie et de l'autre l'augmentation de l'entropie totale du sytème et de son environnement au cours du temps. Ces deux quantitiés sont liées au travers des notions de travail et de chaleur. En effet, historiquement, c'est en constatant que le travail extrait à partir d'un flux de chaleur est borné que Sadi Carnot énonça pour la première fois le second principe de la thermodynamique. Le premier principe reconnait quant à lui ces deux flux comme les deux facettes d'une même quantité: l'énergie et érige la conservation totale de cette énergie au niveau d'une loi.

Comme l'avait déjà compris Carnot en 1824, il est possible de définir une quantité, à partir des flux de chaleurs, qui n'est nulle que pour un cycle reversible et positive en cas d'irreversibilité. Cette quantité est la variation d'entropie totale des bains thermiques et du système utilisé pour extraire du travail. Puisque même lors de l'évolution inverse, donc en utilisant un moteur thermique en réfrigérateur par exemple, la variation totale d'entropie reste positive ou nulle, cette quantité révèle une disymétrie fondamentale dans l'évolution des échanges énergétiques. Si, lors d'un processus, l'entropie totale augmente, alors c'est que le temps augmente: c'est la notion de flèche du temps. Autrement dit, l'entropie totale, au sens strict: l'entropie de l'univers, est un indicateur qui additionne les effets des phénomènes irréversibles.

En remontant jusqu'à une description atomique de la matière, force est de constater que cette description classique suppose beaucoup d'idéalisation qui, bien que généralement légitimes à l'échelle macroscopique, s'avèrent inexacte à plus petite échelle. On pourra notamment penser aux dynamiques non markoviennes et aux régimes de couplage forts. En outre, la manipulation d'objets toujours plus petits permet d'accéder à des régimes jusqu'alors inaccessibles où les fluctuations deviennent mesurables et jouent un rôle considérable. Deux implémentations identiques d'une expérience conduisent ainsi à des évolutions différentes dont la distribution statistique donne accès à de nouvelles informations. C'est le cas notamment lors de l'étude des processus hors-équilibres par le biais des théorèmes fluctuations.

Lorsque les systèmes considérés sont suffisamment bien isolés pour exhiber des comportements et états purement quantiques, tels que l'intrication par exemple, de nouvelles possibilités apparaissent. Les systèmes quantiques sont en particulier connus pour la taille exponentielle, en fonction du nombre de systèmes élémentaires considérés, de l'espace algébrique auquel ils donnent accès. Si les ordinateurs quantiques espèrent tirer partie de cette propriété, la thermodynamique n'est pas en reste puisque les phénomènes quantiques ont déjà montré leur potentialité en terme d'efficacité énergétique.

Une autre conséquence de la possibilité pour un système quantique d'être en état de superposition, c'est-à-dire dans un état parfaitement connu et pourtant pouvant donner lieu à des résultats différents lorsqu'il est mesuré puis repréparé à plusieurs reprises, donne également lieu au phénomène de "Rétroaction de la mesure" ("Measurement Backaction" en anglais). Comme son nom l'indique, la rétroaction de la mesure correspond à la modification de l'état du système quantique mesuré sous l'effet de cette action.

L'ensemble de ces possibilités vient alors completer notre compréhension et le domaine d'applicabilité de la thermodynamique comme illustré en Figure. I.1.

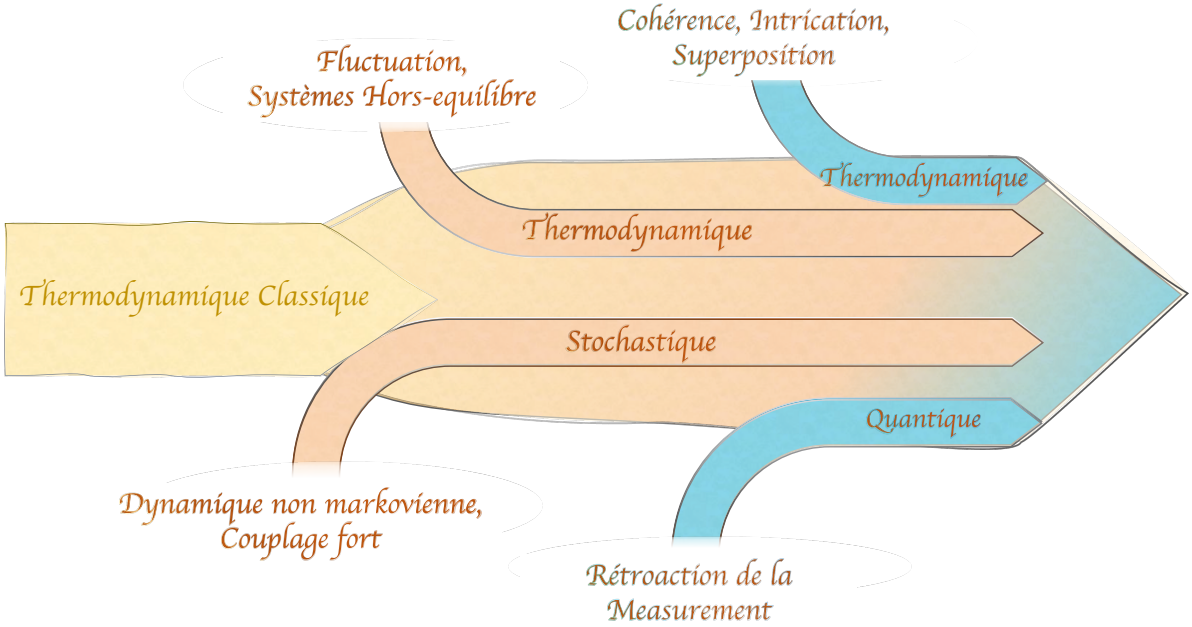

Figure I.1: De la thermodynamique classique à la thermodynamique quantique

Mesure quantique

Une des mesures quantiques les plus simples est la mesure projective. D'après le postulat de la mesure, le résultat sera une des valeurs propre o_i de l'observable mesuré $\mathcal{O}^S$ suivant la

probabilité $P_i = |\langle e_i| \rho^S |e_i\rangle|$ où ρ^S est l'état du système mesuré avant la mesure. La rétroaction de la mesure projettera cet état sur le vecteur propre de $\mathcal{O}^S$ correspondant à la valeur propre o_i: $|e_i\rangle$. Cette mesure projective est dite "lue" ou "sélective". En répétant la mesure, si le système est bien repréparé à chaque fois dans sont état de départ ρ^S, le résultat et l'état final pourront être différents: c'est la stochasticité de la mesure. En moyennant sur tous les états finaux obtenus, chacun avec sa probabilité associée, on obtient alors l'état final correspondant à une mesure "non-lue" ou "non sélective". Il s'écrit alors $\sum_i P_i |e_i\rangle \langle e_i| = \sum_i \Pi_i \rho^S \Pi_i$, où $\Pi_i = |e_i\rangle \langle e_i|$. Cet état sera identique à l'état initial ρ^S, si et seulement si ρ^S est diagonal dans la base des états propre de $\mathcal{O}^S$.

Ainsi, en mesurant l'état d'un objet quantique, il est possible (et même très commun) de modifier son état. Plus surprenamment encore, lorsque l'observable mesuré $\mathcal{O}^S$ et l'Hamiltonien propre du système H^S ne commutent pas, l'énergie moyenne du système peut être modifiée. Ce changement d'énergie parfois appelé « chaleur quantique » s'écrit alors :

$$E_{\mathcal{M}} = \mathrm{Tr}(H^S \Pi_i \rho^S \Pi_i) - \mathrm{Tr}(H^S \rho^S), \tag{5.33}$$

et peut être utilisé comme ressource pour alimenter de nouveaux types de machines quantiques: les moteurs quantiques à mesure.

La chaleur quantique peut être négative ou positive suivant l'état initial et l'opérateur mesuré et est dû à l'interaction du système avec l'appareil de mesure. Pour mieux comprendre son origine, il est cependant necessaire de connaitre la dynamique du processus de mesure.

Cette évolution temporelle de l'état d'un système mesuré au cours de la mesure n'est pas aujourd'hui connu à cause du phénomène de réduction du paquet d'onde. En effet, les postulats de la physique quantique permettent de décrire l'évolution d'un système quantique isolé par l'équation de Schrödinger mais un traitement différent doit être utilisé pour décrire l'effet de la mesure. Cela vient du fait que l'équation de Schrödinger est linéaire et deterministe tandis que les mesure quantiques projectives ne le sont pas.

Il est possible cependant d'obtenir l'état final prévu suite à une mesure projective non-séléctive en faisant interagir le système mesuré avec un autre object quantique, appelé mesureur quantique, dont l'état va se corréler à celui du système mesuré. C'est le processus de pré-mesure. L'évolution globale de ce système reste régit par l'équation de Schrödinger et offre donc un cadre idéal pour l'étude des échanges energétiques causés par la mesure.

Il est important de noter que pour obtenir de l'information à propos du système, la mesure doit être lue et conduire à un résultat en particulier parmi tout ceux possible. Suite à l'étape de pré-mesure, voir de plusieurs étapes de pré-mesure à la manière de Von Neumann, il est donc nécessaire d'invoquer une mesure selective et donc une interface avec le monde classique: c'est la séparation de Heisenberg (Heisenberg cut).

Contenu de la thèse

Cette thèse se concentre sur l'étude des conséquences énergetiques et entropiques de la mesure en physique quantique. La mesure est décomposée en: une étape de pré-mesure durant laquelle le système mesuré S interagit avec un système quantique intermediaire appelé "mesureur quantique" et noté M, suivi d'une étape de mesure projective non lue de ce mesureur. Si cette mesure projective n'affecte pas l'énergie moyenne du système total SM, alors l'énergie de la mesure peut être étudié entièrement au sein du formalisme quantique, i.e., sans invoquer le postulat de la mesure.

En utilisant ce principe, je remonte l'origine de la chaleur quantique utilisée comme source d'énergie dans un moteur quantique à mesure. En utilisant les notions de travail et chaleur généralisées, je caractérise la nature de cette énergie et généralise ce cas particulier. Je montre alors que l'énergie reçue par le système correspond à celle nécessaire pour allumer et éteindre l'interaction entre le système et l'appareil de mesure et qu'elle est idéalement reću sous forme de chaleur.

En remontant encore la source de cette énergie, nous proposons une version autonome de ce mécanisme. Pour cela, le système choisi est un qubit se déplaćant à travers une cavité dont le champ constitue l'appareil de mesure. L'interaction entre eux étant dépendante de leur position relative, l'énergie cinétique apporte l'énergie nécessaire à faire interagir ces deux systèmes. En modélisant cette évolution de manière purement quantique, nous caractérisons l'impact de l'extension spatiale finie du paquet d'onde sur la nature de ces échanges d'énergie.

Du point de vue opposé, nous comparons le cout énergétique de la mesure d'un qubit en fonction de l'état initial du champ utilisé pour le mesurer. Dans le cas d'un circuit d'électrodynamique quantique, nous trouvons que les états cohérents et thermiques permettent une même qualité de mesure à énergie fixée.

Les résultats présentés et décrits dans cette thèse contribuent à améliorer notre compréhension profonde des effets et mécanismes surprenants induits par la mesure quantique. En particulier, ils permettent de mieux comprendre le fonctionnement des moteurs quantiques à mesure et d'identifier précisément la ressource et le coût que constitue la mesure en physique quantique.

Caractériser les échanges d'énergies entre systèmes quantiques

Afin de caractériser les échanges énergétiques au sein d'un système quantique bipartite fermé et pouvant seulement échanger de l'énergie sous forme de travail avec le monde exterieur, un ensemble cohérent de définitions a récemment émergé. Bien que d'autres définitions existent, celle-ci permet de traiter les deux sous systèmes de manière agnostique, sans émettre d'hypothèse sur aucun d'eux et n'invoque aucun système classique. Ainsi, afin de quantifier la chaleur et le travail, j'utilise dans cette thèse les définitions issues de ce paradigme que j'appellerais : «Énergétique quantique bipartite » (EQB, ou BQE en anglais).

Ces définitions, résumées dans la Figure. 2.2, sont les suivantes. Soit un système quantique

bipartite AB évoluant selon le Hamiltonien dépendant du temps:

$$H^{AB}(t) = H^{A}(t) + H^{B}(t) + V^{AB}(t) \tag{5.34}$$

où H^A et H^B sont les Hamiltoniens propre des sous parties A et B respectivement et avec V^{AB} le terme d'interaction entre elles. L'énergie interne de A est alors définie par: $\mathcal{U}_A(t) = \mathrm{Tr}(H^A\rho^A(t))$ avec $\rho^A(t) = \mathrm{Tr}_A(\rho^{AB}(t))$ l'état réduit du système A. Le flux de chaleur reçu par cette sous partie A est quant à lui :

$$\frac{d}{dt}\mathcal{W}_A = -\frac{i}{\hbar}\mathrm{Tr}_{AB}([H^A, V^{AB}]\rho^A(t)\otimes\rho^B(t)) \tag{5.35}$$

tandis que le flux de travail qu'elle reçoit est :

$$\frac{d}{dt}\mathcal{Q}_A = -\frac{i}{\hbar}\mathrm{Tr}_{AB}\left([H^A, V^{AB}]\chi^{AB}(t)\right). \tag{5.36}$$

Nous avons ici introduit la matrice de correlation χ^{AB} qui joue un rôle capital dans EQB et qui est définie par: $\chi^{AB}(t) = \rho^{AB}(t) - \rho^A(t)\otimes\rho^B(t)$. En échangeant les rôles de A et B, on obtient alors les flux de chaleur et travail reçus par le sous système B. L'énergie totale du système n'est cependant pas simplement la somme des énergies internes de chacun des sous systèmes et il faut ajouter à cela l'énergie d'interaction qui s'écrit alors: $\mathcal{V}_{AB}(t) = \mathrm{Tr}(V^{AB}\rho^{AB}(t))$ et dont la dérivé temporelle est elle même divisée en un flux de chaleur $\dot{\mathcal{V}}^{\otimes}_{AB}(t)$ et de travail $\dot{\mathcal{V}}^{\chi}_{AB}(t)$ selon:

$$\begin{aligned}\dot{\mathcal{V}}^{\otimes}_{AB}(t) &= -\frac{i}{\hbar}\mathrm{Tr}_{AB}([V^{AB}, H^{AB}]\rho^A(t)\otimes\rho^B(t))\\ \dot{\mathcal{V}}^{\chi}_{AB}(t) &= -\frac{i}{\hbar}\mathrm{Tr}_{AB}\left([V^{AB}, H^{AB}]\chi^{AB}(t)\right).\end{aligned} \tag{5.37}$$

Les échanges d'énergie lors de la pré-mesure

Durant l'étape de pré-mesure, le système S et le mesureur M intéragissent via l'Hamiltonien :

$$H = H^S + H^M + f(t)\,V^S\otimes V^M \tag{5.38}$$

où l'interaction entre ces sous-systèmes est modulée par la fonction $f(t)$ où $f(t) = 0$ pour tout temps t hors de l'intervalle $\left[t_0, t_\mathrm{m}\right]$, i.e., avant et après l'étape de pré-mesure. Cette interaction est un produit tensoriel entre une partie s'appliquant au système mesuré V^S, qui correspond à l'opérateur mesuré, et une partie s'appliquant sur le mesureur V^M, afin de mesurer l'observable du système V^S via celui sur le mesureur V^M [112, 114, 113].

Durant cette étape, des corrélations sont créées entre système et le mesureur quantique. Idéalement, à la fin de ce processus, l'état réduit du système correspondra à la moyenne des états projetés prévus par le postulat de la mesure lors de la mesure de l'opérateur V^S.

Afin que la mesure n'affecte pas l'énergie du mesureur quantique, il est important que $\left[H^M, V^M\right] = 0$. C'est le cas lorsque les états du mesureur sont dégénérés ou alors lorsque

V^M et H^M sont diagonalisables dans la même base. En outre, si $\left[H^S, V^S\right] \neq 0$, l'énergie du système pourra être modifiée par la mesure, i.e., $E_{\mathcal{M}} \neq 0$.

Le flux de travail reçu par le système S, obtenu en appliquant l'équation. 5.35 est: $d\mathcal{W}^S/dt = -f(t)\left\langle V^M\right\rangle\left(d\left\langle V^S\right\rangle/dt\right)$, et peut être intégré pour obtenir la quantité de travail reçue pendant la pré-mesure:

$$\mathcal{W}^S\left(t_0 \to t_{\mathrm{m}}\right) = -\langle V^M\rangle\left[f(t)\langle V^S\rangle(t)\right]_{t_0^-}^{t_{\mathrm{m}}^+} + \langle V^M\rangle\int_{t_0}^{t_m} dt\dot{f}(t)\langle V^S\rangle \tag{5.39}$$

$$= \langle V^M\rangle\int_{t_0}^{t_m} dt\dot{f}(t)\langle V^S\rangle, \tag{5.40}$$

avec t_0 et t_m, respectivement les instants juste avant et juste après la pré-mesure tels que $f(t_m) = f(t_0) = 0$.

Indépendamment de la fonction f modulant l'interaction, le travail est donc nul lorsque $\langle V^M\rangle_0 = 0$, où l'indice 0 signifie que la moyennne est effectuée sur l'état initial, i.e., à l'instant t_0. La moyenne de cet opérateur étant constante au cours de la pré-mesure, puisque $[V^{SM}, H^M] = 0$, cette condition initiale garantie que sa valeur moyenne restera nulle au cours de l'évolution. Dans ce cas, l'énergie reçue par le système sera uniquement de la chaleur : $\Delta\mathcal{U}^S = \mathcal{Q}^S\left(t_0 \to t_{\mathrm{m}}\right)$ en accord avec le terme "chaleur quantique".

Comme illustré en Figure. 3.7, l'énergie de la mesure correspond donc à la chaleur généralisée reçue par le système qui elle même provient du travail généralisé transmis à l'énergie d'interaction et finalement issue du travail externe nécessaire à la modulation de l'interaction entre le système et l'appareil de mesure. Ainsi, le coût de la mesure est exactement celui de l'allumage et l'extinction du terme de couplage $f(t)V^{SM}$ et ce chemin énergetique conduit à la suite d'égalité suivante:

$$E_{\mathcal{M}} = \Delta\mathcal{U}^S\left(t_0^- \to t_{\mathrm{m}}^+\right) = \mathcal{Q}^S\left(t_0 \to t_{\mathrm{m}}\right) = -\int_{t_0}^{t_{\mathrm{m}}} f(t)\frac{d\langle V^S \otimes V^M\rangle_{\chi^{SM}(t)}}{dt}dt = \int_{t_0}^{t_m}\frac{df(t)}{dt}\langle V^{SM}\rangle_{\rho^{SM}(t)}dt,$$

Il est intéressant de noter qu'une telle mesure idéale est ainsi un processus thermodynamique très inefficace puisqu'elle transforme le travail externe en chaleur reçu par le système.

Flux énergétiques lors d'une mesure autonome

Pour aller plus loin dans l'analyse du coût de la mesure d'un object quantique, il est possible de rendre le processus de modulation de l'interaction purement autonome. L'évolution totale sera donc effectuée selon un Hamiltonien indépendant du temps et tous les échanges énergétiques s'effectueront entre les sous parties d'un système quantique mutlipartite.

Pour cela, nous considérons une particule de masse m avec des degrés de liberté internes (DdLI) et un degree de liberté cinétique (DdLC) et se déplaçant selon un mouvement unidi-

mensionnel vers le potentiel de forme spatiale $f(x)$ selon le Hamiltonien:

$$H = \frac{\hat{p}^2}{2m} + H_0 + f(\hat{x}) \otimes V_1, \tag{5.41}$$

avec $\hat{p}$ l'opérateur moment cinétique, $\hat{x}$ l'opérateur position, H_0 l'Hamiltonian propre des DdLI et V_1 la partie du terme d'interaction agissant sur les DdLIs (potentiellement ceux de la particule et de l'object générant le potentiel).

Lorsque la particule est suffisamment massive pour pouvoir être considérée comme ponctuelle, et donc que sa réflexion sur le potentiel est négligeable, la dynamique des DdLIs est gouvernée par l'Hamiltonien dépendant du temps et donc non-autonome, et son opérateur unitaire associé:

$$H_{\mathrm{NA}}(t) = H_0 + f(x_0 + v_0 t)V_1, \quad U_{NA}(t) = e^{-\frac{i}{\hbar}\int_0^t H_{\mathrm{NA}}(t)dt} \tag{5.42}$$

où x_0 et v_0 sont la position et vitesse initiale de la particule. Dans ce cas, aucune information n'est échangée entre le DdLC et les DdLIs.

Dans le cas où la particule a le DdLI d'un qubit, que ce DdLI constitue le système mesuré S, et que le DdLI du système générant le potentiel est le champ d'une cavité C qui sert alors de mesureur quantique, nous avons obtenu la dynamique globale du qubit et de la cavité. Cette dynamique est donnée à l'ordre 1 par rapport à l'angle entre la base de mesure et celle de diagonalisation de l'Hamiltonien propre du système. Cette contribution réduit les corrélations entre le système et le mesureur quantique en cohérence avec le théorème WAY. De plus, il apparait que l'énergie reçue par le qubit n'est plus seulement de la chaleur mais qu'une part importante lui provient sous forme de travail. Cet apport de travail provient de la moyenne du terme d'interaction agissant sur le mesureur qui n'est pas nul ($\langle V^M \rangle \neq 0$).

Lorsque la particule ne peut plus être considérée comme ponctuelle, mais que sa fonction d'onde est initialement étroite en position par rapport à la largueur de la zone d'interaction, la dynamique engendrée par le Hamiltonien donnée en Equation. 5.41 peut être approximée par celle donnée par le l'Hamiltonien "horloge":

$$H \simeq v_0 \hat{q} + H_0 + f(\hat{x}) \otimes V_1, \tag{5.43}$$

où $\hat{q} = \hat{p} - p_0$ est l'écart au moment cinétique moyen. L'évolution de l'état joint initial: $\int_{-\infty}^{\infty}\int_{-\infty}^{\infty} A_0(x,y)\,|x\rangle\langle y|\,dxdy \otimes \rho_0$, selon ce Hamiltonien peut être calculé à partir de la solution associée au Hamiltonien non-Autonome donné en Equation. 5.42. Pour cela, l'évolution unitaire est linéarisée autour de la position centrale x_0 en fonction de l'écart à cette position δx. Ainsi, il est possible d'obtenir l'état des DdLIs au temps t, qui s'écrit alors:

$$\rho_{\mathrm{DdLIs}}(t) \simeq \rho_C(t) = \rho_{NA}(t) + \left(\frac{E_I(t)\Delta x}{\hbar v_0}\right)^2 \mathcal{C}(\rho_0, t) \tag{5.44}$$

où $\rho_{NA}(t) = U_{\mathrm{NA}}(t)\rho_0 U_{\mathrm{NA}}^{\dagger}(t)$. Le terme correctif $\mathcal{C}(\rho_0, t_m)$ à cette évolution non-autonome est, au temps t_m tel que la particule est loin de la zone d'interaction, est :

$$\mathcal{C}(\rho_0, t_m) = \frac{1}{E_I^2(t)}\left(\left[H_0, U_{\mathrm{NA}}\left[H_0, \rho_0\right]U_{\mathrm{NA}}^{\dagger}\right] + U_{\mathrm{NA}} D_{H_0}(\rho_0) U_{\mathrm{NA}}^{\dagger} + D_{H_0}(U_{\mathrm{NA}}\rho_0 U_{\mathrm{NA}}^{\dagger})\right).$$

sous l'hypothèse que la particule est initialement suffisamment loin du potentiel pour que $\tilde{H}_0(x_0 + v_0 t) = H_{\mathrm{NA}}(t) \approx H_0$ et que $\tilde{H}_0(x + v_0 t_m) = H_{\mathrm{NA}}(\frac{x-x_0}{v_0} + t_m) \approx H_0$ et avec $D_X(\rho) = X\rho X^\dagger - (1/2)\{X^\dagger X, \rho\}$. Ainsi, lorsque l'état initial des DdLIs est un état propre du Hamiltonien H_0, $\mathcal{C}(\rho_0, t_m) = D_{H_0}(\rho_{\mathrm{NA}}(t))/E_I^2(t)$. à partir de ce terme correctif il est possible de calculer l'efficacité du DdLC en tant que source de travail qui est défini par:

$$\eta(\Delta x) \equiv \frac{W_I}{\Delta U_I} \simeq 1 + \frac{W_{\mathrm{I}}^{\Delta}}{\Delta U_{\mathrm{I}}^{NA}} + \varepsilon^2 \left(\frac{W_{\mathrm{I}}^{\mathcal{C}} - \Delta U_{\mathrm{I}}^{\mathcal{C}}}{\Delta U_{\mathrm{I}}^{NA}} \right) \quad \text{where} \quad W_I = \int_0^{t_m} \dot{W}_I \, \mathrm{d}t \ \text{ and } \varepsilon \equiv \frac{E_I \Delta x}{\hbar v_0},$$

et avec les termes W_{I}^{Δ} et $W_{\mathrm{I}}^{\mathcal{C}}$ définis en Eq. (4.51). Le terme W_{I}^{Δ} étant proportionel à $(\Delta x)^2$, cette efficacité est donc affectée par l'extension de la fonction d'onde à l'ordre 2 en Δx. Ainsi, il apparait donc que la nature de l'énergie reçu par les DdLIs et donc par le degré de liberté interne mesuré (car le DdLI de la cavité a une énergie constante) est affectée par la distribution spatiale de la fonction d'onde de la particule. Notamment, plus l'extension spatialle Δx augmente, plus cette énergie est donnée sous forme de chaleur, cette évolution étant d'ordre deux.

Quelles resources pour mesurer?

Nous avons précédemment étudié l'influence de l'état initial de la source de travail fournissant l'énergie de la chaleur quantique sur la qualité de ce transfert d'énergie. Maintenant, la question se pose de l'impact de l 'état du mesureur sur la qualité de la mesure et sur son coût.

Le coût de la mesure quantique de l'état d'un système quantique S via un autre système quantique M, correspond à celui nécessaire pour corréler ces deux systèmes en les faisant interagir via une opération unitaire [68]. L'énergie $\mathcal{W}_{meas}$ transmise au système total SM correspond alors à la variation de leur énergie libre ΔF_{SM} telle que:

$$\mathcal{W}_{meas} = \Delta F_{SM} = \Delta E_S + \Delta E_M - k_B T \Delta S_{SM} = \Delta F_M + k_B T I.$$

où $I = S_M + S_S - S_{SM}$ est l'information mutuelle, après interaction, entre S et M. Lorsque l'état initial du système n'a pas de cohérence dans la base selon laquelle il interagit avec M, son entropie reste constante et donc $\Delta S_S = 0$. Ainsi, pour une mémoire aux états énergétiques dégénérés: $\Delta E_M = 0$, puisque lors d'une opération unitaire l'entropie totale reste constante: $\Delta S_{SM} = 0$ et que l'information mutuelle est initialement nulle: $\Delta I = I$, la variation d'entropie de M est telle que $\Delta S_M = I$. Il en résulte que $\mathcal{W}_{meas} = 0$ et c'est donc pourquoi la mesure quantique n'a pas de coût fondamental. Cependant, comme les expériences de pensée de type démon de Maxwell l'indiquent, à la suite d'une mesure il est nécessaire de restaurer l'état initial du système M pour ne pas simplement tirer partie de son entropie initiale généralement nulle comme s'il s'agissait d'un bain à température nulle. Le coût associé s'écrit alors:

$$\mathcal{W}_{eras} = -\Delta F_M = -\Delta E_M + k_B T \Delta S_M$$

et le coût du cycle de mesure et réinitialisation de l'état du mesureur est:

$$\mathcal{W}_{meas} + \mathcal{W}_{eras} = k_B T I.$$

Ce coût est donc simplement proportionel à l'information mutuelle extraite: on ne paie idéalement que proportionellement à la quantité de la mesure effectuée.

Une manière de quantifier cette qualité est d'introduire une efficacité informationnelle: $\eta_I = I/S_S^0$, définit comme la proportion de l'entropie initial du système S_S^0 qui est communiquée au mesureur M. En outre, l'efficacité energétique $\eta_E = I/\delta S_M$ permet d'évaluer quelle proportion du coût de la réinitialisation du mesureur était vraiment nécéssaire par rapport au coût réel de cette réinitialisation.

Lorsque des cohérences sont présentes dans le mesureur à la fin de son interaction avec S dans la base où il est finalement classiquement mesuré, l'entropie de M augmentera alors plus que par la seule influence de son interaction avec S. Ainsi $\Delta S_M \geq I$ à la fin du processus de mesure total incluant cette mesure classique.

Si le système S a des cohérences dans la base selon laquelle il interagit avec M, alors son entropie augmentera $\Delta S_S \geq 0$ due à la rétroaction de la mesure.

Pour étudier l'impact de ces effets sur η_I et η_E, nous considérons le cas particulier d'un qubit mesuré par le champ d'une cavité de manière dispersive comme précédemment. En revanche, le qubit est cette fois ci mesuré dans une base qui commute avec son Hamiltonien propre et donc aucune chaleur quantique n'est ici impliquée. Inspiré par les possibilités offertes par les plateformes d'électrodynamique quantique sur circuit supraconducteur, l'interaction entre le champ et le qubit est modélisé par la correspondance suivante:

Champ quantique

$$|g\rangle \otimes |0\rangle \to |g\rangle \otimes (\cos(\theta/2)\,|0\rangle + \sin(\theta/2)\,|1\rangle)\,,$$
$$|e\rangle \otimes |0\rangle \to |e\rangle \otimes |0\rangle\,,$$

Champ cohérent

$$|g\rangle \otimes |0\rangle \to |g\rangle \otimes |\alpha\rangle\,,$$
$$|e\rangle \otimes |0\rangle \to |e\rangle \otimes |0\rangle\,,$$

Champ thermique

$$|g\rangle\langle g| \otimes |0\rangle\langle 0| \to |g\rangle\langle g| \otimes \rho_{th},$$
$$|e\rangle\langle e| \otimes |0\rangle\langle 0| \to |e\rangle\langle e| \otimes |0\rangle\langle 0|\,,$$
$$|g\rangle\langle e| \otimes |0\rangle\langle 0| \to |g\rangle\langle e| \otimes \sum_n \sqrt{p_n}\,|n\rangle\langle 0|$$
$$|e\rangle\langle g| \otimes |0\rangle\langle 0| \to |e\rangle\langle g| \otimes \sum_n \sqrt{p_n}\,|0\rangle\langle n|\,,$$

avec $\bar{n} = |\sin(\theta/2)|^2 = |\alpha|^2 = \mathrm{Tr}(a^\dagger a \rho_{\mathrm{th}})$.

Lorsque l'état initial du système est $\frac{|e\rangle\langle e| + |g\rangle\langle g|}{2}$, les états obtenus pour ces trois types de champ: quantique, cohérent et thermique montrent un clair avantage quantique en terme d'efficacité

informationelle et énergétique. En effet, ces indicateurs sont meilleurs pour le champ quantique formé d'une superposition de 0 et 1 photon, puis pour le champ cohérent et enfin pour le champ thermique. En revanche, il est intéressant de noter que l'entropie du champ thermique est moindre que celle du champ coherent, au moins tant que $\bar{n} \leq 3$.

Lorsque l'état inital possède des cohérences dans la base dans lequel il est mesuré par M: $\frac{|e\rangle+|g\rangle}{\sqrt{2}}$, l'information mutuelle finale est supérieure au cas précédent sans cohérences et l'efficacité énergétique des champs cohérents et thermiques décroit avec $\bar{n}$. Les cohérences du système décroissent également et ce d'autant plus à nombre moyen de photon fixé pour le champ quantique puis cohérent et enfin thermique. Cet effet vient de la probabilité p_0 de ces distributions de se trouver dans l'état de Fock $|0\rangle$. En effet, plus p_0 est grand plus la décohérence est importante. En revanche, expérimentalement, des résultats montrent une décohérence similaire due aux champs thermiques et cohérents. Cela peut-être expliqué en première approximation par les formes des fonctions $p_0(\bar{n})$ associées à ces champs, une fois intriqués avec l'état du qubit. Lorsque $\bar{n}$ tend vers 0 ces fonctions tendent toutes les deux vers l'exponentielle décroissante $e^{-n^{(\mathrm{emit})}}$, où $n^{(\mathrm{emit})}$ est le nombre total de photons ayant interagit avec le qubit par petites portions. Ainsi ces champs conduisent donc à la même décohérence dans le cas d'une injection progressive des photons dans la cavité.

Ces résultats, encore très préliminaires, ouvrent la voix à une étude plus générale de l'impact des cohérences sur les performances de la mesure quantique.

Conclusion

LA PHYSIQUE QUANTIQUE est si contre-intuitive que, la possibilité de changer l'énergie d'un système quantique en le mesurant, aussi déroutante soit-elle, aurait presque pu passer inaperçue. Notre intuition classique ne doit pas pour autant être négligée, et il reste légitime d'exiger la conservation de l'énergie moyenne d'un système isolé, même au sein du domaine de la physique quantique.

Les objets classiques étant beaucoup plus gros que les systèmes quantiques, l'énergie qu'ils échangent avec ces derniers pourrait être inaccessible depuis notre point de vue classique. Cependant, les systèmes optomécaniques et électromécaniques, par exemple, ont déjà réussi à montrer que cette énergie pouvait être stockée dans un système mécanique et même mesurée.

Afin de retracer l'origine fondamentale de cette énergie et d'en déterminer la nature, nous nous sommes concentrés sur l'énergie échangée lors du processus de pré-mesure, c'est-à-dire lors de l'étape d'extraction de l'information par le mesureur. En utilisant les notions de chaleur et de travail généralisés, nous quantifions la qualité de l'échange d'énergie entre le système mesuré et le mesureur quantique avec lequel il interagit. Nous constatons que lorsque le système mesuré gagne de l'énergie en moyenne, cette énergie peut provenir du coût d'allumage et d'extinction de l'interaction avec le système de mesure. Nous avons ensuite décrit comment cette modulation pouvait être rendue autonome en rendant l'interaction dépendante de la position relative entre le mesureur et le système. Cela permet d'analyser complètement tous les

échanges d'énergie dus à la pré-mesure dans le cadre du formalisme quantique. On constate que l'énergie transférée du degré de liberté cinétique (DdLC) au système mesuré est reçue sous forme de chaleur. Lorsque l'état initial du DdLC a une extension spatiale finie, il n'agit pas comme une source de travail parfaite et est corrélé avec le système à mesurer et le champ-mètre pendant l'interaction. Même si les corrélations s'annulent à la fin du processus, l'efficacité du transfert de travail entre le DdLC et les autres DdL permet de caractériser l'unitarité de l'évolution du point de vue système et mesureur.

Nous avons ensuite exploré l'impact de l'état initial du mesureur sur le coût de l'énergie pour des performances de mesure similaires, tel que quantifié par la décohérence du qubit mesuré et l'information mutuelle entre le qubit et le champ qui constitue le mesureur quantique. Nous avons constaté que, dans le cadre d'une expérience d'électrodynamique quantique de circuit, le champ thermique et le champ cohérent mixte ont des performances similaires. La superposition quantique des photons 0 et 1 devrait être moins gourmande en énergie pour la même qualité de mesure. Cependant, étant donné que les états thermiques sont souvent traités comme des ressources gratuites car ils sont généralement très faciles à mettre en oeuvre, ce résultat pourrait s'avérer utile afin de mettre à l'échelle le dispositif basé sur la mesure et de réduire l'échauffement de l'échantillon dû au processus de mesure.

Ces résultats aident à clarifier le lien entre la mesure et l'énergie au niveau quantique et pourraient permettre de concevoir des mesures plus économes en énergie pour les futurs objets quantiques. Ils montrent également que la frontière quantique/classique n'est pas nécessairement une vérou empéchant toute étude des aspects fondamentaux liés aux mesures quantiques telles que les mesures énergétiques.

Bibliography

[1] Stéphane Mazouffre. Electric propulsion for satellites and spacecraft: Established technologies and novel approaches. *Plasma Sources Sci. Technol.*, 25(3):033002, April 2016.

[2] Dan Ye, Jun Li, and Jau Tang. Jet propulsion by microwave air plasma in the atmosphere. *AIP Advances*, 10(5):055002, May 2020.

[3] Mohammed Shaheen and Shaaban Abdallah. Development of efficient vertical axis wind turbine clustered farms. *Renewable and Sustainable Energy Reviews*, 63:237–244, September 2016.

[4] Matteo Colombo and Patricia Palacios. Non-equilibrium thermodynamics and the free energy principle in biology. *Biol Philos*, 36(5):41, August 2021.

[5] Ziqing Wang, Robert Malaney, and Ryan Aguinaldo. Temporal Modes of Light in Satellite-to-Earth Quantum Communications. *arXiv:2106.13693 [physics, physics:quant-ph]*, June 2021.

[6] Valentina Marulanda Acosta, Daniele Dequal, Matteo Schiavon, Aurélie Montmerle-Bonnefois, Caroline B. Lim, Jean-Marc Conan, and Eleni Diamanti. Analysis of satellite-to-ground quantum key distribution with adaptive optics. *arXiv:2111.06747 [quant-ph]*, November 2021.

[7] Ajay Kumar and Sunita Garhwal. State-of-the-Art Survey of Quantum Cryptography. *Arch Computat Methods Eng*, 28(5):3831–3868, August 2021.

[8] Christopher Portmann and Renato Renner. Security in Quantum Cryptography. *arXiv:2102.00021 [quant-ph]*, August 2021.

[9] Ninghao Zhou, Zhenyu Ouyang, Liang Yan, Meredith G. McNamee, Wei You, and Andrew M. Moran. Elucidation of Quantum-Well-Specific Carrier Mobilities in Layered Perovskites. *J. Phys. Chem. Lett.*, 12(4):1116–1123, February 2021.

[10] Agustin Pérez-Madrid and Ivan Santamaría-Holek. A Theoretical Perspective of the Photochemical Potential in the Spectral Performance of Photovoltaic Cells. *Entropy*, 23(5):579, May 2021.

[11] John M. Martinis. Quantum supremacy in a superconducting quantum processor. In *Photonics for Quantum 2021*, volume 11844, page 118440D. SPIE, July 2021.

[12] Cyril Branciard. Witnesses of causal nonseparability: An introduction and a few case studies. *Scientific Reports*, 6(1), 2016.

[13] K. Goswami, C. Giarmatzi, M. Kewming, F. Costa, C. Branciard, J. Romero, and A. G. White. Indefinite Causal Order in a Quantum Switch. *Phys. Rev. Lett.*, 121(9):090503, 2018.

[14] Giulia Rubino, Lee A. Rozema, Adrien Feix, Mateus Araújo, Jonas M. Zeuner, Lorenzo M. Procopio, Časlav Brukner, and Philip Walther. Experimental verification of an indefinite causal order. *Science Advances*, 3(3):e1602589, March 2017.

[15] Lorenzo Magrini, Philipp Rosenzweig, Constanze Bach, Andreas Deutschmann-Olek, Sebastian G. Hofer, Sungkun Hong, Nikolai Kiesel, Andreas Kugi, and Markus Aspelmeyer. Optimal quantum control of mechanical motion at room temperature: Ground-state cooling. *arXiv:2012.15188 [physics, physics:quant-ph]*, December 2020.

[16] Neelesh Kumar Vij, Meenakshi Khosla, and Shilpi Gupta. Optimization of ground-state cooling of a mechanical mode using a three-level system. *arXiv:2104.14533 [quant-ph]*, April 2021.

[17] Yannick Seis, Thibault Capelle, Eric Langman, Sampo Saarinen, Eric Planz, and Albert Schliesser. Ground State Cooling of an UltracoherentElectromechanical System. *arXiv:2107.05552 [quant-ph]*, July 2021.

[18] Leonhard Neuhaus, Remi Metzdorff, Salim Zerkani, Sheon Chua, Jean Teissier, Daniel Garcia-Sanchez, Samuel Deleglise, Thibaut Jacqmin, Tristan Briant, Jerome Degallaix, Vincent Dolique, Geppo Cagnoli, Olivier Le Traon, Claude Chartier, Antoine Heidmann, and Pierre-Francois Cohadon. Laser cooling of a Planck mass object close to the quantum ground state. *arXiv:2104.11648 [quant-ph]*, April 2021.

[19] K. S. Lee, Y. P. Tan, L. H. Nguyen, R. P. Budoyo, K. H. Park, C. Hufnagel, Y. S. Yap, N. Møbjerg, V. Vedral, T. Paterek, and R. Dumke. Entanglement between superconducting qubits and a tardigrade. *arXiv:2112.07978 [physics, physics:quant-ph]*, December 2021.

[20] V. Andreev, D. G. Ang, D. DeMille, J. M. Doyle, G. Gabrielse, J. Haefner, N. R. Hutzler, Z. Lasner, C. Meisenhelder, B. R. O'Leary, C. D. Panda, A. D. West, E. P. West, X. Wu, and ACME Collaboration. Improved limit on the electric dipole moment of the electron. *Nature*, 562(7727):355–360, October 2018.

[21] M. Planck. On the Theory of the Energy Distribution Law of the Normal Spectrum. In *The Old Quantum Theory*, pages 82–90. Elsevier, 1900.

[22] Binder and correa. *Thermodynamics in the Quantum Regime*. 2018.

[23] Joule JP. On the mechanical equivalent of heat. *Phil. Trans. R. Soc.*, 140:61–82, 1850.

[24] Sadi Carnot. *Réflexions sur la puissance motrice du feu et sur les machines propres à développer cette puissance*. Gauthier-Villars, 1878.

[25] J. Clerk Maxwell. *Theory of Heat*. 1872.

[26] Leo Szilard. On the decrease of entropy in a thermodynamic system by the intervention of intelligent beings. *Behavioral Science*, 9(4):301–310, 1929.

[27] Charles H. Bennett. Notes on Landauer's principle, reversible computation, and Maxwell's Demon. 2003.

[28] R. Landauer. Irreversibility and Heat Generation in the Computing Process. *IBM Journal of Research and Development*, 5(3):183–191, July 1961.

[29] Marcelo O. Magnasco and Gustavo Stolovitzky. Feynman's Ratchet and Pawl. *Journal of Statistical Physics*, 93(3):615–632, November 1998.

[30] Juan M. R. Parrondo and Pep Español. Criticism of Feynman's analysis of the ratchet as an engine. *American Journal of Physics*, 64(9):1125–1130, September 1996.

[31] Alhun Aydin, Altug Sisman, and Ronnie Kosloff. Landauer's Principle in a Quantum Szilard Engine Without Maxwell's Demon. *Entropy*, 22(3):294, March 2020.

[32] Rafael Sánchez, Janine Splettstoesser, and Robert S. Whitney. Nonequilibrium System as a Demon. *Physical Review Letters*, 123(21), November 2019.

[33] Nahuel Freitas and Massimiliano Esposito. A Maxwell demon that can work at macroscopic scales, April 2022.

[34] H. E. D. Scovil and E. O. Schulz-DuBois. Three-Level Masers as Heat Engines. 1959.

[35] J. E. Geusic, E. O. Schulz-DuBois, and H. E. D. Scovil. Quantum Equivalent of the Carnot Cycle. *Phys. Rev.*, 156(2):343–351, April 1967.

[36] Y. V. Rostovtsev, A. B. Matsko, N. Nayak, M. S. Zubairy, and M. O. Scully. Improving engine efficiency by extracting laser energy from hot exhaust gas. *Phys. Rev. A*, 67(5):053811, May 2003.

[37] Ting Zhang, Wei-Tao Liu, Ping-Xing Chen, and Cheng-Zu Li. Four-level entangled quantum heat engines. *Phys. Rev. A*, 75(6):062102, June 2007.

[38] Marlan O. Scully. Extracting Work from a Single Thermal Bath via Quantum Negentropy. *Phys. Rev. Lett.*, 87(22):220601, November 2001.

[39] Marlan O. Scully. Quantum Afterburner: Improving the Efficiency of an Ideal Heat Engine. *Phys. Rev. Lett.*, 88(5):050602, January 2002.

[40] X. L. Huang, Tao Wang, and X. X. Yi. Effects of reservoir squeezing on quantum systems and work extraction. *Phys. Rev. E*, 86(5):051105, November 2012.

[41] Philipp Strasberg, Gernot Schaller, Tobias Brandes, and Massimiliano Esposito. Thermodynamics of a Physical Model Implementing a Maxwell Demon. *Phys. Rev. Lett.*, 110(4):040601, January 2013.

[42] Bartłomiej Gardas and Sebastian Deffner. Thermodynamic universality of quantum Carnot engines. *Phys. Rev. E*, 92(4):042126, October 2015.

[43] Valentin Blickle and Clemens Bechinger. Realization of a micrometre-sized stochastic heat engine. *Nature Phys*, 8(2):143–146, February 2012.

[44] Jean-Philippe Brantut, Charles Grenier, Jakob Meineke, David Stadler, Sebastian Krinner, Corinna Kollath, Tilman Esslinger, and Antoine Georges. A Thermoelectric Heat Engine with Ultracold Atoms. *Science*, November 2013.

[45] I. A. Martínez, É Roldán, L. Dinis, D. Petrov, J. M. R. Parrondo, and R. A. Rica. Brownian Carnot engine. *Nature Phys*, 12(1):67–70, January 2016.

[46] Johannes Roßnagel, Samuel T. Dawkins, Karl N. Tolazzi, Obinna Abah, Eric Lutz, Ferdinand Schmidt-Kaler, and Kilian Singer. A single-atom heat engine. *Science*, April 2016.

[47] Sudeesh Krishnamurthy, Subho Ghosh, Dipankar Chatterji, Rajesh Ganapathy, and A. K. Sood. A micrometre-sized heat engine operating between bacterial reservoirs. *Nature Phys*, 12(12):1134–1138, December 2016.

[48] Suman Chand and Asoka Biswas. Single-ion quantum Otto engine with always-on bath interaction. *EPL*, 118(6):60003, June 2017.

[49] Jan Klaers, Stefan Faelt, Atac Imamoglu, and Emre Togan. Squeezed Thermal Reservoirs as a Resource for a Nanomechanical Engine beyond the Carnot Limit. *Phys. Rev. X*, 7(3):031044, September 2017.

[50] John P. S. Peterson, Tiago B. Batalhão, Marcela Herrera, Alexandre M. Souza, Roberto S. Sarthour, Ivan S. Oliveira, and Roberto M. Serra. Experimental Characterization of a Spin Quantum Heat Engine. *Phys. Rev. Lett.*, 123(24):240601, 9, 2019.

[51] Gleb Maslennikov, Shiqian Ding, Roland Hablützel, Jaren Gan, Alexandre Roulet, Stefan Nimmrichter, Jibo Dai, Valerio Scarani, and Dzmitry Matsukevich. Quantum absorption refrigerator with trapped ions. *Nat Commun*, 10(1):202, January 2019.

[52] James Klatzow, Jonas N. Becker, Patrick M. Ledingham, Christian Weinzetl, Krzysztof T. Kaczmarek, Dylan J. Saunders, Joshua Nunn, Ian A. Walmsley, Raam Uzdin, and Eilon Poem. Experimental Demonstration of Quantum Effects in the Operation of Microscopic Heat Engines. *Phys. Rev. Lett.*, 122(11):110601, March 2019.

[53] D. von Lindenfels, O. Gräb, C. T. Schmiegelow, V. Kaushal, J. Schulz, Mark T. Mitchison, John Goold, F. Schmidt-Kaler, and U. G. Poschinger. Spin Heat Engine Coupled to a Harmonic-Oscillator Flywheel. *Phys. Rev. Lett.*, 123(8):080602, August 2019.

[54] Baldo-Luis Najéra-Santos, Patrice A. Camati, Valentin Métillon, Michel Brune, Jean-Michel Raimond, Alexia Auffèves, and Igor Dotsenko. Autonomous Maxwell's demon in a cavity QED system. *arXiv:2001.07445 [quant-ph]*, January 2020.

[55] Nathan M. Myers, Obinna Abah, and Sebastian Deffner. Quantum thermodynamic devices: From theoretical proposals to experimental reality. *arXiv:2201.01740 [cond-mat, physics:quant-ph]*, January 2022.

[56] Giovanni Vacanti, Cyril Elouard, and Alexia Auffeves. The work cost of keeping states with coherences out of thermal equilibrium. *arXiv:1503.01974 [quant-ph]*, March 2015.

[57] M. H. Mohammady, A. Aufféves, and J. Anders. Energetic footprints of irreversibility in the quantum regime. *arXiv:1907.06559 [cond-mat, physics:quant-ph]*, July 2019.

[58] P. Kammerlander and J. Anders. Coherence and measurement in quantum thermodynamics. *Scientific Reports*, 6(1), April 2016.

[59] Andrew N. Jordan and Markus Büttiker. Entanglement Energetics at Zero Temperature. *Physical Review Letters*, 92(24), June 2004.

[60] Howard M. Wiseman and Milburn. *Quantum Measurement and Control*. 2010.

[61] Huzihiro Araki and Mutsuo M. Yanase. Measurement of Quantum Mechanical Operators. *Physical Review*, 120(2):622–626, October 1960.

[62] Juyeon Yi and Yong Woon Kim. Role of measurement in feedback-controlled quantum engines. *J. Phys. A: Math. Theor.*, 51(3):035001, January 2018.

[63] Cyril Elouard, David A. Herrera-Martí, Maxime Clusel, and Alexia Auffèves. The role of quantum measurement in stochastic thermodynamics. *npj Quantum Information*, 3(1):9, March 2017.

[64] Hoda Hossein-Nejad, Edward J O'Reilly, and Alexandra Olaya-Castro. Work, heat and entropy production in bipartite quantum systems. *New Journal of Physics*, 17(7):075014, July 2015.

[65] Maria Maffei. Work exchanges between a qubit and a quantum field in Waveguide Quantum Electro-Dynamics. page 6.

[66] M Hamed Mohammady and Janet Anders. A quantum Szilard engine without heat from a thermal reservoir. *New Journal of Physics*, 19(11):113026, November 2017.

[67] Juan M. R. Parrondo, Jordan M. Horowitz, and Takahiro Sagawa. Thermodynamics of information. *Nature Physics*, 11(2):131–139, February 2015.

[68] Takahiro Sagawa and Masahito Ueda. Minimal Energy Cost for Thermodynamic Information Processing: Measurement and Information Erasure. *Physical Review Letters*, 102(25), June 2009.

[69] Kurt Jacobs. Quantum measurement and the first law of thermodynamics: The energy cost of measurement is the work value of the acquired information. *Physical Review E*, 86(4), October 2012.

[70] Sang Wook Kim, Takahiro Sagawa, Simone De Liberato, and Masahito Ueda. Quantum Szilard Engine. *Physical Review Letters*, 106(7), February 2011.

[71] Cyril Elouard, David Herrera-Martí, Benjamin Huard, and Alexia Auffèves. Extracting Work from Quantum Measurement in Maxwell's Demon Engines. *Physical Review Letters*, 118(26), June 2017.

[72] Cyril Elouard and Andrew N. Jordan. Efficient Quantum Measurement Engine. *Phys. Rev. Lett.*, 120(26):260601, June 2018.

[73] Juyeon Yi, Peter Talkner, and Yong Woon Kim. Single-temperature quantum engine without feedback control. *Physical Review E*, 96(2), August 2017.

[74] Xuehao Ding, Juyeon Yi, Yong Woon Kim, and Peter Talkner. Measurement-driven single temperature engine. *Physical Review E*, 98(4), October 2018.

[75] Lorenzo Buffoni, Andrea Solfanelli, Paola Verrucchi, Alessandro Cuccoli, and Michele Campisi. Quantum Measurement Cooling. *Physical Review Letters*, 122(070603):5, 2019.

[76] Arpan Das and Sibasish Ghosh. Measurement Based Quantum Heat Engine with Coupled Working Medium. *Entropy*, 21(11):1131, November 2019.

[77] Michele Campisi. Feedback-controlled heat transport in quantum devices: Theory and solid-state experimental proposal. *New J. Phys.*, page 13, 2017.

[78] Andrew N. Jordan, Cyril Elouard, and Alexia Auffèves. Quantum measurement engines and their relevance for quantum interpretations. *arXiv:1911.06838 [quant-ph]*, November 2019.

[79] Rolf Landauer. Information is physical. page 8, 1991.

[80] Takahiro Sagawa and Masahito Ueda. Second Law of Thermodynamics with Discrete Quantum Feedback Control. *Physical Review Letters*, 100(8), February 2008.

[81] Yelena Guryanova, Nicolai Friis, and Marcus Huber. Ideal Projective Measurements Have Infinite Resource Costs. *Quantum*, 4:222, January 2020.

[82] Wojciech Hubert Zurek. Quantum Darwinism. *Nature Phys*, 5(3):181–188, March 2009.

[83] Wojciech Hubert Zurek. Emergence of the Classical from within the Quantum Universe. *arXiv:2107.03378 [quant-ph]*, July 2021.

[84] Maximilian Schlosshauer. Decoherence, the measurement problem, and interpretations of quantum mechanics. *Rev. Mod. Phys.*, 76(4):1267–1305, February 2005.

[85] tim maudlin. Three measurement problem. 1995.

[86] Craig Callender. The emergence and interpretation of probability in Bohmian mechanics. *Studies in History and Philosophy of Science Part B: Studies in History and Philosophy of Modern Physics*, 38(2):351–370, June 2007.

[87] Alexia Auffèves and Philippe Grangier. Contexts, Systems and Modalities: A New Ontology for Quantum Mechanics. *Foundations of Physics*, 46(2):121–137, February 2016.

[88] Carlo Rovelli. Relational Quantum Mechanics. *Int J Theor Phys*, 35(8):1637–1678, August 1996.

[89] Jonte R. Hance and Sabine Hossenfelder. What does it take to solve the measurement problem?, June 2022.

[90] N. David Mermin. A note on the quantum measurement problem, June 2022.

[91] Maximilian Schlosshauer. Decoherence: From Interpretation to Experiment. *arXiv:2204.09755 [quant-ph]*, 204:45–64, 2022.

[92] *Wigner Book*. 1932.

[93] Wigner.

[94] Mutsuo M. Yanase. Optimal Measuring Apparatus. *Phys. Rev.*, 123(2):666–668, July 1961.

[95] L. Loveridge and P. Busch. 'Measurement of quantum mechanical operators' revisited. *Eur. Phys. J. D*, 62(2):297–307, April 2011.

[96] Mehdi Ahmadi, David Jennings, and Terry Rudolph. The Wigner–Araki–Yanase theorem and the quantum resource theory of asymmetry. *New Journal of Physics*, 15(1):013057, January 2013.

[97] Ronnie Kosloff. Quantum Thermodynamics: A Dynamical Viewpoint. *Entropy*, 15(6):2100–2128, June 2013.

[98] Philipp Strasberg, Gernot Schaller, Tobias Brandes, and Massimiliano Esposito. Quantum and Information Thermodynamics: A Unifying Framework Based on Repeated Interactions. *Physical Review X*, 7(2), April 2017.

[99] Philipp Strasberg and Andreas Winter. First and Second Law of Quantum Thermodynamics: A Consistent Derivation Based on a Microscopic Definition of Entropy. *arXiv:2002.08817 [cond-mat, physics:quant-ph]*, June 2021.

[100] Matteo Lostaglio. An introductory review of the resource theory approach to thermodynamics. *Rep. Prog. Phys.*, 82(11):114001, November 2019.

[101] R. Alicki. The quantum open system as a model of the heat engine. *J. Phys. A: Math. Gen.*, 12(5):L103–L107, May 1979.

[102] S. Alipour, F. Benatti, F. Bakhshinezhad, M. Afsary, S. Marcantoni, and A. T. Rezakhani. Correlations in quantum thermodynamics: Heat, work, and entropy production. *Scientific Reports*, 6(1), December 2016.

[103] Philipp Strasberg and Andreas Winter. Heat, Work and Entropy Production in Open Quantum Systems: A Microscopic Approach Based on Observational Entropy. *arXiv:2002.08817 [cond-mat, physics:quant-ph]*, February 2020.

[104] Cyril Elouard and Camille Lombard Latune. Emergence of the laws of thermodynamics for autonomous, arbitrary quantum systems, July 2022.

[105] Roie Dann and Ronnie Kosloff. Unification of the first law of quantum thermodynamics, August 2022.

[106] A. Auffèves. Quantum technologies need a quantum energy initiative. *arXiv:2111.09241 [quant-ph]*, November 2021.

[107] Marco Fellous-Asiani, Jing Hao Chai, Robert S. Whitney, Alexia Auffèves, and Hui Khoon Ng. Limitations in quantum computing from resource constraints. *arXiv:2007.01966 [cond-mat, physics:quant-ph]*, July 2020.

[108] H. Weimer, M. J. Henrich, F. Rempp, H. Schröder, and G. Mahler. Local effective dynamics of quantum systems: A generalized approach to work and heat. *Europhys. Lett.*, 83(3):30008, August 2008.

[109] Léa Bresque, Patrice A. Camati, Spencer Rogers, Kater Murch, Andrew N. Jordan, and Alexia Auffèves. Two-Qubit Engine Fueled by Entanglement and Local Measurements. *Phys. Rev. Lett.*, 126(12):120605, March 2021.

[110] Y. Masuyama, K. Funo, Y. Murashita, A. Noguchi, S. Kono, Y. Tabuchi, R. Yamazaki, M. Ueda, and Y. Nakamura. Information-to-work conversion by Maxwell's demon in a superconducting circuit quantum electrodynamical system. *Nature Communications*, 9(1), December 2018.

[111] Philippe Grangier, Juan Ariel Levenson, and Jean-Philippe Poizat. Quantum non-demolition measurements in optics. *Nature*, 396(6711):537–542, December 1998.

[112] J. von Neumann. *Mathematische Grundlagen der Quantenmechanik ,Springer, (Verlag Julius ton University Press, Berlin, 1932; English Princeton, 1955).* 1932.

[113] Paul Busch and Pekka J. Lahti. The standard model of quantum measurement theory: History and applications. *Found Phys*, 26(7):875–893, July 1996.

[114] Armen E. Allahverdyan, Roger Balian, and Theo M. Nieuwenhuizen. Understanding quantum measurement from the solution of dynamical models. *Physics Reports*, 525(1):1–166, April 2013.

[115] Stella Seah, Stefan Nimmrichter, and Valerio Scarani. Nonequilibrium dynamics with finite-time repeated interactions. *Phys. Rev. E*, 99(4):042103, April 2019.

[116] Poyatos, Cirac, and Peter Zoller. Quantum reservoir engineering with laser cooled trapped ions. *PRL*, 1996.

[117] Eliot Kapit. The upside of noise: Engineered dissipation as a resource in superconducting circuits. *Quantum Science and Technology*, 2(3):033002, September 2017.

[118] Y. Liu, S. Shankar, N. Ofek, M. Hatridge, A. Narla, K. M. Sliwa, L. Frunzio, R. J. Schoelkopf, and M. H. Devoret. Comparing and Combining Measurement-Based and Driven-Dissipative Entanglement Stabilization. *Phys. Rev. X*, 6(1):011022, March 2016.

[119] Yao Lu, S. Chakram, N. Leung, N. Earnest, R. K. Naik, Ziwen Huang, Peter Groszkowski, Eliot Kapit, Jens Koch, and David I. Schuster. Universal Stabilization of a Parametrically Coupled Qubit. *Physical Review Letters*, 119(15), October 2017.

[120] S. Touzard, A. Grimm, Z. Leghtas, S. O. Mundhada, P. Reinhold, C. Axline, M. Reagor, K. Chou, J. Blumoff, K. M. Sliwa, S. Shankar, L. Frunzio, R. J. Schoelkopf, M. Mirrahimi, and M. H. Devoret. Coherent Oscillations inside a Quantum Manifold Stabilized by Dissipation. *Physical Review X*, 8(2), April 2018.

[121] Ruichao Ma, Brendan Saxberg, Clai Owens, Nelson Leung, Yao Lu, Jonathan Simon, and David I. Schuster. A Dissipatively Stabilized Mott Insulator of Photons. *Nature*, 566(7742):51–57, February 2019.

[122] Seth Lloyd. Quantum-mechanical Maxwell's demon. *Physical Review A*, 56(5):3374–3382, November 1997.

[123] Michele Campisi, Jukka Pekola, and Rosario Fazio. Nonequilibrium fluctuations in quantum heat engines: Theory, example, and possible solid state experiments. *New Journal of Physics*, 17(3):035012, March 2015.

[124] D. Mandal and C. Jarzynski. Work and information processing in a solvable model of Maxwell's demon. *Proceedings of the National Academy of Sciences*, 109(29):11641–11645, July 2012.

[125] A. C. Barato and U. Seifert. An autonomous and reversible Maxwell's demon. *EPL*, 101(6):60001, March 2013.

[126] Sreenath K. Manikandan, Étienne Jussiau, and Andrew N. Jordan. Autonomous quantum absorption refrigerators. *Phys. Rev. B*, 102(23):235427, December 2020.

[127] Philipp Strasberg, Christopher W. Wächtler, and Gernot Schaller. Autonomous implementation of thermodynamic cycles at the nanoscale. *arXiv:2101.05027 [cond-mat, physics:quant-ph]*, January 2021.

[128] Haroche and Raimond. *Exploring the Quantum: Atoms, Cavities, and Photons | Serge Haroche, Jean-Michel Raimond | Download*. 2006.

[129] B.-G. Englert, J. Schwinger, A. O. Barut, and M. O. Scully. Reflecting Slow Atoms from a Micromaser Field. *EPL*, 14(1):25–31, January 1991.

[130] Samuel L. Jacob, Massimiliano Esposito, Juan M. R. Parrondo, and Felipe Barra. Quantum scattering as a work source. *arXiv:2108.13369 [cond-mat, physics:quant-ph]*, August 2021.

[131] Y. Aharonov and T. Kaufherr. Quantum frames of reference. *Phys. Rev. D*, 30(2):368–385, July 1984.

[132] Nicolas Gisin and Emmanuel Zambrini Cruzeiro. Quantum Measurements, Energy Conservation and Quantum Clocks. *ANNALEN DER PHYSIK*, 530(6):1700388, June 2018.

[133] Stanisław Sołtan, Mateusz Frączak, Wolfgang Belzig, and Adam Bednorz. Modelling of weak quantum measurements consistent with conservation laws. *Eur. Phys. J. Spec. Top.*, 230(4):915–921, June 2021.

[134] Sebastian Deffner. Energetic cost of Hamiltonian quantum gates. *arXiv:2102.05118 [cond-mat, physics:quant-ph]*, February 2021.

[135] Jeremy Stevens, Daniel Szombati, Maria Maffei, Cyril Elouard, Réouven Assouly, Nathanaël Cottet, Rémy Dassonneville, Quentin Ficheux, Stefan Zeppetzauer, Audrey Bienfait, Andrew N. Jordan, Alexia Auffèves, and Benjamin Huard. Energetics of a Single Qubit Gate. *arXiv:2109.09648 [quant-ph]*, September 2021.

[136] H. J. Briegel, D. E. Browne, W. Dür, R. Raussendorf, and M. Van den Nest. Measurement-based quantum computation. *Nature Phys*, 5(1):19–26, January 2009.

[137] Tzu-Chieh Wei. Measurement-Based Quantum Computation. *arXiv:2109.10111 [quant-ph]*, September 2021.

[138] Kais Abdelkhalek, Yoshifumi Nakata, and David Reeb. Fundamental energy cost for quantum measurement. *arXiv:1609.06981 [cond-mat, physics:quant-ph]*, September 2018.

[139] Antoine Bérut, Artak Arakelyan, Artyom Petrosyan, Sergio Ciliberto, Raoul Dillenschneider, and Eric Lutz. Experimental verification of Landauer's principle linking information and thermodynamics. *Nature*, 483(7388):187–189, March 2012.

[140] J. von Neumann. *Mathematical Foundations of Quantum Mechanics*. Princeton University Press, Princeton, 1955.

[141] Harold Ollivier and Wojciech H. Zurek. Quantum Discord: A Measure of the Quantumness of Correlations. *Phys. Rev. Lett.*, 88(1):017901, December 2001.

[142] John Archibald Wheeler and Wojciech Hubert Zurek. *Quantum Theory and Measurement*. Princeton University Press, July 2014.

[143] T. Baumgratz, M. Cramer, and M. B. Plenio. Quantifying Coherence. *Phys. Rev. Lett.*, 113(14):140401, September 2014.

[144] Xiayu Linpeng, Léa Bresque, Maria Maffei, Andrew N. Jordan, 4 Alexia Auffèves, and Kater W. Murch. Energetic cost of measurements using quantum, coherent, and thermal light. *arXiv:2203.01329 [cond-mat, physics:quant-ph]*, March 2022.

[145] Jay Gambetta, Alexandre Blais, D. I. Schuster, A. Wallraff, L. Frunzio, J. Majer, M. H. Devoret, S. M. Girvin, and R. J. Schoelkopf. Qubit-photon interactions in a cavity: Measurement-induced dephasing and number splitting. *Phys. Rev. A*, 74(4):042318, October 2006.

[146] A. P. Sears, A. Petrenko, G. Catelani, L. Sun, Hanhee Paik, G. Kirchmair, L. Frunzio, L. I. Glazman, S. M. Girvin, and R. J. Schoelkopf. Photon shot noise dephasing in the strong-dispersive limit of circuit QED. *Phys. Rev. B*, 86(18):180504, November 2012.

[147] Mahdi Naghiloo. Introduction to Experimental Quantum Measurement with Superconducting Qubits. *arXiv:1904.09291 [quant-ph]*, April 2019.

[148] Ken Funo, Yu Watanabe, and Masahito Ueda. Integral quantum fluctuation theorems under measurement and feedback control. *Physical Review E*, 88(5), November 2013.

[149] Alexandre Blais, Ren-Shou Huang, Andreas Wallraff, S. M. Girvin, and R. J. Schoelkopf. Cavity quantum electrodynamics for superconducting electrical circuits: An architecture for quantum computation. *Phys. Rev. A*, 69(6):062320, June 2004.

[150] Alexandre Blais, Arne L. Grimsmo, S. M. Girvin, and Andreas Wallraff. Circuit quantum electrodynamics. *Rev. Mod. Phys.*, 93(2):025005, May 2021.

[151] P. Campagne-Ibarcq, E. Flurin, N. Roch, D. Darson, P. Morfin, M. Mirrahimi, M. H. Devoret, F. Mallet, and B. Huard. Persistent Control of a Superconducting Qubit by Stroboscopic Measurement Feedback. *Phys. Rev. X*, 3(2):021008, May 2013.

[152] Nathanaël Cottet, Sébastien Jezouin, Landry Bretheau, Philippe Campagne-Ibarcq, Quentin Ficheux, Janet Anders, Alexia Auffèves, Rémi Azouit, Pierre Rouchon, and Benjamin Huard. Observing a quantum Maxwell demon at work. *PNAS*, 114(29):7561–7564, July 2017.